MATHEMATICAL MODELLING AND CONTROL OF AGITATED EXTRACTION COLUMNS

FAROUQ SABRI MJALLI

Doctor of Philosophy

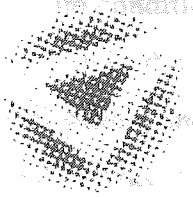

ASTON UNIVERSITY

October 2003

ASTON UNIVERSITY

MATHEMATICAL MODELLING AND CONTROL OF AGITATED EXTRACTION COLUMNS

FAROUQ SABRI MJALLI
Doctor Of Philosophy, 2003

ABSTRACT

Liquid-liquid extraction has long been known as a unit operation that plays an important role in industry. This process is well known for its complexity and sensitivity to operation conditions. This thesis presents an attempt to explore the dynamics and control of this process using a systematic approach and state of the art control system design techniques.

The process was studied first experimentally under carefully selected operation conditions, which resembles the ranges employed practically under stable and efficient conditions. Data were collected at steady state conditions using adequate sampling techniques for the dispersed and continuous phases as well as during the transients of the column with the aid of a computer-based online data logging system and online concentration analysis.

A stagewise single stage backflow model was improved to mimic the dynamic operation of the column. The developed model accounts for the variation in hydrodynamics, mass transfer, and physical properties throughout the length of the column. End effects were treated by addition of stages at the column entrances. Two parameters were incorporated in the model namely; mass transfer weight factor to correct for the assumption of no mass transfer in the settling zones at each stage and the backmixing coefficients to handle the axial dispersion phenomena encountered in the course of column operation. The parameters were estimated by minimizing the differences between the experimental and the model predicted concentration profiles at steady state conditions using non-linear optimisation technique. The estimated values were then correlated as functions of operating parameters and were incorporated in the model equations. The model equations comprise a stiff differential-algebraic system. This system was solved using the GEAR ODE solver. The calculated concentration profiles were compared to those experimentally measured. A very good agreement of the two profiles was achieved within a percent relative error of ±2.5%.

The developed rigorous dynamic model of the extraction column was used to derive linear time-invariant reduced-order models that relate the input variables (*agitator speed, solvent feed flowrate and concentration, feed concentration and flowrate)* to the output variables (*raffinate concentration and extract concentration*) using the asymptotic method of system identification.

The reduced-order models were shown to be accurate in capturing the dynamic behaviour of the process with a maximum modelling prediction error of 1%. The simplicity and accuracy of the derived reduced-order models allow for control system design and analysis of such complicated processes.

The extraction column is a typical multivariable process with *agitator speed* and *solvent feed flowrate* considered as manipulative variables; *raffinate concentration and extract concentration* as controlled variables and the *feeds concentration and feed flowrate* as disturbance variables. The control system design of the extraction process was tackled as multi-loop decentralised SISO (*Single Input Single Output*) as well as centralised MIMO (*Multi-Input Multi-Output*) system using both conventional and model-based control techniques such as IMC (*Internal Model Control*) and MPC (*Model Predictive Control*). Control performance of each control scheme was studied in terms of stability, speed of response, sensitivity to modelling errors (*robustness*), setpoint tracking capabilities and load rejection.

For decentralised control, multiple loops were assigned to pair each manipulated variable with each controlled variable according to the interaction analysis and other pairing criteria such as relative gain array (RGA), singular value analysis (SVD) and Jacobi eigenvalue criterion. Loops namely *Rotor speed-Raffinate concentration* and *Solvent flowrate-Extract concentration* showed weak interaction. Multivariable MPC has shown more effective performance compared to other conventional techniques since it accounts for loops interaction, time delays, and input-output variables constraints.

KEYWORDS: **SCHEIBEL, EXTRACTION DYNAMICS, LIQUID-LIQUID, BACKMIXING, BACKFLOW MODEL, STAGEWISE, SYSTEM IDENTIFICATION, CONTROL, SISO, MIMO, MPC.**

DEDICATION

To my beloved parents, and my family who have provided me with support throughout this long journey toward this thesis and were a source of encouragement and inspiration to me throughout my life.

ACKNOWLEDGEMENTS

I would like to express my gratitude to all those who gave me the possibility to complete this thesis. Special thanks to Dr. John Fletcher for being my advisor and his valuable help and support. Also I would like to express heartfelt thanks to my co-supervisor Dr. Nabil Abdul Jabbar for his valuable scientific comments, guidance and continuous encouraging support throughout the work of this thesis.

I will not forget the valuable support of Dr. C. J. Mumford and Dr. Imad Alatiqi who guided me during the early stages of the research.

I would also like to express my appreciation to Dr. Salah E. M. Hamam who have given help for the preparation of my thesis.

Finally, I feel especially indebted to my family and wife whose patient love enabled me to complete this work.

TABLE OF CONTENTS

LIST OF FIGURES

LIST OF TABLES

LIST OF SYMBOLS

a	Interfacial area per unit height (cm^2).
A	Cross sectional area of column (cm^2).
$A(s)$	Overall system transfer matrix.
CV	Controlled variable.
d_{32}	Sauter mean drop diameter (cm).
D	Column diameter (cm).
DV	Disturbance (load) variable.
D_c	Continuous phase diffusion coefficient (cm^2/s).
D_d	Dispersed phase diffusion coefficient (cm^2/s).
D_E	Extract phase diffusion coefficient (cm^2/s).
D_R	Raffinate phase diffusion coefficient (cm^2/s).
E	Extract phase flowrate (cm^3/s).
f	Mass transfer weighting factor.
F	Flow ratio.
$g_{ij}(s)$	Transfer function of element at i^{th} row and j^{th} column.
$G_c(s)$	Controller transfer function matrix.
$G_d(s)$	Disturbances transfer function matrix.
$G(s)$	Process transfer function matrix.
h_x	Holdup for the aqueous phase (cm^3).
h_y	Holdup for the organic phase (cm^3).
H_s	Stage height (cm).
I	Identity matrix.
k_c	Continuous phase mass transfer film coefficient (cm/s).
k_d	Dispersed phase mass transfer film coefficient (cm/s).
K	Overall mass transfer coefficient (cm/s).
K_E	Extract phase mass transfer coefficient (cm/s).
K_R	Raffinate phase mass transfer coefficient (cm/s).
K_p	Process steady state gain.
m	Mass transfer distribution coefficient.
MR	Magnitude ratio.
MV	Manipulated variable.
n	Stage number n.
N	Rotor speed (s^{-1}).
$N.I.$	Niederlinski stability index.
Q_x	Volumetric mass transfer rate in aqueous phase (cm^3/s).
Q_y	Volumetric mass transfer rate in organic phase (cm^3/s).
R	Raffinate phase flowrate (cm^3/s).
R^2	Regression coefficient squared.
Re	Reynolds dimensionless number.
R_f	Feed flowrate (cm^3/s).

R_{out}	Raffinate phase outlet flowrate (cm^3/s).
s	Laplce operator.
S	Extract phase flowrate (cm^3/s).
Sc	Schmidt dimensionless number.
S_f	Extract phase feed flowrate (cm^3/s).
S_{out}	Extract phase outlet flowrate (cm^3/s).
t	Time (s).
$u(t)$	Input to the process at time t.
$v_{dispersed}$	Velocity of the dispersed phase (cm/s).
$v_{continous}$	Velocity of the continuous phase (cm/s).
v_o	Average agitator tip speed (cm/s).
V	Stage volume.
We	Weber dimensionless number.
W_E	Extract phase holdup (cm^3).
W_R	Raffinate phase holdup (cm^3).
W_{MA}	Holdup in the aqueous mixing stage (cm^3).
W_{MO}	Holdup in the organic mixing stage (cm^3).
x_f	Feed concentration (wt fraction).
x_n	Aqueous phase concentration at stage n (wt fraction).
x_{out}	Raffinate outlet concentration (wt fraction).
x^*	Aqueous phase equilibrium concentration (wt fraction).
y_f	Solvent feed concentration (wt fraction).
y_n	Organic phase concentration at stage n (wt fraction).
y_{out}	Extract outlet concentration (wt fraction).
y^*	Organic phase equilibrium concentration (wt fraction).
$y(t)$	output to the process at time t.
z	Discrete domain operator,

Greek letters :

α	Aqueous phase backmixing coefficient.
β	Organic phase backmixing coefficient.
$\gamma(G)$	Condition number.
$\gamma_d(G)$	Disturbance condition number.
λ	Relative gain array element.
μ	Viscosity (Poice = gm/cm s).
θ	Dead time (s).
ρ	Density (gm/cm^3).
σ	Interfacial surface tension (dyn /cm = gm/s^2).
$\bar{\sigma}$	Largest singular value.
$\underline{\sigma}$	Smallest singular value.
τ	Process time constant (s).
τ_1, τ_2	First and second time constant (s).
τ_f	IMC filter time constant (s).

ω	Frequency (Hz).
$\Lambda(i\omega)$	Relative gain array matrix at frequency ω.
Θ	Phase shift.

Subscripts:

0	Aqueous mixing stage.
1	Stage number 1.
A	Acetone.
c	Continuous phase.
d	Dispersed phase.
f	Feed.
i	Stage number ***i.***
N	Last stage.
N+1	Organic mixing stage.
Out	Exit.
set	Set point.
T	Toluene
W	Water

Superscripts:

-1	Matrix inverse
T	Matrix transpose.
*	Equilibrium.

CHAPTER ONE
INTRODUCTION

1.1 PROBLEM STATEMENT AND MOTIVATION

During the early thirties of last century, research was devoted for the development of extraction contactors in which, the use not only of rotational motion to promote phase mixing but also of a reciprocating motion. In the following decade liquid-liquid extraction processes depended solely on the use of mixer-settlers which limited their economic application. In the same period, The Scheibel extractor [Scheibel, 1948] was introduced as the first multistage extractor column, which employed a column with more than twenty theoretical stages in a unified contactor. This column was proved to be simple in design and efficient in laboratory and pilot plant scales. Later, this contactor was modified for commercial scales processes. The solvent is typically chosen so that the solute in the solution has more affinity towards the added solvent. Therefore, mass transfer of the solute from the solution to the solvent occurs. Further separation of the extracted solute and the solvent will be necessary. However, these separation costs may be favourable to distillation and other separation processes for situations where extraction is applicable such as:

- when chemicals involved are temperature sensitive and need special precautions against reactions and degradation at higher temperatures.
- when separation by distillation is ineffective or difficult (e.g. zoetropes).
- when boiling points of mixtures are close and it is not possible to get the components without contamination due to small range of boiling points.
- when flexibility in operation conditions choice is desired.
- if more than two components are present and to be separated completely.

Solvent extraction was realized as a commercially important process operation only during the fifties as a result of intensive work for nuclear fuel reprocessing. Other important applications have been introduced later in separation of metals, aromatics, pharmaceutical, petrochemical industries, waste water treatment, hydrometallurgy and many others using counter-current extractors. The operation of

counter-current extractors is very complex and needs careful consideration. Some of these complexities and operational variables can be mentioned here:

- An increase in agitator speed increases the drops dispersion time resulting in more surface area of contacts and consequently promotes the efficiency of separation. On the other hand, this effect will produce finer uniform dispersion which increases the time for phases to disengage, and consequently reduces the column throughput [Scheibel, 1983].
- Efficiency can be also affected by the interfacial properties of the system. If surfactants favour continuous phase, they will be accumulated at the interface, which results in stabilizing emulsion and reducing efficiency. To remedy this problem, agitator speed and/or column throughput must be reduced [Scheibel, 1983].
- The presence of trace impurities and minor variations in concentration on the distribution coefficients are important to the analysis of the stability and flexibility of an extraction process. Thus, the uniformity of the feedstock and the cleanliness of the solvents and the feed are critical to the operation. These factors will have considerable effects on the degree of separation and the throughput to the limit that they become unreliable.
- The changes in interfacial tension due to solute concentration, temperature and interfacial electrical potential causes spontaneous interfacial flows referred to as the Maragoni phenomena [Ortiz, 1992]. This phenomenon contributes to the rate of solute transfer and modifies the hydrodynamics of the fluid layers adjacent to the interface, which affects drop coalescence and jet break-up. This added factor increases the non-ideality of the process [Ortiz, 1992].
- Hydrodynamics, expressed as axial holdup, is a function of the operating conditions such as the inlet flow rates, agitator speed and droplets characteristic velocities [Chiang et al., 1990]. This variability necessitates the accurate prediction of the column hydrodynamics during all phases of operation.
- The circulatory flow of continuous phase and the velocity distribution of the dispersed phase arising from entrainment of droplets cause vortex or reverse flow within the wake of droplets. This behaviour results in a phenomenon called back-mixing [Anderson et al., 1978]. It results in an overall degradation

in separation process. The simulated behaviour of a column must take this factor into consideration and its effect on the transients of the contactor.

- Solute Mass transfer in specified direction (i.e. continuous to dispersed or vice versa) is a complex function of flow rates and agitator speed. Its value changes during the operation of the column and the change of transient conditions (i.e. during drop formation, drops travel and drop coalescnce [Al-Faize et. al., 1987]). This effect results in discrepancy of predicted mass transfer coefficient. Hence, a reliable mass transfer model should cope with such variation in operational parameters.

- The best performance of extractors is achieved by operating the column near flooding conditions [Scheibel, 1983], which is a region very sensitive to changes in operational parameters. This acts as a physical constraint on the column throughput and phase separation.

On the other hand, safe operation has to be emphasized. Statistical records [Critchfield, 1976] showed that most accidents in the solvent extraction industry are caused not so much by technological failures (10%) as by human errors (90%). This adds up to the complexities involved in operating extraction columns.

Motivated by the above-mentioned complexities, an interest has focused on modelling and simulation of extractors for better control system design. This was also triggered by the need to understand the process behaviour under start up, shut down and stable operation ranges of the column.

The modelling of extractor equipment depends on its type and configuration. Two main categories are in use, namely the diffusion model which assumes turbulent axial diffusion of solute superimposed on plug flow of the phase under consideration and the backflow model, which assumes well-mixed non-ideal stages between which backflow occurs [Sleicher, 1960]. These two models represent idealized limiting cases. For multi-compartment agitated contactors like the Scheibel column, the later model is usually adopted.

Modelling studies for the stagewise contactors reported in the past described the cascade of stages as perfectly mixed with constant volume [Franks, 1966]. The main concern in the development of these models was to simulate the hydrodynamics and mass transfer within the contactor. Previously reported models suffer from either heavy assumptions that limit their real applications [Marshall, 1947; Gray, 1961] or involving detailed specifications of behaviour through the use of empirical correlations that made the applicability of these models specific for the equipment used [Staffin, 1959; Nabeshima, 1987].

Assumptions like fixed holdup profile, specific mass transfer correlation, constant physical properties and fixed operational parameters are common. This imposed a great need for adopting a modelling strategy that is capable of explaining the highly complex behaviour of the column efficiently over the whole range of operation under varying conditions of hydrodynamic and mass transfer conditions. These modelling difficulties can be tackled by using a rigorous dynamic model with variable parameters. The model parameters should be estimated as a function of operational parameters so that their values vary during simulation. This can be attained by correlating these parameters to the operating variables through a wide range of column operation. For liquid-liquid agitated extraction columns, the mass transfer weigh factor and the backmixing coefficients for both phases need to be estimated in order to simulate the column. Model parameter estimation is usually performed using non-linear optimisation techniques to minimise the difference between the model predictions and the experimental data. The target here is to derive a model that can be employed for transient operations and be adequate for further control system design and analysis studies. The feasibility of using reduced order models also has to be investigated and compared to the rigorous one [Najim et al., 1987].

Achievable control performance is limited by how much we know about the process. A good control system design should maintain satisfactory setpoint tracking and load rejection characteristics in terms of response time, stability, and sensitivity to modeling errors (*robustness*). Consequently, after dealing with the problem of process modelling, the engineering practice targets towards achieving a stable operation and robust performance of the process under regulatory and supervisory conditions [Ogunnaike et al., 1994]. The control of the feed and solvents flowrates, coupled with

the ability to maintain the compositions of all streams entering and leaving the extractor, is of paramount importance to the extraction operation.

Extraction processes have not been considered as prime targets for control studies and were often a neglected part of process plants. The slow response time of the process encouraged engineers to use local control of inlet flows, alarms to indicate abnormal conditions, off-line analysis, and operator experience in correcting for process deviations. These approaches were hindered by the complex nonlinear nature of the process and the varying physico-chemical phenomena present in their operations [Burkhart, 1984]. Yet, the key points for successful extractor control are hydrodynamic stability, changes in mass transfer rates, and chemical stability.
The classical control strategy for an extraction column was to control the flow ratio of inlet solvent to feed (ratio control). In addition, control the interface level by varying the column hydrostatic pressure via a control valve in the extract line. Product composition may be used as a set point to the ratio controller [Burkhart, 1984]. This arrangement assumes that the system is insensitive to total flow rate changes and feed concentration changes and depends also on a fixed product quality that is pre-specified during the design stage.

In order to maintain the column in its optimal behaviour zone, in spite of flowrates and physical properties of solvent and solute fluctuations, more sophisticated control system design techniques are needed. The advancement in computer technology and the great evolution of new control algorithms has made it possible to achieve this task efficiently and economically. Several control techniques have been evolved and tested industrially with great success in the past decade for the extraction processes. Yoswathana and co-workers used an adaptive control scheme, where the plant parameters were recursively estimated using recursive least square methods [Yoswathana et. al., 1985]. The PID (Proportional-Integral-Derivative) controller parameters were adjusted accordingly to the closed loop system characteristic equation. Najim et al. (1988) used linear quadratic self-tuning control algorithm from the minimization of quadratic cost function. This algorithm, involves a parameter identification procedure and feedback control law which uses the estimated parameters. Tsouris and Tavlarides (1991) used a first order-reduced model of the process to control the dispersed phase volume fraction. The Dahlin controller

algorithm was used. Wichterlova and Rod (1999) studied the control of the extractive separation of the rare earth metals. The final design wasn't tested for stability and robustness under the whole range of operating conditions.

Despite the good control theory involved in the application of the above mentioned techniques, the authors did not give the control system synthesis a proper attention and they have built their control law based on practical considerations only. Before any control system design of a MIMO process (Multiple Input Multiple Output), the control synthesis must be carried out. The synthesis of control configurations for multivariable system involves selection of controlled and manipulated variables, pairing manipulated inputs and controlled outputs (loop pairing), and selection of the best control configuration. Generally, input variables can be classified into manipulated variables (MV's) and disturbances or load variables (DV's). In liquid-liquid extraction systems, the manipulated variables typically include *Rotor speed* and *solvent feed flowrate*. Load variables include *feed concentration, solvent feed concentration* and *feed flowrate*. The controlled variables (CV's) in extractors are *outlet concentrations* for both phases.

Model-based control techniques such as internal model control (IMC) (Garcia and Morari, 1982; Morari *et. al.*, 1989) and model predictive control methods (MPC) (Rawlings *et. al.*, 1994) including dynamic matrix control DMC (Cutler and Ramaker, 1980) and model algorithmic control (MAC) (Mehra and Rouhani, 1980), which have shown to be very effective in controlling dynamic systems, do use dynamic models explicitly for on-line process predictions and control action calculations. The complexity of dynamic models can be very computationally intensive and hence may prohibit on-line implementation of MPC. Thus, model identification is a critical step towards designing model-based control schemes that can cope with process nonlinearity and complexity. The accuracy of the obtained reduced-order models via system identification will determine the success of the control system design.

Although process models can be derived based on the fundamental principles, obtaining a reduced-order time-invariant dynamic model from plant test data via system identification techniques, has proved to be more efficient and is the currently accepted industrial practice (Andersen *et al.*, 1991). In this approach, selected step

changes sequence in the input variables (manipulated and disturbances) is introduced into the process system and the output variables response data are collected in response to these step changes. Usually, the input/output plant data that are generated from plant step testing are used to derive reduced-order simple models that can adequately describe the dynamic behavior of the process. Different types of models can be derived via system identification including transfer function, state-space, step response, or finite impulse response models. These models can be in continuous or in discrete forms. The advantages of this type of models stems from the fact that they are simple to use with no intensive computations needed for on-line implementation of model-based control schemes.

1.2 RESEARCH OBJECTIVES

Based on the previous presentation, this research has been set primarily to achieve the following objectives:

1. Experimental investigation of the Scheibel liquid-liquid extraction column at different modes of operation in order to gain a close insight of steady-state and dynamic behaviour of the contactor under varying operating conditions and disturbances. This part of the study involves data logging and analysis techniques.
2. Development of a rigorous dynamic mathematical model based on the physical principles of mass transfer, hydrodynamics, and phase equilibria involved in the extraction processes. The model also includes auxiliary equations that correlate dispersed phase holdup, mass transfer coefficient, drop size, and physical properties. Model correlations take the same general form in order to facilitate the generality of applying such a model to other column geometries. The process simulation model will be validated with the obtained experimental data.
3. Perform system identification to construct a reduced-order MIMO model for the process, which can be utilized for further control system design and analysis. The model predictions obtained using the reduced-order models should be compared to those obtained from the rigorous dynamic model to test the accuracy of the identified models.

4. Propose a multivariable control system that can handle the extraction process efficiently. Multivariable control design techniques must be considered here in order to account for dynamic interactions between the control loops. The performance of advanced model based control strategies will be compared to the classical ones. The control system will be tested for efficiency, stability, robustness and its ability to handle process variables constraints.

1.3 THESIS OVERVIEW

This thesis presents a methodological framework for modelling, simulation and control system design of extraction processes. It can be implemented to any contactor provided that data regarding chemical system, column geometry and operating conditions are available. The body of the thesis consists of eight chapters and seven appendices. In chapter one, an overview of the problem is introduced with the motivation of the proposed work and the main objectives. In chapter two, the literature related to liquid-liquid extraction modelling, identification and control are critically reviewed. In chapter three, the experimental investigation is explained in detail and the results are presented in a form suitable for comparison with theoretical ones. In the fourth chapter, the rigorous dynamic model is developed, and simulated with experimental data. Chapter five involves the calculation of reduced order models using system identification techniques followed by open loop dynamics and model validation of the developed simplified linear time-invariant models. In chapter six, control system synthesis is considered and a classical approach to a control system design is presented. The control system is analysed and tested. Chapter seven presents the model predictive control (MPC) system design and investigation of multivariable control strategies that involves system testing for reliability, and robustness. The MPC algorithm will be implemented for the two cases of control with and without input-output variables constraints. The last chapter presents and discusses the major conclusions for this study and provides some recommendations for further work related to this area. The appendices cover some experimental and computational details implemented within the context of the thesis in addition to a listing of the programs used in the simulation and control system design and analysis.

CHAPTER TWO
LITERATURE SURVEY

A prior knowledge of the previous work accomplished in the area of modelling, simulation and control of liquid-liquid extraction contactors is essential to achieve further advancement in the field. The following is a critical review of both the experimental and theoretical studies conducted on these areas listed in chronological order. The emphasis is given to studies for both continuous and stagewise contactors. In this chapter, the three areas; modeling, simulation and control of extractors will be reviewed.

2.1 Dynamic Modelling and Simulation of Extractors :

As far as the method of operation is concerned, Liquid-liquid solvent extraction equipment can be divided into two main categories; (a) continuous or differential contactors and (b) stagewise contactors. Dynamic modelling studies of these contactors have gone into the same categorization and previous work done in these two areas will be enlightened in the following subsections. Interesting reviews of this topics have been given by Pollock and Johnson (1974), Weinstein *et al.* (1998) and recently by Swati (2000).

2.1.1 Modelling and Simulation of Continuous Columns Contactors

Marshall and Pigford (1947) studied the transient behaviour of diffusional operations. They developed differential model for a section of the column as shown in figure (2.1). It was further assumed that the holdups, flow rates and mass transfer coefficient are constant and that only solute transfer between phases. An equivalent stagewise form of the model was developed. To solve the stagewise model equations, ideal mixing in each phase and linear equilibrium relationship were assumed for simplicity. Laplace transform was used to solve the previous equations. This was a pioneering effort in this field and many restrictive assumptions were put for simplicity such as constant inlet solvent concentration, outlet concentration, and an initial concentration profile. These

assumptions had put some limitations on the application of the model. Fig (2.1) illustrates the two models used in the study [Pollock and Johnson 1970].

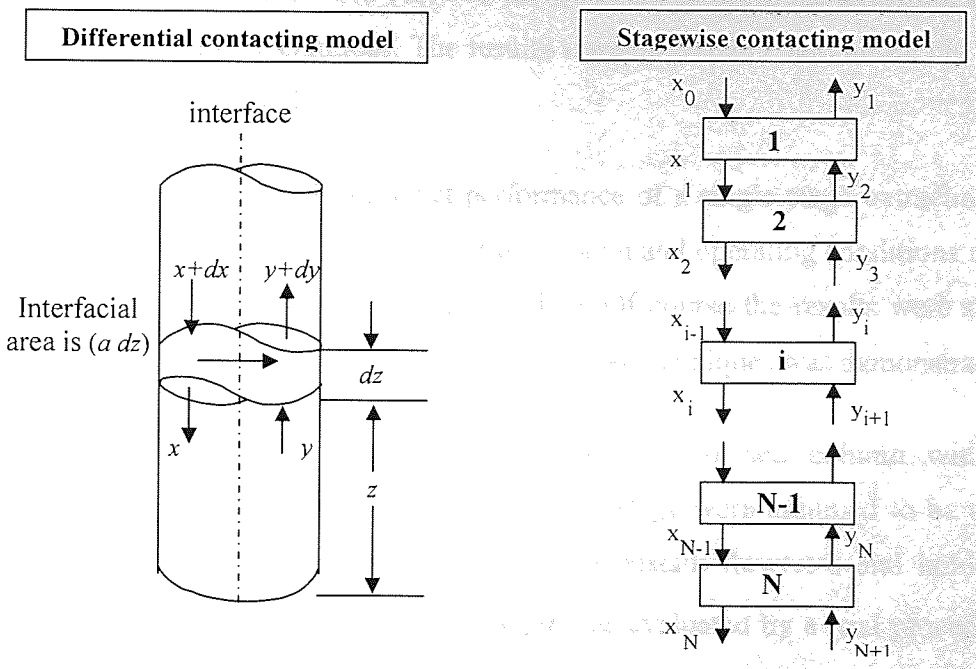

Figure(2.1) General Schematic diagram of continuous and stagewise extraction models.

Lapidus and Amundson (1950) generalized and extended the work of Marshall and Pigford for unsteady state feed compositions. An analytical approach was adopted for the simulation but without any experimental verification. The solution was complex and impractical , also the assumption of linear equilibrium relation restricted its application.

Jaswon and Smith (1954) have transformed the model equations developed by Marshal and Pigford (1947), by introducing new independent variables, α and β, into a single dimensionless partial differential equation. The ordinary differential equation (ODE) developed had very complex boundary conditions and hence the analytical solution was lengthy and not easy to apply. Their solution showed mathematical discontinuity, which can be attributed to the assumption of no diffusional effects. This was a major drawback of the model. Lavergne (1956) attempted to simplify the model developed by Jaswon and Smith (1954) and compared it with experimental data, although comprehensive, no significant improvements were obtained due to simplifications in the analytical solution of the model.

Huang (1956), conducted experimental studies on the transient startup behaviour of extraction columns but his work suffered from human errors in establishing zero time, and improper sampling techniques. The results were not reliable and hence his analytical solution was very restricted.

Staffin (1959), attempted to predict performance of a single stage extraction column as a first step for design. The properties of the system and operating conditions in relation to transient response characteristics were studied. Of course the results were specific to the equipment used, and the need for better analytical techniques was demonstrated.

Biery (1961), studied the dynamic response of a pulsed column with a non-equilibrium stage model where the phases in each stage were assumed to be uniformly mixed but not at equilibrium with each others. Constant flowrates and holdups were assumed and the mass transfer coefficient $K_E a$ was evaluated by a trial procedure. This gave a set of $2n$ equations, where n is total number of stages. These were solved using a fourth order Runge-Kutta procedure, and compared his predicted results with the experimental raffinate response only. They were reasonably good with some deviations. Further it was assumed that each stage was uniformly mixed with concentration gradient (in each phase) and used arithmetic averages to approximate the gradients. An oscillation of the numerical solution was observed, so the modified model was rejected.

Using frequency response methods to study the dynamics of a packed absorber, Gray (1961), formulated and solved three models. This study paved the way for later extraction studies that used that same mathematical background. The first model attempted was a plug flow model with hyperbolic partial differential equations similar to the equations used by Marshal and Pigford (1947) using linear equilibrium relationship. This were transformed to Laplace domain and solved analytically. Complete extraction takes place at infinite column length was assumed. The second model was a stagewise model similar to Beiry (1961) equations. It was solved with linear relationship, and constant holdups and flowrates by Laplace transform to predict the frequency response.

The third model was an axial diffusion model similar to that developed by Marshal and Pigford (1947) with the addition of axial diffusion term. The model was solved by Laplace transform. A fourth order differential equation was obtained for which no general solution was found. After comparing experimental and theoretical frequency response of the first and second models, he concluded that only Magnitude Ratio (defined as $MR = \sqrt{\mathrm{Re}^2 + \mathrm{Im}^2}$ where Im and Re the imaginary and real parts) should be used for the comparison. The phase shift (defined as $\theta = \tan^{-1}(\mathrm{Im}/\mathrm{Re})$) was similar for the two models. This result contradicts with findings of other studies conducted later. The assumption of single-phase flow made the models inapplicable where absorption is present.

Later, Champagne (1962), solved the model developed by Gray (1961) using finite difference techniques for a pulsed column for start-up and step change in feed concentration and solvent flowrate. Much detailed experimental information and long computer time were needed. Using finite difference techniques with finely divided grid, his solution required 35min on an IBM709 computer. This was the main disadvantage as far as control and modelling work is concerned where model simulation time is a critical factor. This problem is rapidly disappearing as faster computers are available.

Watjen (1963), conducted experiments on a pulsed column both theoretically and experimentally (using pulse testing techniques). The axial diffusion model equations developed by Gray (1961), were solved using finite differences. Murphree stage efficiency for eliminating the light phase concentration was utilized. This efficiency with the diffusivities were found experimentally and substituted in the model. The use of Murphree efficiency was a disadvantage as was shown previously by Dillido (1961). A more sophisticated model was required, especially for the case of turbulent mass transfer. The stagewise model was used while the extractor was operating outside the mixer-settler region of operation where backmixing occurs.

Takamatsu and Nakanishi (1963) used a single stage ideally mixed vessel to study the effects of mass transfer expressions on the dynamic response shape. Their model consists of three ODEs. The equations were Laplace transformed and four transfer functions were

derived relating outlet concentration to inlet concentrations. The transfer functions were compared for the case where mass transfer coefficient was based on the extract phase. It was concluded that the results were consistent with each other, and the choice of which fluid the mass transfer coefficient was based on was not important. This wasn't the case when they try to do the same investigation using Murphree efficiency instead of mass transfer coefficient. The use of a single stage apparatus limited the generality of their study and more investigation was needed to include the case of multi-stage extraction units.

Chiu (1963), used a 6 ft high by 4 inch internal diameter Scheibel column to study the transient behaviour to a disturbance in feed composition, assuming constant holdups; flow rates; and an experimental pseudo-equilibrium relationship. The model used a combined form of the model developed by Biery (1961) with a pseudo-equilibrium relation. Poor agreement was obtained between experimental and theoretical results due to the effect of poor sampling technique.

In studying the transient response of a packed column using pulse methods, Clements (1963), tried to model the system by a differential model equation similar to Marshal and Pigford (1947) model, but without axial mixing. He Laplace transformed the differential model and derived the transfer function. An attempt was made to evaluate the only unknown parameter, which was the mass transfer coefficient by fitting the experimental data to the equation but with no success. Pulse testing was used to determine the axial diffusivity without extraction. An attempt to fit the models in the Laplace domain was carried out. However, it was difficult to relate deviations in the s-plane to the model error. The program he used to calculate the frequency response gave response curves that were similar in shape but displaced from each other.

Justice (1964), studied the dynamics of packed bed columns, using pulse testing. Axial diffusivity was calculated by minimizing a residual function that includes both Magnitude Ratio (***MR***) and phase shift (Θ). Good agreement was obtained between predicted and experimental results. In a later paper by Justice and Schnelle (1965) a variation of the axial differential model developed by Gray (1961) but without extraction

was considered with the addition of a reaction term and assuming that dispersed phase concentration is constant and that transfer mechanism is analogous to a first order reaction. The model was transformed and three parametric equations were obtained, and then the parameters were evaluated by least squares minimization between the experimental and theoretical values. The assumption of a constant dispersed phase concentration was unrealistic and limiting.

Foster (1964), solved a stagewise model with axial mixing terms. The axial mixing terms were expressed as constants representing the fractions of each phase, which is entrained by the other phase into the adjacent stage. Figure (2.2) represents a simplified flow diagram of the model. A linear equilibrium relation was used and the solution was in an explicit matrix exponential form. He solved the ***2n*** ODE equations for both cases of linear and nonlinear equilibrium relationship. The predicted response curves agreed reasonably with those obtained by Champagne (1962) and Biery (1961). The solution suffered from the difficulty of evaluating the operational parameters (i.e. the backmixing coefficients ***r*** and ***s***) and the calculations needed so much time, which is inappropriate for control studies where simulation time is major factor.

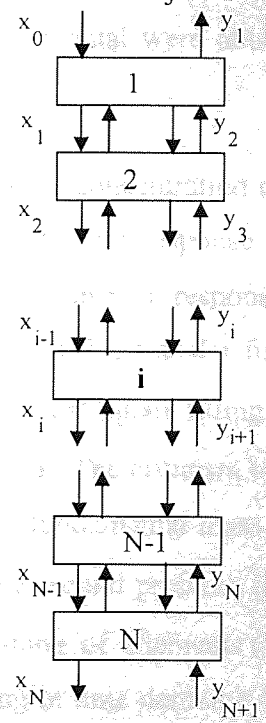

Fig.(2.2) Schematic diagram of the Stagewise backflow model

Doninger (1965), used a packed extraction column and compared his experimental frequency response obtained by pulse testing of the feed concentration to the frequency response obtained from the mixing cell model of Gray (1963). It was found that by adjusting the number of cells or stages, the normalized ***MR*** (Magnitude Ratio) of the theoretical transfer function obtained from the mixing cell model could be made to agree with the normalized ***MR*** of the experimental results. This was achieved by adding correlation factors to the theoretical results. Those correlation factors were found by trial and error and have no experimental significance.

Using pulse testing on a spray and a packed columns, Elkins (1966), tried to solve the axial differential model both with and without extraction. The results were simulated using an analogue computer. The time response predicted for the one-dimensional model using different values of diffusivity coefficients was compared to the experimental. The diffusivity coefficients were calculated then substituted in the model developed by Gray (1961). The time response curves were generated. The use of analogue computer limited the number of differencing modules in the approximation and consequently, no good agreements with the experimental were obtained. It was concluded that a digital computer should be used instead.

Hale (1966), used colourimetric concentration measurements of the feed and product streams to study the frequency domain response of a pulsed column. A pulse testing technique was used to get the transient response data (frequency response). These responses were fitted to a first order lag transfer function with a dead time. The number of cells ***n*** was calculated using a least square fitting algorithm in terms of the ***MR*** only to minimise a given residual function. The criticism to this work is the use of a mixing cell model rather than one based on fundamental mass transfer phenomenon. This restricted the range of its application. The second problem is the use of ***MR*** in the minimization algorithm, which was shortcoming of Clements (1963) and Justice (1964) work. This gave only approximate matching in time domain. A rigorous method for minimizing the frequency response residual was reported later by Hays, Clements and Harris (1967). The frequency response residual was expressed as:

$\mathbf{R} = \sum(\Delta\mathbf{Re})^2 + \sum(\Delta\mathbf{Im})^2$ where **Re** and **Im** are the real and imaginary parts. This method is dependent on the squared vectorial deviations of the experimental and theoretical values. The conclusion of this work is that importance of the correspondence of the frequency and time domain was emphasized and the model must ultimately predict the time domain behaviour if it is to be useful.

Foster (1967), studied the dispersed phase holdup of a 22 plate, 2 inch ID pulsed column both experimentally and theoretically for operation in the emulsion region. Liquid flowrate and pulse frequency were used as input disturbances. The experiments were done without mass transfer. An inter-stage mixing term was included from a previous study. It was concluded later that this term has little effect on the overall performance of the model. A slip velocity defined as the ratio of dispersed phase velocity to the continuous phase velocity was introduced to account for variation of flowrates through the stages. This was correlated from steady state as a function of pulse velocity and holdup. The column hydrodynamics were expressed in terms of the dispersed phase flowrate, the slip velocity and dispersed phaseholdup. The set of n equations were solved using Runge-Kutta algorithm. The main limitations to this work were the lack of mass transfer coefficient and the dependency of slip velocity on pulse velocity and holdup volume only.

McSwain (1966), used Foster's backflow model with backmixing coefficients changing between stages. The Backmixing coefficients, at each stage were evaluated at the steady state by comparing the predicted with experimental profiles. An exponential behaviour for the holdup variation was assumed. In this model the responses of both phases could be determined, but the main criticism for this work is the way the parameters where estimated.

Pollock and Johnson (1969) studied a Scheibel column, and used a non-equilibrium mixing model, and used the Runge-Kutta-Gill method for the solution assuming solute transfer only, with holdups and mass transfer coefficient obtained experimentally. The holdups were averaged, and the mass transfer coefficient was changed linearly as a

function of the number of column stages between the initial and final values. Their work suffered from several limitations. The response was unreliable due to poor sampling at the column exits. Column end effects on mass transfer were not considered. The method of calculating mass transfer coefficient was not practical since it requires the final steady state conditions to be known a priory and this is not available at hand always.

Souhrada, Landau and Prochazka (1970), studied the dynamics of a reciprocating plate column by modelling it with a stagewise backflow model similar to that used by Foster (1964). The model equations were added to form one equation. They used constant Backmixing coefficient and holdup, with both cases of linear and non-linear equilibrium relation. Stage efficiency similar to Murphree efficiency was used.
The parameters were obtained experimentally from the steady state runs. The model equations were integrated and the response was compared to experimental ones. Some comparison discrepancies of response were encountered at the column outlets. This work is similar to that of Foster (1964) except for the experimental part.

Pollock and Johnson (1970), studied the dynamic characteristics of a three stage multi-mixer column. They tried various testing techniques and concluded that step testing is as reliable as pulse methods. Various mathematical models without backmixing using frequency and time domain techniques were compared. It was concluded that for a realistic extraction model to be applied, the mass transfer coefficient should be allowed to vary with concentration column length, and the ends effects should be considered.

Pang (1971), extended Pollock's work and applied signal flowgraph and matrix inversion methods, for obtaining the theoretical frequency response of the extractor. Both the effluent and the extract streams were simulated using a large digital computer. They changed the extract phase composition from one to another in a minimum time, and varied the specification while minimizing the production of off-specification material. Since no experimental study was conducted, this work suffers from the same limitations of Pollock's original work. The same study was repeated by Jarvis (1971) on a minicomputer, with similar results.

Pollock and Johnson (1974), investigated the dynamics of a mechanically agitated sieve plate extraction column in a three part study. In the first part pulse and step testing were used to generate the response data. A double pulse was recommended to minimize the effect of random noise. In the second part of the study, they concentrated on exploring the best techniques for sampling the two phases dynamically, and concluded that more experimental investigations were needed and variable mass transfer coefficient should be used in the modelling of extractors. In the last part the extractor was modelled using an ideally mixed, non-equilibrium stage form. Starting with equations similar to those developed by Beiry (1961), the equations were Laplace transformed and solved analytically. A single phase mixing cell was added to each phase to approximate the damping and delaying action of the phase separation zones at the ends of the column i.e. end effects as shown in Fig (2.3). The two mixing cells were modelled assuming no mass transfer. The model parameters namely; number of stages and mass transfer coefficient were determined by optimising the residual function between experimental and predicted responses.

A comparison of the methods of Justice (1964), Hays (1967) and Clements (1963) indicated that Hays' method for calculating frequency response residual was the only acceptable one since it is the only method directly related to the minimization of the deviation in the time domain. Solution of the previous differential equations with the calculated mass transfer coefficient values was performed and compared to the experimental responses. poor results were obtained due to the assumption of constant mass transfer coefficient. The main criticism of this work is the reliance on the single stage model, without further comparison with other models such as the backmixed model of McSwain (1966).

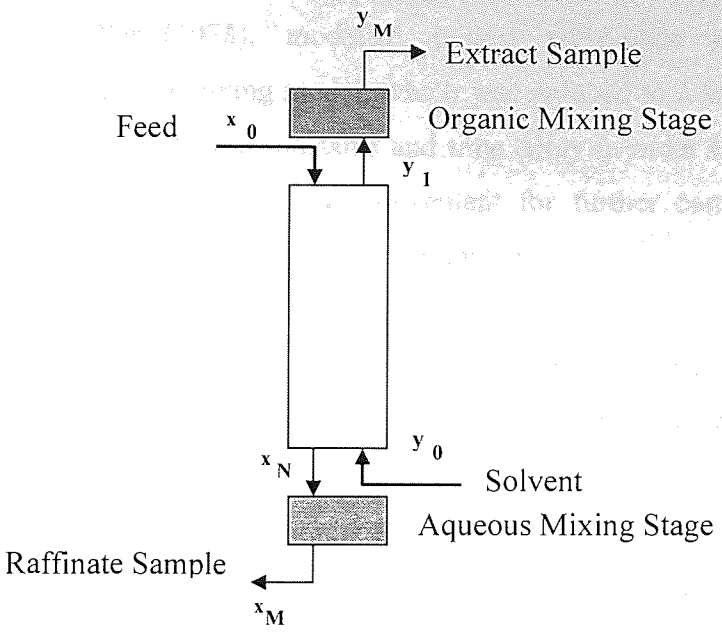

Fig (2.3) Single-phase mixing stage model

Chartres and Korchinsky (1975), improved a stagewise model to represent the physical processes occurring in liquid-liquid extraction. The influence of drop size distribution was first included. The model was solved numerically with a range of parameter values in order to predict the extent of drop size distribution on extraction rates.

Wang et al. (1977), modelled the dynamic concentration changes in Graesser raining-bucket contactor using the MIMIC digital simulation language. He employed both non-equilibrium stage wise model and finite difference axial dispersion flow model with back mixing. The models gave similar results but weren't able to representing the actual dynamic behaviour of the column accurately. This was due to the exclusion of end effects and constant mass-transfer and hydrodynamic effects assumptions.

Stiner *et al.* (1978), modelled a spray column using a modification of non-equilibrium stagewise model in which the dispersed phase was assumed to consist of non-coalescing drops. The computational time was reduced, but no experimental verification was conducted.

Bauermann and Blass (1978), modelled pulsed sieve-plate column using the non-equilibrium stage backmixing model, which was reduced to a second order transfer function with two identical time constants and time delay in order to reduce number of model parameters. This approach was convenient for further control studies but no further testing and analysis of the model was conducted.

Sovova *et al.* (1986), studied experimentally a reciprocating plate column and determined transfer functions relating the holdup to the intensity of plate reciprocation and the velocity of the dispersed phase. The transfer functions were of first order with a time lag. They used ultrasonic technique for the online holdup measurement. Mass transfer wasn't included in their study and there wasn't a thorough investigation of the effect of column operational parameters on the efficiency of the column and consequently on the transfer function parameters.

Zimmermann *et al.* (1990), used a nonequilibrium drop population stage model for describing the hydrodynamics of the extraction column. They avoided the use of empirical correction factors like efficiencies or HETP. The effects of drop breakage, transport and inter-drop coalescence were incorporated by the use of the so-called production terms. Molar densities were assumed constant for both phases. They used Newton's method to solve the set of non-linear equations using a tri-diagonal matrix. This method is very sensitive to initialisation and not appropriate for further control system design and analysis.

2.1.2 Modelling and Simulation of Stagewise Contactors:

The other mode of operation of extractors is on stage-wise basis. Burns and Hanson (1964) used a five-stage mixer-settler to study the effect of variations of feed concentration on contactor response experimentally. The results showed that the extractor behaviour was different for the cases where the feed concentration increases than for decreases. It was further recommended that there were shortcomings in the experimental techniques used and the need to improve them.

Halligan and Smutz (1966) conducted experimental and theoretical study on a cascade of mixer-settlers. A typical stage is shown in Figure (2.4). They modelled the mixer and the settler separately. The mixer was assumed to be a perfectly mixed equilibrium stage with constant holdup. The material balance revealed equation similar to that used by Biery (1961). The settler was modelled in four different ways with different assumptions; perfectly mixed model, plug flow model, hybrid model (organic phase moves in plug flow while aqueous phase is perfectly mixed) and equilibrium model, where both mixer and settler constitute a single perfectly mixed stage. The last was the simplest. Their simulation revealed that for the single stage investigation, the hybrid model was the best choice but as the number of stages increases the response curves for the four models become close to each other, as a result they recommended the use of a simple model such as the equilibrium model for the case of large number of stages.

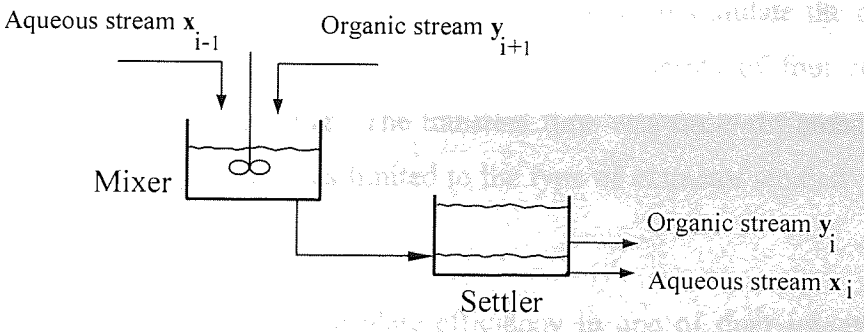

Fig (2.4) A typical mixer-settler stage flow diagram

Using a single-stage lab-scale mixer-settler unit, and a highly complex equilibrium relationship, Kikiudai *et al.* (1967) tried to simulate the behaviour of the mixer-settler response using an analogue computer and they suggested the use of hybrid computers for large scale equipment. This was a computational limitation at that time.

Hanson and Sharif (1970) studied the hydrodynamics of mixer-settlers, and found that the perfect mixing in the settler is better assumption than plug flow.
Assuming perfect mixing in both mixer and settler, instantaneous mass balance, and empirical holdup relationships, Cadman and Hsu (1973) derived a nonlinear equation for the system. Without any assumptions of linear equilibrium relation or constant flow rate

they linearized the equations and transformed them by Laplace transform in order to find the transfer function.

With parallel studies Rouyer *et al.* (1970) and Hoclet *et al.* (1970) studied the hydrodynamics of mixer-settlers; they investigated upward and downward steps in aqueous feed concentration. Their work was complex to be used for computer control.

Bobrow *et al.* (1971) employed the DYNSIS modular computer program for studying the dynamics of a multistage butadiene extraction plant. It is a steady state modular flow-sheeting program. Equipments are represented by separate blocks in the flow diagram. The application to extraction was limited by the type of model used and the assumptions associated in its synthesis.

Beetner *et al.* (1973) presented a simulation technique for a 10-stage box-type pump-mix mixer-settler where its volume was divided into 20 regions to simulate the organic phase in the settler, and the aqueous phase was described in terms of four regions, perfectly mixed with two recycle mixing. The transient time was finite differenced and the model was solved. This approach was limited to the type of extractor studied, and no generalization was introduced.

Aly *et al.* (1973) introduced Murphree plate efficiency in one of their mixer-settler and used the state space representation to solve their model. They compared their model to the experimental results obtained from pseudo-random binary sequence changes and concluded that the use of stage efficiency was not adequate and it is rather better to use simple models with assumptions.

Libhaber *et al.* (1974) modelled the extraction of phosphoric acid using IMI phosphoric acid process with an equilibrium stagewise model where each of the mixer and settler were treated as one constant volume equilibrium stage.

El-Rifai *et al.* (1975) derived linear dynamic models for counter-current mixer-settler cascades with a first order reaction occurring in the organic phase. They obtained the

effects of dynamical rate constant; residence time; extraction factor; and number of stages on the frequency response of the two outlet streams.

In their study of thermodynamic characteristics of a horizontal liquid-liquid settler, Drown and Thomson (1977) divided the settler into three distinct regions: the entrance region; the emulsion band region, and the exit region. They found that the velocity distribution was not a plug flow pattern distribution and that the emulsion band zone was capable of absorbing momentum from both bulk phases and as a result the dynamic coalescence rate was enhanced due to the deceleration of the emulsion band.

Ochsenfeld *et al.* (1977) employed a multistage, multi-component equilibrium stage to confirm the dynamic behaviour of a laboratory scale hot cell mixer settler cascade used for the extraction of fast breeder reactor fuel. This study highlighted important effects that could be caused by relatively small changes in the feed flowrate on outlet concentrations. They also concluded that the control of such effects is possible due to the slow nature of the transient response.

Tsouris et al. (1994) used a population balance equation model to study the multistage behaviour of extraction contactors. The model considered drop breakage, coalescence, and exit phenomena. A photomicrographic technique for the drop size distribution and an ultrasonic technique for the transient holdup measurements were used.

Wichterlova and Rod (1999) studied the dynamics of a 6 stage box-type mixer-settler cascade using the pulsed-flow model to predict the operating conditions, and performance of the extractive separation of the rare earth metals. The main criticisms of this work are; first, discrete sequences of pulses in time domain were used to approximate the dynamic model. Secondly, stage efficiency was calculated from steady state profiles and this does not necessarily represent the true transient approach to equilibrium in the stage. Finally, the use of constant flowrates and constant holdups restricted the applicability of this work.

Ribeiro et al. (2000) studied the unsteady state behaviour of liquid-liquid dispersions in single and continuous batch-stirred vessels. They simulated a population balance equation model using a parallel processing architecture. The study revealed that the parallel algorithm pays off for the study of extraction dynamics. The adoption of these algorithms presents a promising research area that lends itself for further control study applications.

2.2 Control of Extractors

The control studies of liquid-liquid extraction followed the same categorization of the modelling studies i.e. Control of continuous contactors and control of stagewise contactors. During the past forty years, the research in this area concentrated on the analysis and design of conventional and advanced control systems to liquid-liquid extraction contactors. The following is a general review of work done in this area.

2.2.1 Control of Continuous Columns

Diliddo (1961) was the first to study the controllability of extraction columns. The transient behaviour of a pulse column was modelled by a stagewise differential equation. A hydrodynamic equation described the flows and predicted flooding. The model was solved for step changes in pulse frequency, solvent flowrate, and solvent inlet concentration. The analysis revealed that a PI controller on aqueous feed rate must be used to control the extract phase concentration. It was noticed that changes in the pulse frequency could cause the most rapid extract response. The control study wasn't complete and lacks the details of a systematic control system design.

Evans (1965) conducted experimental work still on a pulsed column to study its controllability. The aims were to test the applicability of pulse testing for large columns, to select control variables and assign the best control scheme. It was concluded that, for obtaining an efficient column model, pulses with high frequency content are needed to obtain high order models. This conclusion is doubtful since an extraction column can be

modelled fairly well by assuming its behaviour similar to a mixed tank with a first order ODE (Pollock and Johnson 1970).

Allen, Kropholler and Spikins (1966) were among the first who conducted exploratory studies on the digital control of a small-scale spray column. Their work lacks a systematic control design methodology and was incomplete.

Erskine (1968) studied theoretically the control of a centre fed rare earth extraction column having an extract reflux. A simple equilibrium stage model similar to the one used by Beiry (1961) was adopted. The steady state concentration profiles were calculated and used regression analysis to find two predictive control models. The set of equations were simulated using an Analogue simulator DIAN. The results were compared to a conventional PID control scheme and found to be 5 to 10 times faster. This study relied on the steady state model for determining the control equations and this did not give a true evaluation of the process. This scheme also requires an accurate measurement of feed concentration, which is not attained in all situations. As far as the PID controller response is concerned an ON-OFF response of the controller is not suitable for mechanical reasons.

Flett *et al.* (1973) discussed the application of direct digital computer control (DDC) to a projected rare metal separation process. Work was performed on an actual plant in Norway for Nickel-Cobalt separation that uses DDC, with a DEC PDP 8 minicomputer. The plant has been described by Vembe (1977). This control system has been shown to run economically, reliably and to the overall benefit of the process.

McDonald and Wilkinson (1977) studied a multiple mixer column with a non-linear equilibrium stagewise model with backmixing. Feed flow rate $\boldsymbol{R}$ was chosen as a manipulative variable to control the raffinate composition $\boldsymbol{X_{raf}}$. Three control schemes were proposed; conventional feedback, feedforward and their combinations. They compared the predicted and experimental values from a 23-stage, 150 mm diameter Oldshue-Rushton column for a Nitric acid-Water-Tributylphosphate chemical system. Variations in feed flowrate resulted in an improper functioning of the concentration

feedforward controller. They recommended the use of dynamic compensation to adjust the development of erroneous intermediate concentration profiles during the startup using feedforward control scheme. Still the selection of controlled and manipulated variables pairing was not based on a proper analysis of the process.

Gaudernack *et al.* (1979) described a computer based stream analytical system for the control of rare earth separation process, but no decision has been made concerning its application to computer closed loop control.

Yoswathana *et al.* (1985) studied experimentally the application of self-tuning PID controller to a pulsed extraction column operating at the flooding point by controlling the pulse frequency. They used pole assignment to derive the controller parameters. The adequacy of using self-adaptive control was indicated but the use of a simplified single input single output (SISO) process model restricted the generality of the control algorithm.

Al Khani et al. (1986), applied a model reference adaptive control system to a sieved plate pulsed extraction column. The column was maintained near its optimal operating zone, which was close to the flooding point. The control law was based on a low order discrete model with time varying parameter. An APPLE II computer was used for data acquisition and control. The operation of the control scheme was applied into three steps; first the column was operated manually to reach a desired steady state, then computer controlled was started and finally the reference value of control action was modified in a stepwise manner until the desired final operating point was achieved. The applied algorithm produced reasonable overall behaviour, but it wasn't able to handle the nonlinearity of the process caused by the effect of operational parameters and the effect of startup on the dynamics of the process.

Le Lann et al. (1986), studied the generalised predictive control of a pulsed column using a low order linear discrete model with time varying parameters. The controller is designed by minimizing a cost function that depends on a reference trajectory function and on-line parameter estimation using a recursive identification algorithm. It was

concluded that a time varying parameter controller algorithm must be used to obtain good result. The practical application of the adaptive control algorithms involves problems such as: the critical choice of model order and time delay and also the difficulty of parameter estimation. Apart from these problems, these algorithms suffer from lack of stability of the identified model. In an extended study, Najim and Lann (1988) used multilevel system of automata based control algorithm operating in a random environment to adapt a learning control algorithm for the same column. This approach is based on Artificial intelligence. Both studies suffer from the lack of investigating the control system design and were only for SISO system where outlet continuous phase conductivity is controlled by pulse frequency.

2.2.2 Control of Stagewise Contactors:

Control research work for stagewise contactors started later than its continuous counterpart. Hsu (1970) conducted a theoretical dynamic and control study of a multi-stage mixer-settler extractor. Analytical transfer functions from the Laplace equivalents of the model equations was developed using a complex procedure. Different combinations of Manipulated, Load and controlled variables to study the controllability of a two-stage apparatus were considered. The effects of different control approaches such as: steady state feedforward, three mode feedback and feedforward-feedback combination control schemes were compared. It was concluded that feedforward is most beneficial when the feed back system has a measurement lag and when the steady-state feedforward effectiveness is high. It must be emphasized here that this work is the first systematic approach for the control system design, but it is very difficult to apply the same analytical procedure for larger systems. The feedback controllers were designed using Ziegler-Nichols procedure, which is known for its modest performance under varying operating conditions.

Mills et al. (1971) described the difficulties in the control of uranium extraction in a mixer-settler plant. The system was Tributylphosphate-[$UO_2(NO_3)$-2TBP]-Water. A proportional controller was used to control the feed using a pump and a concentration

analyser located in the sensitive region of the profile. The set points for the two end feed flow controllers were set by calculated results obtained from the steady state SIMTEX computer program. It was reported that this control scheme gave good results, corresponding to ±1% of the desired concentration value. This scheme was tested for changes in the solvent and the feed flow rates.

Tsouris and Tavlarides (1991) used a first order-reduced model of the process to control the dispersed phase volume fraction. The Dahlin controller algorithm was used. This study was concerned mainly with the hydrodynamic control of the contactor and no emphasis was given to the mass transfer control, which is of a great importance to the process.

Wichterlova and Rod (1999) studied the control of a 6 stage box-type mixer-settler cascade. They used the pulsed-flow model to represent the behaviour of the extractive separation of the rare earth metals. The control system design was selected based on practical experience, and not on a systematic approach. The final design wasn't tested for stability and robustness under the whole range of operating conditions.

Up to this point it appears that for better modelling of liquid-liquid extraction the following comments has to be put forward:

- In most cases the holdup and flowrates are assumed to be constants, and their dynamics were not considered.
- A reservation has been expressed on the use of Murphree stage efficiency to express displacement from equilibrium state.
- Equilibrium was handled by simplified linear relations, which wasn't adequate for all situations. Efficient equilibrium calculation schemes should be considered.
- The majority of extraction models ignored the end effects of the column. This affected the overall prediction accuracy of the mass transfer characteristics and consequently the concentration transient profiles.
- The effect of backmixing was ignored in most of the cases and should be taken into consideration, with its value estimated throughout the column.
- The ready-made simulation packages ignore most of the details of the contactor and treat the process as an equilibrium separation unit. A proper design for the specific case has to be considered.

- The effect of variations in physical properties of the system during the transient of the column was ignored.

Therefore a work methodology is needed that takes the above-mentioned observations into account for proper build up of the model. This will be covered in the scope of this work.

As far as control is concerned it appears that the control system design of liquid-liquid extraction equipments suffered from serious limitations. Some of these limitations are listed below:

- Effect of operational parameters and startup wasn't considered for the whole range of operation.
- Most control design was developed using conventional single loop procedures ignoring the multivariable nature of the process.
- System identification was based on experience and rules of thumb with no solid numerical analysis techniques that are directly related to control system design. The use of efficient system identification techniques is recommended.
- Most previous control work either considered the process from the hydrodynamic point of view or mass transfer one but not both.
- The use of computers in control was hindered by the technological limitations of computers at that time. The availability of high-speed computers can be used efficiently to overcome previous difficulties such as simulation time and cost.
- There is a demanding need for studying the control system design of the Scheibel contactor by the implementation of model based control algorithms such as IMC and MPC algorithms and explore their efficiency, stability and robustness.
- The control of extractors under physical constraints imposed on the actuating variables as well as output variables has to be investigated and proper control algorithms that can handle this frequently implemented practical type of operation must be considered and investigated.

Hence, the objective of the control system design to be developed in this work is to attempt to eliminate these limitations and develop a more realistic and robust control scheme.

CHAPTER THREE
EXPERIMENTAL INVESTIGATION

The experimental investigation of the Scheibel extraction column is a crucial part of this study. It consisted of two main parts namely; the steady state and the dynamic parts.

The steady state investigation was aimed towards exploring the different factors that affect the extraction operation and determine the most practical ranges of column's operating parameters. The study explored the hydrodynamic and flooding limits of the column under varying operating conditions. Furthermore, drop distribution characteristics and estimation of mass transfer and phase equilibria of the chemical system were considered. Finally, sampling techniques for both phases were examined and adequate sampling probes were constructed and used for the rest of the study.

On the other hand, the dynamic part of the study considered the time variation of the column response due to step changes in operating variables in order to collect the transient data needed for the validation of the rigorous dynamic model.

The apparatus, experimental techniques, and procedures used in this work will be presented in this chapter. The details of the Scheibel Type(I) extraction column and its accessories will be considered first.

3.1 Description of Experimental Apparatus:

A schematic diagram of the experimental apparatus is shown in Figure(3.l) and also in Figure(A.1) in the appendix (A). It is composed basically of a Scheibel extraction column of type I. In this type, the column is divided into a series of wire mesh packed calming sections followed by mixing sections. The column is made of a QVF borosilicate pipe of 8.7cm diameter, and 185cm length. It is divided into nine compartments each of 14.5cm height with a Dual Coalescer wire gauze packings of 12cm height inserted in each compartment making a stage of a mixing zone and coalescence zone. The mixing zone of each stage was supplied with a hole of 15mm in diameter on the column's wall to support the single phase sampling head probe and needle.

The wire mesh packing mentioned above is a (S.S.-Polypropylene) of type 9201SL with a filament diameter (1×0.12mm S.S. and 1×0.133 mm PPL) with 6×7 stitches/inch and 97% voidage. It is used for two purposes first for isolating the agitator flow patterns between adjacent mixing zones to prevent loss of efficiency due to backmixing, and second it provides baffling effect to remove the rotational motion due to agitation.

The feed streams are introduced counter-currently. The aqueous inlet stream is introduced at the top of the column 1.5cm above the ninth stage whereas the solvent inlet stream is introduced at the bottom of the column through a stainless steel distributor of 4.5cm diameter and 2mm hole diameter. The process streams tubes are made of either stainless steel or glass pipes of 1.25 cm diameter so as to prevent any kind of corrosion or material deterioration to occur due to the presence of solvents. The feed tanks are constructed of stainless steel plates (2mm) thick for the same reason. They were installed on wall-mounted support 2.5 meters above ground to give enough head for the feed pumps. Two centrifugal feed pumps (Loher Gmbh, Type: eA63b-2) are installed to give steady flow for both feed steams and to eliminate any head deterioration due to the constant decrease of the liquid levels in the two feed tanks during the experimental run. The pumping suction head for both pumps was 2m.

3.2 Chemical system:

The chemical system *Water-Acetone-Toluene* was chosen for the experimental study. This system has the following characteristics;

1. This system was chosen as a test system by the European Federation of Chemical Engineering Working Party on Distillation and Extraction and Absorption. This will facilitate good comparison of our results with others, available from their investigations.
2. This system has a high interfacial tension, which means that the dispersed drops are large and clear to distinguish, and relevant for any size or drop distribution measurements.
3. Availability, low cost, low toxicity and ease of solvent recovery.

4. The solute concentration measurements can be performed using gas chromatography (GC), ultra violet (UV), or refractive index (RI) analysis methods with high degree of accuracy.

Table (3.1) presents the properties of the three liquids used which can be monitored constantly by GC analysis as well as Refractometry.

Table (3.1) Physical Properties of the *Water-Acetone-Toluene* System.

	Toluene	**Water**	**Acetone**
Density (kg/m^3)	$0.866\pm0.02\times10^3$	$0.997\pm0.002\times10^3$	$0.792\pm0.02\times10^3$
Viscosity (Ns/m^2)	$0.55\pm0.01\times10^{-3}$	$1.019\pm0.01\times10^{-3}$	$0.32\pm0.01\times10^{-3}$
Boiling Range(°C)	110.0-111.0	100	56.0-56.5
RI @ 20°C	1.4940-1.4970	1.3329-1.3330	1.3589-1.3591
Impurities	0.03% Water	Conductivity 0.67 µS/cm	0.05% max Water
	0.003% Sulfer		0.002% max Aldehydes
	10 max (colour APHA)		0.05 max Isopropyl Alcohol
			.05% max Methanol

3.3 Steady State Experimental Work:

The first phase of the experimental work was at steady state. This is a primary step that aims towards better understanding of modelling. Thus, the main objectives for conducting this type of study are:

- Determination of the practical ranges of column operational parameters including rotor speed and flowrates.
- Understanding the hydrodynamics and flooding characteristics of the column.
- Characterization of the drop distribution and estimation of mass transfer effects.
- Study the Phase equilibria of the chemical system (Water-Acetone-Toluene) during the operation of the extractor.

The experiments were conducted at ambient temperature with a carefully controlled surroundings temperature. This was achieved by passing all input streams through a constant temperature water bath and running the experiments in a carefully controlled ambient air temperature.

3.3.1 Column Cleaning Procedure:

The column used has to be clean and free of contamination. The presence of surface-active impurities reduces the rate of mass-transfer per unit area. It also increases the interfacial tension with consequent effects on coalescence, dispersion and the column hydrodynamics. Special precautions have been taken to insure the operation of the column under consistent and surfactant free conditions. An anti-surfactant detergent solution (DRY-DECON from Decon Laboratories Limited) was prepared to clean the equipment before each experimental run.

The Decon solution was prepared by dissolving the powder with distilled water to a concentration of 2% v/v. The column was filled with the solution and left several hours and some time until next day, then the column was emptied and rinsed a minimum of four times with distilled water. The joints, pipes, sampling ports, valves and pumps were washed to insure that no traces of detergent still exist.

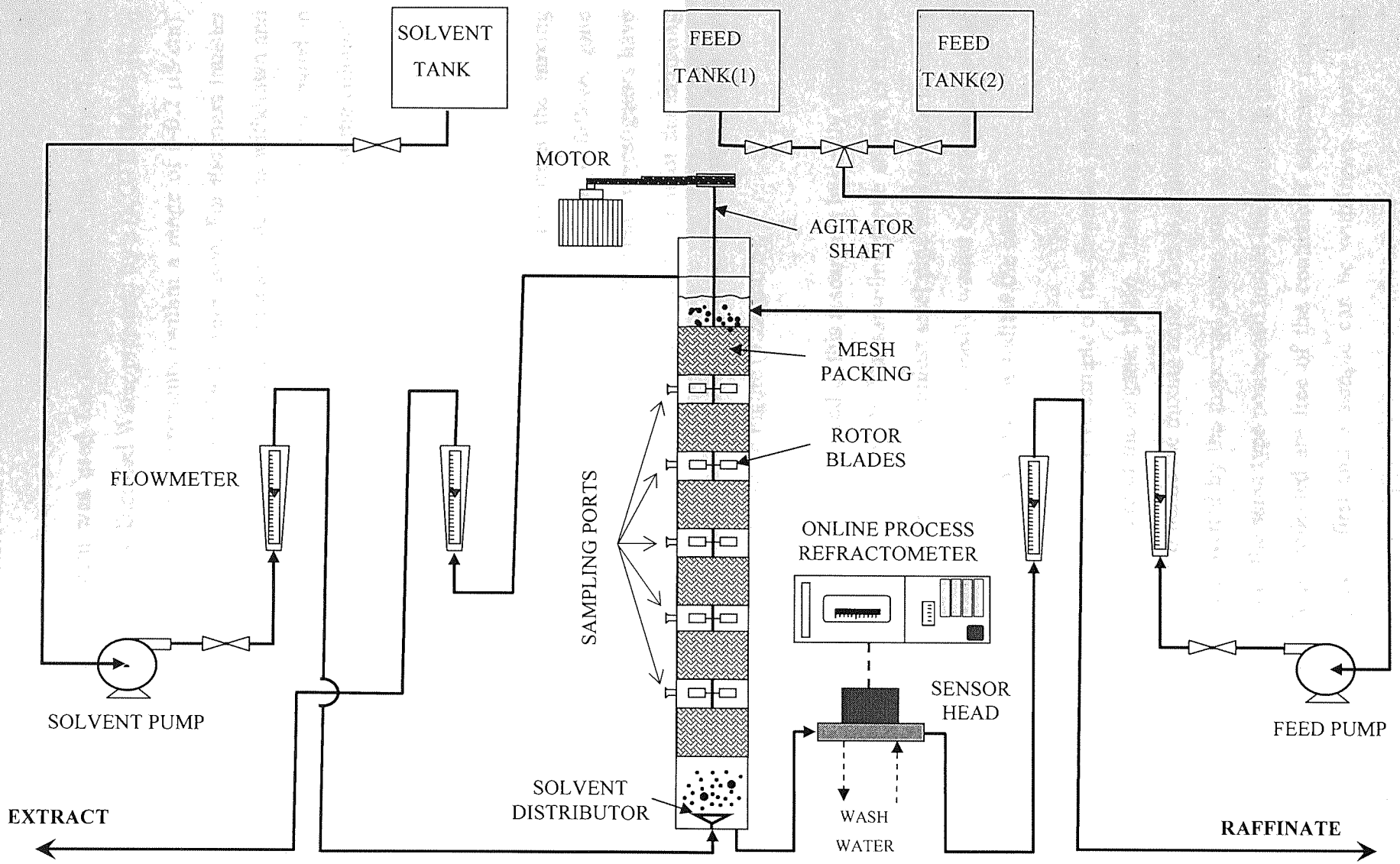

Figure (3.1) Schematic diagram of the experimental apparatus.

3.3.2 Preparation of Feed Solutions:

Water-Acetone-Toluene system was used for the purpose of this study. Toluene purity was monitored, by GC analysis. Distilled Water prepared by a (KOTERMAN 1035) distiller, was monitored by conductivity measurements (within a range of 0-0.2 μS/cm). For flooding experiments, pure water and toluene feeds were used. For the mass transfer runs, known amounts of Acetone and Water were mixed and a sample was withdrawn and fed to GC to determine the exact solution composition. All solutions were prepared in clean Pyrex glassware, and then a pump was used to transfer them to one of the column's three tanks at the top of the apparatus.

3.3.3 Sampling Technique:

The sampling of a pure uncontaminated single phase sample from the mixing chamber of the Scheibel column is very difficult. The movement of drops follows quite closely a torroidal flow pattern created by the turbine impellers. Many investigators have tried different types of samplers. Bonnet (1982) presented a good review of the sampling techniques employed for agitated contactors. The sampling assemblies employed in this work for both phases are shown schematically in Figure (3.2a and b).

The continuous phase sampling technique used in this research is basically similar to that developed by Bonnet (1982) and Staffin (1959). The sampling probe shown in figure (3.2a) behaves as a drop filter. It is constructed of stainless steel pipe with several layers of stainless steel micromesh positioned inside it. It can be easily wetted by the aqueous phase which will be trapped inside it. A syringe was used to withdraw the sample.

On the other hand, obtaining a representative sample of the dispersed phase is much more difficult due to the discrete structure of the organic phase. Therefore a coalescence nucleus of the bubbles must be formed inside the mixing zone. This is achieved by using a sampling probe made of a material wetted by the dispersed phase such as P.T.F.E., with multi-layers of micro mesh cloth of the same type positioned inside the sampling probe as shown in figure (3.2b). The drops collected are free of the continuous aqueous phase. However, the line should be purged first and a sample can be withdrawn slowly and carefully by syringe.

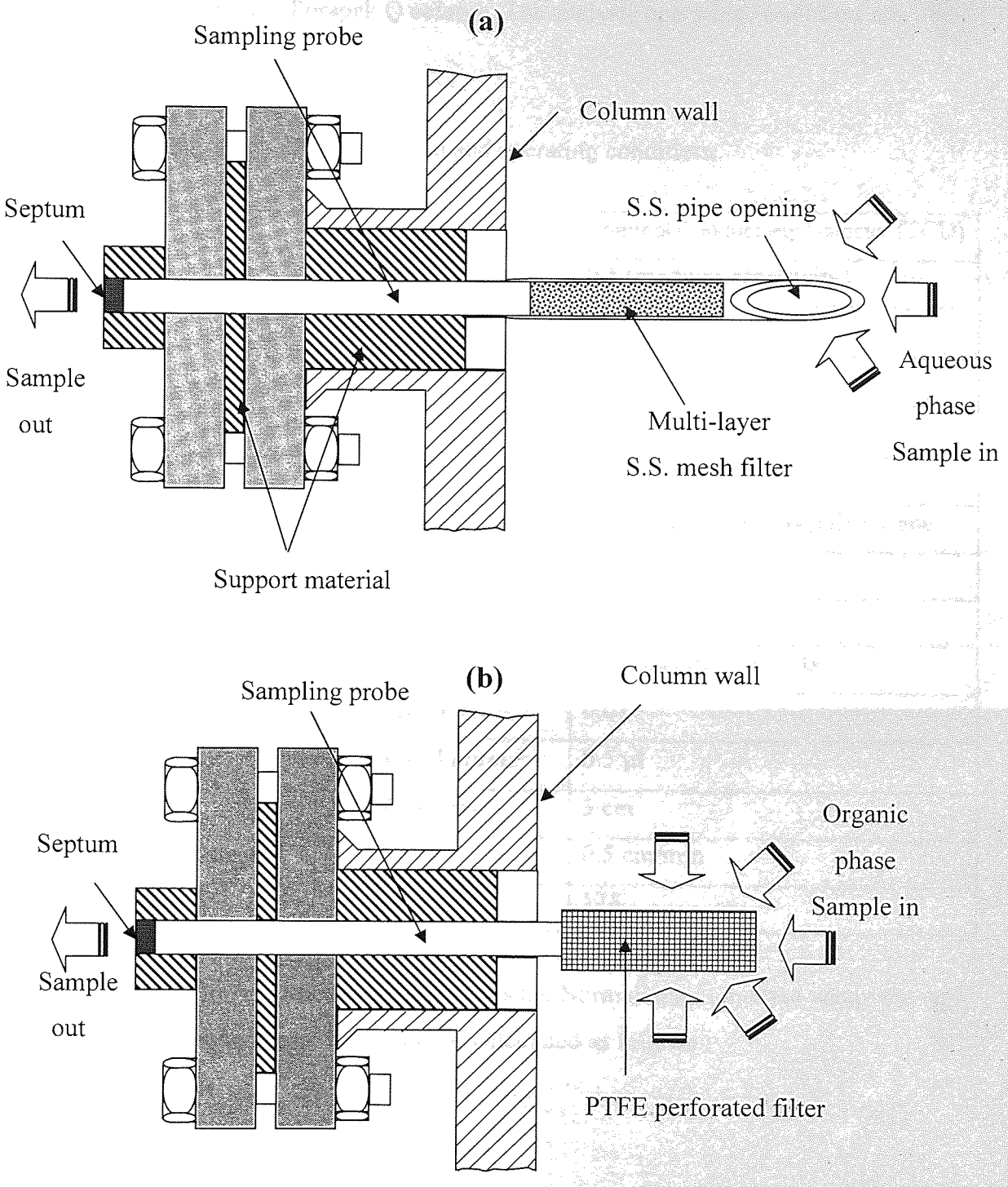

Figure (3.2) schematic diagram of the sampling assembly for:

(a) Aqueous phase.
(b) Organic phase.

Samples were analysed using Gas Chromatography (VARIAN VISTA 6000) for the acetone content utilizing Porapak Q column. The analysis operating conditions are given in table (3.2).

Table (3.2) GC specification and operating conditions.

Detector	***Type:***	Thermal Conductivity Detector (TCD)
	Range:	0.5 (medium sensitivity)
	Temperature:	275 °C
	Filament Temp.:	300 °C
	Injector Temp.:	250 °C
Column	***Type:***	Porapak Q
	Stationary Phase:	Cross-linked porous polystyrene
Carrier Gas	***Type:***	He
	Flow rate:	25 ml/min
Integrator	***Min. peak rejection:***	1000 electrical counts
	Noise filter set:	0.01
Syringe	***Injection Volume:***	0.5 µl
	Needle length:	5 cm
Recorder Chart Speed		0.5 cm/min
Ionisation Amplifier Att.		128

The method used for the wt. fraction calculation is the Normalization method where the wt. fraction for any component k in the mixture is calculated as follows :

$$wt\ frac. = \frac{RF_k\ A_k}{\sum RF_i\ A_i} \qquad (3.1)$$

where:

A_k :is the area percentage of the ***k***th component in the sample.

RF_k :is the response factor of the ***k***th component in the sample.

Values of RF for *Acetone, Water,* and *Toluene* are given as 0.68, 0.55, and 0.794 respectively.

3.3.4 Experimental Procedure:

In general the procedure for conducting the experiments was done following one of two methods depending on whether mass transfer is involved or not. The first was with no mass transfer to investigate the hydrodynamics and flooding characteristics of the column, and the second was the mass transfer experiments. Description of the two procedures is given after:

3.3.4.1 Flooding Experiments (no mass transfer):

Flooding is a very important phenomena that may occur during the operation of liquid-liquid extraction columns. It is characterised by the appearance of a second liquid interface in the column either at the end of the column opposite to that at which it is being controlled, or more immediately through a phase inversion in one of the stages that will ultimately result in a second interface at the opposite end of the column. Flooding is undesirable. It is caused as a result of increased agitator speed at a certain throughput and also if the velocities of the two phases were increased up to a specific maxima.
Therefore, a series of exploratory experiments were performed to investigate the flooding characteristics of the extractor and determine an operational range of the equipment far enough from the critical flooding conditions. The procedure given below is for a single flooding experiment:

1. The column was filled with the continuous aqueous phase up to the interface level about 7 cm below the extract outlet stream.
2. The dispersed organic phase is introduced at a low flow rate without continuous phase flow or rotation speed. When the dispersed organic phase reaches the top and overflows out through the extract outlet stream, the rotor is then started and set to the desired value.
3. The continuous phase flow is then started and set for a certain value, and the interface is continuously monitored by controlling its outlet flow rate.
4. The dispersed flow rate is then increased gradually in a stepwise manner with interval duration of 10 min for the system to reach steady state after each step.
5. The flooding is monitored where it is characterized by the formation of a second interface under the packing of any stage. When this occurs, the

dispersed phase flow rate is recorded and all inlets and outlets are closed. The column is emptied. The experiment is repeated for the reproducibility of results.

6. Steps 1-3 were repeated at constant phase flow ratio and the rotor speed was increased gradually. The flooding is monitored after each step increase. Thus, two sets of results were obtained at different phase ratios and agitator speed.

3.3.4.2 Extraction Experiments (with mass transfer):

For steady state extraction experiments, the following procedure was followed to collect a steady state sample at each stage:

1. The column was cleaned according to the procedure previously described and it was filled slowly with the continuous aqueous phase from the bottom of the column, in order to prevent air from being trapped inside the packing zones.
2. The inlet aqueous phase valve was closed and the agitator was started and set to the desired value. The organic phase feed valve was then opened and its flow rate was set also to the desired speed.
3. The continuous phase feed valve was then opened and set to the required condition. The interface level was fixed by manipulating the continuous exit stream valve and the levelling arrangement attached to it.
4. The column was kept in operation under these conditions by monitoring flow rates and interface level until constant outlet concentration were obtained. The experiment was run for 45 min, chosen based on previous runs to insure that steady state conditions have been attained.
5. The single-phase samples were collected from each mixing compartment by a stainless steel syringe withdrawing slowly and carefully a 2cc clear sample. Each sample collected was injected into a tightly sealed sampling vial and stored in the refrigerator when necessary for later analysis. Samples of the outlet streams were also collected.
6. The agitator was then stopped and all inlet and exit valves are closed. The two phases are left to settle for the determination of the dispersed phase hold-up, using the displacement technique that will be presented in the next section.

3.3.5 Hydrodynamic Experiments:

Hydrodynamics behaviour of the extractor is expressed in terms of dispersed phase holdup.

The holdup is measured to facilitate later statistical correlation with the operational parameters. Two types of hold-up measurements were tested; the sampling technique and the displacement technique.

In the sampling technique a large sample containing both phases is withdrawn from the middle stage of the column through a sampling valve connected directly to the wall of the column.

The displacement method consists of shutting off simultaneously all input and output streams, and letting the column contents to settle for a sufficiently enough time to form two separate layers of the immiscible phases, then the dispersed phase layer is displaced and measured by introducing an equivalent volume of continuous phase to the column. This volume is called the normal or freely falling hold-up. To measure the permanent hold-up, which is trapped within the packing interstices, the column is drained and washed several times with the continuous phase to collect all trapped drops. The total hold-up or the average column hold-up is defined as the sum of the free falling and the permanent hold-ups.

Both techniques of hold-up measurements were carried out. Results showed that the sampling method did not give reproducible results, and large deviations were noticed in the measured sample volume. This may be attributed to the large errors associated with the withdrawal of large samples.

On the other hand, using the displacement technique, the phase volume within the column closely represents the true average hold-up of the contactor at certain operating conditions. Therefore the displacement method was adopted.

3.3.6 Interfacial surface tension measurements:

In addition to the previously mentioned steady state experiments, other lab measurements of the interfacial surface tension were conducted. The aim of these experiments was to generate experimental values of this property at different acetone concentrations. These data will be used for correlating the interfacial surface tension as a

function of Acetone concentration. The correlations are used later in the modelling study in chapter(4). The procedure for the experiments is given in appendix(A).

3.4 Dynamic Step Testing:

This is the second part of the experimental program. The purpose of this part is to study the transient dynamics of the column under different operating conditions and to obtain profiles that will be used later for modelling the column under these conditions.

3.4.1 Procedure for Dynamic Step Testing:

The same procedure of column preparation for the steady state experiments was followed in the dynamic step testing experiments. The 10% step changes were performed in both positive and negative directions. The general experimental procedure was as follows:

1- Two feed concentrations were prepared and pumped to the feed tanks (1 and 2) at the upper part of the apparatus as shown in figure (3.1).
2- The column was then started at certain operating conditions until steady state conditions were reached. A duration of 30 min was enough to attain the steady state conditions. The concentration logging was started and monitored.
3- The rotor speed was altered by changing the calibrated potentiometer setting located on the motor and RPM was measured with an optical tachometer and the experiment was repeated as before.
4- For the phase ratio step testing experiments, the flow of the solvent (Toluene) feed stream was changed to achieve a desired phase ratio.
5- Now, for the concentration step testing experiments, with aid of the three way valve joining the two feed tanks as shown in figure (3.1) the feed tank(2) was introduced to the column at constant flowrate. Of course tank(1) will be disconnected. The experiment was repeated as before.
6- In each experiment the raffinate was analysed for its refractive index using the process refractometer. The refractometer output signal was fed to PC after A/D conversion. These signals were calibrated and the concentration profile was recorded and plotted on screen.

3.4.2 Online concentration measurement:

Chromatography is a very accurate concentration measurement technique, however, due to its high sample residence time, and high maintenance overhead it is not preferred for the on-line measurement of concentration. It can be used where the process is slow enough to justify its use such as steady-state measurement.

On the other hand refractometry is an alternative concentration measurement technique. It can be used in a variety of applications, and has a very fast response. Very good accuracy is achieved using this method for the chemical system used.

Details of the theory of online refractometry and the specifications of the equipment used in this study are given in appendix (A.1).

Some preliminary experiments were conducted to calibrate the refractometer with the used chemical system. The calibration range was set to vary from 0 to 0.1 wt fraction Acetone which is within the expected range of samples to be collected in this work.

The raffinate outlet stream was connected to the measuring cell of the refractometer. The refractive index signal generated by the equipment is sent to the PC via a data acquisition card. There, it is conditioned, calibrated and stored in the hard disk. A plot is generated for the transient change of Acetone wt fraction throughout the experiment.

3.4.3 Data acquisition and logging:

The concentration measurements carried out by the online refractometer were in the form of analogue signals. These signals were conditioned and transformed into digital form by means of a data acquisition board fitted on an IBM compatible PC. The specifications of this board are given in Appendix (A.3).

The collected data was displayed in the form of a continuous graph with respect to time and finally saved in computer text files for later analysis.

3.4.4 Variables and operational ranges investigated:

The variables that affect the overall performance of the Scheibel column are the *rotor speed* and the *phase flowratio* [Bonnet et al. 1985]. These two variables were investigated and their ranges were chosen in such a way to achieve good extraction of

the solute as well as to cover broad range of operation far from the flooding limits of the column tested before. To gain a good picture of the column practical operational ranges, the dynamic limits (characterized as flooding) at different phase flow ratios were investigated. The flooding points were determined using the procedure described above. Table(3.3) gives the rotor speed at start of flooding at typical phase flow ratios.

Table(3.3) Column flooding conditions investigated.

Phase flow ratio	Rotor speed at start of Flooding (s^{-1})
1:1	9.8
1.5:1	9.4
2:1	8.9

Based on the flooding experiments findings, nine operational conditions were selected covering a broad range of column rotor speed and phase flow ratio. The following are the selected operational conditions adopted for this work:

Rotor speed (N): 5, 6.7 and 8.33 s^{-1}

Phase flow ratio (F): 1:1, 1.5:1 and 2:1

These ranges were chosen in such a way to achieve good extraction of the solute. Also these operating conditions cover broad range of operation including those far from the flooding limits of the column.

3.5 Experimental results and error analysis:

The holdup, surface tension, and concentration were measured and the results are given below. The holdup measured for the selected operating conditions is given in table(3.4). The results show the direct proportionality of the fractional holdup with both rotor speed and phase ratio for the studied operating conditions. The fractional holdup increases with the increase of phase flow ratio and rotor speed.

Table(3.4) Experimental fractional holdup measurements.

Run No.	Rotor Speed (RPM)	Rotor Speed (s^{-1})	Phase Flow Ratio	Fractional Holdup
1	300	5	1.0	0.069
2	300	5	1.5	0.081
3	300	5	2.0	0.097
4	400	6.667	1.0	0.099
5	400	6.667	1.5	0.144
6	400	6.667	2.0	0.148
7	500	8.333	1.0	0.300
8	500	8.333	1.5	0.325
9	500	8.333	2.0	0.367

The interfacial surface tension data were collected for different continuous phase Acetone concentrations. Results are shown in Table(3.5). The interfacial surface tension decreases with the increase of Acetone concentration.

Table(3.5) Measured interfacial surface tension at different Acetone concentrations in aqueous phase.

x (wt. Fraction)	σ (dyn/cm)
0.0100	32.450
0.0152	32.012
0.0185	31.530
0.0245	31.370
0.0315	30.710
0.0409	30.083
0.0503	29.445
0.0598	28.773
0.0678	28.317
0.0811	27.599

For the steady state concentration profiles experiments, the samples for each phase were collected at the end of each experiment using the sampling techniques described previously. The samples were analysed and plotted vs. stage number. The profiles are shown in the next chapter figures (4-7 to 4-9) in conjunction with profiles from the model predictions.

The dynamic tests data were also collected online and stored using the data logging system described previously. The profiles for each test are given in the next chapter

figures (4-10 to 4-14). The profiles were compared to those generated from the developed model.

The experimental measurements obtained were analysed to calculate the probable size of their errors. There are many types of experimental errors, which affect the measured quantities, and there are many ways to classify them. The most general classification is *determinate (systematic)* , *indeterminate (random)* and *illegitimate* errors.

(1) *Indeterminate (random) errors* are random fluctuations in the experimental measurements. These errors cannot be corrected for. It is this type of errors that our intuition suggests that repeated measurements allow us to "average" them out.

(2) *Determinate (systematic) errors* are frequently constant and related to the measuring device. These errors can normally be corrected for if the systematic effect is identified.

(3) *Illegitimate errors*: this type of error accounts for inexplicable "events", which result in a measurement whose value deviates significantly from what is expected. (e.g. an error reading a number), [Young, 1962].

A measurement with relatively small indeterminate error is said to have high precision. A measurement with relatively small determinate error is said to have high accuracy. A measurement, which has both high precision and high accuracy, is sometimes called highly reliable.

Every possible effort must be done to avoid illegitimate errors by conducting careful and exact experimental procedures. The effect of indeterminate errors can be reduced by averaging the values of repeated measurements for each set of readings.

On the other hand the determinate errors can be more serious than indeterminate errors for the following reasons; First of all, they can not be identified by looking at the experimental data. Second, their effects can not be reduced by averaging repeated measurements and lastly, their size and sign for each measurement in a set of repeated measurements are fixed, so there is no opportunity for positive and negative errors to offset each other [Young, 1962].

The error bounds for the operational variables, concentration measurements and other measured quantities conducted are listed in Table(3.6). The absolute errors were calculated for each variable by conducting repeated measurements of a known quantity and recording

the bounds of the measurements. These errors will be used later in the correlations error analysis.

Table (3.6) Error bounds in experimental measured quantities.

Measured Variable	Absolute Error	Error bounds
Rotor speed (s^{-1})	0.0833	$N \pm 0.0833$
Flow rate (cc/min)	2.0	S or $R \pm 2.0$
Fractional holdup	0.013	$\varepsilon \pm 0.013$
Concentration (wt. fraction)	0.0001	x or y ± 0.0001
Refractive Index	0.0001	$R.I.$ ± 0.0001

The percent relative errors $(\frac{\text{Absolute Error}}{\text{True Value}} \times 100)$ for the variables given in Table(3.6) are 1.2%, 0.8%, 4.3%, 0.5% and 0.003% respectively. The only value of percent relative error which is greater than 1.5% is the fractional holdup value. Its error bounds are relatively high with a percent relative error of 4.3%. This high error was due to the difficulty of obtaining repeatable experimental values for this variable. Nevertheless, the table indicates that the error bounds are within acceptable limits for the modelling study, and further theoretical study based on these experimental values is possible.

In the next chapter the modelling of the contactor will be carried out and the experimental data will be correlated as functions of rotor speed, phase flow ratio, and Acetone concentration in the aqueous phase. The calculated values from the correlations will be analysed for reliability.

CHAPTER FOUR
MODELLING OF SCHEIBEL LIQUID-LIQUID EXTRACTOR

4.1 Introduction:

For production purposes, mass transfer contactors are usually designed to operate under steady state conditions for long periods of time. Practically, the operation of liquid-liquid contactors cannot be dealt with completely until the transient performance was studied for the whole range of operation. The unsteady state modelling is concerned with the mathematical representation of the behaviour of the equipment under the full span of its operation with respect to time. This is useful for the following situations:

- The dynamic response of the extractor to excitations in feed rates, compositions, and other operational parameters is essential to the development of reliable control algorithms.
- Estimation of operational parameters under unsteady state conditions. This involves hydrodynamic, mass transfer and backmixing coefficients.
- Situations like start-up, load disturbances and shut down necessitate the presence of accurate unsteady state models for testing and analysis.

In this chapter, the dynamic modelling of the Scheibel extractor is explained with the method of solution employed and at the end the accuracy and validation of the model is considered.

At the beginning, a brief look at the axial dispersion phenomenon that resembles the real operation of extractors and the attempts employed to model it is given in the following sections.

4.2 Axial dispersion:

This phenomenon is encountered in the operation of liquid-liquid extraction equipment especially at conditions near flooding region where the optimum efficiency of separation is attained. The plug flow nature of the two phases is the ideal case, and occurs only for discrete-stage mixer-settlers and perforated plate columns where the phase separation is virtually complete between stages. Scheibel and other types of contactors suffer adversely in performance from the non-uniform flows in both phases. The contributing factors to these flow non-idealities, which are referred to as axial dispersion are given below: [Pratt and Stevens 1992]:

1. Circular flow of continuous phase in the direction of drop motion, due to the dissipation of the dispersed phase potential energy.
2. Circulation of continuous and entrained dispersed phase.
3. The formation of wakes attached to the rear of droplets in motion.
4. The frictional drag of packing causes a distribution of residence time and this in turn will cause non-uniform velocity profiles for both phases to develop.
5. Channelling and the resulting irregular distribution of phases.

Two models are used to describe axial dispersion; the diffusion model for continuous differential contactors, and the backflow model for stage wise contactors. These two models represent limiting cases, and the best choice of the best model to adopt varies extremely depending on its structure and operational parameters [Burns and Hanson 1964].

The diffusion model approach was used mainly to describe the behaviour of truly differential columns such as RDC, spray and pulsed plate columns. In this approach, extraction phenomena are represented by distributed parameter models in the form of a set of partial differential equations (PDEs) to describe the dispersion.

The other approach is to represent the behaviour of the contactor by a non-equilibrium stagewise model. This is more convenient for mixer-settlers and columns with stagewise type of operation like the Scheibel column.

In this study we will be concerned with the backflow model, which is a form of the stagewise model.

4.3 The Backflow model:

As described in Chapter (2), the backflow model was one of the first attempts to describe axial dispersion. This model assumes well-mixed non-ideal stages between which backflow occurs. It has proven to be a good approximation for modelling rotary agitated, pulse plate, and reciprocating plate contactors [Pratt and Stevens, 1992].

This model assumes a series of interconnected stages where backflow occurs by entrainment of the phases between stages. The backflow is expressed in terms of backmixing ratios α and β between the backmixed and the net forward flow.

4.4 The Mixing Stage model:

Kramers and Alberda (1953) developed this model to describe axial mixing of a single-phase, non-absorbing medium. Gray (1963) later extended this model to two-phase absorption systems. The model was used to derive the theoretical frequency response of the gas phase composition. Later, Doninger (1965) used the same model to calculate the frequency response of the raffinate phase for and extraction process. In their study, Gray, and Doninger did not solve the model equations in the time domain. Following that, Biery (1961) used the same model to study the transient startup behaviour of a pulsed column without using frequency response information. In all these formulations, the following assumptions were used:

1- Ideal mixing occurs in each stage, i.e. the outlet concentration of a phase is the same as the bulk concentration in the cell.
2- Only solute transfer occurs, and hence the solute-free phase flows are constant.
3- Phase holdups are equal in all stages and are independent of time.
4- Interphase mass transfer rate at any stage (n) is expressed by an equation of the form:

$$Q_{y_n} = K_{y_i} a V (y_i^{\star} - y_i) \qquad (4.1)$$

where: $K_{y_i} a$ is an overall transfer coefficient which is independent of time and concentration.

5- Linear equilibrium relation expressed as:

$$y_i^{*} = m x_i^{\star} \qquad (4.2)$$

The inter-phase mass transfer at any stage (n) was written for the two phases as follows:

$$R(x_{i-1} - x_i) - K_{y_i} a.V(y_i^* - y_i) = W_R \frac{dx_i}{dt} \quad (4.3)$$

$$E(y_{i+1} - y_i) + K_{y_i} a.V(y_i^* - y_i) = W_E \frac{dy_i}{dt} \quad (4.4)$$

In order to approximate the damping and delaying action of the phase separation volumes (single phase) located between the interfaces and the contactor ends, a form of delay must be added to the theoretical model. This was attained by considering the volume between the interface and sampling tube as comprising a perfectly mixed, single-phase stage without mass transfer. This arrangement is shown in figure(4.1).

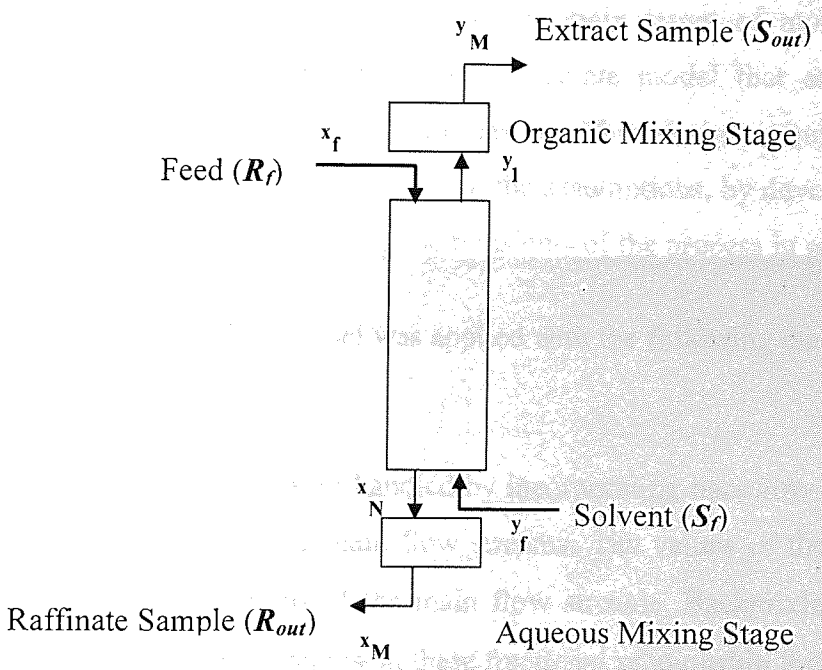

Figure (4.1) Schematic diagram of the mixing stage model

The aqueous and organic mixing stages are modelled by equations similar to (4.3 and 4.4) but without the mass transfer rate term. This is given in the following two equations:

$$R(x_N - x_M) = W_{MA} \frac{dx_M}{dt} \quad (4.5)$$

$$S(y_1 - y_M) = W_{MO} \frac{dy_M}{dt} \quad (4.6)$$

Pollock and Johnson (1974) used this model to study the frequency, and time domain modelling of a mechanically agitated extractor. The equations were interpreted in terms of perturbation variables about an initial steady state, after that the equations were solved using Laplace transformation. The transfer function of the process relating the input and output transformed aqueous phase concentrations was derived using the developed equation.

4.5 The mixing stage with backmixing model:

In the previous modelling attempts, a lot of serious assumptions were made to simplify the analytical solution of the model. This was at the cost of quality of the model, and its practicality. In this work, the main target of modelling task was directed towards developing a reasonably accurate model that can be used with confidence for further control system design. This design requirement made it necessary to rethink in eliminating some of the assumptions, by developing the model further to include variables affecting the transients of the process in practice.

The mixing stage backflow model was applied with the following main features and assumptions:

1- Flow non-idealities were handled by incorporating backflow streams opposite to the direction of the main flow streams. The values of these streams were expressed as fractions of the main flow streams. Backmixing coefficients α and β, were used to represent these fractional relationship for the two phases.

2- Physically, each stage comprises of two parts, one mixing zone and another settling zone. Mass transfer mainly occurs in the mixing zones, which are considered perfectly mixed. In the settling zones, coalescence of the dispersed phase, and phase separation occurs.

3- Mass transfer coefficient is calculated for each stage as a function of physical properties, operational parameters and stage design specifications. Oscillating drop behaviour was assumed to model the dispersed phase due to the high degree of turbulence in the mixing zones. The Rose-Kintner (1966) correlation

was used for the dispersed phase mass transfer coefficient, and the Garner and Tayeban (1960) correlation for the continuous phase.

4- To account for the mass transfer occurring in the settling zones, a weighting factor f was introduced in the calculation of mass transfer rate term to approximate the ratio of mass transfer as $Q_{x_a} = f \cdot Q_{x_m}$ where a and m represent settling and mixing zones respectively. These weighting factors were calculated at each stage by reconciling model predictions with the experimental data using non-linear optimisation techniques.

5- Equilibrium between phases at each stage was expressed as a distribution coefficient $m_i = y_i^* / x_i^*$. Its value was calculated for each stage from experimental data as a function of solute concentration in the raffinate phase.

6- Hydrodynamics within stages was expressed as a fractional volume holdup ε_i and calculated for each stage. The initial holdup profiles were predicted experimentally as a function of agitator speed and the two phases flowrates.

7- Physical properties of the two phases are variable throughout the column and calculated for each stage as functions of concentration, column geometry and operational parameters.

4.6 Model Equations:

A schematic drawing of the modelled contactor is given in Figure (4.2). The stages were modelled utilising the previous assumptions to predict flowrates and concentrations of both phases. The details of the inside streams for the contactor are shown in Figure (4.3). In this figure, the stages were numbered starting at the bottom of the contactor towards the top, with stages number 0 and $N+1$ denoting the bottom and top mixing stages (without mass transfer) respectively.

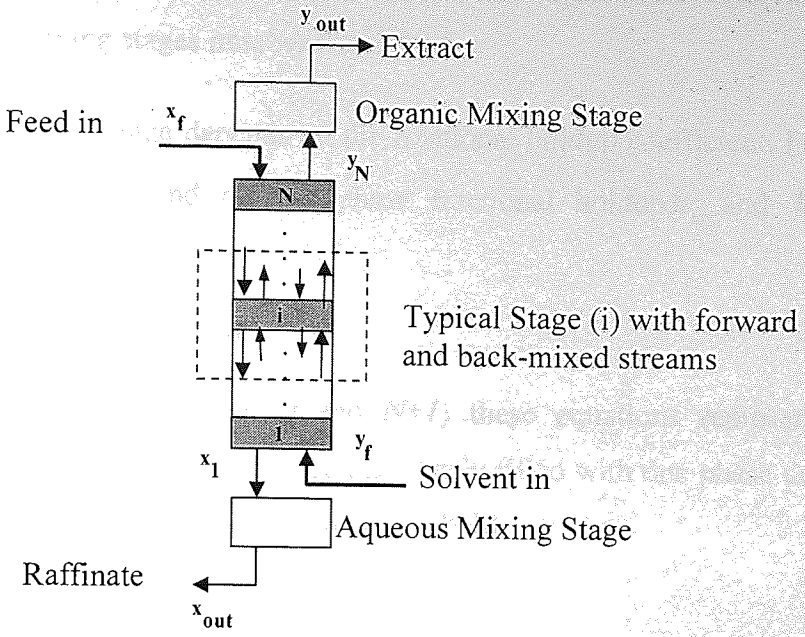

Figure (4.2) Schematic diagram of the modified mixing stage model with backmixing.

The model equations are composed of the following types of equations:

- Solute Free Material Balance for calculating stage flowrates.
- Component Material Balance for calculating stage concentrations.
- Hydrodynamic equations for calculating stage holdup.
- Equilibrium equations.

These equations will be explained in the following subsections.

4.6.1 Equations at each stage:

At each column stage, there are eight equations that model its hydrodynamics and mass transfer characteristics. These equations are categorized as follows:

(a) Stage holdup of the raffinate phase (cm^3).

(b) Stage holdup of the extract phase (cm^3).

(c) Rate of change of raffinate phase Acetone concentration (wt. frac./ min).

(d) Rate of change of extract phase Acetone concentration (wt. frac./ min).

(e) Extract phase flowrate (cm^3/min).

(f) Raffinate phase flowrate (cm^3/min).

(g) Mass Transfer rate equation.

(h) Equilibrium stage relation.

The following is a description of the details of model equations at each stage including the mixing stages number ***0*** and ***N+1***.

The holdup at each stage depends on the fractional holdup coefficient. For any stage $i:1\cdot\cdot N$, the aqueous and organic phase fractional holdup h_{x_i} and h_{y_i} can be expressed as:

$$h_{x_i} = V(1-\varepsilon_i)\ ,\ h_{y_i} = V\varepsilon_i \tag{4.7a}$$

For the mixing stages (stages ***0*** and ***N+1***) these equations represent boundary conditions. Each mixing stage will be completely filled with one phase depending on its location and hence the following equations hold:

$$h_{x_0} = V\ ,\quad h_{y_0} = 0 \tag{4.7b}$$

$$h_{x_{N+1}} = 0\ ,\ h_{y_{N+1}} = V \tag{4.7c}$$

The Solvent and the Feed can be assumed to be practically immiscible, hence solute free material balance can be performed over each stage to calculate the flowrates at each stage. After rearranging variables, the flowrates of the two phases at any stage $i:2\cdot\cdot N-1$ are expressed as:

$$S_i = \left[\beta S_{i+1}(1-y_{i+1}) + (1+\beta)S_{i-1}(1-y_{i-1}) + h_{y_i}\frac{dy_i}{dt}\right] \Big/ \left[(1+2\beta)(1-y_i)\right] \tag{4.8a}$$

$$R_i = \left[(1+\alpha)R_{i+1}(1-x_{i+1}) + \alpha R_{i-1}(1-x_{i-1}) + h_{x_i}\frac{dx_i}{dt}\right] \Big/ \left[(1+2\alpha)(1-x_i)\right] \tag{4.8b}$$

and for stages 1 and N the equations will be expressed as:

$$S_1 = \left[\beta S_2(1-y_2) + S_f(1-y_f) + h_{y_1}\frac{dy_1}{dt}\right] \Big/ \left[(1+\beta)(1-y_1)\right] \tag{4.8c}$$

$$R_1 = \left[(1+\alpha)(1-x_2)R_2 + h_{x_1}\frac{dx_1}{dt}\right] \Big/ \left[(1+\alpha)(1-x_1)\right] \tag{4.8d}$$

$$S_N = \left[(1+\beta)S_{N-1}(1-y_{N-1}) + h_{y_N}\frac{dy_N}{dt}\right] \Big/ \left[(1+\beta)(1-y_N)\right] \tag{4.8e}$$

$$R_N = \left[R_f(1-x_f) + \alpha R_{N-1}(1-x_{N-1}) + h_{x_N}\frac{dx_N}{dt}\right] \Big/ \left[(1+\alpha)(1-x_N)\right] \tag{4.8f}$$

For the mixing stages the feeds are the input to the stages, hence the flowrates boundary values can be expressed as:

$$S_0 = S_f \tag{4.8g}$$

$$R_0 = \left[R_1(1-x_1) + h_{x_0} \frac{dx_0}{dt} \right] \Big/ (1-x_0) \tag{4.8h}$$

$$S_{N+1} = \left[S_{out}(1-y_{out}) + h_{y_{N+1}} \frac{dy_{N+1}}{dt} \right] \Big/ \left[(1-y_N) \right] \tag{4.8i}$$

$$R_{N+1} = R_f \tag{4.8j}$$

The concentrations at each stage are calculated from a solute mass balance. The general equations are expressed as:

$$\frac{dx_i}{dt} = \left[(1+\alpha) R_{i+1} x_{i+1} + \alpha R_{i-1} x_{i-1} - (1+2\alpha) R_i x_i - Q_{x_i} \right] / h_{x_i} \tag{4.9a}$$

$$\frac{dy_i}{dt} = \left[\beta S_{i+1} y_{i+1} + (1+\beta) S_{i-1} y_{i-1} - (1+2\beta) S_i y_i + Q_{x_i} \right] / h_{y_i} \tag{4.9b}$$

For the stages *1* and *N* the equations are expressed as:

$$\frac{dx_1}{dt} = \left[(1+\alpha) R_2 x_2 - (1+\alpha) R_1 x_1 - Q_{x_1} \right] / h_{x_1} \tag{4.9c}$$

$$\frac{dy_1}{dt} = \left[\beta S_2 y_2 + S_f y_f - (1+\beta) S_1 y_1 + Q_{x_1} \right] / h_{y_1} \tag{4.9d}$$

$$\frac{dx_N}{dt} = \left[R_f x_f + \alpha R_{N-1} x_{N-1} - (1+\alpha) R_N x_N - Q_{x_N} \right] / h_{x_N} \tag{4.9e}$$

$$\frac{dy_N}{dt} = \left[(1+\beta) S_{N-1} y_{N-1} - (1+\beta) S_N y_N + Q_{x_N} \right] / h_{y_N} \tag{4.9f}$$

At the mixing stages, the mass balance equations include one phase depending on the location of each mixing stage. The equations are expressed as:

$$\frac{dx_0}{dt} = \left[R_1 x_1 - R_{out} x_{out} \right] / h_{x_0} \text{ and } \frac{dy_0}{dt} = 0 \tag{4.9g}$$

$$\frac{dy_{N+1}}{dt} = \left[S_N y_N - S_{out} y_{out} \right] / h_{y_{N+1}} \text{ and } \frac{dx_{N+1}}{dt} = 0 \tag{4.9h}$$

No mass transfer is assumed in the mixing stages, and the single solute mass transfer rate at each stage is expressed as: $Q_{x_i} = K_{x_i} a_i V (x_i - x_i^*)$ where x_i^* is the concentration of solute in the aqueous phase which would be in equilibrium with the local organic phase concentration.

Equilibrium concentrations are expressed as a function mass distribution coefficient at any stage as: $y_i^* = m_i x_i^*$.

Values of backmixing coefficients (α, β) and mass transfer weighting factor (f) are determined using steady state optimization of the experimental profiles, where as values of fractional holdup coefficient (ε), mass transfer distribution coefficient (m), diffusion coefficients (D_c,D_d) for both phases and physical properties ($\rho_c, \rho_d, \eta_c, \eta_d, \sigma$) for both phases are correlated as functions of operational parameters. The details of these model parameters are explained in the next section.

Correlation analysis of the dependency of the variables (α, β, f and ε) on combinations of rotor speed N and phase flow ratio F and their logarithms such as (N, F, NF, $log(N)$, $log(F)$ and $log(NF)$) revealed that the best correlation index was for the variables (N, F, and NF). Based on this result, only these variables were used as independent variables in the model's parameter correlations.

In the above equations, each combined mixing and calming zone is represented by a single stage in the model, the number of these stages N was set to nine plus two mixing stages at the two ends of the column. This set of $8(N+2)-4$ equations are sorted starting from the bottom of the column where the light phase enters the column and proceeds towards the top of the column where the heavy phase enters.

4.6.2 Hydrodynamic Equations:

As mentioned previously, the hydrodynamics in each stage was expressed in terms of fractional holdup coefficient ε_i. The dispersed phase droplet diameter was expressed as Sauter mean diameter d_{32}. These two parameters (ε_i and d_{32}) were calculated as explained in the following sections.

4.6.2.1 Fractional hold-up coefficient (ε_i):

The extract phase fractional holdup coefficient at each stage was correlated as a function of rotor speed (N) and the phase flow ratio at each stage F_i. The correlation is given as:

$$\varepsilon_i = b_0 + b_1 N^{b_2} + b_3 (N.F_i)^{b_4} \qquad (4.12)$$

where : $F_i = \frac{S_i}{R_i}$: phase flow ratio at stage (i).

b_i: are correlation constants given in table (4.1)

Table (4.1) Parameters of the Dispersed Phase Hold-up Coefficient Correlation.

b_0	b_1	b_2	b_3	b_4
0.05596	5.07×10^{-9}	8.2835	8.28×10^{-4}	1.7736

The average dispersed phase operational holdup was measured experimentally after each run using the displacement technique described in chapter (3). The holdup data were correlated using the Marquart-Levenberg optimisations method. The details of this method are given in Appendix (B). The regression coefficient squared of this correlation was $R^2=0.980$. The correlation is valid for the experimental conditions investigated for phase ratios ranging from 1:1 to 2:1 and agitator speed from 5.0 to 8.3 s^{-1}. It is noticed that the coefficients b_1 and b_3 have small values. These coefficients are multiplied by exponent terms with high values, so the overall effect will be the reduction of these terms.

The values of dispersed phase holdup coefficient at different rotor speeds and phase flow ratios are calculated using the obtained correlation (4.12) and are compared with the experimental ones as shown in Figure (4.4).

4.6.2.2 Sauter Mean Drop Diameter (d_{32i}):

For calculating the mass transfer interfacial area, an estimate of the average drop diameter is needed. The average drop size is usually expressed using Sauter mean diameter evaluated as:

$$d_{32} = \frac{\sum_i n_i d_i^3}{\sum_i n_i d_i^2} \qquad (4.13)$$

where n = total number of drops.

The correlation given by Bonnet (1982) for the same ternary system was used for the prediction of drop diameter as a function of holdup and Weber dimensionless number as:

$$d_{32i} = d_r (1.763 + 16.117\varepsilon_i) We_i^{-0.907} \qquad (4.14)$$

where : We_i : Weber dimensionless number $= \frac{d_r^3 N^2 \rho_{ci}}{\sigma_i}$

N : rotor speed (s^{-1}).
d_r : rotor diameter (cm).
ρ_{ci} : continuous phase density at stage (i). (gm/cm^3)
σ_i : interfacial surface tension (gm/cm^2).

4.6.3 Mass Transfer and Equilibrium Equations:

4.6.3.1 Overall mass Transfer coefficient (K_{xi}):

Acetone mass transfer from one phase to another depends significantly on the drop state. Using single drop models Al-Aswad et al. (1985) have related the overall mass transfer coefficient to the three drop regimes namely; *stagnant*, *circulating* and *oscillating* drops. They calculated the overall mass transfer coefficient from the following equation:

$$K_{cal} = K_S P_S + K_C P_C + K_O P_O \qquad (4.15)$$

where P_S, P_C and P_O are the volume fraction of drops in the stagnant, circulating and oscillating drop regimes respectively and K_S, K_C and K_O are the overall mass transfer coefficients relating to each regime.

For the Scheibel column under investigation and the range of operating conditions considered, it was observed from the experimental runs that the stagnant and circulating drops comprise much less proportion than the oscillating type out of the total population, so it was assumed that only oscillating drops were effectively present.

The overall mass transfer coefficient based on the raffinate phase was calculated by applying the two-film theory of Whitman (1923). This was done for each stage i, as a function of the two mass transfer film coefficients; k_c for the continuous phase and k_d for the dispersed phase and distribution coefficient m_i as follows:

For the dispersed phase, the oscillating drop model proposed by Rose and Kintner (1966) was chosen. It is expressed as a function of dispersed phase diffusion coefficient D_d and the frequency of oscillation ω_i at each stage :

$$k_{di} = 0.45\sqrt{\omega_i D_d} \qquad (4.16)$$

where ω_i is calculated from:

$$\omega_i = \sqrt{\sigma_i \frac{(d_{32i}^{0.225}/1.242)}{(d_{32i}^{3}/2)} \frac{(n(n+1)(n-1)(n+2)}{(n+1)\rho_{di} + n\rho_{ci}}} \quad (4.17)$$

where n:=2, and σ_i: Interfacial surface tension (gm/s^2) at stage (i).

For the continuous phase the mass transfer coefficient was calculated using the penetration theory-based prediction equation of Garner and Tayeban (1960).

$$k_{ci} = \frac{D_c}{d_{32i}}\left(50 + 0.0085 Re_i Sc_i^{0.7}\right) \quad (4.18)$$

where :

D_c: continuous phase diffusion coefficient (cm^2/sec).

v_o: the average agitator tip speed = $\frac{\pi d_r N}{2}$ (cm/sec)

and d_r : agitator diameter (cm).

4.6.3.2 Mass transfer interfacial area coefficient (a_i):

It was assumed that the interfacial area for mass transfer is equal to the total surface area of all dispersed drops, and hence the interfacial area coefficient at any stage a_i can be expressed as (Oloidi et al. 1987):

$$a_i = \frac{6\varepsilon_i V_i}{d_{32i}} \quad (4.19)$$

where : $V_i = \frac{(\pi D^2)}{4} h_s$,

D: column diameter (cm),

h_s: stage height (cm).

4.6.3.3 Mass Transfer Weight Factor (f_i) and backmixing coefficients (α, β) :

As mentioned in the model assumptions, a weight factor was introduced in the calculation of mass transfer rate Q_{xi} to account for the limitation in the assumption of drop behaviour, and also for the assumption of no mass transfer in the settling zone. To account for backmixing in the two phases, the backmixing coefficients (α, β) were considered in the modelling study.

Due to lack of experimental measurements of the mass transfer weighting factor and backmixing coefficients, there was a need to estimate these model parameters using well-established estimation techniques. Nonlinear optimisation methods were used for the parameter estimation by matching the model predictions with experimental data. The experimental concentration profiles at different operating conditions were used to fit the model under consideration with the model parameters (mass transfer weight factor f_i and the backmixing coefficients α, β). The objective function used was set as the following:

$$min\left[f(x)\right] = min\left[\sqrt{\frac{\sum_{i=1}^{N}(x_i^e - x_i^p)^2}{N}} \times 100\right] \tag{4.20}$$

where x_i^e and x_i^p are the i th stage experimental and model predicted Acetone concentration values.

The parameter estimation in this study was performed by adopting the *Quasi-Newton* optimisation technique. The details of this technique are given in Appendix(B). Here, nine experiments covering a wide range of operating conditions were employed.

Parameter estimation via optimization is a computationally intensive task as the model needs to be solved at each simulation run for a given set of parameters until the objective function is minimized. Therefore, the values of the model parameters that were estimated from the parameter estimation over wide range of operating conditions were related to a set of operational variables in order to infer these parameters using simple correlations.

The mass transfer weight factor was correlated to the rotor speed and phase flow ratio in the form of:

$$f_i = k_0 + k_1 N^{k_2} + k_3 F_i^{k_4} + k_5 (NF_i)^{k_6} \tag{4.21}$$

where:

N: rotor speed (s^{-1})

F_i: phase flow ratio at stage i.

Pratt and Stevens (1992) and Heyberger (1982), reported that true backmixing in mechanically agitated columns is less common within the dispersed phase, as droplets normally move only in the forward direction relative to the continuous phase. The main cause of backmixing is the circulation of continuous phase due to agitation in mixing zones. The results of the optimization study enforced the previously mentioned findings. For the dispersed phase backmixing coefficient(β), the calculated values were very small. Therefore it was assumed that its effect is negligible and was assumed zero for all runs. On the other hand, the values calculated for the continuous phase backmixing coefficient were significant and variable with variation of operating conditions. The calculated values of the backmixing coefficient were correlated to the rotor speed, and phase flow ratio in a form similar to that used for the mass transfer weight factor (4.20) as follows:

$$\alpha_i = h_0 + h_1 N^{h_2} + h_3 F_i^{h_4} + h_5 (NF_i)^{h_6} \qquad (4.22)$$

4.6.3.4 Distribution coefficient (m_i):

Hackl et al. (1978) used the same chemical system and correlated the distribution coefficient m at each stage as a function of acetone molar concentration in the continuous phase. The exponential correlation was given as follows:

$$m_i = \exp\left(\sum_{l=0}^{6} c_l \ln(x_i)^{l-1}\right) \qquad (4.23)$$

The concentration of Acetone is expressed in mole fraction and the range of validity of this correlation is for $x_i \in [0, 0.3]$. The numerical values of the c_l coefficients are given in table (4.2)

Table (4.2) Constants of the Equilibrium Distribution Coefficient Correlation.

c_0	c_1	c_2	c_3	c_4	c_5	c_6
-8.394	-16.319	-11.187	-4.011	-0.7891	-.0804	-0.0033

In this work, another simplified correlation was predicted for m_i in which the concentration was expressed in terms of Acetone mass fraction in the continuous phase x_i:

$$m_i = 0.86852 + 0.08681 x_i^{-0.483142} \quad (4.24)$$

The range of validity of this correlation is for $x_i \in [0, 0.1]$, which is sufficient for the range of operating conditions investigated. This correlation proved to be more convenient for simulation due to its simplicity.

4.6.4 Physical Properties:

As mentioned earlier that the physical properties were variable throughout the column, so they were calculated at each stage continuously. The following are calculation methods used in the model for the physical properties (Density, diffusion coefficient, Interfacial tension and viscosity) for both phases.

4.6.4.1 Continuous and Dispersed Phase Densities:

The density of each phase was estimated as a function of pure component densities ρ_A, ρ_T and ρ_W. and concentration in x_i and y_i for both phases as:

$$\rho_c = \rho_A x_i + \rho_W (1 - x_i) \quad (4.25a)$$

$$\rho_d = \rho_A y_i + \rho_T (1 - y_i) \quad (4.25b)$$

4.6.4.2 Continuous and Dispersed Diffusion Coefficients:

The diffusion coefficients for the continuous and the dispersed phase were calculated using the correlations (4.26 and 4.27) given by Bibaud and Treybal (1966).

$$D_c = \frac{V_c h_s}{1 - \varepsilon}\left[-0.171 + 0.02\frac{d_R N (1 - \varepsilon)}{V_c}\right] \quad (4.26)$$

$$D_d = d_R^2 N \left[1.3 \times 10^{-8} We_R^{1.54} \left(\frac{\rho_c}{\rho_c - \rho_d}\right)^{4.18} Re_R^{0.61}\right]^{-1} \quad (4.27)$$

where

We_R and Re_R : impeller Weber and Reynolds numbers.

V_c : the continuous phase velocity term (cm/s).

d_R : rotor diameter (cm).

and h_s : section height (cm).

4.6.4.3 Interfacial Surface Tension (σ_i):

The variation in interfacial surface tension between the two phases plays an important role on the coalescence and dispersion behaviour of droplets. To account for the variation of this property, it was correlated experimentally and used in the model. The Interfacial tension between the two phases for different concentrations of Acetone was measured experimentally. The details of the experimental procedure and the equipment used for measurements are given in Appendix (A). The apparatus used for experimental measurements is shown in Figure(A.4). Interfacial tension data for the range $x_i \in [0 , 0.1]$ were correlated as a polinomyal function of Acetone mass fraction available in the two phases with a correlation factor of $R^2=0.987$. The correlation obtained is given below:

$$\sigma_i = 33.4793 - 95.0502x_i + 275.9171x_i^2 \qquad (4.26)$$

4.6.4.4 Continuous and Dispersed Phase viscosities:

It was assumed that the organic phase viscosity is a function of pure component viscosities. The method of Grunberg and Nissan (1949) was used for the calculation of the dispersed phase viscosity as:

$$\ln \eta_d = x_T \ln \eta_T + x_A \ln \eta_A + x_T x_A G_{TA} \qquad (4.27)$$

where: x_T and x_A are Toluene and Acetone concentrations respectively.

η_T and η_A are Toluene and Acetone pure component viscosities respectively.

G_{TA}: binary interaction parameter at 298 °K.

Isdale et al (1985) proposed a group contribution method for the estimation of the binary interaction parameter G_{TA}. It is calculated as:

$$G_{TA} = \sum \Delta_i + \sum \Delta_j + W \qquad (4.28)$$

where:

W : is a parameter that depend on type of atoms present, and number of carbon atoms.

Δ_i and Δ_j are the group contributions for G_{TA} , and i and j refer to the binary components. In our case i refers to Toluene and j refers to Acetone. These parameters are calculated from experimental values given in table (4.3).

Table (4.3) Group Contributions for G_{ij} at 298°K

Group	Notes	Value
$-CH_3$		-0.1
$>CH_2$		0.096
>CH-		0.204
>C<		0.433
Benzene ring Ortho- Meta- Para-		0.766 0.174 - 0.154
Cyclohexane ring		0.416
-OH	Methanol Ethanol Higher aliphatic alcohol	0.887 -0.023 -0.0443
>C=O	Ketones	1.046
-Cl		$0.653-0.161N_{Cl}^*$
-Br		-0.116
-COOH	Nonassociated liquids Ketones Formic acid with ketones	$-.411+0.06074N_C^*$ 1.130 0.167

*N_{Cl} and N_C are number of chlorine and carbon atoms in the molecule

The pure components viscosity as a function of temperature is calculated using the correlation:

$$\ln \eta = A + \frac{B}{T} + CT + DT^2 \qquad (4.29)$$

the coefficient A,B,C and D for the three components is given by Yaw et al. (1979) and Van Velzen et al. (1972) and listed in table (4.4).

Table (4.4) Coefficients for components viscosity correlation

Component	A	B	C	D
Water	-24.71	4.209×10^{3}	4.527×10^{-2}	-3.376×10^{-5}
Acetone	-4.033	8.456×10^{2}	0.0	0.0
Toluene	-5.878	1.287	4.575×10^{-3}	-4.499×10^{-6}

The continuous phase viscosity was determined by correlating the experimental data reported by Weast et al. (1993) as a quadratic function of Acetone concentration as:

$$\eta_c = 0.99694 + 2.611x - 1.231x^2 \qquad (4.30)$$

The correlation coefficient is $R^2 = 0.9996$

4.7 Method of Solution

The above set of equations represents a system of Differential Algebraic Equations (DAEs) system. This system consists of algebraic equations as well as ordinary differential equation. It is very difficult to solve these equations analytically, and the only practical way to achieve this is by numerical techniques.

Many DAE integration algorithms exist, but selecting the most suitable one depends primarily on the accuracy and degree of stability of the solution sought. For obtaining accurate calculations, the integration step size was chosen automatically and updated by the integrator algorithm.

The DAE system of the modelled Scheibel extractor was classified as a stiff system. Stiffness arises in dynamic systems as a result of having slowly changing components (having high response time constants) with rapidly changing ones (with small response time constant). For these types of systems the integration step size is determined by solution stability and not accuracy. If stability cannot be achieved with a reasonable step size, a class of new algorithms must be considered. Such algorithms are called implicit stiff methods. The drawback of using these methods is that they involve more computational algebra than the non-stiff explicit algorithms, so for non-stiff problems, implicit stiff integrators should not be used.

Examples of non-stiff methods include:

- Explicit Euler's method
- Rung-Kutta methods.
- Adams method

Examples of stiff methods include:

- implicit Euler's method
- implicit Runge-Kutta method
- Gear's Backward Differentiation Formula (BDF) method

The set of DAEs were solved with respect to time using the Gear's (BDF) method which implemented in the well-known DDASSL stiff DAE equation solver [Petzold, 1982].. The details of theory and implementation of this integrator is given in Appendix(D).

4.8 Simulation of the model

A Fortran program was written for the simulation of the model. A user-friendly interface was written using MS Excel Macro language to facilitate the ease of use of the program. The user interface enables the user to run the program in one of two modes; steady state mode and dynamic mode. The user is prompted to enter input and operating parameters of the column and the step changes in one of the variables. The Simulation program is then executed in the background, and the calculated results stored in two formats; text files and spreadsheet format. The transients of the column are displayed as graphs within the created spreadsheet. The details of the simulation program and the user interface are given in Appendix(C).

4.9 Model Solution Validation and Parameter Estimation

The model parameters described previously namely; mass transfer weight factor, and backmixing coefficients were estimated via performing simultaneous steady-state simulation and optimization. The estimated values of the model parameters were correlated to the operational parameters and were employed in the dynamic model. Next, dynamic simulation of the model was performed and the transient profiles were compared to the experimental ones at the same feed and operating conditions.

4.9.1 Parameter Estimation

The steady state experimental data were collected using the procedure explained in Chapter (3). The concentration profiles for both phases along the column length were used to calculate the optimum values of the model parameters via optimisation. This procedure was conducted in a simultaneous simulation of the model and minimization of the objective function (Equation 4.20). The Quasi-Newton optimisation algorithm was used to minimize the objective function until the termination tolerance of 0.0001 was satisfied. The estimated model parameters at different operating conditions are presented in Table(4.5)

Table(4.5) Estimated values of model parameters at different operating conditions

Run No.	Rotor Speed (N) RPM	Phase Flow Ratio (F)	Mass transfer weight factor (f)	Continuous phase backmixing coeff. (α)	$MRAE_x$	$MRAE_y$
1	300	1:1	0.0450	0.0491	0.00597	0.03351
2	300	1.5:1	0.0599	0.1077	0.00019	0.00785
3	300	2:1	0.0770	0.2873	0.00655	0.01101
4	400	1:1	0.0927	0.0915	0.00745	0.01681
5	400	1.5:1	0.1109	0.1540	0.00805	0.00994
6	400	2:1	0.1305	0.3362	0.01190	0.00599
7	500	1:1	0.1719	0.1062	0.00441	0.02229
8	500	1.5:1	0.1941	0.1716	0.00457	0.00525
9	500	2:1	0.2169	0.3558	0.00978	0.00657

The results indicate the dependence of mass transfer weight factor (f) and the continuous backmixing coefficient (α) on the values of operational parameters. From table (4.5) we can notice that the rotor speed has more effect on the mass transfer weight factor whereas the phase flow rate is more effective on the backmixing coefficient. This result is expected since the rotation speed has the effect of increasing solute transfer by increasing area of contact, whereas the backmixing phenomena is more dependent on the phases flows. The dispersed phase backmixing coefficient (β) was of negligible values and therefore was ignored in this study.

Table(4.8) shows also the *Mean Relative Absolute Error (MRAE)* for the two phases ($MRAE_x$ and $MRAE_y$) at each set of operating conditions.

The *Mean Relative Absolute Error* for both phases were calculated as:

$$MRAE = \frac{1}{N}\sum_{i=1}^{N}\frac{\left|x_i^{exp} - x_i^{pre}\right|}{x_i^{pre}} \qquad (4.31)$$

where the x_i^{exp} : the experimental concentration value at the ith stage.

x_i^{pre} : the model predicted concentration value at the ith stage.

N : number of stages.

Figures (4.7-9) gives a comparison between the experimental concentration profiles and the model predicted concentration profiles at the estimated model

parameters as a function of stage number. The low error values ($MRAE_x$ for the raffinate phase and $MRAE_y$ for the extract phase) from table (4.5) and the close match of the experimental and model predicted results indicate the good agreement of the model to the actual column behaviour under a wide range of operating conditions.

The calculated values of the model parameters were correlated as a function of rotor speed (***N***) and phase flow ratio (***F***) as given in equations (4.21 and 4.22). The correlation constants for both parameters are listed in Table(4.6). The regression coefficients of the two correlation fits were 0.998 and 0.997.

Table (4.6) Constants of the model parameters correlations.

Constant Number	***0***	***1***	***2***	***3***	***4***	***5***	***6***
Mass transfer weight factor	0.2	3.6131	-2.2565	0.2798	0.5526	-0.2582	0.2775
Continuous Phase Backmixing Coeff.	-2.859	-2.463	-0.8	0.156	2.0	4.031	-0.1

Values of the two model parameters from both the rigorous model optimisation and from the fitted correlations are compared in figures 4.5 and 4.6. It was observed that there was a good agreement between the two values, which gives confidence in incorporating the correlations in the dynamic model to predict the model parameters at any instant of simulation depending on the values of the operational parameters.

4.9.2 Model Validation

The validation of dynamic response of the rigorous model was done by conducting positive and negative step tests on the five input variables namely; *rotor speed, solvent feed flowrate, solvent feed concentration, feed flowrate and feed concentration*. For each run the outlet raffinate concentration profile as function of time was calculated. A 24 *min* run time was enough to show the complete dynamics of the model for all tested variables. The computer-logged raffinate phase concentration profiles were compared with the model predicted transient profiles of the model at the same conditions. The results are shown in Figures(4.10-14). In order to get an insight of how these profiles are close to each other statistically, the relative percentage error profiles for each of the previously mentioned runs are given in Figures(4.15-19) respectively. These figures show the location of modelling error

with respect to the 97.5% confidence interval indicated by the two horizontal dotted lines. Also the *Mean Relative Absolute Error (MRAE)* was calculated for each profile and included within the error profiles plots. The *MRAE* was calculated as given previously in equation (4.31) but in this case the subscript ***i*** represents the sampling point at a certain time.

In general, the experimental transient responses have good agreement with the model simulated profiles with acceptable degree of deviations. Following, is a discussion of the behaviour of each one of these profile.

Figure (4.10) shows the transients of the column due to a ±10% disturbance in the rotor speed. There is a little mismatch during the start of response. This is due to the fast dynamics at the first five minutes and the measurement lag at this period. For the +10% there were some oscillations in the last 10 min of the experimental profile. These observations are clearly shown in the relative percentage error plots shown in Figure(4.15).

Same mismatches were noticed for the ±10% disturbance in the raffinate feed flowrate but no oscillations in response were observed and the error sizes were less than the previous one, which is shown in Figure(4.11) and the corresponding relative percentage error plot in Figure(4.16).

The column's transient due to step in the solvent feed flowrate and the equivalent error plots are shown in Figure (4.12) and Figure(4.17) respectively. The figures indicate some mismatch during the first 10 min but better performance at the end of simulation and both experimental and simulated responses reached the same final concentrations. Again startup conditions were the major cause for this behaviour.

Figure (4.13) shows the column transient to a step in feed concentration. Figure (4.18) gives its relative percentage error. It is clear that the -10% step response shows high gap between the two profiles for the second part of the response. The +10% step response is more stable and good match of profiles was attained.

In all the previous profiles the calculated *MRAE* were below *0.01* which is a reasonable profiles matching accuracy. Probably the greatest disagreement of transient profiles was noticed for the step change in the solvent feed concentration shown in Figure (4.14) and its equivalent error plot in Figure(4.19). The calculated *MRAE* value of *0.01431* was relatively high. The probable reason for this may be stated as follows. The sudden large disturbance in the solvent feed concentration from

a pure Toluene to an Acetone contaminated feed causes the column to behave in such a way that new equilibria must be attained. This unusual mismatch was expected in view of the fact that the model was run using pure solvent feed which makes the column transient more sensitive to any feed disturbance. This enforces the practical need to control the column's outlets against such undesirable disturbances. Despite this small discrepancy, the experimental profile traced the same path of the modelled one, which makes the model acceptable with reasonable accuracy.

As a whole, the predicted responses follow reasonably the experimental profiles for all tested variables. The discrepancies noticed in some of the profiles were due to:

- Unmeasured disturbances in feed flowrates and the rotor speed. These were difficult to control during the experiments.
- The fluctuations of the position of the interface level at the top of the column affect its hydrodynamic behaviour and this in turn affects its throughput.

The close agreement of the rigorous model to the actual process gives confidence in adopting the model for further system identification study which will be the theme of the next chapter.

4.10 Error Analysis of the Fitted Model Parameters Correlations:

The model parameters fitted correlations in the previous sections depend on experimental measurements. These measurements suffer from experimental errors as was indicated in the previous chapter. Hence, these correlations should be analyzed for their reliability by calculating the *Maximum Indeterminate Error* (*MIE*) [Donald, 1996]. The *MIE* propagates according to the following rules:

- Addition and subtraction rule: The *absolute* indeterminate errors add.
- Product and quotient rule: The *relative* indeterminate errors add.
- Power rule: When a quantity is raised to a power, the *relative* error in the result is the power times the *relative* error in base.

Table (4.7) gives a summary of these rules assuming operations between two quantities $A \pm a$ and $B \pm b$ where a and b are absolute errors in A and B respectively.

Table (4.7) Maximum Indeterminate Error propagation rules.

Operation	Error Type	Calculation
$A + B$	Absolute	$a + b$
$A - B$	Absolute	$a - b$
$A . B$	Relative	$(a/A+b/B)$
A / B	Relative	$(a/A+b/B)$
A^B	Relative	$B*(a/A)$

The error propagation rules were applied for each of the experimental correlations used in the model. The absolute errors given in table (3.6) were used in the calculations. Table (4.8) gives the *Maximum Indeterminate Absolute Error* (*MIAE*) formula for each of the experimental correlations. The relative errors are given as ζ_A to represent (***a/A***).

Table (4.8) Maximum Indeterminate Absolute Error (*MIAE*) calculation formulae of experimental correlations.

Correlation	*MIAE* Formula*
Fractional holdup	$\left(b_2 N^{b_3}\right)\left(b_3 \xi_N\right)+\left(b_4 (NF)^{b_5}\right)\left(b_5 \left(\xi_N + \xi_F\right)\right)$
Mass transfer weight factor	$\left(k_1 N^{k_2}\right)\left(k_2 \xi_N\right)+\left(k_3 F^{k_4}\right)\left(k_4 \xi_F\right)+\left(k_5 (NF)^{k_6}\right)\left(k_6 \left(\xi_N + \xi_F\right)\right)$
Backmixing coefficient	$\left(h_1 N^{h_2}\right)\left(h_2 \xi_N\right)+\left(h_3 F^{h_4}\right)\left(h_4 \xi_F\right)+\left(h_5 (NF)^{h_6}\right)\left(h_6 \left(\xi_N + \xi_F\right)\right)$
Distribution coefficient	$\left(m_2 x^{m_3}\right)\left(m_3 \xi_m\right)$
Interfacial tension	$(bx)(\xi_x)+\left(cx^2\right)(2\xi_x)$

* ξ_N , ξ_F and ξ_x are relative errors in the variable shown as subscripts.
b_i, k_i, h_i, m_i and (b, c) are parameters of the experimental correlations.

The error formulae were used for calculating the *MIAE* in each run used in the experiments. The calculated values of errors are shown in Table(4.9) for the fractional holdup, mass transfer weight factor, backmixing coefficient, distribution coefficient and interfacial surface tension correlations.

The *MIAE* generated from the holdup correlation at high rotor speed and that from the backmixing coefficient at high phase flow ratio are relatively high compared to the rest of calculated values. This is due to the effect of the size of the absolute error

of the components forming total absolute error formula. The absolute errors of the $b_2 N^{b_3}$ term in the holdup correlation and in the $h_3 F^{h_4}$ term in the backmixing correlation were relatively high.

As a whole, the small values of absolute errors generated from the experimental correlations indicate that the mathematical correlations are reliable and can be used confidently in the prediction of variables values in the model.

Table(4.9) ***MIAE*** bounds between experimental and correlated values.

Run No.	Fractional Holdup (ε)	Mass Transfer Weight factor(f)	Backmixing Coefficient (α)	Distribution Coefficient (m)	Interfacial Tension (σ)
1	7.027E-02±0.0011	0.0450±0.0016	0.0491±0.0028	1.6983±0.0039	32.450±0.0090
2	8.204E-02±0.0017	0.0599±0.0015	0.1077±0.0085	1.5260±0.0021	32.012±0.0087
3	9.732E-02±0.0024	0.0770±0.0014	0.2873±0.0149	1.4591±0.0016	31.530±0.0085
4	1.085E-01±0.0044	0.0927±0.0024	0.0915±0.0009	1.3952±0.0010	31.370±0.0082
5	1.281E-01±0.0053	0.1109±0.0023	0.1540±0.0065	1.3326±0.0007	30.710±0.0078
6	1.535E-01±0.0063	0.1305±0.0023	0.3362±0.0128	1.2805±0.0005	30.083±0.0072
7	2.979E-01±0.0190	0.1719±0.0048	0.1062±0.0001	1.2162±0.0004	29.445±0.0067
8	3.270E-01±0.0201	0.1941±0.0048	0.1716±0.0057	1.2117±0.0003	28.773±0.0062
9	3.653E-01±0.0214	0.2169±0.0048	0.3558±0.0119	1.1956±0.0002	28.317±0.0058
10	-	-	-	1.1587±0.0002	27.599±0.0050

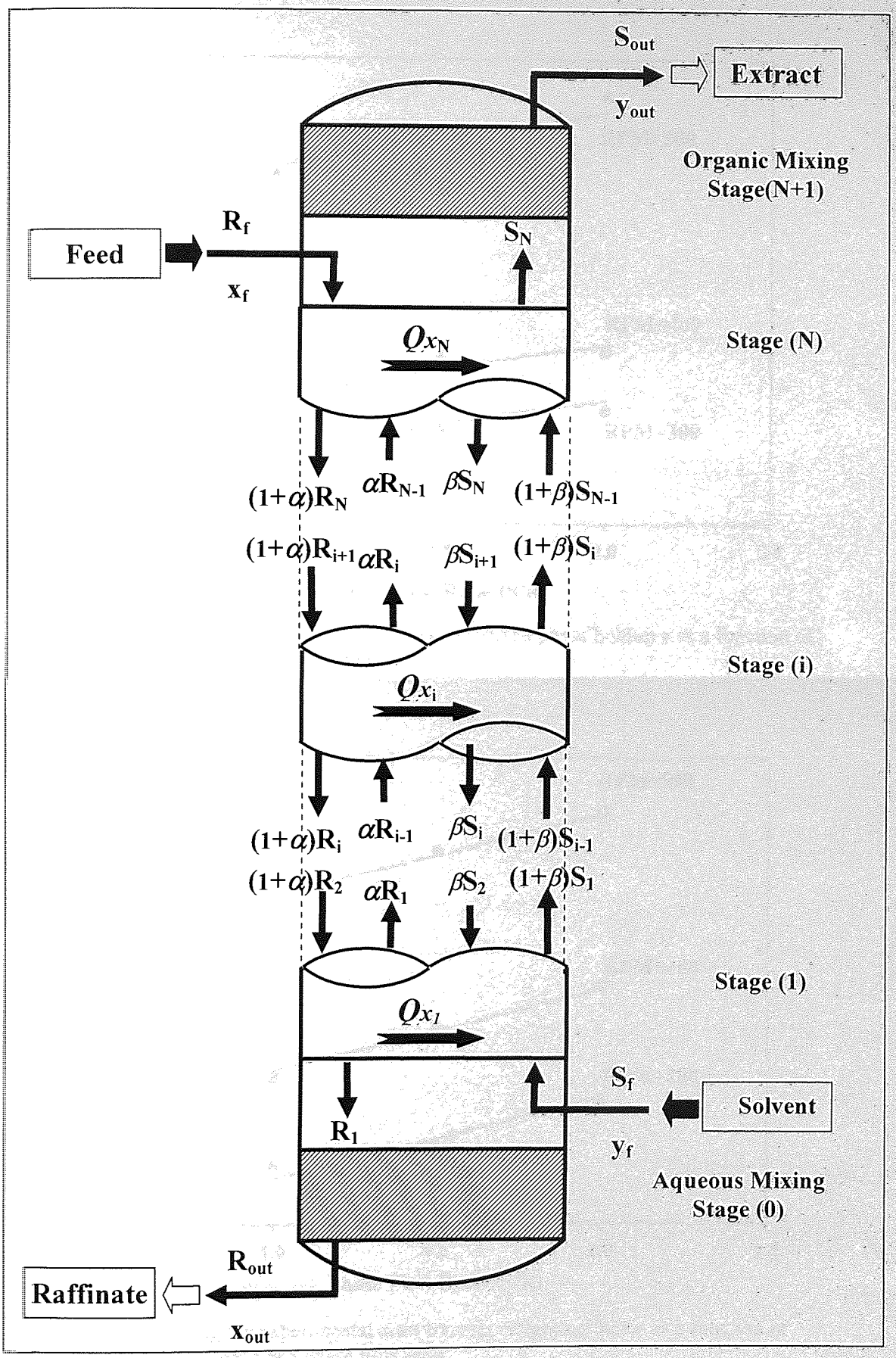

Figure (4.3) Stagewise backmixing model with single-phase mixing stage.

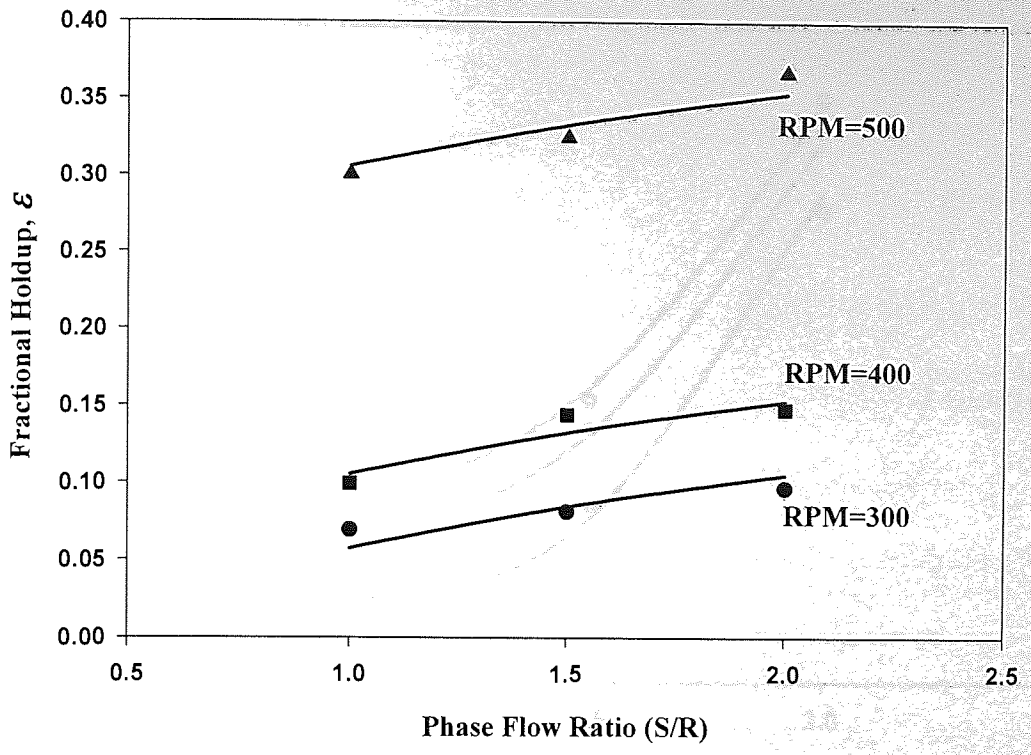

Figure(4.4) Fitting the experimental fractional despersed phase holdup ε as a function of rotor speed and phase flow ratio.

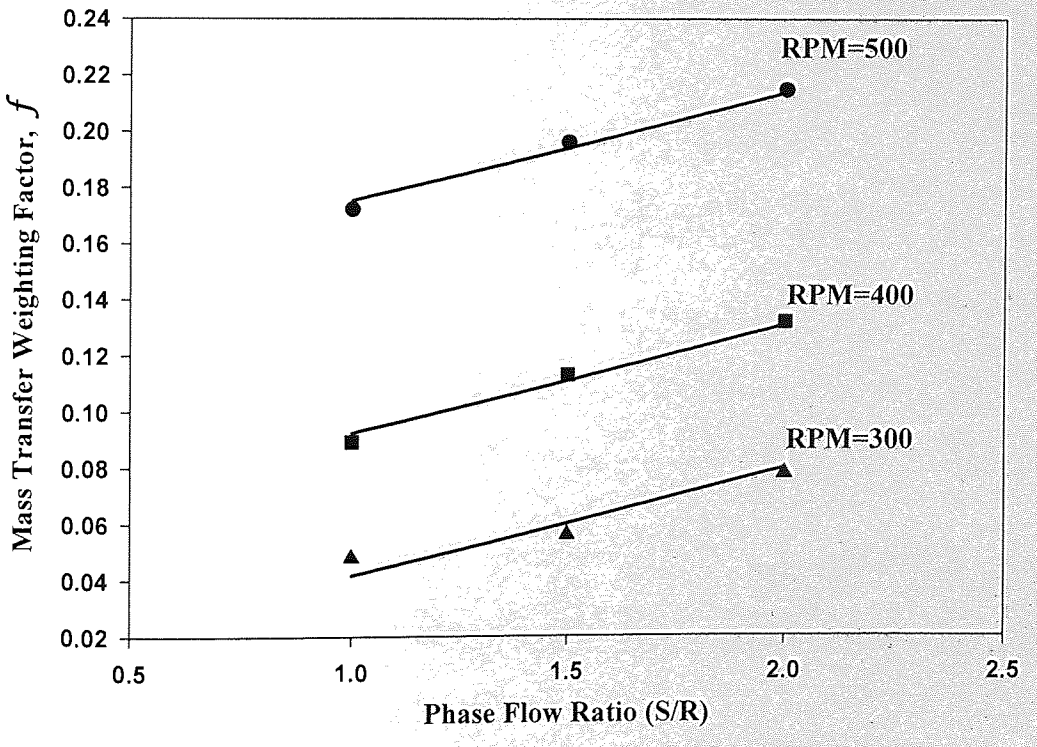

Figure(4.5) Fitting the experimental mass transfer weighting factor as a function of rotor speed and phase flow ratio.

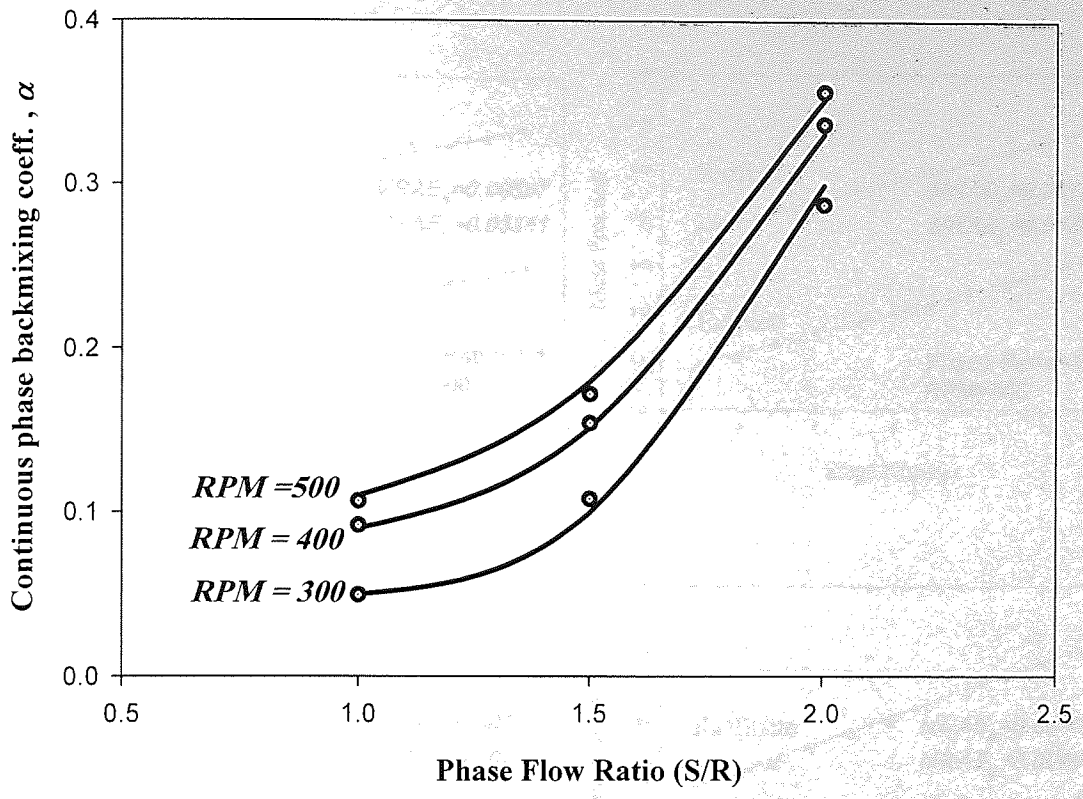

Figure(4.6) Fitting the experimental continuouos phase backmixing coefficient as a function of rotor speed and phase flow ratio.

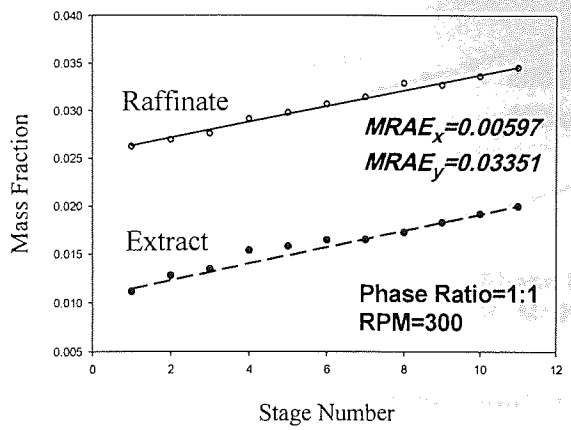

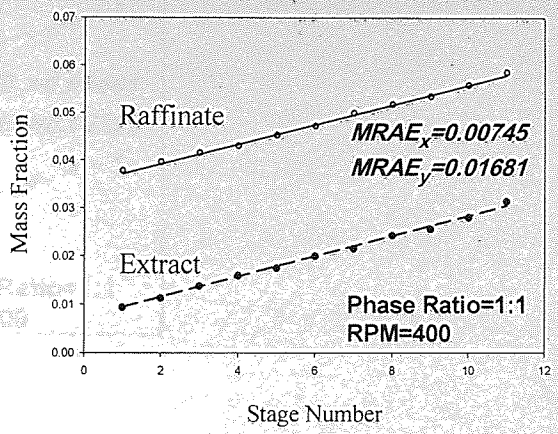

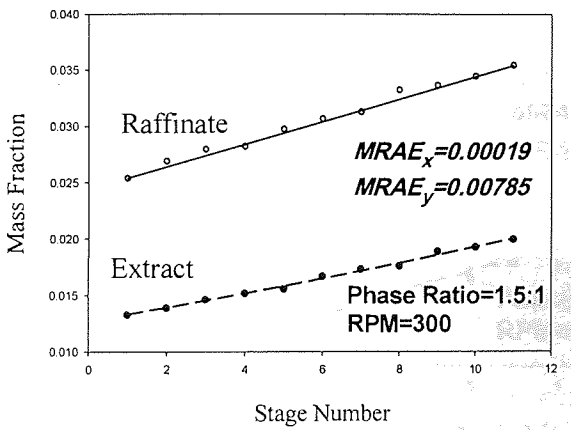

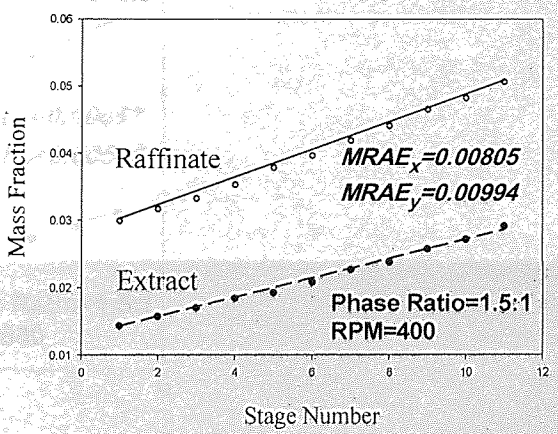

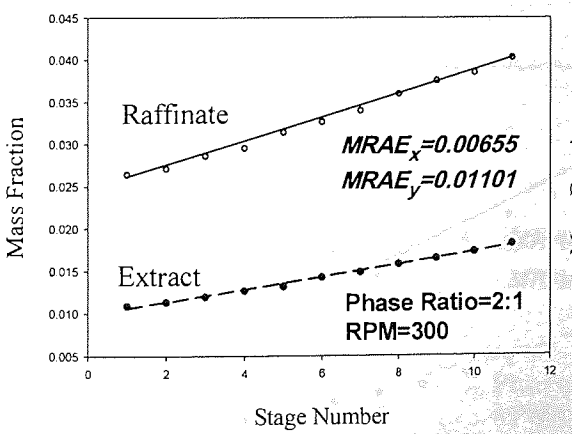

Figure(4.7) Experimental and calculated concentration profiles at an agitator speed of 5.0 s^{-1} for three different phase ratios.

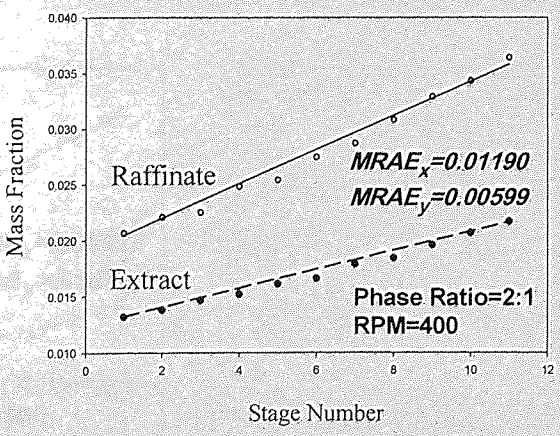

Figure(4.8) Experimental and calculated concentration profiles at an agitator speed of 6.7 s^{-1} for three different phase ratios.

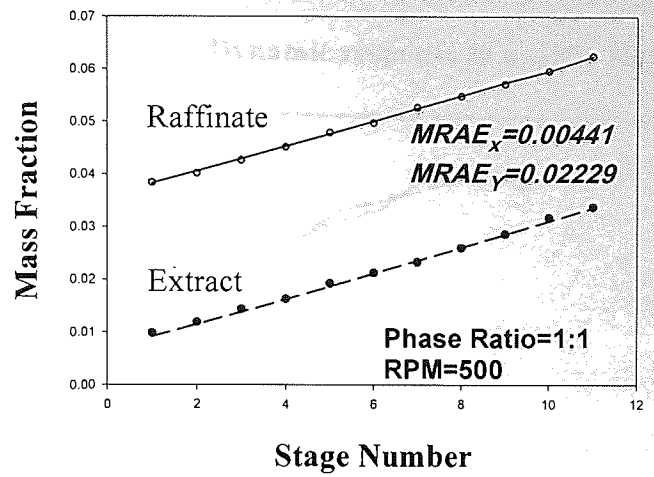

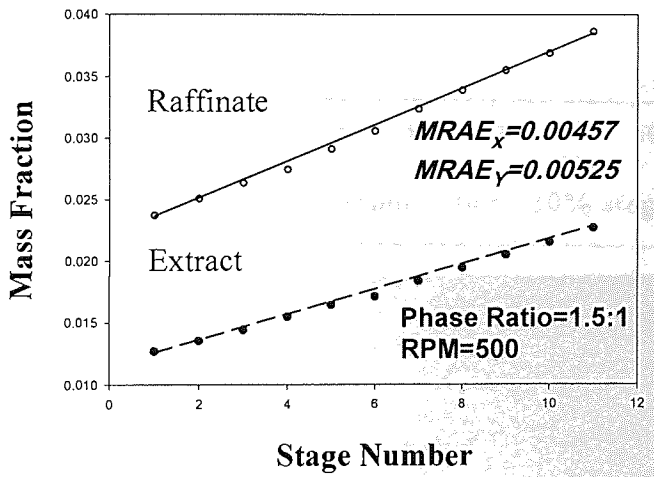

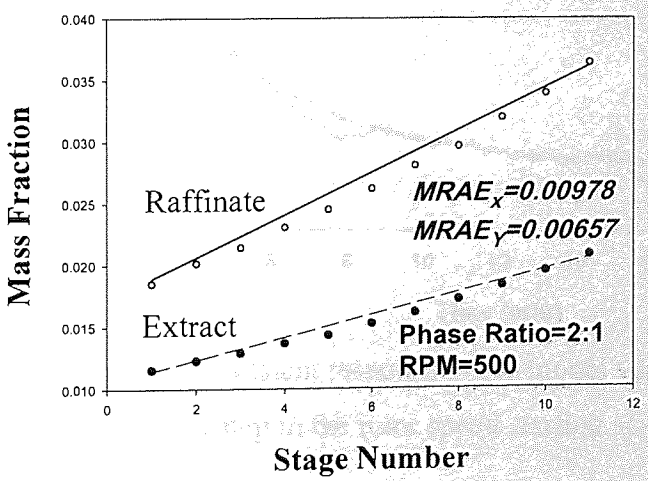

Figure(4.9) Experimental and calculated concentration profiles at an agitator speed of 8.33 s^{-1} for three different phase ratios.

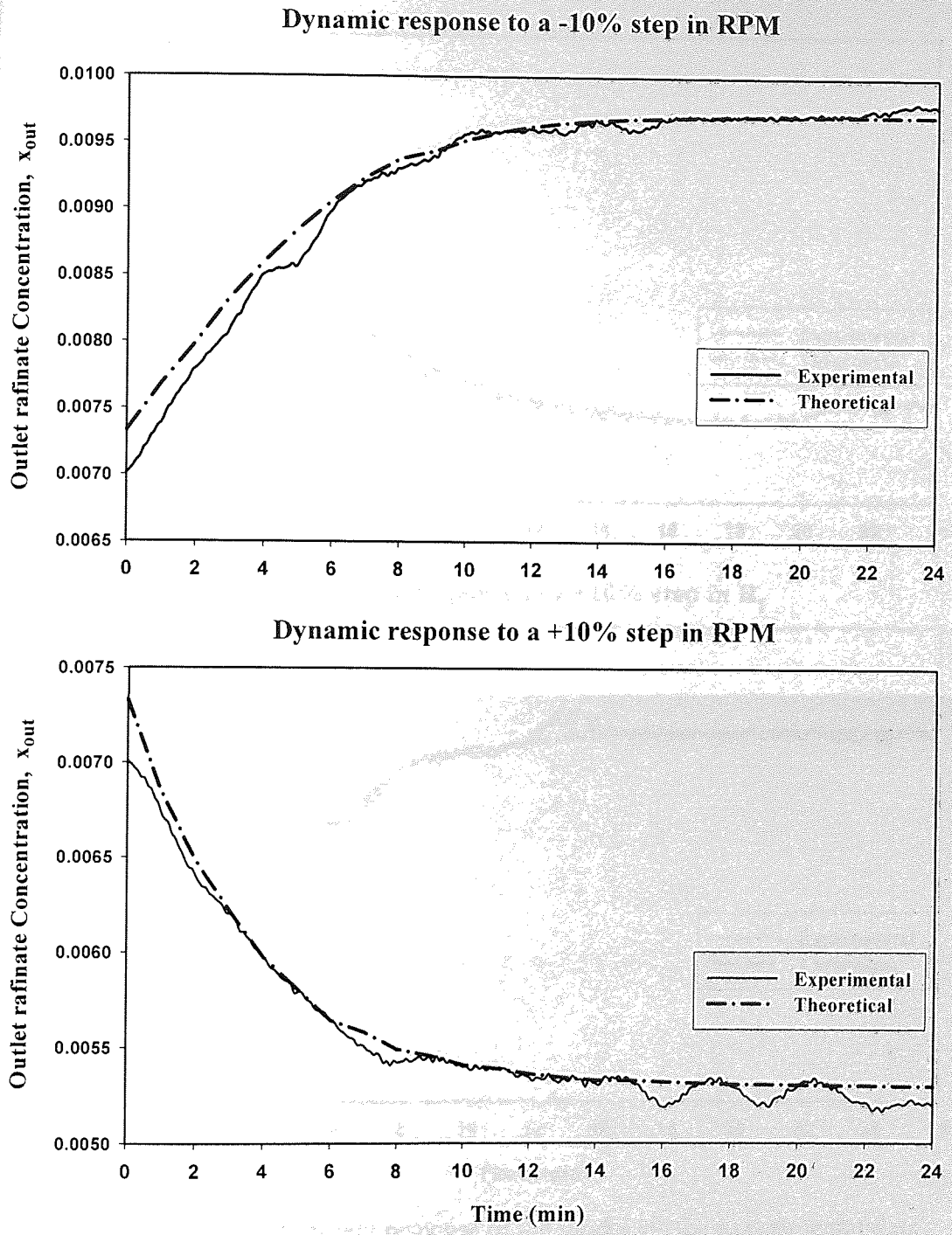

Figure (4.10) Dynamic transient response of the model vs. the experimental data for a ±10% step in the rotor speed starting at 400 RPM.

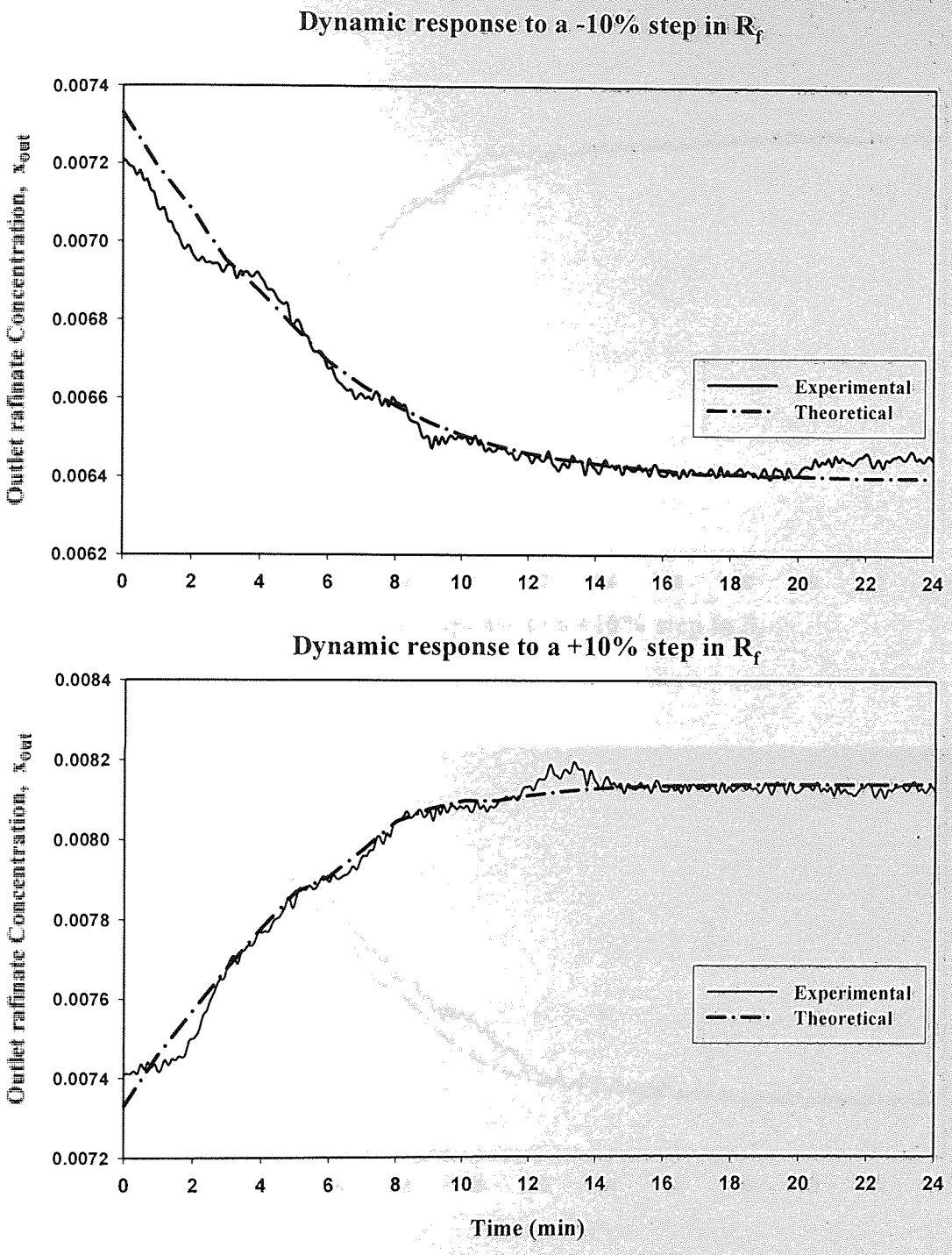

Figure (4.11) Dynamic transient response of the model vs. the experimental data for a ±10% step in the feed flowrate at 250 cm^3/min.

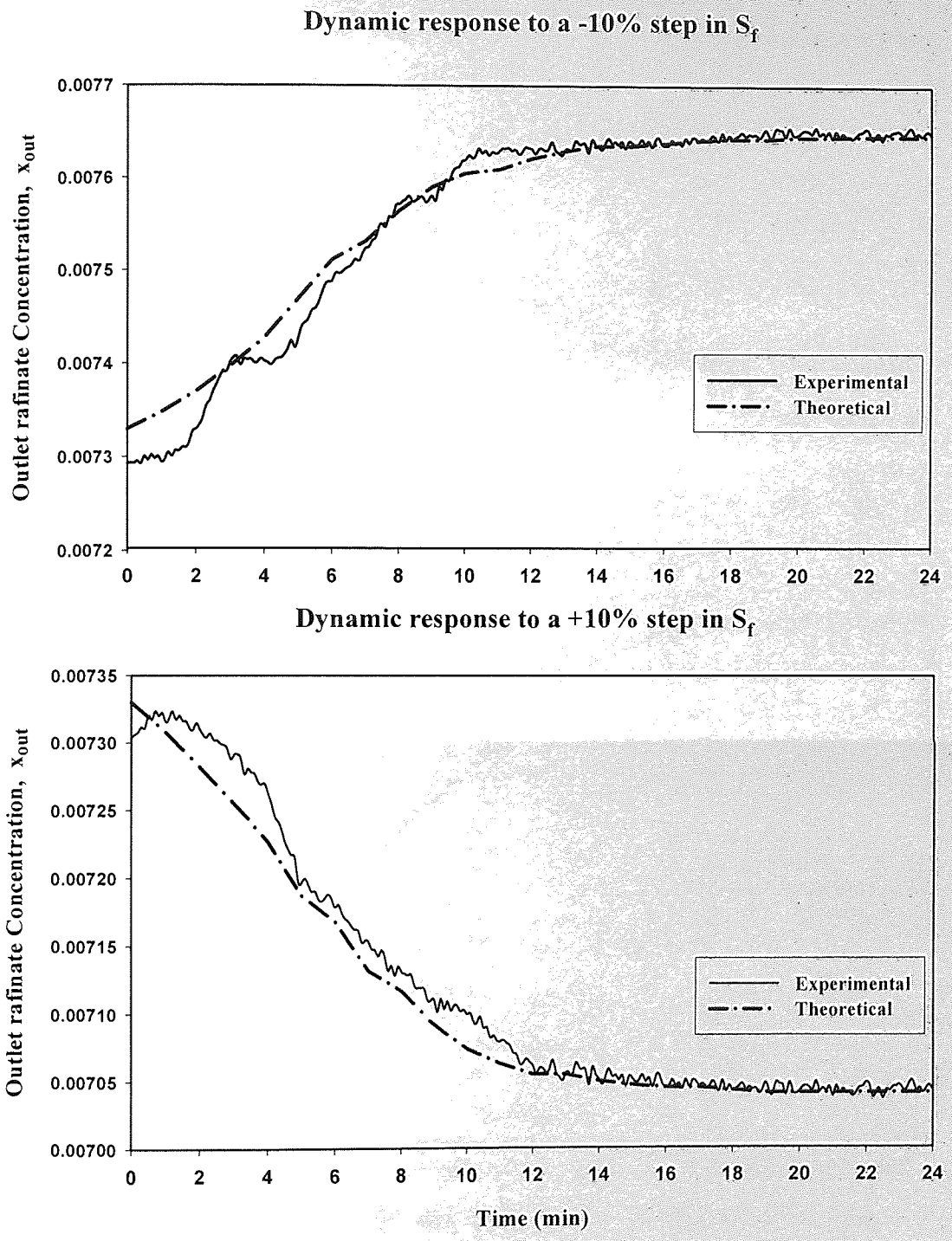

Figure (4.12) Dynamic transient response of the model vs. the experimental data for a ±10% step in the solvent feed flowrate at 250 cm^3/min.

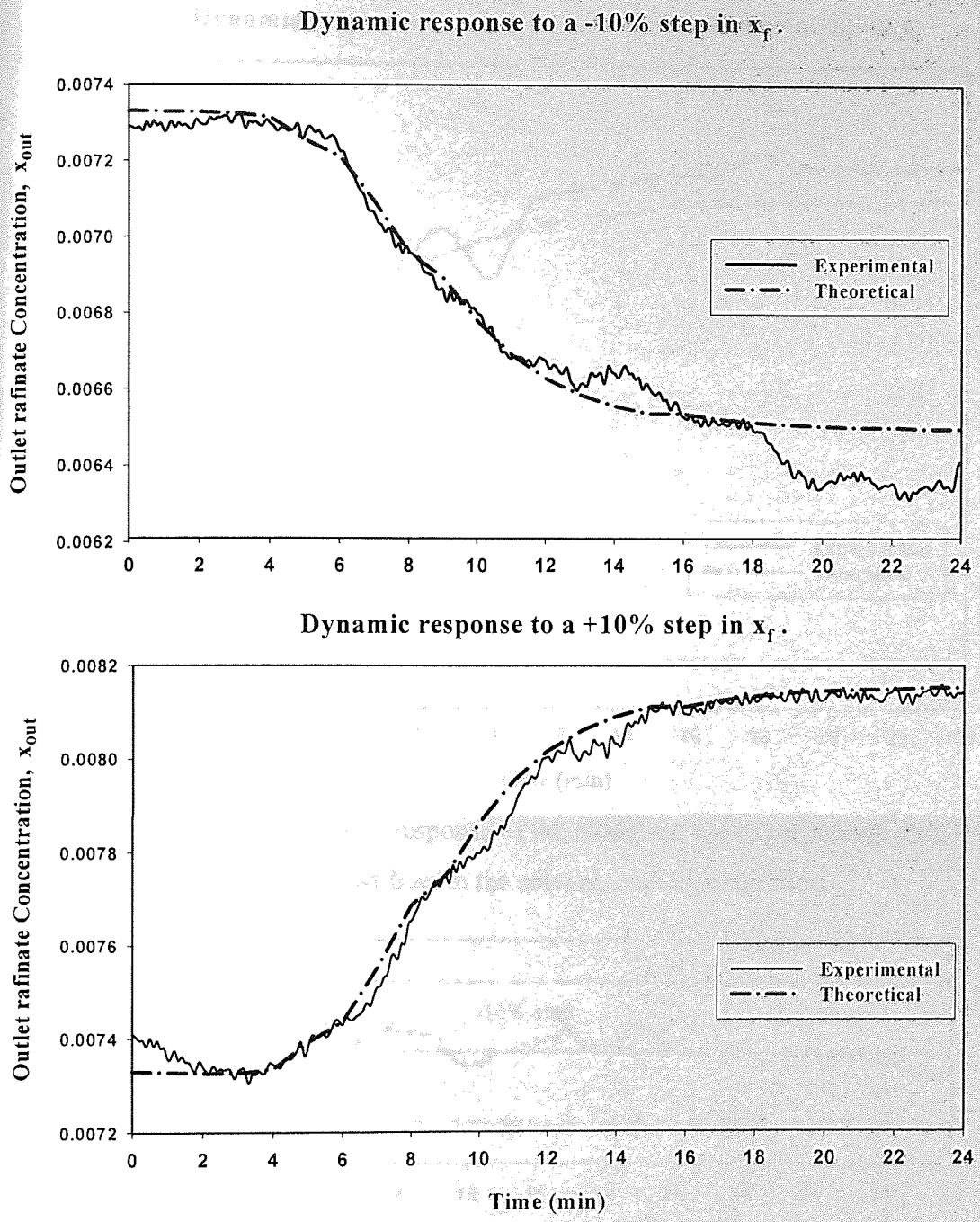

Figure (4.13) Dynamic transient response of the model vs. the experimental data for a ±10% step in the feed concentration starting at 0.02 wt frac.

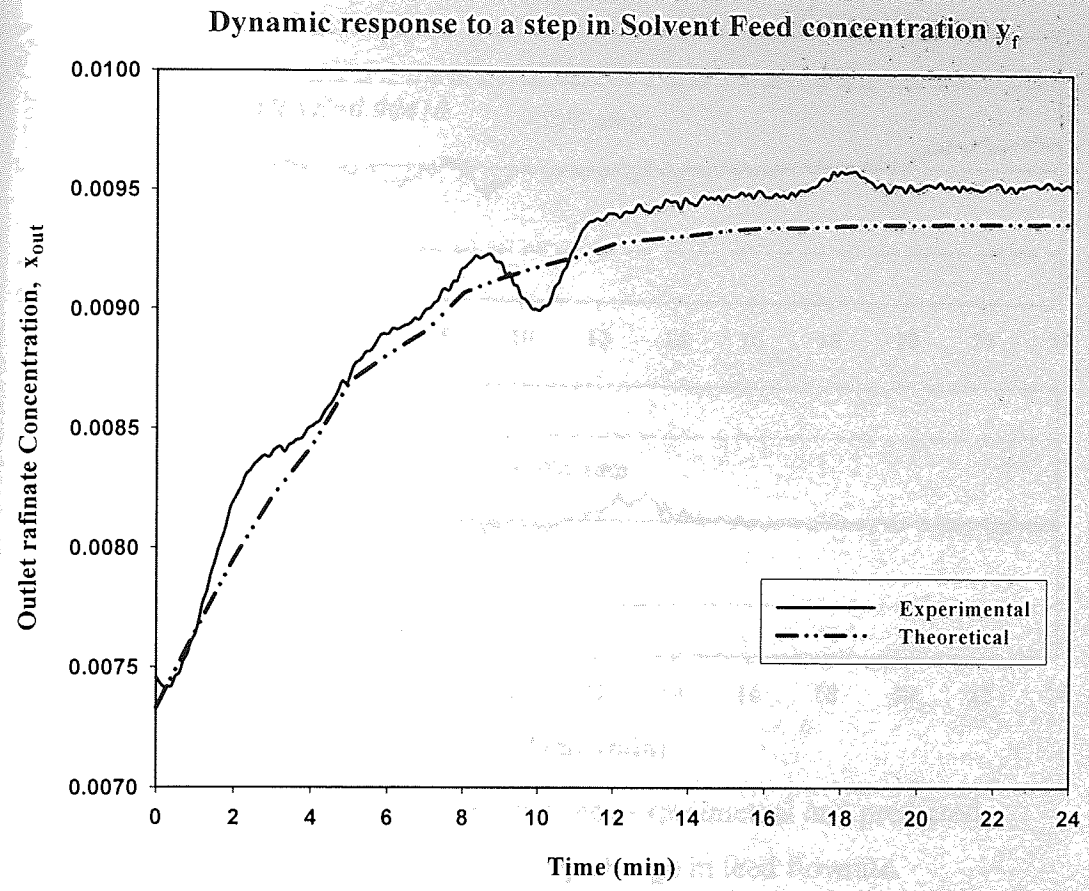

Figure (4.14) Dynamic transient response of the model vs. the experimental data from 0.0 to 0.05 wt frac. in the solvent feed concentration.

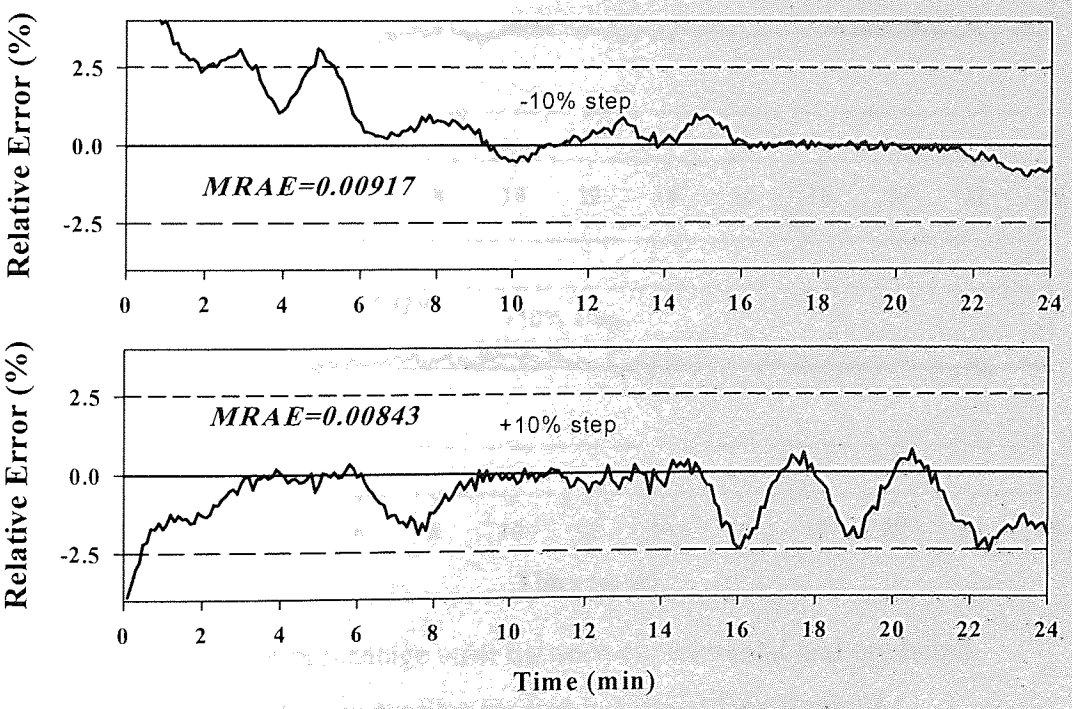

Figure(4.15) Relative percentage error between experimental and predicted concentration profiles for step change in rotor speed.

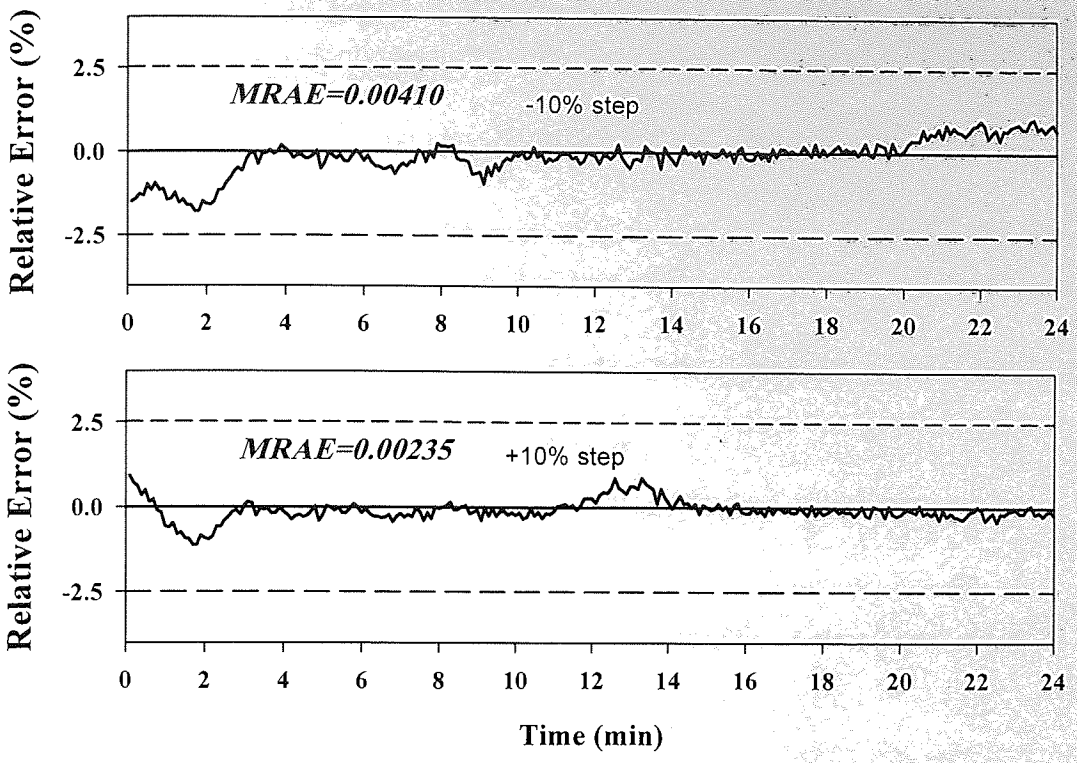

Figure(4.16) Relative percentage error between experimental and predicted concentration profiles for step change in feed flowrate.

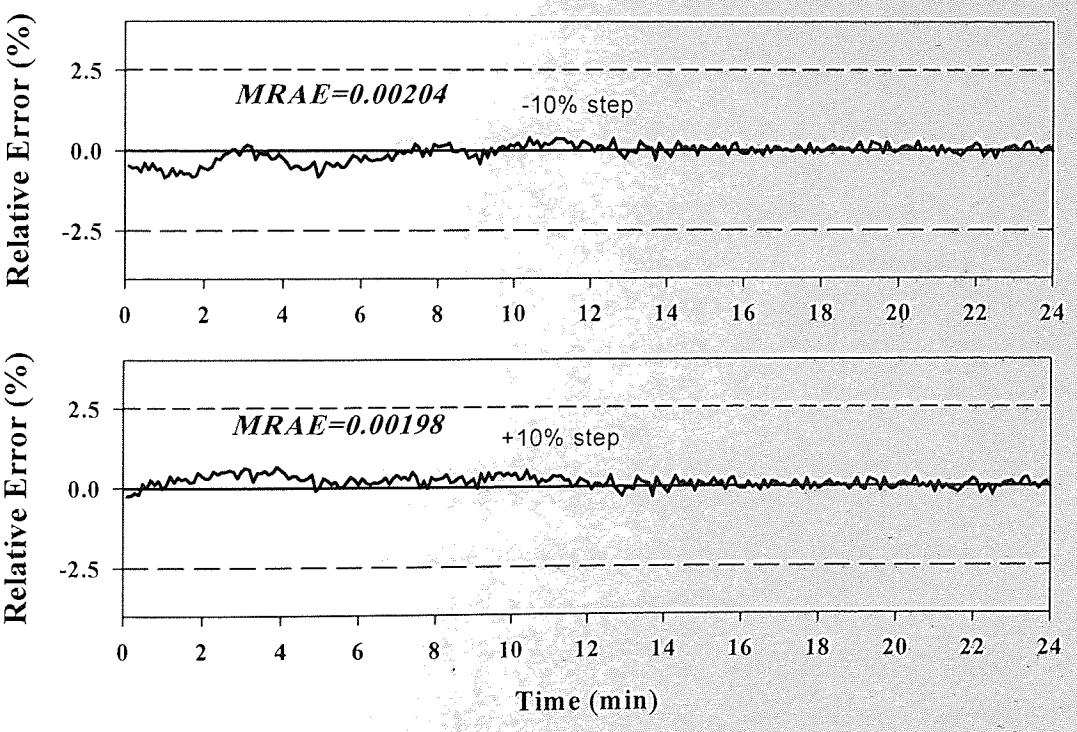

Figure(4.17) Relative percentage error between experimental and predicted concentration profiles for step in solvent feed flowrate.

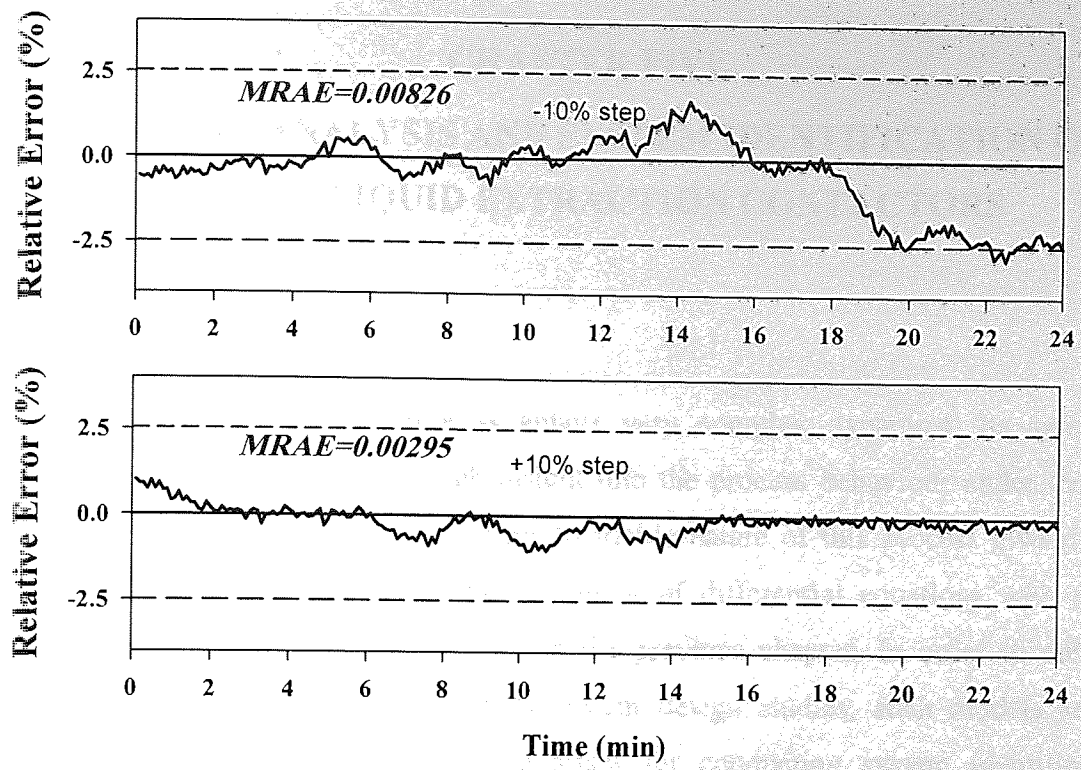

Figure(4.18) Relative percentage error between experimental and predicted concentration profiles for step in feed concentration.

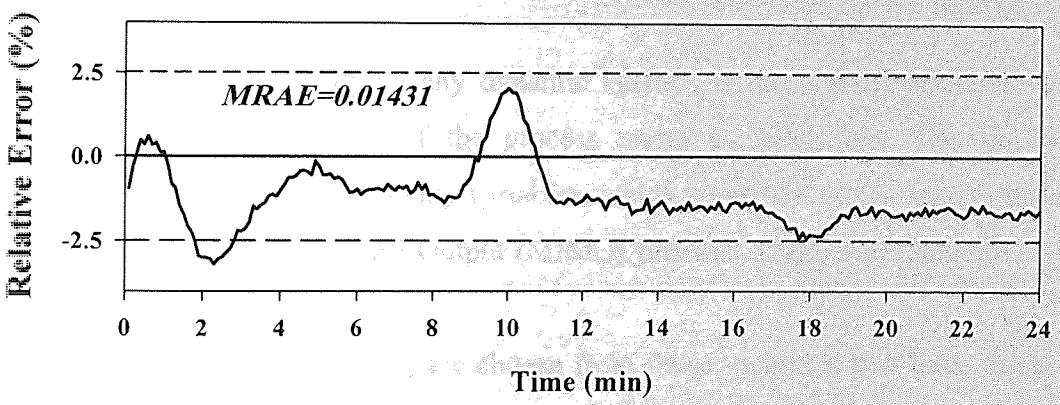

Figure(4.19) Relative percentage error between experimental and predicted concentration profiles for step in solvent feed concentration.

CHAPTER FIVE

DYNAMIC ANALYSIS AND SYSTEM IDENTIFICATION OF LIQUID-LIQUID EXTRACTION CONTACTORS

5.1 Introduction

Liquid-liquid extraction process entails very complex dynamics. Its safe and efficient operation needs thorough insight into the process behaviour under the full range of operating conditions. The multivariable nature of this process give rise to mathematical models involving large number of differential equations with many algebraic equations as was discussed in the previous chapter. In order to conduct system dynamic analysis and control system design studies, such models are of limited usefulness and a great need arises for conducting system identification strategies to arrive at more relevant models for such applications.

System identification involves building a dynamical model from an input/output data and without use of any laws concerning the fundamental nature and properties of the system.

The first step in studying any dynamic system, is the classification of variables involved in the operation of the process under consideration. The liquid-liquid extraction process involves many variables, which contribute to its operation, and this makes it a Multi-Input Multi-Output (MIMO) process. These variables are classified as follows:

Manipulated variables (MVs) are chosen from those variables that have direct effect on the process performance, and practically easy to actuate. In our case, these are: rotor speed (N) and solvent feed flowrate (S_f). The *Load variables* (DVs) involve variables that may experience fluctuation which causes instability during the operation of the column. Three variables fall in this category namely; the feed concentration (x_f), the solvent feed concentration (y_f) and the raffinate feed flowrate (R_f). The *controlled variables* (CVs) are selected from the process outlet streams that are usually of foremost importance such as the outlet raffinate concentration (x_{out}) and the extract outlet concentration (y_{out}). A schematic diagram representing the previously mentioned variables is shown in Figure(5.1).

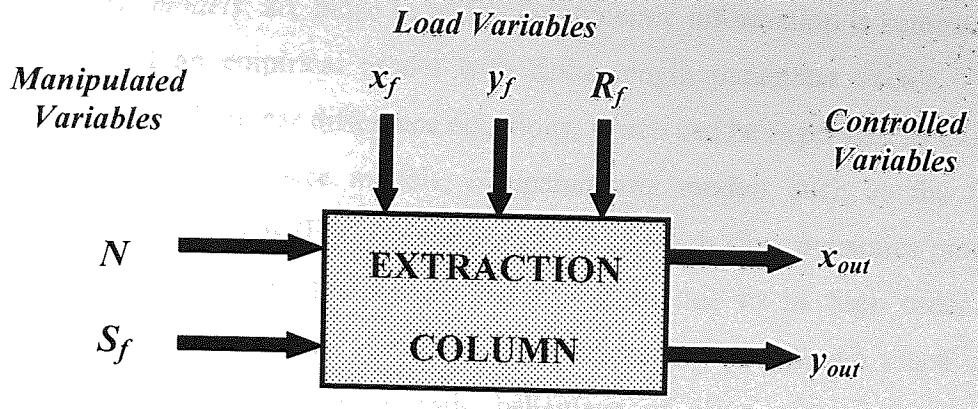

Figure 5.1: Representation of variables in an extraction column as a MIMO system.

Studying the system dynamic behaviour under different operational conditions is a prerequisite to the good selection of the control scheme. This could be achieved by making some deterministic tests either in real plant or in the physical model that properly and adequately fits the actual process. The input-output relationships are studied using the open-loop dynamic response of the process, which can be determined from the process model by stepping different inputs and recording output responses. Starting from steady state conditions, each input is perturbed with certain magnitude that is enough to show the effect on the system dynamics.

The input-output data obtained from the step testing are useful in verifying that the process is stable and in determining the approximate settling time, which will be used to design the test signal to be employed in system identification.

In the identification process, a test signal such as pseudorandom binary sequence (PRBS), sum of sinusoids or a sequence of step changes is introduced to the system. For multivariable systems, manipulated variables are either stepped separately or together. In order to utilize the data obtained from signals introduced for estimation and control system design it is necessary to select model structure to represent the data. The reduced-order model representation of data can be classified into two main categories:

1- *Nonparametric models*: are those in which the dynamic information is summarized in the form of plots, tabulated data or frequency functions which cannot be represented as a set of finite parameters. These models are identified using nonparametric identification methods such as *step response model*, and *impulse response model*.

2- *Parametric models*: are those in which the dynamic information is summarized in the form of an empirical model with finite length parameter vector. These models are typically linear difference equations, which can be expressed as transfer functions or as state space models. Nonparametric models such as the finite impulse response models (FIR) are irrelevant for use with slow dynamics process. This is because their model variance error is high due to its high order and truncation causes bias errors to increase. The parametric models are much more efficient in representing the dynamic behaviour of slow processes than the truncated impulse response models (Zhu Y. 1998). Another advantage of these models is that they are able to utilize data having relatively large noise or disturbances in the output.

Among the many different types of models, the linear time-invariant (LTI) models gained popularity for their use in petrochemical plants. Figure (5.2) shows the different types of the LTI models and the relation between them. The arrows indicate existence of reliable transformation algorithms.

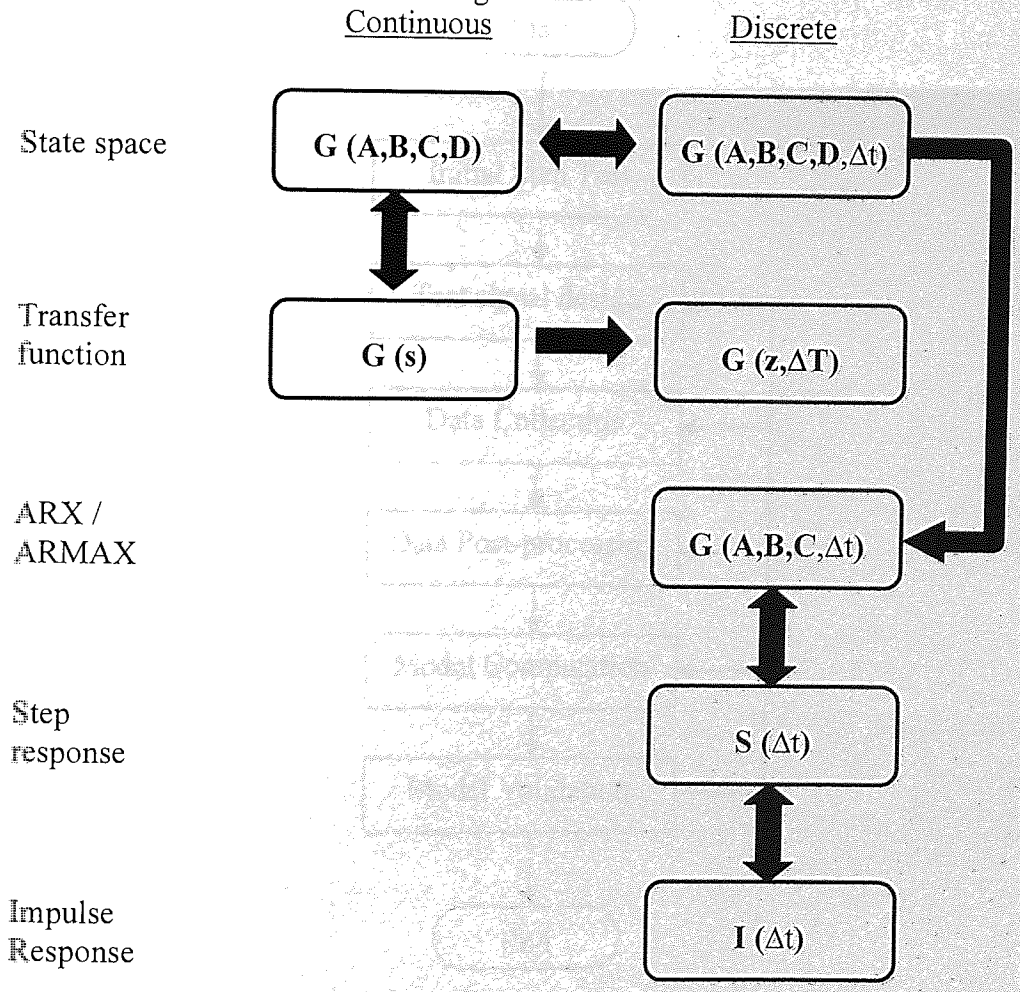

Figure(5.2): Linear time-invariant models and the relations between them.

In the figure (5.2), the ARX (Auto-Regressive with Exogenous input) has the form:

$$A(z^{-1})y(t) = B(z^{-1})u(t) + e(t) \quad (5.1)$$

And the ARMAX (Auto-Regressive with Moving Average Exogenous input) has the form:

$$A(z^{-1})y(t) = B(z^{-1})u(t) + C(z^{-1})\, e(t) \quad (5.2)$$

where $A(z^{-1})$: system poles polynomial.

$B(z^{-1})$: input zeros polynomial.

$C(z^{-1})$: noise zeros polynomial.

$y(t), u(t),$ and $e(t)$: output, input and noise vectors respectively.

The term auto-regressive indicates that the output depends explicitly on past outputs.

Process identification is an iterative process. It can be pictured as shown in Figure(5.3).

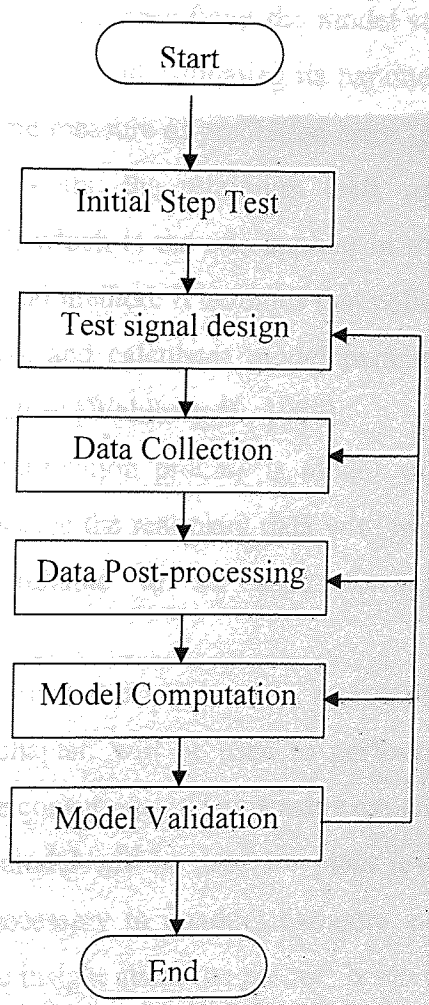

Figure(5.3) The system identification procedure flowchart

Initial single step testing is a preliminary practice done to verify that subsequent testing will be performed correctly, and give an insight about the process to be identified concerning linearity, stability, settling time and give the engineer a proper value of input signal amplitude to be used later in the test. The test signal is designed to be long enough to be sufficient for identifying process gain. Also short steps should be available to enable identification of dead time.

Data collection should be done carefully putting in mind consistency of operating conditions during testing. It should be done avoiding undesired limits of the process such as flooding and phase inversion of the column. Also all disturbances should be noted during the test.

After test data is collected, pre-processing of data is performed to remove unwanted effects on the model to be designed, and to discard things like high frequency noise, unwanted data sections, spikes, outliers (unwanted individual data points), and steady state information (using hi-pass filtering) (Ljung L. 1987).

The next step is concerned with specifying the model structure (from the list of LTI models mentioned previously) and estimating its parameters. The parameters are calculated by minimizing some measure of prediction error (prediction error method). Available estimation methods are; the minimum least squares method, and the maximum likelihood method, which is the one applied in this work. The maximum likelihood method is a statistical method. It assumes that collected data is the one that most likely to have observed, and calculates model parameters that maximize the probability of the observed values [Wahlberg B., 1989].

The final step in the identification process is model validation. The identified model is the one that can describe the real plant data with minimal deviations so that the derived models are reliable to be used for control system design [Andersen et al. 1991].

The rigorous model described and validated to represent the process behaviour efficiently, in the previous chapter, will be used to perform plant testing and this eliminates the need to do time consuming and expensive experimental plant testing. Since the rigorous dynamic model will be used for plant testing for the purpose of system identification, it is necessary to conduct dynamic analysis on the rigorous model. This analysis will give insight about the process behaviour in terms of settling time, gains, and nonlinearlity for different process variables.

After plant testing, the collected input-output transient profiles will be utilized to derive simplified reduced-order linear models. These models can be implemented in different control design strategies instead of the rigorous model.

In the field of liquid-liquid extraction modelling, previous studies were concerned principally on rigorous dynamic modelling in time domain and very modest amount of work dealt with system identification for the purpose of control system design and analysis. Even for the limited literature available in this area, the Scheibel extraction column was not considered for such studies, and work was concentrated on mixer-settlers, and other columns such as pulsed, and reciprocating plate columns. The reported work was concerned with identifying the process by studying each variable separately, without the effect of other variables.

5.2 Process Identification technique:

5.2.1 General approach

The control of industrial processes must be carried out using a multivariable approach to handle interaction of process variables and make sure of the process stability under different regulatory and servo types of operations. Despite this, the process identification is achieved using single-variable techniques. Identification experiments are performed by carrying what so called step tests, in which, each manipulating variable (MV) and disturbance variable (DV) is stepped separately and the process variables responses are used for estimating a reasonable transfer function relating this MV to all controlled variables (CVs) of the process.

In practice this approach works fine for stable processes, but the cost is very high. The product qualities may be disturbed by stepping the MVs. The test time is very long, which occupies much manpower and makes production planning difficult. The tests are done manually, which dictates extremely high commitment of the engineers and operators; it is not unusual that such tests are carried out around the clock.

To reduce these consequences and to improve the identification, other alternatives can be adopted. One approach is the use of PRBS (pseudo random binary sequence) for the single variable tests, which will reduce disturbances to product qualities. Another approach is to estimate multivariable finite impulse response (FIR) models using the data from a sequence of single variable tests. This reduces disturbance to production

by allowing operator intervention during the tests. The engineer has still to do some trial-and-error tests, and hence the costs of identification remain high.

5.2.2 Asymptotic Method of Identification (ASYM)

In this study, the asymptotic identification method was used for the multivariable process identification. This method was originally developed for the purpose of linear robust control by Zhu *et. al.* (1993), and later was modified for using it with model predictive control (MPC) applications.

The power of ASYM approach stems from the fact that it provides systematic solutions to the four fundamental problems of identification: 1) test design for control, 2) order/structure selection, 3) parameter estimation and 4) model validation.

The name *asymptotic method* is based on the asymptotic theory of identification developed by Ljung (1985), for single variable version and Zhu (1989) for multivariable extension. The highlight of the method is described in Appendix (B). The ASYM method was implemented in the identification software *Tai Ji ID* [Zhu, and Ge 1987]. ASYM was applied successfully to over 50 industrial processes for MPC control, mainly in refinery and petrochemical industries.

The generated input/output response data from the plant testing are read into the Tai-Ji ID friendly user interface driver that uses these data to determine a number of different but equivalent reduced linear models such as discrete linear state space model, discrete and continuous linear first order with dead time transfer function models.

The final step in the system identification is model validation. The best identified model is the one that can describe the real plant data with minimal deviations so that the derived models are reliable to be used for control system design. Tai-Ji ID has implemented a strategy for grading the model by comparing the relative size of the error bound with the model over the low and middle frequencies. Four grades can be realized as follows:

Grade **A**: very good transfer function, error bound $\leq$ 30% model.

Grade **B**: good transfer function, error bound $\leq$ 60% model.

Grade **C**: marginal transfer function, error bond $\leq$ 90% model.

Grade **D**: poor or no transfer function exists, error bound > 90% model.

It has been indicated from project experience and extensive simulations that usually models with grade *A* or *B* can be used in control design, where as those of grades C and D are rejected.

5.3 Results and Discussions

Before conducting the system identification technique described above, the rigorous model was tested to gain a good picture of its behaviour in order to set the basis for the plant testing to be used for system identification.

5.3.1 Dynamic Analysis

The rigorous dynamic model of the extractor is used here to study the dynamic behaviour of the process via step testing of each of the input variables and observing the transients of the output variables. The step for each variable is selected large enough to acquire the sought dynamics, and at the same time not to exceed the operational physical limits of the process under investigation. The same step is repeated in the negative direction in order to inspect the non-linear behaviour of the process. The profiles of each variable are compared for consistency. This technique gives a very good picture of the effect of each variable and the behaviour of the process under the presence of excitations.

The previous procedure was applied for the Scheibel extraction column model, and the step testing was performed on the following five variables: *rotor speed* (N), *solvent feed flowrate* (S_f), *inlet feed concentration* (x_f), *inlet solvent concentration* (y_f), and *feed flowrate* (R_f). The interface level at the top of the column was assumed to be fixed during simulations. In practice this can be achieved by installing an interface level feedback controller with either, the outlet extract flowrate or the outlet raffinate flowrate as manipulated variables. In the following paragraphs, the effect of each one of the tested variables is explained in terms of process dynamics.

The effect of rotor speed was the first variable to be studied. Figure (5.4) shows the effect of positive and negative steps on the outlet concentrations profiles. The ±10% steps around the operating speed of 400 rpm ensures the operation of the column within the stable region far away from flooding which will occur at 588 rpm. Under such conditions the effect of backmixing is not significant, and as a result the

stage efficiency experiences an increase in value as a function of rotor speed. As a result a positive step in rotor speed increases mass transfer within mixing zones. Consequently, the raffinate solute concentration decreases with time while the extract concentration increases. This observation was indicated by the transients of outlet concentrations.

Examining the figures reveals that the process reaches steady state after 10 min in the case of extract concentration profile with a time constant of less than one minute, where as it needed 15 min for the raffinate to settle with a time constant of about 3 min. This indicates that the extract concentration has a faster dynamics. From the small difference in the process gains and the presence of overshoot, it is clear that the process has some non-linearity at these conditions.

Figure(5.5) shows the effect of solvent feed flowrate step testing on the column outlet concentrations. The ±10% steps around the operating solvent feed flowrate of 250 cc/min are within the safe operation of the column. As the solvent feed flowrate increases, more Acetone is extracted from the aqueous phase. This causes the outlet raffinate concentration to decrease. Consequently, the extract outlet concentration decreases because the solvent residence time gets shorter and the Acetone content per unit volume of solvent becomes relatively less. The converse of this behaviour was realized for the decrease in solvent flowrate.

The speeds of responses for both concentration profiles were the same as those attained from the rotor speed step change dynamics. Again it is clear that the extract dynamics is faster, and it has higher gain than that of the raffinate. The profiles of the positive and negative steps were consistent in terms of trend, but the presence of small gains difference indicates that some non-linearity is available at these operating conditions.

The dynamics of the process due to changes in the feed concentration is shown in Figure(5.6). An increase in the feed concentration affects the Acetone concentration throughout the column and consequently, the raffinate outlet concentration will exhibit a steady increase during the whole spectrum of the process transient. This increase in the Acetone concentration increases the mass transfer driving force and as a result, more Acetone will be extracted by the solvent and consequently the extract concentration profile will build-up continuously.

From the figure it can be observed that the process has a slow dynamics with a settling time of 15 min (i.e. 60% of the total simulation time), and a time constants of about 4 min.

It is also noticed that a time delay of about 4 min was present in the raffinate concentration profile. This was due to the fact that any change in feed concentration needs some time for it to propagate through the column and reach the other end at the raffinate exit. This is similar to the presence of a transportation lag in the raffinate concentration dynamics. This behaviour was not observed for the case of the extract phase where the feed inlet is close to the extract outlet, and any change in the former is reflected spontaneously in the later.

The dynamics is uniform for both directions of step changes and both phases exhibit approximately equal gains. This is expected since the dynamics of this disturbance is mainly due to mass transfer effects and the process hydrodynamic was not involved.

Figure(5.7) shows the effect of change in solvent feed concentration. The profiles indicate that an abrupt increase in solvent concentration causes both phases outlets solute concentration to increase. This behaviour is due to the fact that the sudden increase in Acetone concentration in the solvent feed decreases the mass transfer driving force and less Acetone will transfer between the two phases and consequently the raffinate will be richer in Acetone than before the step change. For the extract phase the increase in the feed concentration results in overall increase of Acetone in the organic phase throughout the column which will eventually reach the end of the column where the outlet extract exits. That's why both phases have the same change trend, but it is noticed that the extract phase was much faster than the raffinate phase as the case with other disturbances. Comparing this behaviour to that of changing the aqueous phase feed concentration it is found that the solvent behaviour is so fast that there is negligible delay of response. This is because the solvent phase droplets travel through the column with fast speed due to the effect of buoyant force and this makes any change in the feed travel throughout the column almost promptly.

It can be noticed that this transient response was similar in trend to that due to an opposite direction change in solvent flowrate with some difference in response gains magnitude.

Again the two profiles for the opposite step changes were consistent with each other, which supports the idea of process linearity under the studied operating condition.

The effect of raffinate phase inlet flowrate on the dynamics of the process is shown in figure(5.8). Honekamp et al. (1962) reported that, the continuous phase flowrate has negligible effect on the dispersed phase holdup but has significant effect on mass transfer. A positive step in the feed flowrate reduces the residence time of the aqueous phase in the column and consequently more Acetone will transfer through the column. This is also reflected on the organic phase, more Acetone will be transferred to it and its concentration will increase with time. The negative step in raffinate inlet flowrate has an opposite effect on both phases. Both profiles were slightly slow attaining steady state after about 15 min with time constants of about 3 min. The extract phase was slightly faster than the raffinate phase.

5.3.2 System Identification

From the above dynamic analysis, plant testing on the rigorous model was prepared for system identification. The identification step tests were performed using a series of step signals introduced for each manipulated and disturbance variable separately. The signals were alternating between positive and negative square steps with lengths and amplitudes appropriate to identify process gain and dead time. The number of these steps was chosen large enough to make sure of the efficient identification of the process with acceptable accuracy. Several positive and negative square steps were adopted in each test, spaning a simulation time of 350 min.

As mentioned previously, the *Tai-Ji ID* identification program was used for processing the simulated input/output data. This program calculates a number of different order but equivalent reduced order linear models in one of three forms:

Linear state space model:

$$\begin{aligned} \mathbf{x}_{k+1} &= \mathbf{A}x_k + \mathbf{B}\mathbf{u}_k \\ \mathbf{y}_{k+1} &= \mathbf{C}x_k + \mathbf{D}\mathbf{u}_k \end{aligned} \tag{5.8}$$

Discrete model:

$$\mathbf{y}(z) = \frac{z^{-m}\mathbf{B}(z^{-1})}{\mathbf{A}(z^{-1})}\mathbf{u}(z) \tag{5.9}$$

Continuous model:

$$y(t) = \frac{k_p e^{-\theta s}}{\tau s + 1} u(t) \qquad (1^{st} \text{ order}) \qquad (5.10a)$$

$$y(t) = \frac{k_p (\tau s + 1) e^{-\theta s}}{(\tau_1 s + 1)(\tau_2 s + 1)} u(t) \qquad (2^{nd} \text{ order}) \qquad (5.10b)$$

The most commonly used form of process models is the continuous Laplace domain form. Here the (N) output variables y_i are related to the (M) input variables m_i and (L) disturbance variables d_i by a set of N equations as follows:

$$\begin{aligned}
\mathbf{y}_1 &= \mathbf{g}_{11}\mathbf{m}_1 + \mathbf{g}_{12}\mathbf{m}_2 + \cdots + \mathbf{g}_{1M}\mathbf{m}_M + \mathbf{g}_{d_{11}}\mathbf{d}_1 + \mathbf{g}_{d_{12}}\mathbf{d}_2 + \cdots + \mathbf{g}_{d_{1L}}\mathbf{d}_L \\
\mathbf{y}_2 &= \mathbf{g}_{21}\mathbf{m}_1 + \mathbf{g}_{22}\mathbf{m}_2 + \cdots + \mathbf{g}_{2M}\mathbf{m}_M + \mathbf{g}_{d_{21}}\mathbf{d}_1 + \mathbf{g}_{d_{22}}\mathbf{d}_2 + \cdots + \mathbf{g}_{d_{2L}}\mathbf{d}_L \\
&\vdots \\
\mathbf{y}_N &= \mathbf{g}_{N1}\mathbf{m}_1 + \mathbf{g}_{N2}\mathbf{m}_2 + \cdots + \mathbf{g}_{NM}\mathbf{m}_M + \mathbf{g}_{d_{N1}}\mathbf{d}_1 + \mathbf{g}_{d_{N2}}\mathbf{d}_2 + \cdots + \mathbf{g}_{d_{NL}}\mathbf{d}_L
\end{aligned} \qquad (5.11)$$

where :

g_{ij} *and* $g_{d_{ij}}$: SISO transfer functions for process and disturbance relating output variable i to input or disturbance variable j. For convenience this set can be represented in MIMO matrix representation as follows:

$$y = G\begin{pmatrix} m_1 \\ \vdots \\ m_M \end{pmatrix} + G_d \begin{pmatrix} d_1 \\ \vdots \\ d_L \end{pmatrix} \qquad (5.12)$$

Here G is the process transfer function matrix and G_d is the disturbance transfer function matrix.

For the extraction process, where two output variables are modelled with two input variables and three disturbance variables, equation (5.12) will be expressed as follows:

$$\begin{bmatrix} x_{out} \\ y_{out} \end{bmatrix} = G\begin{bmatrix} N \\ S_f \end{bmatrix} + G_d \begin{bmatrix} x_f \\ y_f \\ R_f \end{bmatrix} \qquad (5.13)$$

where $G = \begin{bmatrix} g_{11} & g_{12} \\ g_{21} & g_{22} \end{bmatrix}$ and $G_p = \begin{bmatrix} d_{11} & d_{12} & d_{13} \\ d_{21} & d_{22} & d_{23} \end{bmatrix}$

The identified matrices G and G_d are given below:

$$G = \begin{pmatrix} \dfrac{-5.4782\times10^{-5}e^{-0.5s}}{3.1121s+1} & \dfrac{-0.8036\times10^{-5}e^{-s}}{5.0295s+1} \\ \dfrac{8.2015\times10^{-5}(4.276s+1)e^{-0.5s}}{(0.2524s+1)(6.2667s+1)} & \dfrac{-3.047\times10^{-5}e^{-s}}{0.6281s+1} \end{pmatrix} \quad (5.14)$$

$$G_d = \begin{pmatrix} \dfrac{0.5907e^{-4s}}{3.312s+1} & \dfrac{0.3005e^{-0.5s}}{2.3449s+1} & \dfrac{3.117\times10^{-5}e^{-0.5s}}{2.0552s+1} \\ \dfrac{0.57599e^{-0.5s}}{3.015s+1} & \dfrac{0.69612e^{-0.5s}}{0.38208s+1} & \dfrac{0.7077\times10^{-5}e^{-s}}{3.2779s+1} \end{pmatrix} \quad (5.15)$$

As can be seen, all elements of the two matrices are of first order and the only exception is the N-y_{out} element which is of second order. This particular transfer function has the fastest dynamics among the other transfer functions due to the fast effect of the rotor speed changes on the solute mass transfer and consequently on the outlet extract concentration. Nevertheless, the first time constant of this element is of small magnitude which makes it close to a first order dynamics. So practically speaking, the two matrices have elements with first order dynamics with time delay.

Other equivalent forms of the identified process model were calculated and listed in Appendix (E). The selection of the models was done on the basis of minimum prediction error calculated by the program. These errors are shown in Table(5.1) below:

Table (5.1) Identification Errors and Type index for the modelled variables.

Modelled variable pairs	Modelling Error%	Model grade index
N - x_{out}	0.76239	A
N - y_{out}	0.38540	A
S_f - x_{out}	0.96830	A
S_f - y_{out}	0.63551	A
x_f - x_{out}	0.12356	A
x_f - y_{out}	0.2114.5	A
y_f - x_{out}	0.01413	A
y_f - y_{out}	0.54656	A
R_f - x_{out}	0.68792	A
R_f - y_{out}	0.74589	A

The step tests data and the corresponding transient responses for all variables studied are shown in the figures (5.9 to 5.14) as dotted lines. The corresponding identified model predicted responses are shown as solid lines. The profiles of both step trains are very close to each other with some gain offsets in certain cases. These small offsets indicate the non-linear behaviour of the process.

Models validation is done by comparing the simulation predicted profiles to the identified models ones. As can be observed from the figures (5.9 to 5.14), the reduced-models and the rigorous model gave excellent agreement with each other's. This agreement is supported by the percentage prediction error of models estimation given in Table (5.1) where all error values are below 1%. The degree by which the approximate models represent the dynamics of the system is the only measure for the reliability of system identification. Nevertheless, for this work, the identified models fit the process with high accuracy.

In order to used these models confidently for control purposes, the grade index generated by the identification program *Tai-Ji ID* should be examined. A model with grade A or B can be used for control system design, where as that of grade C or D is not appropriate, and it should be re-identified. Table(5.1) shows that the grades for all the identified reduced order models are of index A, which indicate that they are absolutely appropriate for control purposes.

The remarkable results obtained for the system identification give a great impetus for going on with control system design utilizing the calculated models. In the next two chapters the problem of control system design will be tackled utilizing the reduced order model developed in this chapter.

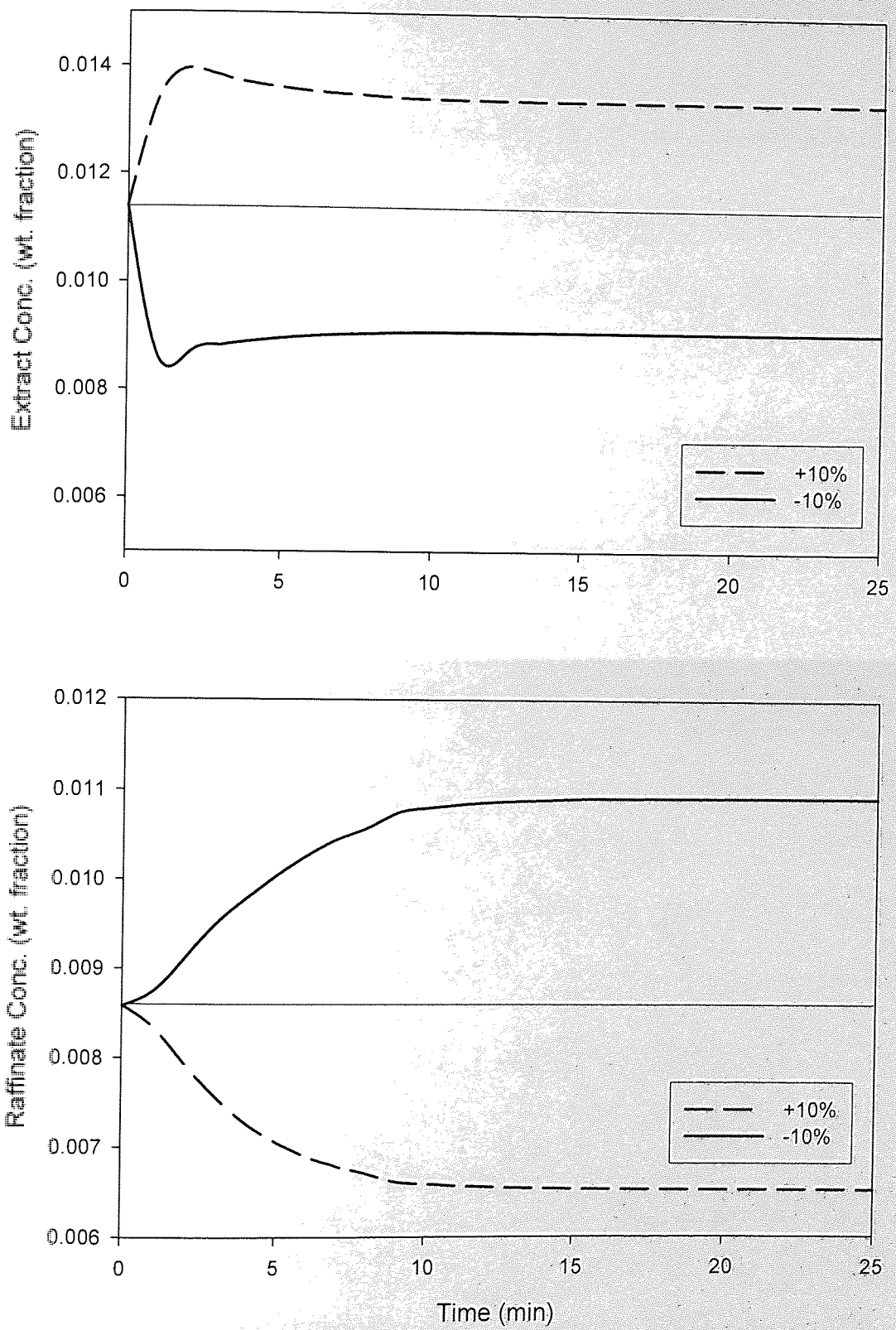

Figure (5.4) Column outlet profile for positive and negative 10% step change in the rotor speed Starting at a value of 400 rpm.

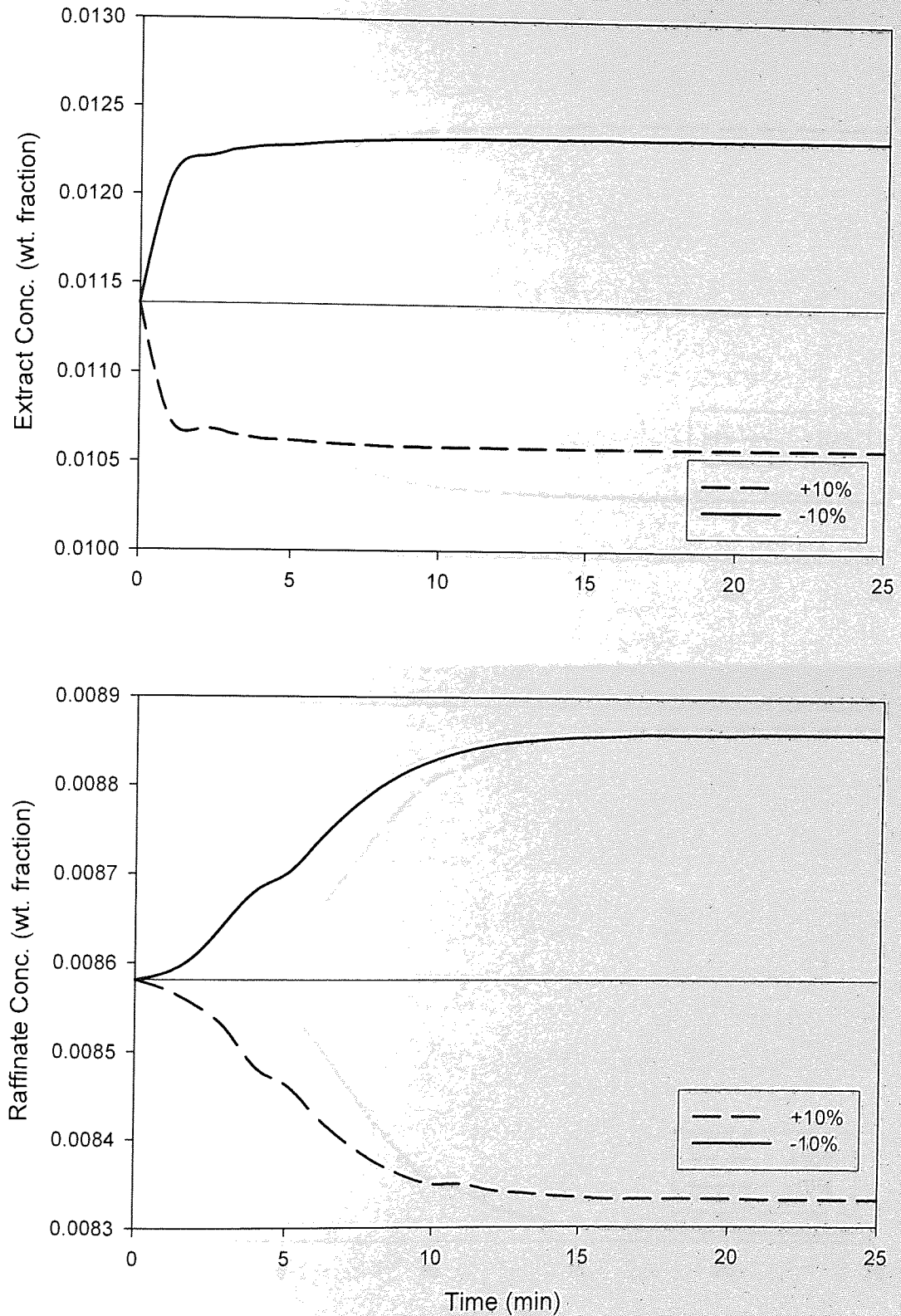

Figure (5.5) Column outlet profile for positive and negative 10% step change in the solvent feed flowrate starting at a value of 250 cc/min.

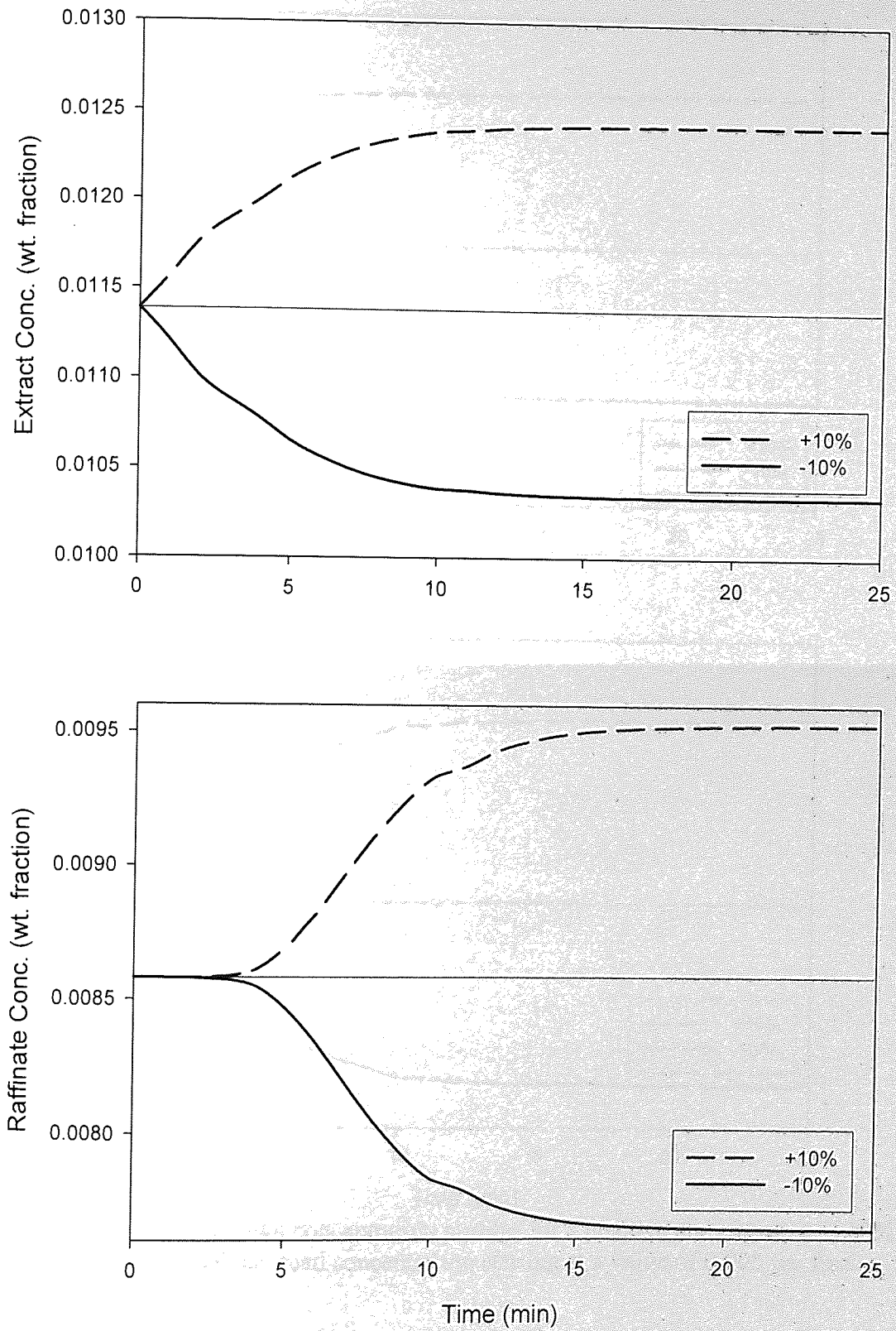

Figure (5.6) Column outlet profile for positive and negative 10% step change in the aqueous feed concentration starting at a value of 0.02 wt frac.

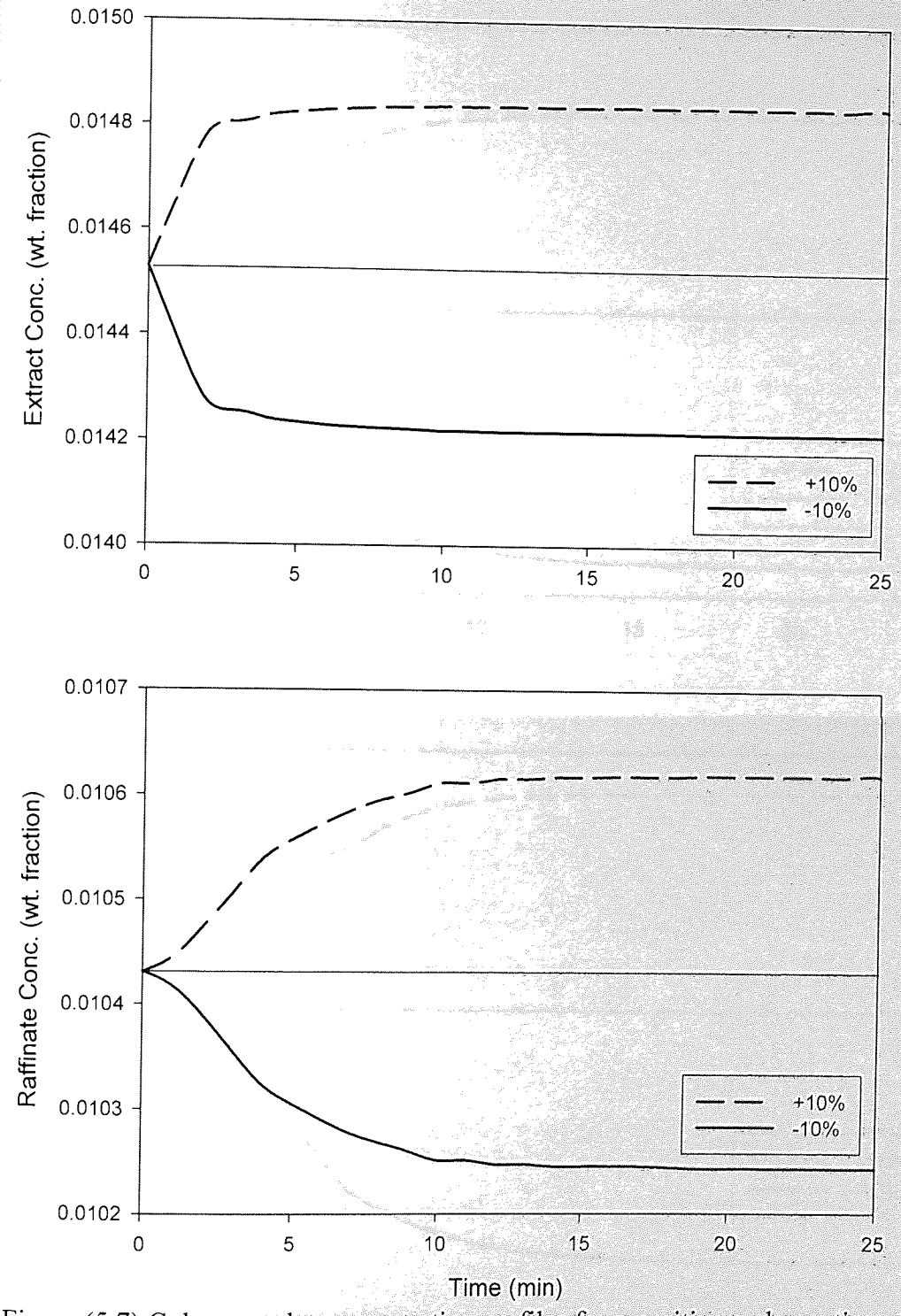

Figure (5.7) Column outlet concentration profiles for a positive and negative of 10% step change in the solvent feed concentration starting at a value of 0.005 wt. frac.

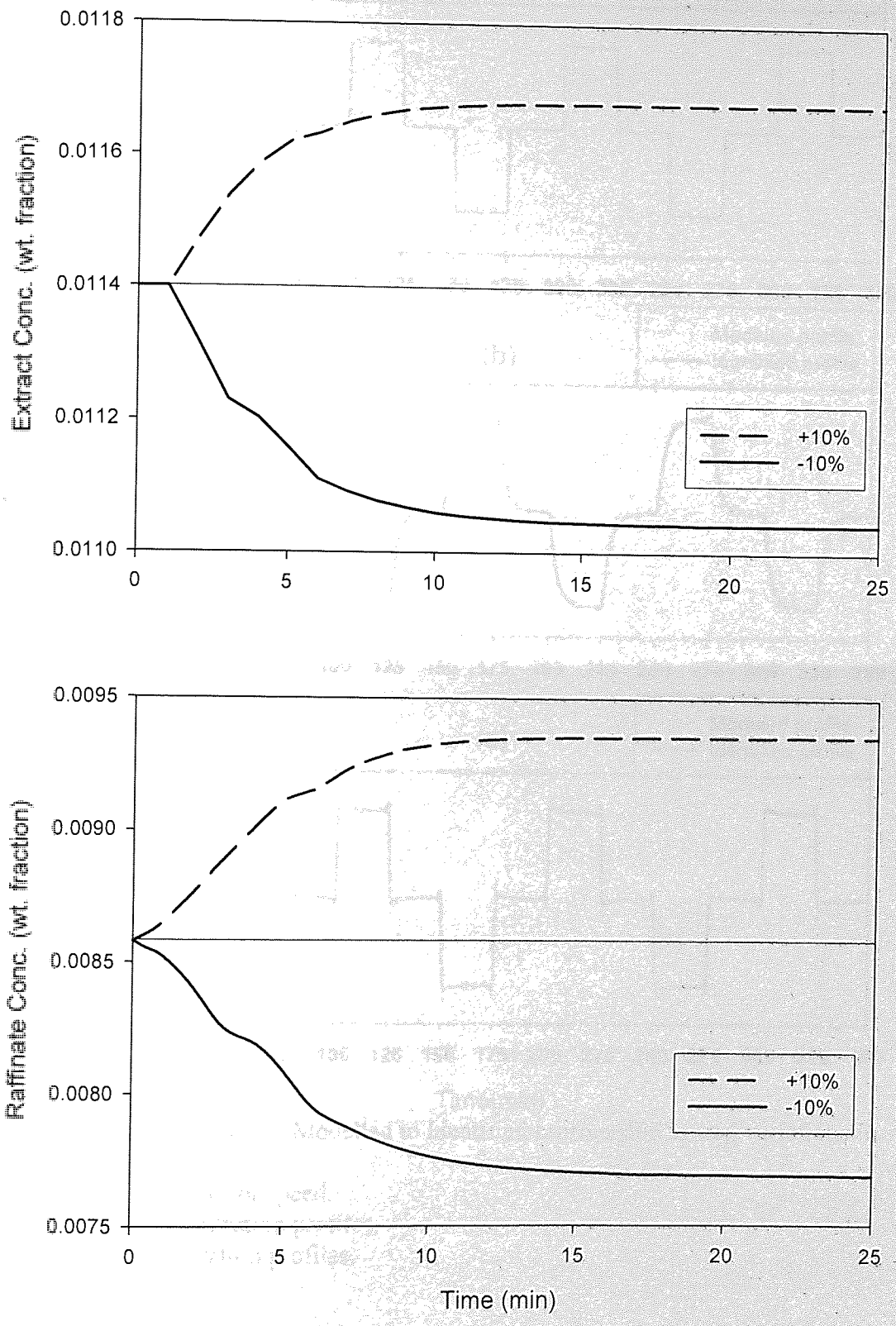

Figure (5.8) Column outlet profile for positive and negative 10% step change in the aqueous feed flowrate starting at a value of 250 cc/min.

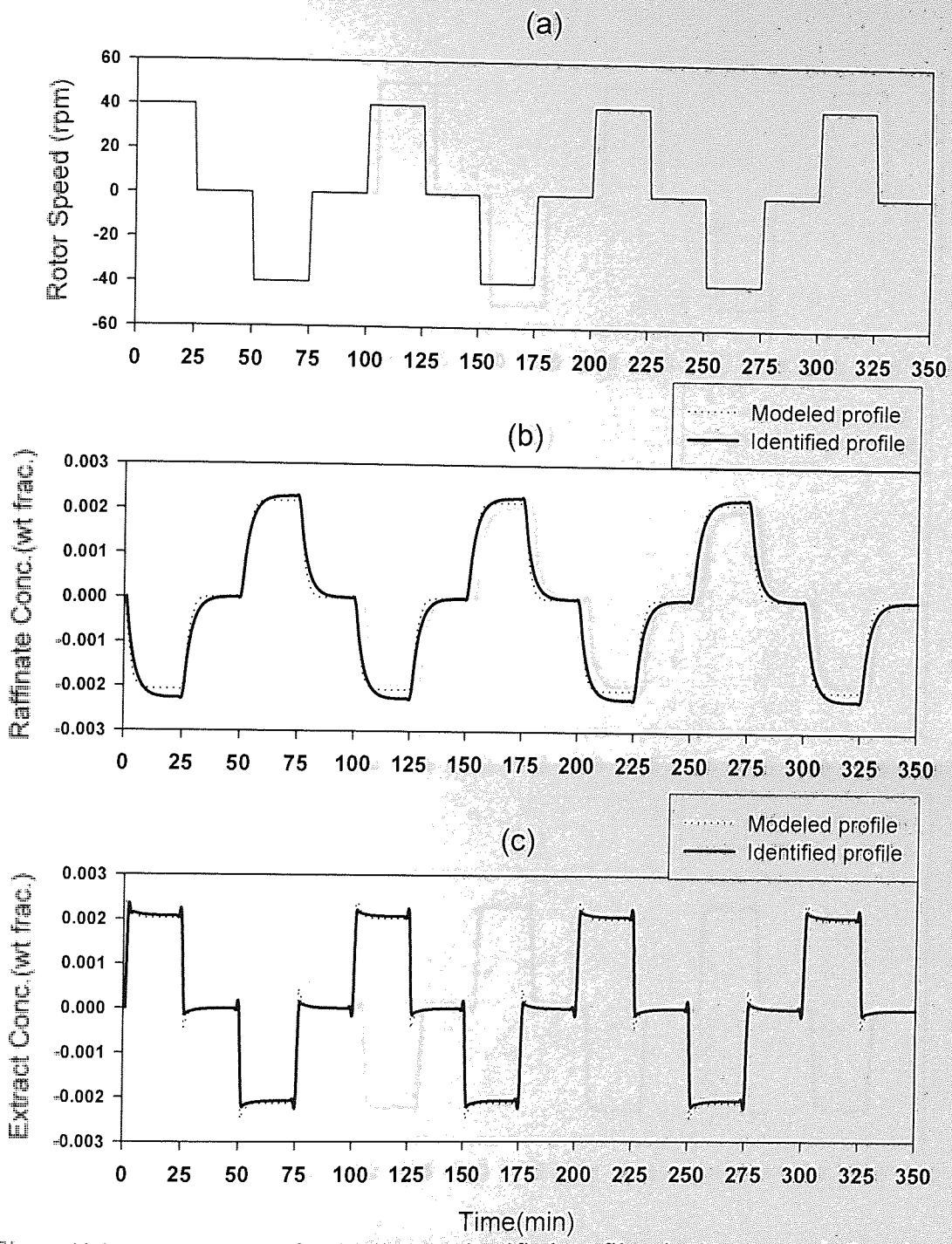

Figure(5.9) Comparison of Modelled to Identified profiles due to step variations in rotor speed:
(a) Step changes in rotor speed.
(b) Raffinate concentration profiles.
(c) Extract concentration profiles.

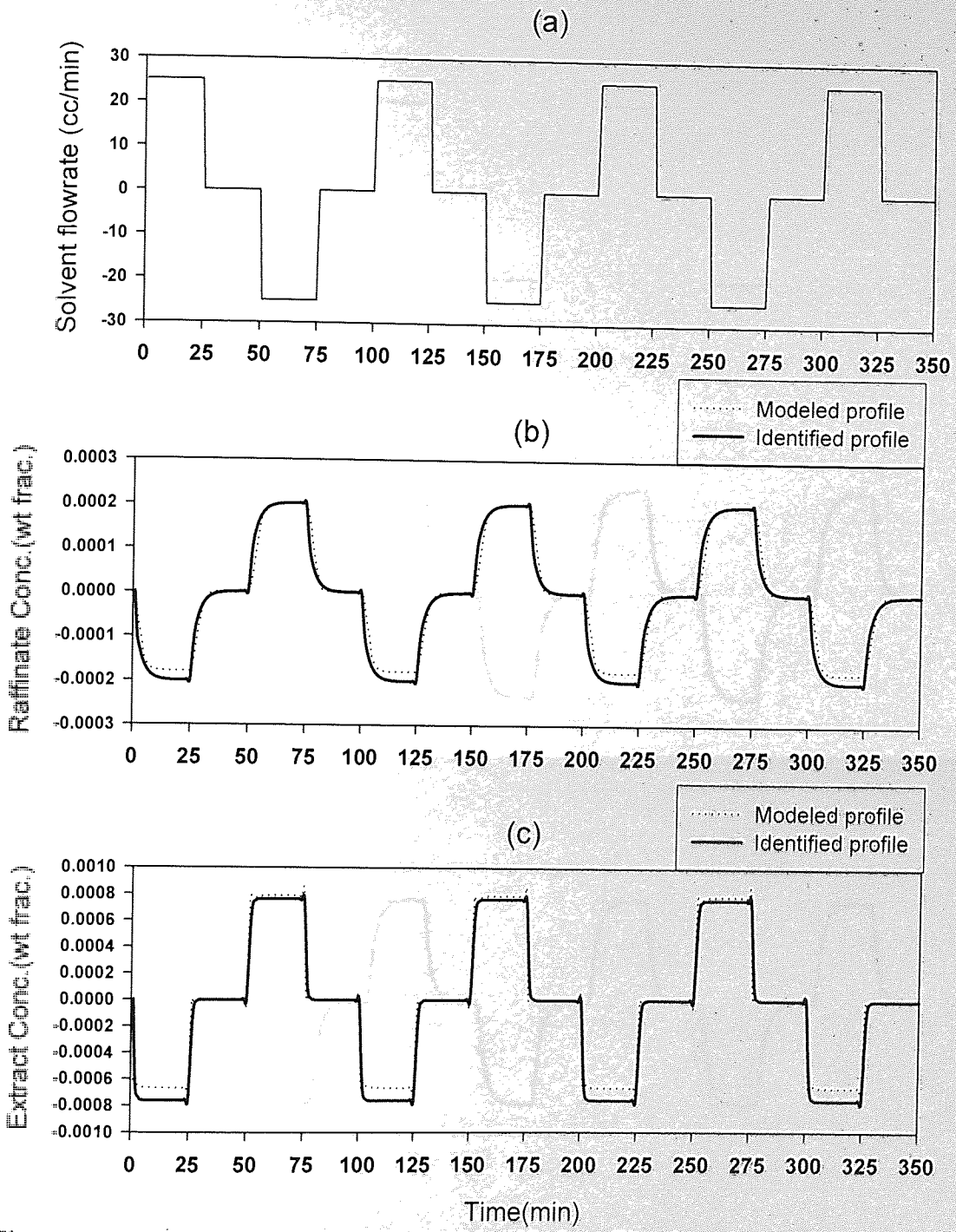

Figure(5.10) Comparison of Modelled to Identified profiles due to step variations in solvent flowrate:
(a) Step changes in solvent flowrate.
(b) Raffinate concentration profiles.
(c) Extract concentration profiles.

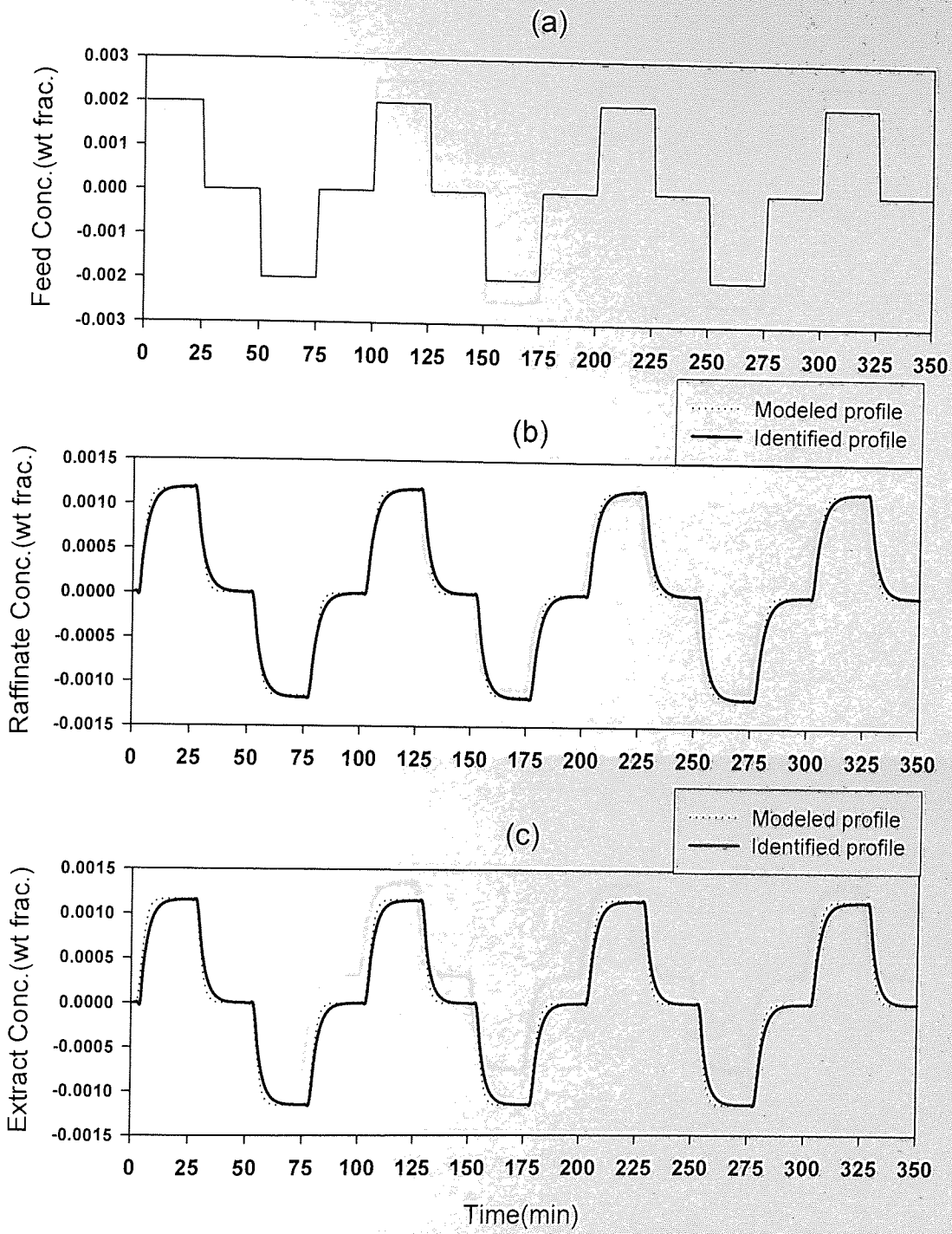

Figure(5.11) Comparison of Modelled to Identified profiles due to step variations in aqueous feed concentration:
(a) Step changes in aqueous feed concentration.
(b) Raffinate concentration profiles.
(c) Extract concentration profiles.

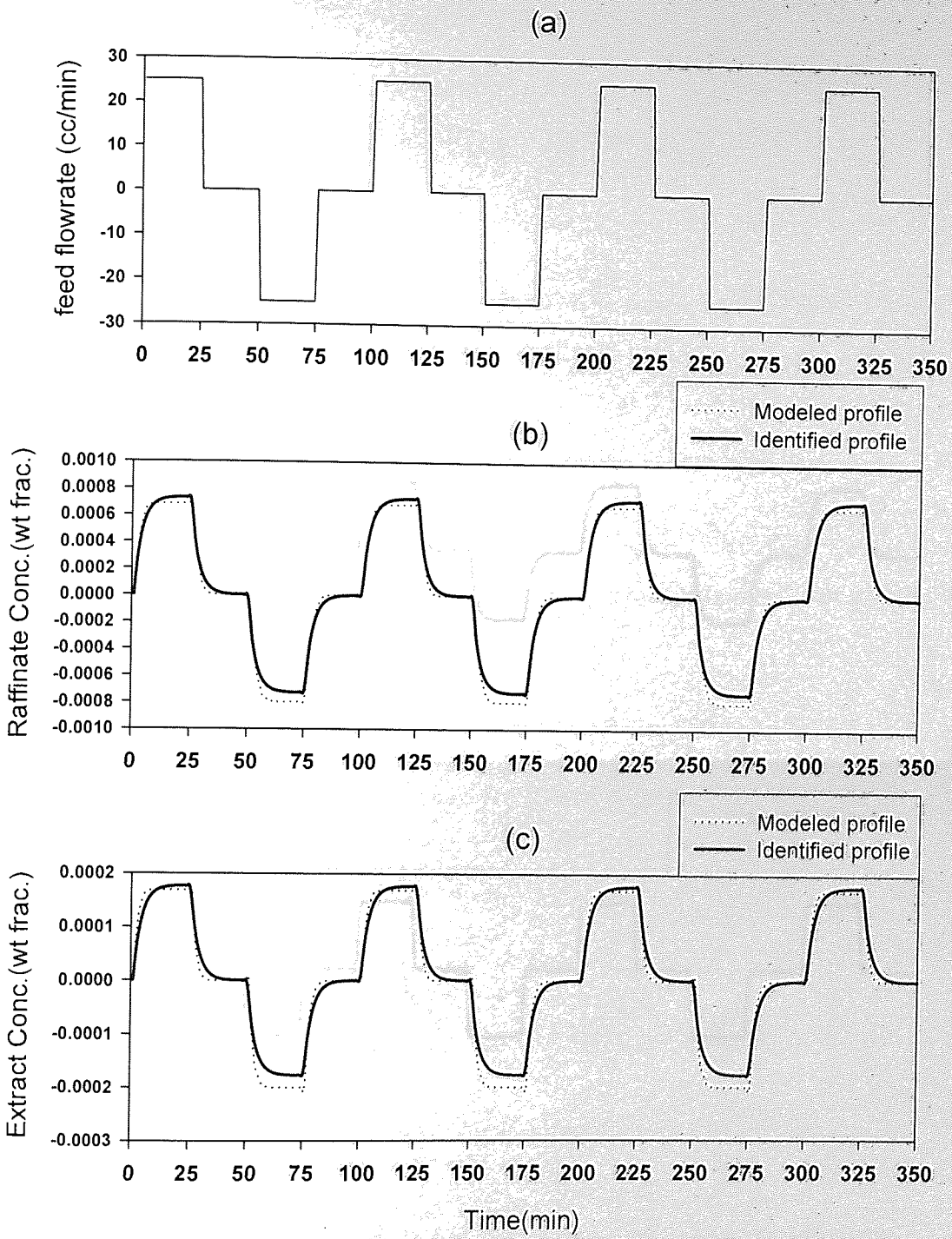

Figure(5.12) Comparison of Modelled to Identified profiles due to step variations in aqueous feed flowrate:
(a) Step changes in aqueous feed flowrate.
(b) Raffinate concentration profiles.
(c) Extract concentration profiles.

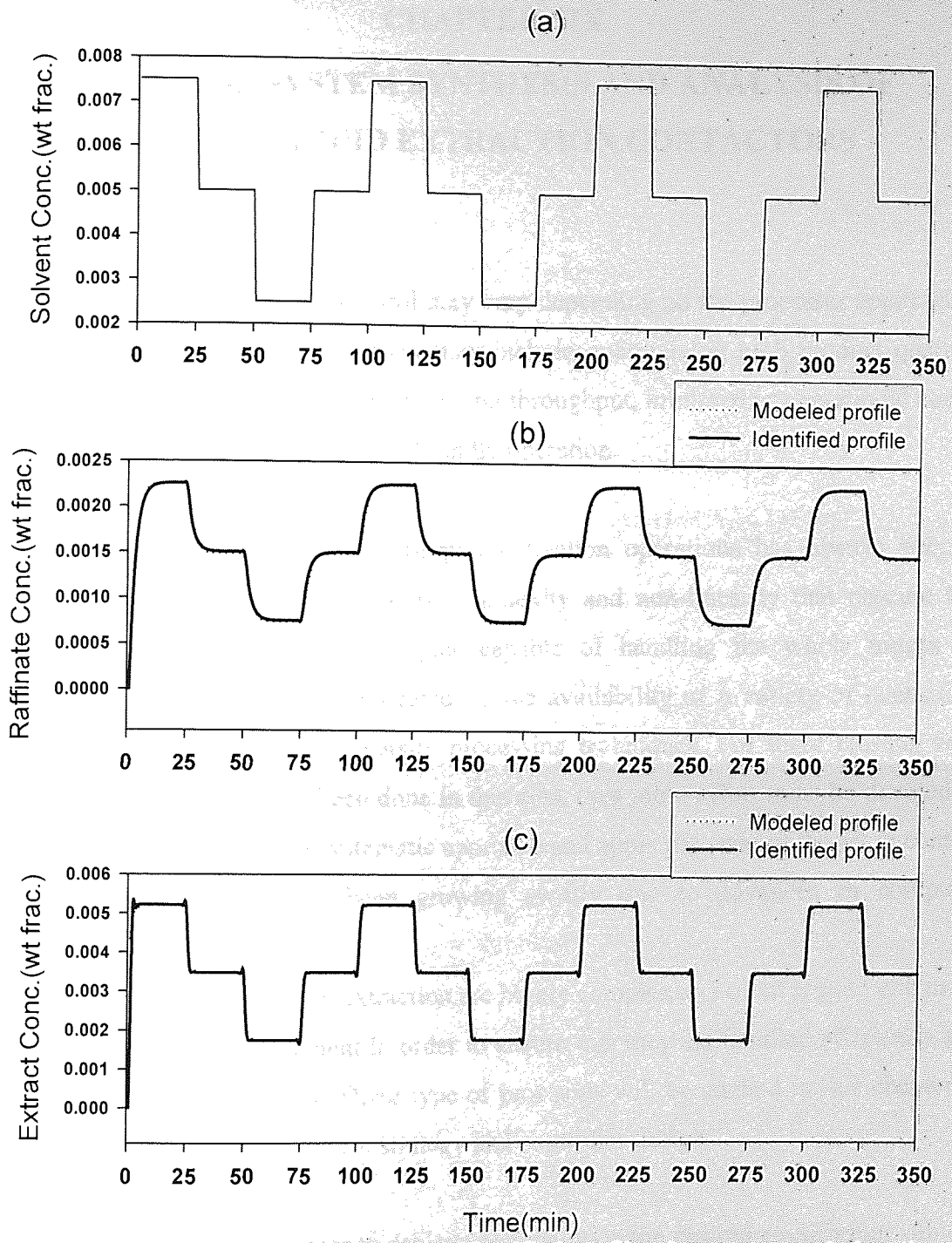

Figure(5.13) Comparison of Modeled to Identified profiles due to step variations in solvent concentration:
(a) Step changes in solvent concentration.
(b) Raffinate concentration profiles.
(c) Extract concentration profiles.

CHAPTER SIX

CONTROL SYSTEM SYNTHESIS AND ANALYSIS OF LIQUID-LIQUID EXTRACTION CONTACTORS

6.1 Introduction

The incentive for process control may vary depending on the processes application under consideration. The objectives may include: maintaining high product quality, avoiding or minimizing losses, maximizing throughput, minimizing operational costs, and ensuring safe and environment friendly operation.

Studying the control of liquid-liquid extraction operations has always been a research hungry area because of its complexity and non-linearity that obscure the design of optimum control strategies capable of handling the whole ranges of operation. This is further complicated by the availability of a variety of contacting geometries, and the use of diversity processing techniques. For these reasons very limited research work has been done in this area, thus more effort must be devoted to fill this area and provide a systematic approach and apply the state of the art in control system design which has been growing swiftly due to advances in computer technology.

The processes entailed in extraction are highly complex and often require extensive coordination and management in order to ensure that they are handled efficiently and with high safety standards. These type of processes will be studied in this chapter in terms of controllability, control strategy and controller design.

The ability of the process to achieve and maintain the desired equilibrium value is termed as the controllability of the process. This is measured by considering a range of properties of the process [Ziegler and Nichols, 1943]. However, in engineering practice a plant is called controllable if it is possible to achieve the specified control objectives [Rosenbrock, 1970]. Control strategy involves the design of control systems and studying them for stability and robustness. Controller design involves tuning the process controllers and implementing them to achieve certain performance of controlled variables.

6.2 Tools for controllability analysis

Before embarking on the controller design procedure, it would certainly be useful to know how well this process may be controlled with the best possible configuration. A number of methods for evaluating model controllability will be applied, these measures are controller independent [Wolff 1994]. The analysis tools considered will be reviewed and applied to the extraction process under consideration.

6.2.1 Functional controllability:

The plant should be checked for its functional controllability. A plant is not functional controllable if the rank of ***G(s)*** is for all ***s*** less than the number of outputs to be controlled. For square plants the requirement is that we should not have $det(\boldsymbol{G}(s)) \neq 0$ [Rosenbrock 1970]. From the reduced-order models of the extraction plant with two inputs and two outputs (2x2 system), which were calculated by system identification, the steady state gain matrix ***G(0)*** is given as:

$$\boldsymbol{G}(0) = \begin{pmatrix} -5.4782\times10^{-5} & -0.8036\times10^{-5} \\ 8.2015\times10^{-5} & -3.047\times10^{-5} \end{pmatrix} \qquad (6.1)$$

For this system the calculated $\boldsymbol{rank}\left(\boldsymbol{G}(s)\right) = 2$ for all values of ***s***. This means that it requires as many inputs as outputs to achieve the plant control and therefore, the model is functional controllable.

6.2.2 RHP zeros

Plant zeros are defined as values for ***s*** for which the plant transfer function matrix ***G(s)*** looses rank. For square plants the zeros may be computed as the solutions to ***det(G(s))=0***. A more careful definition involving the system matrix may be needed in the case the model has internal pole zero cancellations.

A *Right-Half-Plane* (RHP) transmission zero of ***G(s)*** limits the achievable bandwidth of the plant. This holds regardless of the type of controller used [Holt and Morari 1985]. One way of seeing this is to note that a RHP transmission zero becomes a RHP pole of the plant inverse and inverting the plant perfect control is therefore not possible. Thus plants with RHP transmission zeros within the desired bandwidth should be avoided. If we use a multivariable controller then RHP zeros in the

elements do not imply any particular problem. However if decentralized controllers are used then we generally avoid pairing on elements with significant RHP zeros (RHP zeros close to the origin) because such a loop may go unstable if it is closed while the other loops left open.

The upper limit on the bandwidth is approximately $\omega_z < z$ where z is the location of the RHP zero. The exact expression depends on the direction of the RHP zero. If a RHP transmission zero cannot be avoided, it should preferably be at as high a frequency as possible and lie in a plant direction such that it affects an output where the performance requirements (as required e.g. for disturbance rejection) are not significant [Morari and Zafiriou 1987]. The implications of RHP-zeros are not clear for non-square plants. Solving the equation ***det(G(s))=0*** for the extraction plant under consideration, gives the zeroes as:

[-3.9726 -0.3244 -0.2501]

As can be noticed, that all zeroes lie in the *Left-Half-Plane* (LHP), which indicates that the plant is stable for the whole range of bandwidth.

6.2.3 RHP poles

Poles of ***G(s)*** in the right half plane also put limitations on the control system through stability considerations. The bandwidth of the closed loop system must be above the frequency of the **RHP**-pole to ensure a stable system. Freudenberg and Looze (1985) have derived some interesting relationships, which quantify the effect of **RHP**-poles and **RHP**-zeros. These are summarized in Hovd and Skogestad (1992). If there are **RHP**-zeros and **RHP**-poles in the same direction it is important that the **RHP**-pole at p is located at a lower frequency than the **RHP** zero at z i.e. $|p| < |z|$.

For the extraction system under consideration, the poles are:

[-0.3213 -3.9612 -0.1596 -0.1988 -1.5921]

As can be seen that there are no **RHP**-pole. This indicates that the open loop stability is not a problem at this operating point.

6.2.4 The effective gain:

For a SISO system, the gain is defined as $K_p = \frac{\Delta y}{\Delta u}$. For a MIMO system the input and output signals are vectors, and to gain an appreciation of the effective process

gain, the magnitudes of these vectors must be used. The 2-norm representation is used as :

$$K_p = \frac{\sqrt{\sum_j |y_j|^2}}{\sqrt{\sum_j |u_j|^2}} = \frac{\|\Delta y\|_2}{\|\Delta u\|_2} \tag{6.2}$$

The wider the range of effective gains, the more sensitive the system is. Effective gains can therefore be used to study the robustness of the system to process model mismatch.

For the system under study, the input and output vectors are:

$$\Delta u = \begin{bmatrix} 40 \\ 25 \end{bmatrix} \text{ and } \Delta y = \begin{bmatrix} -2.338 \times 10^{-3} \\ 1.04 \times 10^{-3} \end{bmatrix} \tag{6.3}$$

the effective gain is calculated as:

$$K_p = \frac{\|\Delta y\|_2}{\|\Delta u\|_2} = \frac{2.56 \times 10^{-3}}{47.17} = 5.42 \times 10^{-5} \tag{6.4}$$

This small effective gain value indicates that the system is less sensitive to input signals and that proper scaling for input signals is needed. This can be taken care of by the careful selection of transmitter gains.

6.2.5 Condition Number:

The ratio between the largest singular value $\bar{\sigma}$ and the smallest nonzero singular value $\underline{\sigma}$ is often denoted as the condition number $\gamma(G) = \frac{\bar{\sigma}(G)}{\underline{\sigma}(G)}$. Plants with a large condition number are called ill-conditioned and require widely different input magnitudes depending on the direction of the desired output. Note that $\gamma(G)$ depends on the scaling of the inputs and outputs and it is important that these are scaled properly. If γ is large then the plant is sensitive to unstructured uncorrelated input uncertainty [Skogestad et al., 1988]. The calculated condition number for the extraction process is $\gamma(G) = 3.85$ which is fairly small. This indicates that the plant is a fairly well conditioned plant. Also to verify this for the whole range of process dynamics, the condition number is calculated as a function of frequency as shown in

figure(6.1). It is clear that for low frequencies the process is well conditioned, but this is not the case for high frequencies, where it reaches a value of 66 at a frequency of 1 rad/min. This calls attention to the special precautions that should be taken into consideration when controlling the process at these conditions. Fortunately the process we are dealing with will not be operated for such high frequencies because of other mass transfer and hydrodynamic constraints. But still we have to investigate the whole range of operation of the process.

6.2.6 Disturbance condition number:

To study specifically the direction of a disturbance Skogestad and Morari (1988) introduced the disturbance condition number of the process matrix G. It is defined as:

$$\gamma_d(G) = \frac{\left\| G^{-1} g_d \right\|_2}{\left\| g_d \right\|_2} \bar{\sigma}(G) \qquad (6.5)$$

where $\|.\|_2$ denotes the 2-norm or the Euclidian norm and g_d is the disturbance transfer function for a particular disturbance.

The disturbance condition number of G, $\gamma_d(G)$ tells us for a particular disturbance how much larger the input magnitude needs to be in order to reject a unit disturbance compared to the case when the disturbance was in the best possible direction of the plant (corresponding to the direction of $\bar{\sigma}(G)$). $\gamma_d(G)$ is thus bounded by 1 and $\gamma(G)$. A value of 1 indicates that the disturbances are in the "easy" plant direction and a value of $\gamma(G)$ indicates that it is in the "bad" plant direction. $\gamma_d(G)$ depends on scaling as it is based on the condition number.

Figure(6.2) gives the disturbance condition number as a function of frequency for the three disturbances. It indicates that the disturbances are well aligned with the plant directions.

6.2.7 Input magnitudes

For perfect disturbance rejection of square plants we need $u = -G^{-1}G_d d$. If we have several disturbances that all are less than unity in magnitude (i.e. $\|d\|_\infty \leq 1$) then the input magnitude measured in terms of the infinity norm needed for perfect rejection of the worst disturbance is given by:

$$\|u\|_\infty = \left\|G^{-1}G_d\right\|_\infty \tag{6.6}$$

which is equal to the largest row sum of the matrix $G^{-1}G_d$.

i.e. $\|u\|_\infty = \max_i \sum_j \left|G^{-1}G_d(i,j)\right|$

A frequency dependent plot of the elements in $G^{-1}G_d$ gives useful information about the possibility for reaching input constraints and which disturbances that cause problems.

The largest row sum of the matrix $G^{-1}G_d$ corresponds to the S_f row. This means that it has more power to reject disturbances. Figure(6.3) shows input magnitude measured in terms of the infinity norm needed for perfect rejection of the disturbances. This figure indicates that $\left\|G^{-1}G_d\right\|_\infty$ corresponds to y_f being the most difficult to reject (perfect control possible) and that S_f holds little power for handling high frequency disturbances. We should avoid running the process under high frequency disturbances to make sure that input variables have enough power to reject any disturbance completely.

6.3 Control Configuration Synthesis

By this we mean the selection of the best manipulated-controlled variables pairs that can be used to control the plant. Many analytical methods are available for variables pairing. The pairing techniques that will be used in this study:

- Relative Gain Array.
- Singular Value Decomposition.
- Jacobi Eigenvalue Criterion.

6.3.1 Relative gain array RGA

The most widespread measure for loop pairings is probably the RGA, which was introduced by Bristol (1966). For a square plant $G(s)$ the relative gain is defined as the ratio of the open-loop and closed-loop gains between input j and output i. It is defined at each frequency as

$$\lambda_{ij} = \frac{\left(\partial y_i / \partial u_j\right)_{u_{i\neq j}}}{\left(\partial y_i / \partial u_j\right)_{y_{i\neq j}}} = g_{ij(s)}\left[G^{-1}(s)\right]_{ji} \tag{6.7}$$

and an RGA matrix is computed from

$$\Lambda(j\omega) = G(j\omega) \times \left(G^{-1}(j\omega)\right)^T \tag{6.8}$$

where $\times$ denotes element by element multiplication. It is worth noting that the RGA is independent of scaling and need only be rearranged (not recomputed) when considering different control pairings.

Plants with large RGA values are ill-conditioned ($\gamma(G)$ is also large) irrespective of input and output scaling. Triangular plants yield $\Lambda = I$, and plants where Λ is different from I are called interactive (G has significant 0 diagonal elements). It is well established that plants with large RGA values in particular at high frequencies are fundamentally difficult to control. In particular it is known that one should never use decouplers in such cases because of a strong sensitivity to (structured) input uncertainty in each channel i.e. one should never use a controller with large RGA values [Skogestad and Morari 1987].

For interactive plants, which do not have large RGA elements, a decoupler may be useful. In particular, this applies to the case where the RGA elements vary in magnitude with frequency (e.g. between 10^0 and 10^2), and it may be difficult to find a good pairing for decentralized control. A steady-state decoupler may be used if the directions do not change too much with frequency.

The general rules for selecting variables pairing based on RGA as follows:

1- *Avoid pairings that give negative RGA element ($\lambda < 0$) because these pairings may produce instability to the system [Yu and Luyben, 1986]).*

2- *Avoid pairings with RGA elements much greater than one ($\lambda >> 1$). These pairings will result in hard to control loops or at least ill-conditioned (i.e. very sensitive to modelling errors).*

3- *Select pairings with RGA elements close to unity ($\lambda \approx 1$). These pairings are ones that free of interaction with other loops.*

The steady state RGA for the extraction process is calculated from G(0) as:

$$\Lambda(0) = \begin{pmatrix} 0.76 & 0.24 \\ 0.24 & 0.76 \end{pmatrix} \tag{6.9}$$

This gives us only one set of possible pairings $N\text{-}x_{out}$ and $S_f\text{-}y_{out}$ that corresponds to pairing on the main diagonal positive RGA elements. At these conditions of steady state, the previously mentioned RGA elements are relatively close to one, which indicates that loop interaction is relatively small.

One of the shortcomings of the RGA pairing method is that it relies solely on the steady state conditions of the system and ignores the dynamics. To overcome this limitation, the magnitude of the RGA elements is calculated as a function of frequency. This dynamic RGA for the extraction process is calculated and shown in figure(6.4). As can be noticed from the figure, the RGA elements are close to one for the whole range of frequencies [10^{-3}-10^{2}] rad/min and decrease at high frequencies. This means that loop interaction for the whole spectrum of frequencies is low though it gets larger at high frequencies and pairing at such extreme conditions gets less sensitive to the choice of input-output variables. The dynamic RGA gives a good indication of the previously reached results with more details.

6.3.2 Singular Value Analysis (SVD).

This is an eigenvalue-eigenvector matrix decomposition technique. The process gain matrix G is decomposed into three matrices as:

$$G = U\,\Sigma V^{T} \tag{6.10}$$

The column vectors of the orthonormal matrix V (i.e. $V^{T}V = VV^{T} = I$) represents the input directions of the plant from maximum to minimum gain. The column vectors of the orthonormal matrix (i.e. $U^{T}U = UU^{T} = I$) U represents the output directions of the plant from maximum to minimum gain. The diagonal matrix Σ contains the singular values of G. The SVD pairing rule [Burns and Smith 1982] can be stated as follows:

Pair the input corresponding to the row containing the element of the largest magnitude in the corresponding right singular vector with the output corresponding

to the row containing the largest magnitude element in the corresponding left singular vector.

The SVD for the extraction process matrix under consideration is calculated as:

$$U = \begin{pmatrix} -0.4717 & 0.8817 \\ 0.8817 & 0.4717 \end{pmatrix} \quad \Sigma = \begin{pmatrix} 0.102\times10^{-3} & 0 \\ 0 & 0.0265\times10^{-3} \end{pmatrix} \quad V^T = \begin{pmatrix} 0.955 & -0.297 \\ -0.297 & -0.955 \end{pmatrix}$$

Applying the pairing rule to the three matrices. It can be seen that the largest element in the first column of $\boldsymbol{U}$ corresponding to $\boldsymbol{y_{out}}$ is to be controlled by manipulating it with the largest element in the first column of $\boldsymbol{V}$ corresponding to $\boldsymbol{N}$, and the largest element in the second column of $\boldsymbol{U}$ corresponding to $\boldsymbol{x_{out}}$ is to be controlled by manipulating it with the largest element in the second column of $\boldsymbol{V}$ corresponding to $\boldsymbol{S_f}$. This implies that the pairing loops are $\boldsymbol{N}$-$\boldsymbol{y_{out}}$ and $\boldsymbol{S_f}$-$\boldsymbol{x_{out}}$. This is a different configuration than that resulted from the RGA analysis.

The failure of the SVD to suggest the RGA pairing is due to the fact that the SVD is a scale dependent method and since the process gain matrix under consideration varies considerably in terms of variable scales, then it is expected that it will not suggest the appropriate pairing.

6.3.3 Jacobi Eigenvalue Criterion:

This pairing criterion is based on an analysis of the difficulty of finding the inverse of the steady state gain matrix [Gerardo M. et al. 1986]. The pairing rule can be stated as:

Select the pairing whose corresponding Jacobi iteration matrix $\boldsymbol{A}$ has the smallest-largest eigenvalue in modulus of all possible pairings. For a 2×2 system the pairing with the smallest-largest eigenvalue corresponds to the pairing with relative gains closest to unity.

The Jacobi iteration matrix $\boldsymbol{A}$ is defined as:

$$A = -\begin{bmatrix} 0 & a_{12} & a_{13} & \cdots & a_{1n} \\ a_{21} & 0 & a_{23} & \cdots & a_{2n} \\ \cdots & \cdots & \cdots & \cdots & \cdots \\ a_{n1} & a_{n2} & \cdots & a_{n,n-1} & 0 \end{bmatrix} \qquad (6.11)$$

where $a_{ij} = g_{ij} / g_{ii}$.

For a 2×2 system the matrix becomes:

$$A = -\begin{pmatrix} 0 & g_{12}/g_{11} \\ g_{21}/g_{22} & 0 \end{pmatrix} \tag{6.12}$$

Table (6.1) The calculated results for the two expected pairings using the Jacobi criterion.

Pairing	Jacobi iteration matrix A	$\lambda(A)^*$	$S(A)^{**}$
N-x_{out} and S_f-y_{out}	$-\begin{pmatrix} 0 & 0.152 \\ -2.128 & 0 \end{pmatrix}$	$0 \pm 0.569i$	0.569
N-y_{out} and S_f-x_{out}	$-\begin{pmatrix} 0 & 6.570 \\ -0.470 & 0 \end{pmatrix}$	$0 \pm 1.757i$	1.757

* eigenvalue of Jacobi iteration matrix A.

** spectral radius of A (largest eigenvalue of A in modulus).

The calculated results in Table(6.1) suggests that the N-x_{out} and S_f-y_{out} pairing is more suitable than the second one. This is in agreement with the RGA results.

To check the stability of the suggested pairing, the Niederlinski stability index [Niederlinski, 1971] is calculated as:

$$N.I. = \frac{\det(G)}{\prod_i g_{ii}} = 1.3239 \tag{6.13}$$

This positive value of the index implies that the suggested loop pair is stable.

To support the argument that the SVD pairings were not suitable, the *N.I.* was calculated based on the SVD pairings. The *N.I.* calculated value was –4.087, which indicates that the paring suggested by SVD was not stable.

6.4 Discussion of Results of the Controllability study:

The previous controllability study analysed the properties and expected behaviour of the plant under closed loop conditions. From this study, it is concluded that our model is functional controllable, stable for the range of operation considered and is less sensitive to input signals. At low frequencies the model is well conditioned and

less sensitive to modelling errors, whereas at high frequency this tendency becomes weak and more consideration should be given to these conditions.

The disturbances are well aligned with the direction of the plant inputs, which means that disturbance rejection is easily attained by carefully manipulating inputs. The three disturbances vary in terms of difficulty to be rejected.

The variables pairing study revealed that the best feedback loop configuration is achieved by pairing the diagonal elements of the gain matrix (i.e. N-x_{out} and S_f-y_{out}). These loop configurations are well suited for most of the range of operation of the plant. At regions of high frequency, the pairing becomes less dependent on the choice of input-output variables, and more advanced control scheme must be used to eliminate interaction that develop at such conditions. In the next sections attention is focused on the problem of designing and evaluation of a relevant control structure for the process under consideration. The tuning of feedback controller can be done either by classical direct design approach or model based one.

6.5 Control System Design Strategies

6.5.1 Introduction:

The key step in designing a control system is the design of the controller element. Conventional PID controllers have been developed and used in industry for the past fifty years, and it is believed that over 90% of process control loops in industry are of PID type. One of the basic challenges for engineers is the tuning of these controllers.

The Ziegler-Nichols tuning rules [Ziegler and Nichols, 1942] were the very first tuning rules for PID controllers, and it is surprising that they are still widely used today. The reason for their popularity lies in their simplicity and efficiency. This is why so many different tuning rules, which are based on the same tuning procedures have been developed later on [Gorez, 1997].

After the work of Ziegler and Nichols, a variety of PID tuning methods have been developed. In general, these methods can be divided into two main groups: the *direct* and the *indirect* tuning methods [Gorez, 1997]. The direct tuning methods do not require a process model, while the indirect methods calculate controller parameters from an identified model of the process (model based). In the following sections,

some of these tuning methods will be outlined and applied to the process under consideration, and an evaluation of the viability of these techniques in terms of process control criteria is shown.

6.5.2 Direct Tuning methods:

The most popular direct tuning methods are based on the measurement of particular points on the process Nyquist curve. The best-known rules are the [Ziegler-Nichols (1942), Cohen-Coon (1953), Chien-Hrones-Reswick (1952)] tuning rules. In all these methods tuning is based on measurements of the process lag and rise time (or ultimate point), so their applicability to a wide range of processes still remains problematical. The refined Ziegler-Nichols [Hang et al. 1991] was an improvement to the ZN method by using the so called "set point weighting". New tuning rules like the Gain Phase assignment [Ho et al. 1995] were introduced but they were still suffering from the same limitations of the previous methods.

The other type of direct tuning methods are based the whole range of transient response of the process. This is accomplished by optimisation of controller criteria, which is defined as a cost function, mainly derived on how the controller reacts to a given disturbance. Given that we want to optimise the controller so that the process variable stays around the set point, a "time integral" performance criteria can be used. The tuning process usually involves minimizing a function of $\varepsilon(t) = y_{set} - y$. This method depends on the form of integral function used. The following, is a list of the different forms used for these methods:

- **IAE**: Integral of absolute value of error i.e. $J_n(\theta) = \int_0^\infty |\varepsilon(\theta,t)|\,dt$.
- **ITAE**: Integral of time by absolute value of error i.e. $J_n(\theta) = \int_0^\infty t.|\varepsilon(\theta,t)|\,dt$.
- **ISTAE**: Integral of time squared by absolute value of error i.e. $J_n(\theta) = \int_0^\infty t^2.|\varepsilon(\theta,t)|\,dt$.
- **ISE**: Integral of error squared i.e. $J_n(\theta) = \int_0^\infty \varepsilon(\theta,t)^2\,dt$.
- **ITSE**: Integral of time by error squared i.e. $J_n(\theta) = \int_0^\infty t\cdot\varepsilon(\theta,t)^2\cdot dt$.
- **ISTSE** :Integral of time squared by error squared i.e. $J_n(\theta) = \int_0^\infty t^2\cdot\varepsilon(\theta,t)^2\cdot dt$.

In all these methods, the only difference is the form of integral cost function used in the optimisation criteria. Any PID tuning algorithm will have the purpose of minimizing one or more of these cost functions.

Some of the previously mentioned methods will be used for comparing their applicability to the process considered. These methods can be summarised as follows:

1. One-shot Tuning Direct Design methods like:
   - Ziegler-Nichols (**ZN**).
   - Cohen-Coon (**CC**).
   - Chien-Hrones-Reswick (**CHR**).
   - Modified Ziegler-Nichols (**MZN**).
   - Gain Phase Margin Assignment (**GP**).
2. Optimum Tuning Direct Design Methods
   - **ISE**: Integral of error squared.
   - **ITSE**: Integral of time multiplied by error squared.
   - **ISTSE** : Integral of time squared multiplied by error squared.

The details and rules of these controller design methods are given in Appendix (F).

6.5.3 Model Based Tuning methods:

These methods use a more advanced approach to tune the controller. The tuning of the controller parameters is based on the mathematical model of the system. The process model is *explicitly* used in the control system design procedure. The standard feedback structure uses the process model in an *implicit* fashion, that is, PID tuning parameters are tweaked on a transfer function model, but it is not always clear how the process model effects the tuning decision.

One benefit of these methods is that the design is done off-site, eliminating the risk of component damage. The procedure of parameter tuning is performed on the computer, which makes the design time short. The Internal Model Control (IMC) is good example of these methods [Morari, and Zafiriou, 1989]. Appendix (F) gives the details of two model based control procedures namely; the Direct synthesis and the IMC.

IMC is a general design technique, and its use for PID design is a special case. This is an analytical method of PID design based on First Order Process Dynamics

(FOPD) model or a Second order Process Dynamics (SOPD). IMC has very good robustness [Scali et al., 1992]. One of the good features of IMC is that its performance is dependant on only one parameter, namely τ_f the filter time constant. As this parameter gets smaller, the response gets faster, and this induces more aggressive system response.

6.5.4 Multi-loop Controller Strategy

Extraction is a multivariable process; nevertheless most of the research in the process control area has been conducted regarding it as a multi-SISO system. Besides, most of the researchers used conventional strategies instead of using advanced schemes. Since the early seventies, the area of research done on the control of extraction contactors, has gained good deal of attention. Yet, it has been concerned with conventional design techniques, and specific cases of application.

Due to the diverse nature of contactor designs and the complexities involved in the separation of different chemical systems, there is no one unified approach for the solution of the extraction control problem. Most of the work done so far was concerned with pulsed columns and mixer-settlers because of their wide use in industry. To my knowledge, there is no comprehensive control study for the Scheibel columns despite the appealing industrial features of high throughput and efficiency of these contactors.

The multivariable nature of the extraction process necessitates the use of an efficient control algorithm for handling variables interaction, time delays, constrained operation of variables, and most importantly the effective use of computers to predict process future behaviour under complex operating conditions. Hence a control strategy that handle the system as one multi-loops system should be investigated and its performance compared to the conventional single loops control stratigies.

6.6 Results and Discussions for the Simulation of Conventional PID Controllers:

The feedback control loop elements and loads transfer functions have to be specified in order to conduct the control system design study. In the following section, the main elements of the two closed loops are studied.

6.6.1 Construction of Feedback loop elements

Figure(6.5) shows a block diagram of the extraction process with all elements and I/O signals indicated and annotated. The process consists of two closed loops. The control loop elements were designed for the two loops selected from the preliminary system analysis, namely S_f-y_{out} and N-x_{out}. The transfer functions of sensor, transmitter, and final actuating elements are given below for each loop:

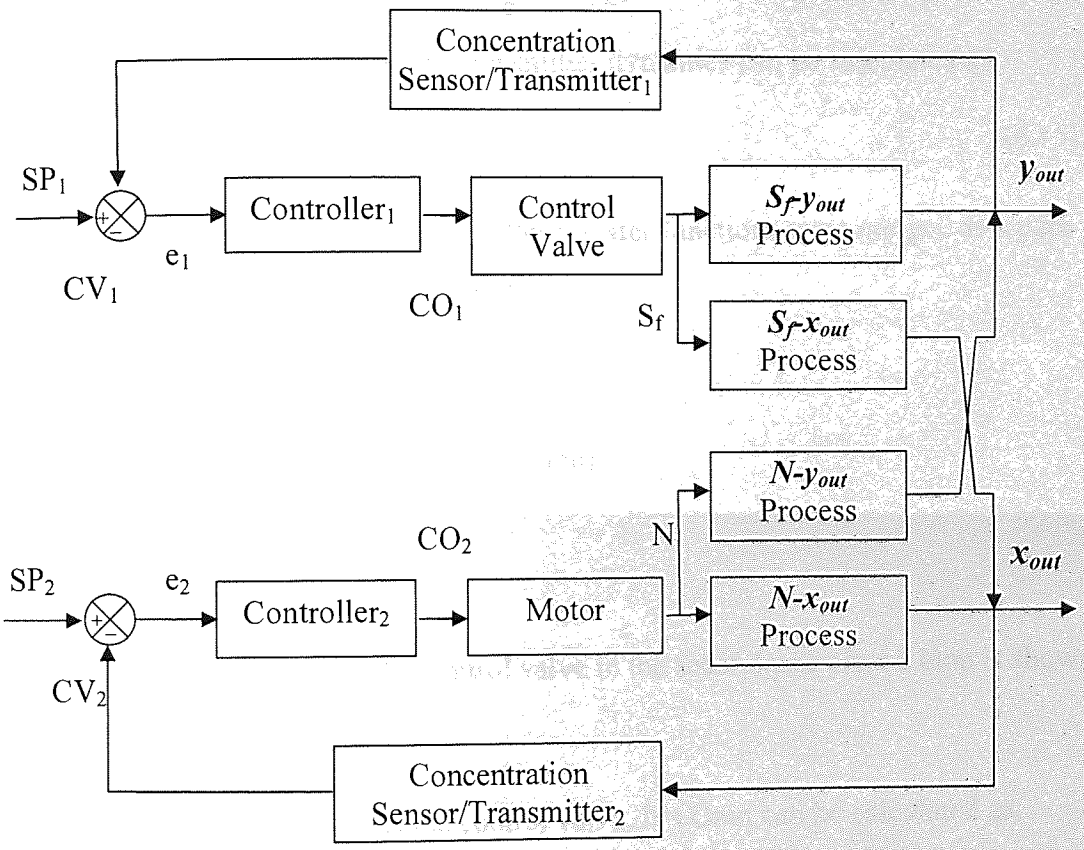

Figure(6.5) Feedback loop of the extraction process.

N-x_{out} Loop:

Here, the stirrer acts as the actuating element and it is driven by the motor. So we will be concerned with the motor transfer function. The I/O signal through the motor is shown Figure(6.6).

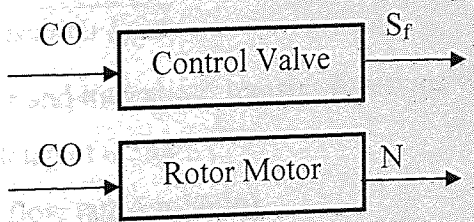

Figure(6.6) Signals through the control valve and motor actuating elements.

As indicated, the signal from the controller through the motor changes as follows:

***Controller output*(mA) → *Controller output*(%) → *Voltage*(V) → *Rotor speed*(RPM)**

Assuming the motor as a pure gain element, its gain can be calculated as:

$$\text{Motor Gain} = \frac{\Delta N}{\Delta CO} = \frac{\Delta N}{\Delta V} \times \frac{\Delta V}{\textit{Controller range}} \times \frac{\textit{Controller range}}{\Delta CO}$$

$$= \frac{600}{240} \times \frac{240}{100} \times \frac{100}{16} = 37.5\ \text{RPM/mA} \qquad (6.14)$$

Knowing the transmitter span, the transmitter dynamics can be calculated as:

$$\text{Transmitter Gain} = \frac{100\%}{\textit{Transmitter Span}} \qquad (6.15)$$

For simplicity, the sensor and transmitter transfer functions were merged as a pure gain of 0.5 with a time delay of 0.5min.

where N: Rotor speed (RPM).

V: voltage (V).

x_{out}: outlet raffinate conc. (wt fraction).

S_f-y_{out} Loop:

The I/O signal through for the control valve in the second pair closed loop is shown in Figure(6.6).

Here the actuating element is the control valve. It's Gain can be calculated as:

$$\text{Control Valve Gain} = \frac{\Delta S_f}{\Delta CO} = \frac{\Delta S_f}{\Delta V} \times \frac{\Delta V}{\textit{Controller range}} \times \frac{\text{Controller range}}{\Delta CO}$$

$$= \frac{500}{240} \times \frac{240}{100} \times \frac{100}{16} = 31.25\ \text{cm}^3/(\text{min.mA}) \qquad (6.16)$$

The transfer function of the control valve is regarded as a first order lag. Its time constant is selected as 0.022 min in order to give fast and smooth response.

$$\text{Transmitter Gain} = \frac{100\%}{\textit{Transmitter Span}} \qquad (6.17)$$

For simplicity, the sensor and transmitter transfer functions were merged as a pure gain of 0.5 with a time delay of 0.5min.

where S_f: Solvent feed flow rate (cm^3/min).

y_{out}: outlet extract conc. (wt fraction).

Table(6.2) summarizes the details of all control loop elements that were used in the control system design.

Table(6.2) Transfer functions of the feedback loops elements.

Loop element	N-x_{out} loop		S_f-y_{out} loop	
	Transfer Function	Eqn. No.	Transfer Function	Eqn. No.
Process	$\frac{x_{out}}{N} = \frac{-5.4782\times10^{-5}e^{-0.5s}}{3.112s+1}$	6-18	$\frac{y_{out}}{S_f} = \frac{-3.047\times10^{-5}e^{-s}}{0.6281s+1}$	6-19
Load	$\frac{x_{out}}{x_f} = \frac{0.5907e^{-4s}}{3.312s+1}$	6-20	$\frac{y_{out}}{x_f} = \frac{0.57599e^{-0.5s}}{3.015s+1}$	6-21
Load	$\frac{x_{out}}{y_f} = \frac{0.3005e^{-0.5s}}{2.3449s+1}$	6-22	$\frac{y_{out}}{y_f} = \frac{0.69612e^{-0.5s}}{0.38208s+1}$	6.23
Load	$\frac{x_{out}}{R_f} = \frac{3.117\times10^{-5}e^{-0.5S}}{2.0552s+1}$	6-24	$\frac{y_{out}}{R_f} = \frac{0.7077\times10^{-5}e^{-S}}{3.2779s+1}$	6-25
Transducer	$0.5e^{-0.5s}$	6-26	$0.5e^{-0.5s}$	6-27
Final Control Element	37.5	6-28	$\frac{31.25}{0.022s+1}$	6-29

The transfer functions of the two loops processes were used to tune the two controllers. The details of controller tuning algorithms are given in Appendix(F). Table(6.3) gives the calculated controller parameters for both loops. The PID controller is used for all tuning methods described above.

Table(6.3) Tuning parameters for different methods for both loop using SISO loops.

Tuning method	N-x_{out} loop			S_f-y_{out} loop		
	K_c	τ_I	τ_D	K_c	τ_I	τ_D
ZN	2148	3.770	0.3304	1082	1.0270	0.2465
M-ZN	1139	2.116	0.5290	573.6	1.5780	0.3946
Cohen-Coon	2929	1.714	0.2647	1256	1.2320	0.2062
CHR	1981	4.637	0.3506	741.7	0.8821	0.3149
IMC	1100	3.685	0.3352	968.7	0.9650	0.2187
ISE	1874	2.978	0.4311	925.2	0.7749	0.3224
ISTE	1863	3.548	0.3304	914.9	0.8559	0.2547
IST2E	1749	3.600	0.2769	849.8	0.8793	0.2089
GP	1822	1.531	0.3442	917.5	1.1420	0.2567

6.6.2 Simulation and Closed-loop characteristics of PID control:

The feedback elements and the tuned controllers were simulated using SIMULINK dynamic simulation package. Figures (F.3 and 5) in Appendix(F) give the structure of simulation loops. The PID controller used in the simulation is of standard type. Each of the two loops were simulated separately, and then both of them were implemented in one control structure.

The transient response of the different PID controllers for a positive set point step in raffinate outlet concentration is shown in Figures(6.7-6.8). The characteristics of the dynamic responses are calculated and given in Table(6.4). The missing values in the table indicate no value or an inapplicable measure. These tests were based on SISO loops in order to eliminate effect of loop interactions, and study the effect of each loop separately.

Table (6.4) Dynamic response characteristics for a positive step in raffinate outlet concentration.

Tuning Method	LOOP	Rise Time (min)	Overshoot	Settling Time (min)	Decay Ratio	Period of Oscillation (min)
ZN	N-x_{out}	2.5	0.778	15	0.36	4.5
	S_F-y_{out}	3	-	25	0.85	5
CC	N-x_{out}	2.5	-	Unstable	-	5.3
	S_F-y_{out}	3.5	-	Unstable	-	5.5
M-ZN	N-x_{out}	4	-	>25	-	6.1
	S_F-y_{out}	-	-	Oscillatory	1	5
CHR	N-x_{out}	3	0.278	10	0.05	6
	S_F-y_{out}	3.5	-	13	0.3	6.5
ISE	N-x_{out}	3	0.415	21	0.38	5.5
	S_F-y_{out}	3.6	-	21	0.51	6
ISTE	N-x_{out}	3.2	0.366	21.5	0.43	6
	S_F-y_{out}	3.5	-	21	0.51	5.5
IST2E	N-x_{out}	3.3	0.341	22	0.42	6.4
	S_F-y_{out}	3.3	-	22	0.38	6.4
GP	N-x_{out}	3	0.854	>25	0.39	7.5
	S_F-y_{out}	4	-	>25	0.6	7.5

From the response characteristics of the different tuning algorithms the following can be noticed:

- For the N-x_{out} loop :

  ZN controller has the lowest rise time with high overshoot, and settling time and the decay ratio was high. The CC was the worst, despite the low rise time, the response was unstable

  M-ZN gave the highest rise time with a settling time greater than the actual process time (25 min) and a long period of oscillations (6.1 min). The CHR gave the best response of all the conventional controllers. It is fast, with minimum overshoot and decay ratio.

  Despite the fast response of the GP, it was not satisfactory as a whole because of its high settling time (>25 min) and overshoot.

  The optimisation based tuning algorithms (ISE, ISTE, and IST2E) have good response in general but they have high settling time. IST2E has the lowest overshoot and ISE is the fastest in response.

- For the S_f-y_{out} loop :

  ZN controller gave good rise time with high overshoot, settling time and decay ratio. For the CC tuning, the rise time is high but the response was unstable. The M-ZN response is critical and oscillatory. The CHR gave the best response of all the conventional controllers; it is fast, with minimum overshoot and decay ratio. The GP gave the slowest response without overshoot and a settling time greater than 25 min.

  The optimisation based tuning algorithms (ISE, ISTE, and IST2E) have good response in general without overshoot, but they have high settling time (>21min). IST2E has the fastest response.

In general we can see that the CHR tuning algorithm gave the best response and the Cohen-Coon gave the worst.

The stability of the controller algorithms was tested using the Nyquist stability criterion. This is shown in Figure (6.20) for all controller algorithms. The plots show that the Cohen-Coon was the only unstable algorithm, and the ZN algorithm was on the limit of stability. However, all other algorithms are stable. This enforces the previous note of the inadequacy of the ZN and CC algorithms in terms of stability.

6.6.3 Simulation and Closed-loop characteristics of IMC control:

IMC control scheme was tested and simulated using the MATLAB SIMULINK simulation package. The SIMULINK block diagrams for both single and multi-loop testing are shown in figure (F.4 and 6) in Appendix (F).

The effect of filter time constant τ_f on the overall response of the process was investigated by testing different values of τ_f for a +10% step change in raffinate outlet conc. τ_f with both loops closed. This is indicated by Figure(6.9) . It is noticed from the behaviour of both loops that the response gets faster and more oscillatory as τ_f is decreased. A value of $\tau_f = 0.1\tau_p$ is reasonable for both loops. A smaller value of $\tau_f = 0.05\tau_p$ makes the second loop ($S_f - y_{out}$) closer to oscillatory behaviour. On the other hand, a value of $\tau_f = 0.05\tau_p$ was reasonable for the case of a +10% step in extract concentration y_{out}. This is shown in Figure(6.10). This indicates the importance of tuning this parameter for a desirable IMC setting.
The selected τ_f was implemented and the transients of the controlled variable and manipulated variable for both loops are shown in figures (6.11) and (6.12).The IMC response was the most appropriate in terms of speed, overshoot and damping ratio.
The characteristics of these transient responses are given in Table(6.5). Both loops tracked the step change smoothly and gave very low overshoot and decay ratio and the settling time were short. The N-x_{out} loop response was a little bit slower than the S_f-y_{out} which was relatively fast in response. The reason for this can be associated to the smaller time constant of the S_f-y_{out} loop compared with that of the N-x_{out} equivalent (about one fifth).

Table (6.5) Dynamic response characteristics for IMC controller tuning.

LOOP	Rise Time (min)	Overshoot	Settling Time (min)	Decay Ratio	Period of Oscil. (min)
N-x_{out}	6.6	0.125	14	0.1	4.5
S_f-y_{out}	3.7	0.1	7	0.05	5

The effects of steps in load variables (10% in x_f, 0 to 0.002 wt fraction in y_f and 10% in R_f) on the outlet raffinate concentration x_{out} for the N-x_{out} closed loop using

IMC scheme is shown in figure(6.13). The effects of steps in loads on the outlet extract concentration y_{out} for the S_f-y_{out} closed loop using IMC scheme is shown in figure(6.14). For both loops, it is clear that their transients follow the step change with a larger overshoot in the case for solvent feed concentration disturbance. This result is in agreement with the disturbance rejection test findings from the controllability analysis conducted previously. It was noticed that the y_f load has higher effect on the process dynamics than the other two loads and that the R_f has the least effect.

For the case of both loops closed, the IMC servo responses for steps in output concentrations are shown in Figures(6.15 and 6.16). From Figure(6.15) it is noticed that the effect of steps in raffinate concentration on the extract concentration response is profound as indicated on Figure(6.15a) compared to the negligible effect of the extract concentration on both loops. Figure(6.16) shows the same interaction effects when both steps are applied for the two loops at different instances of time (0 and 10 min). It can be inferred that some degree of loop interaction is present for the case of excitations in the raffinate outlet concentration. Consequently, some treatment for this interaction must be considered for any practical implementation of the IMC controller.

6.7 Robustness of the closed loop MIMO system:

Any industrial process is subject to changes in its parameters during its operation. This is due to non-linearities of the process, changes in operating conditions, etc. Robustness of a control system is the term given to indicate the ability of the system to be tolerant to changes in process parameters or modelling errors. Two methods for testing the control system robustness will be presented.

6.7.1 Robustness test by model mismatch:

The most important limitation to satisfy control criteria is imposed by inaccuracies in the model assumed for design. Models used for design will not be accurate for several reasons:

- Assumption of linear behaviour for a nonlinear one.
- Equipment degradation.
- Unknown disturbance characteristics.

- Unreliable model identification techniques.

The control system is robust if it is tolerant to changes in process parameters. To investigate the robustness of the control system, i.e. its sensitivity to modelling errors, model mismatches in process gains and process time constants were introduced into the models and the controllers behaviour were studied. 50% model mismatch in model parameters was chosen for the robustness study. The *time response* of both the perturbed and the original models were compared using the IMC algorithm, and a conclusion can then be drawn about the reliability and sensitivity of the model to modelling errors.

The 10% set-point step response for the raffinate (x_{out}) and the extract (y_{out}) outlet concentrations for both loops using the IMC algorithm are shown in figure(6.17-6.19). A 50% mismatch in process parameters namely; *process gain, response time* and *time delay* are also shown in the same figures.

The perturbed responses are all slower than the original ones. For the (N-x_{out}) loop, the responses for process gain and delay time mismatch are more oscillatory whereas for the (S_f-y_{out}) loop they are characterised by less oscillatory transients. This gives an indication that there is some effect of model mismatch on the behaviour of the response, and that a more robust control algorithm is needed.

6.7.2 Robustness test using Doyle-Stein criterion:

Doyle and Stein (1981), have developed a method for checking the robustness of multivariable systems. The robustness of a closed loop multivariable system is measured by plotting the minimum singular value of the matrix: $I + (G_p G_c)^{-1}_{(i\omega)}$ as a function of frequency (ω). The structure and parameters of the feedback controller are changed until a minimum dip in the curve is within a value of –12dB as recommended by Doyle and Stein (1981).

The minimum singular values and corresponding frequencies are given in Table(6.6). The table gives an indication that IMC, GP, CHR, and the IST2E are close to robustness whereas the other algorithms are far away. The IMC value of minimum singular value is 2.465 dB away from the recommended value of Doyle and Stein. This supports the conclusion drawn from the model parameters mismatch test

discussed above that the closed loop extraction system using the IMC controller is capable to tolerate model uncertainties reasonably. Appendix (G) gives a listing of this procedure, programmed in Fortran PowerStation language.

The above criterion was applied for all controller algorithms as shown in figure(6.21).

Table(6.6) Minimum dip of the singular value curves of the Doyle-Stein criterion for different controllers.

Tuning method	**Min singular value**	**frequency**
ZN	-22.440	2.291
M-ZN	-1.456	2.512
Cohen-Coon	-39.703	2.317
CHR	-9.843	2.114
IMC	-14.465	2.163
ISE	-20.125	2.291
ISTE	-14.572	2.163
IST2E	-10.688	2.042
GP	-11.173	2.265

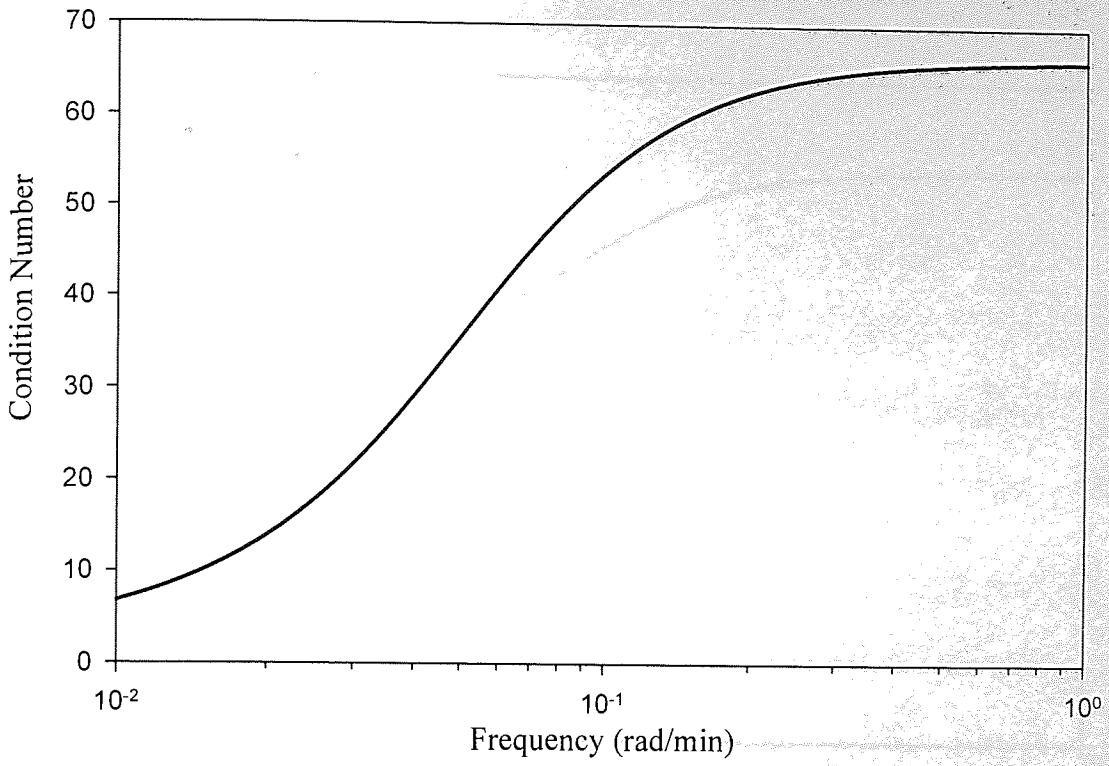

Figure (6.1) Plant condition number as a function of frequency.

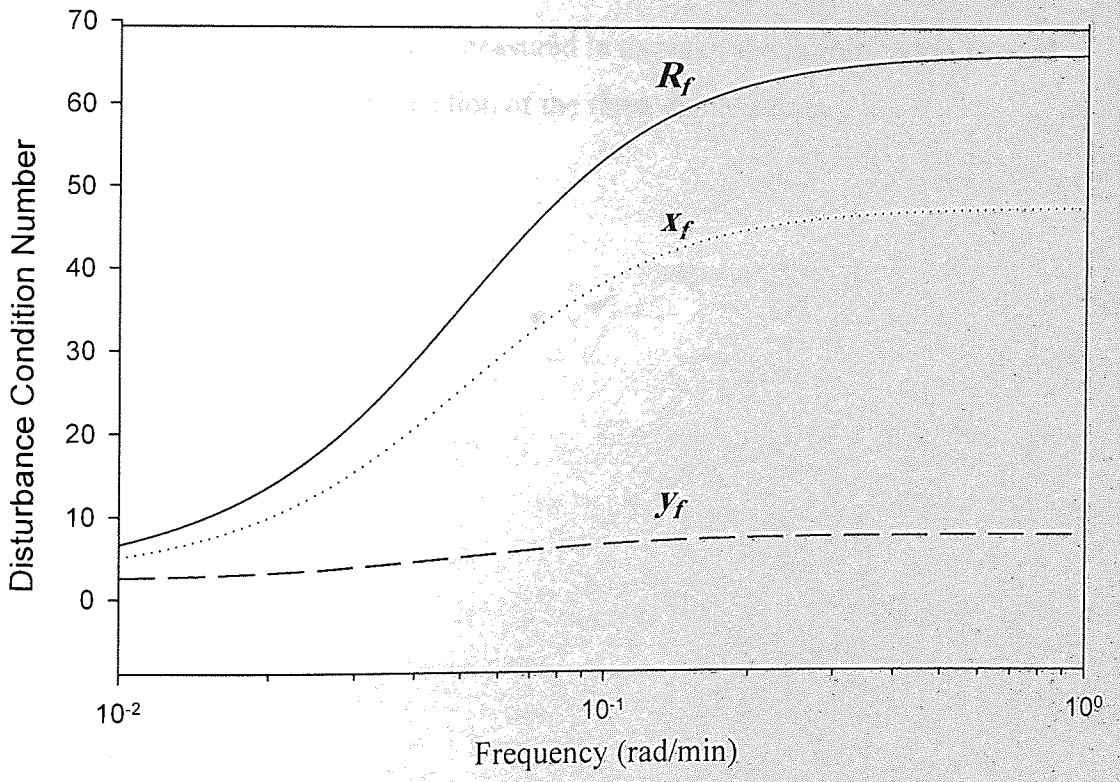

Figure (6.2) Disturbance condition number for each of the three disturbances as a function of frequency.

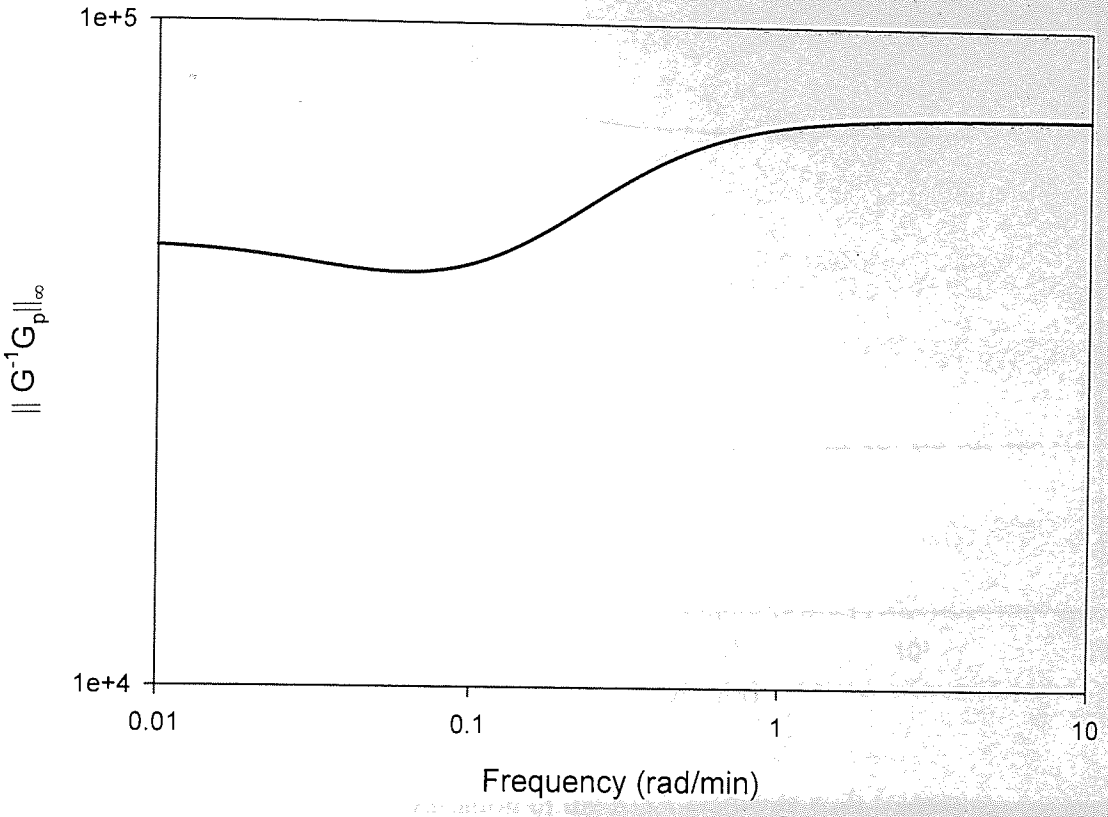

Figure(6.3) The Input magnitude measured in terms of the infinity norm needed for perfect rejection of the three disturbances.

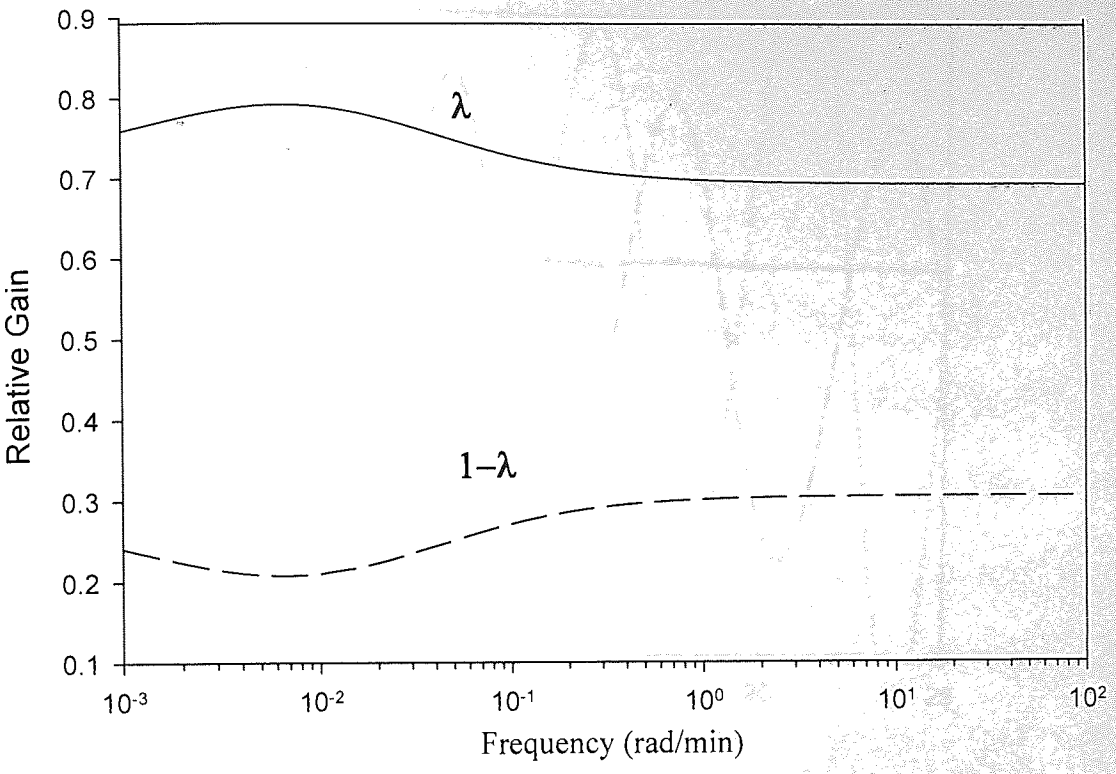

Figure(6.4) The variation of the RGA elements with frequency.

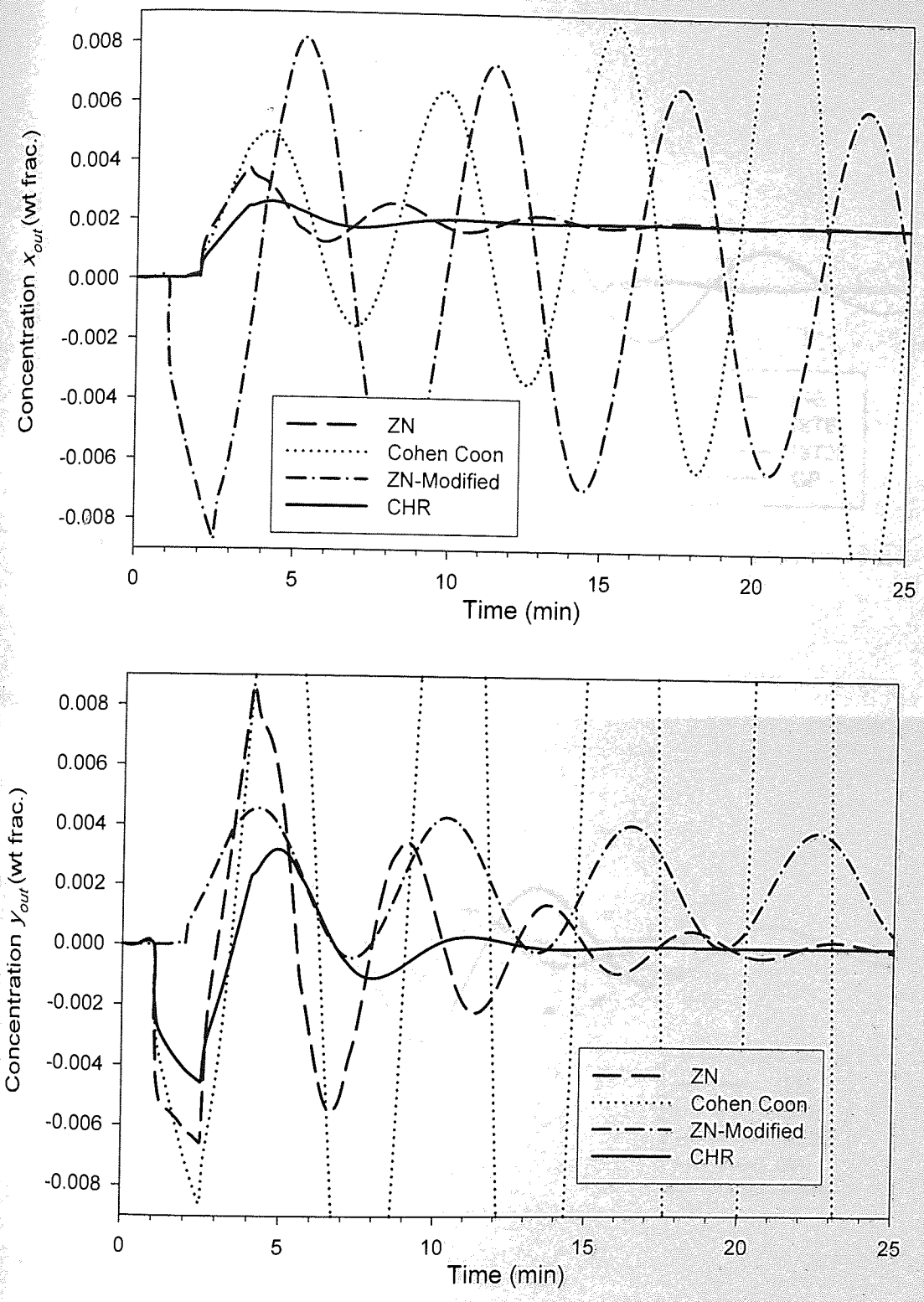

Figure(6.7) Comparison of different conventional loop tuning methods (ZN, Cohen-Coon, Modified ZN and Chein) for a +10% step in raffinate outlet concentration x_{out} when both loops are closed.

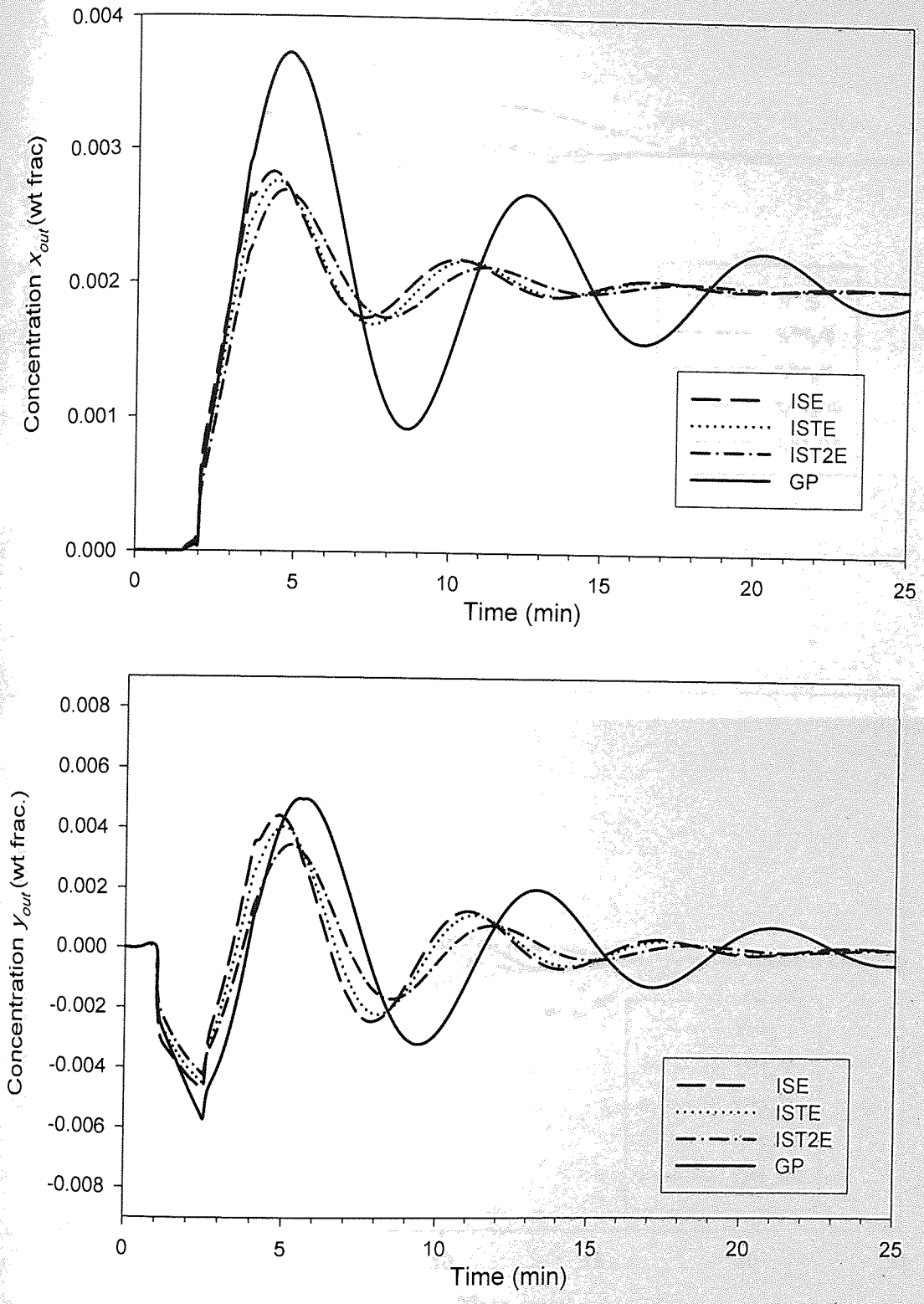

Figure(6.8) Comparison of different conventional loop tuning methods (ISE, ISTE, IST2E and GP) for a +10% step in raffinate outlet concentration x_{out} when both loops are closed.

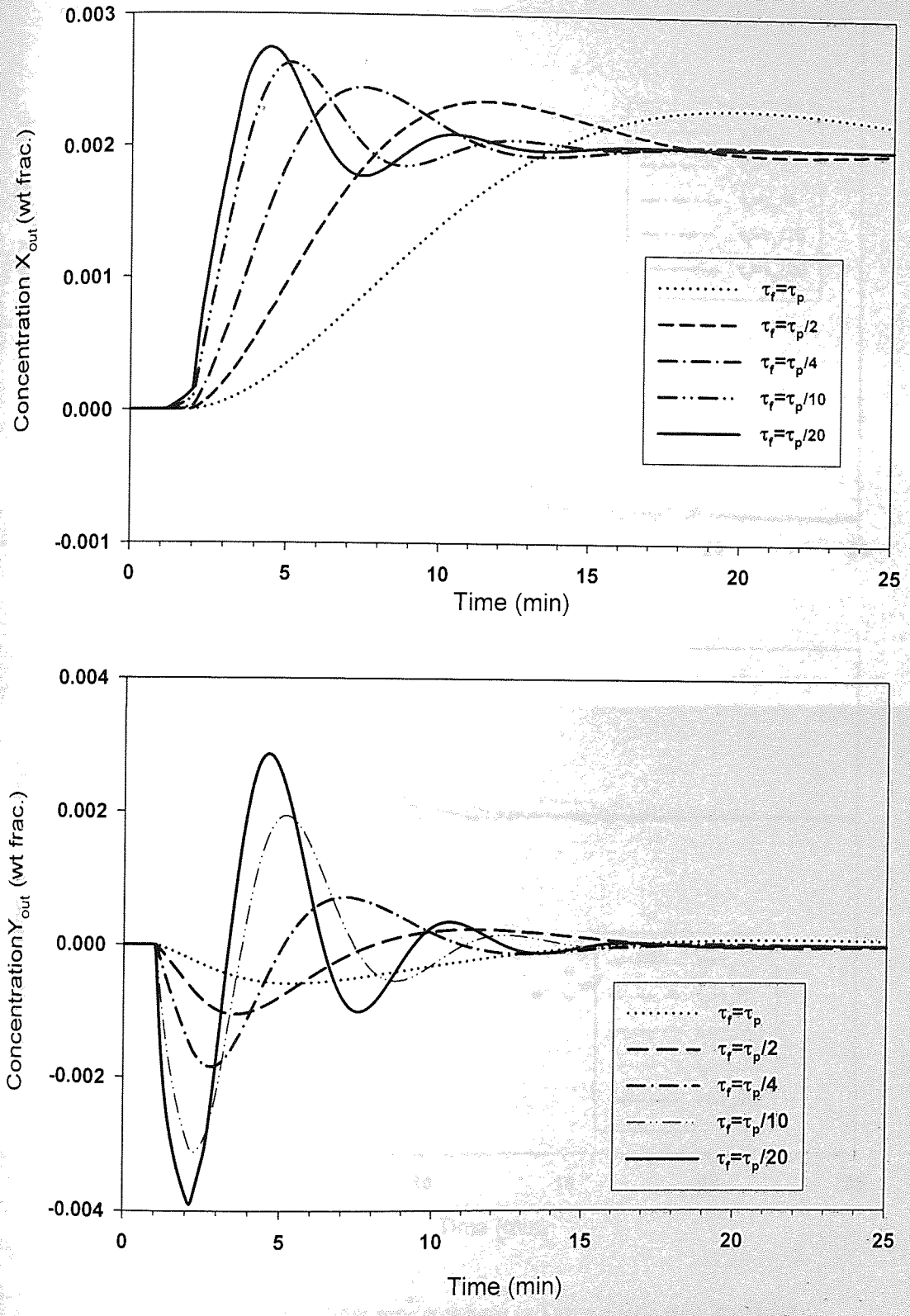

Figure(6.9) Effect of IMC filter time constants (τ_f) for a +10% step in raffinate outlet concentration x_{out} when both loops are closed.

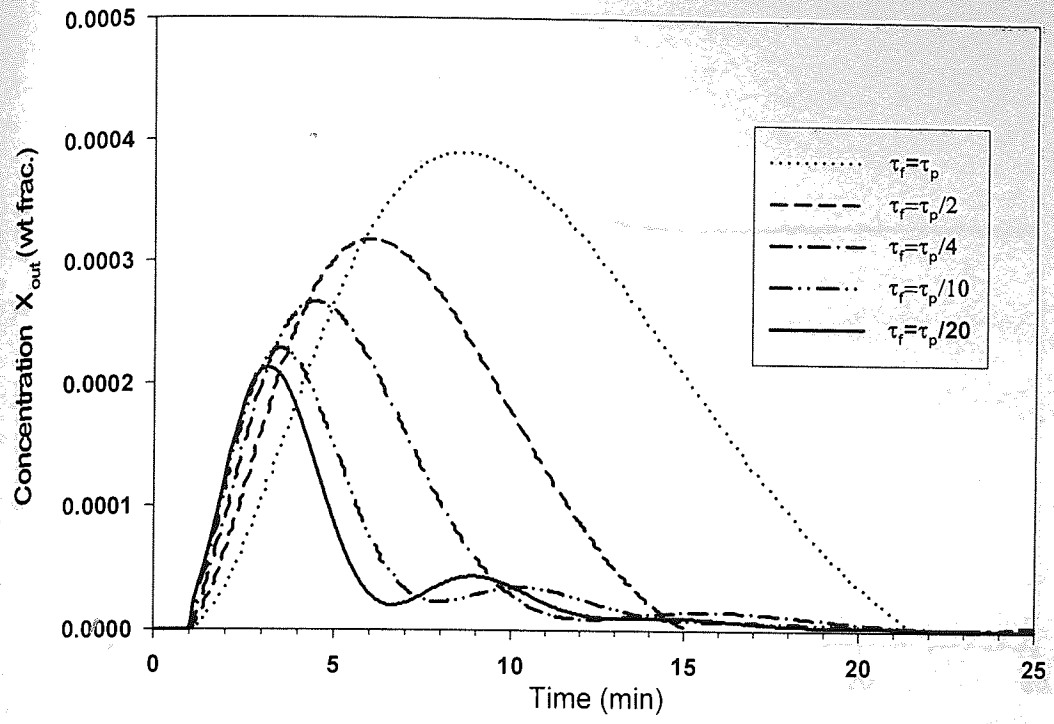

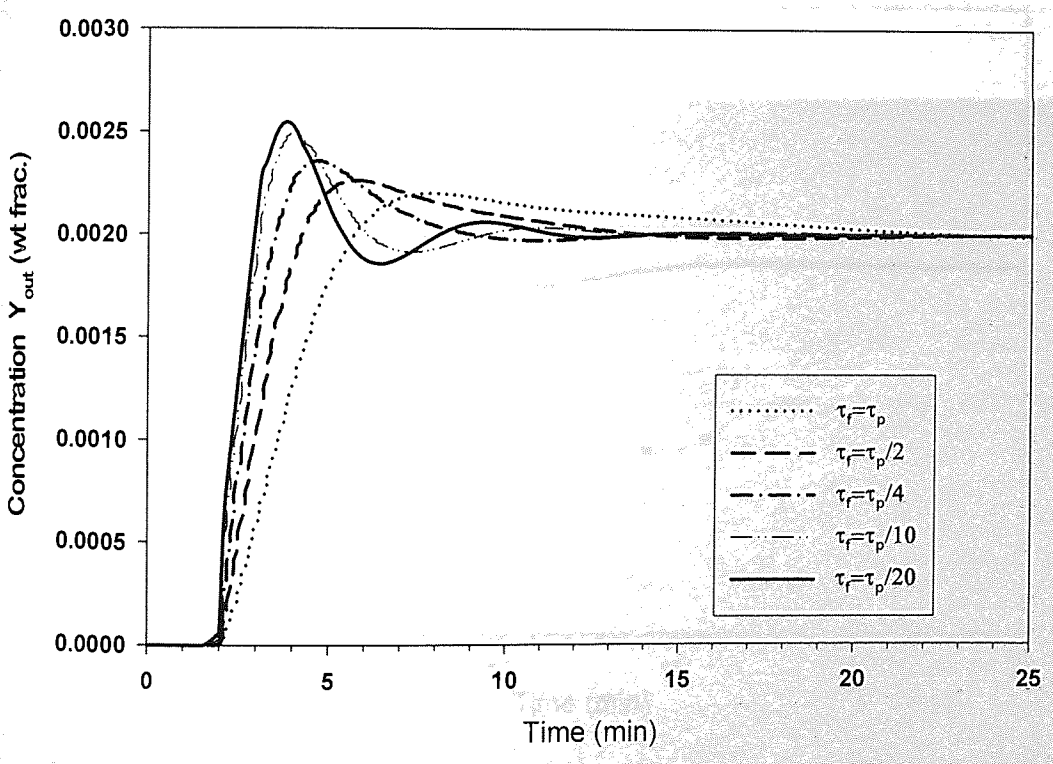

Figure(6.10) Effect of IMC filter time constants (τ_f) for a +10% step in extract outlet concentration y_{out} when both loops are closed.

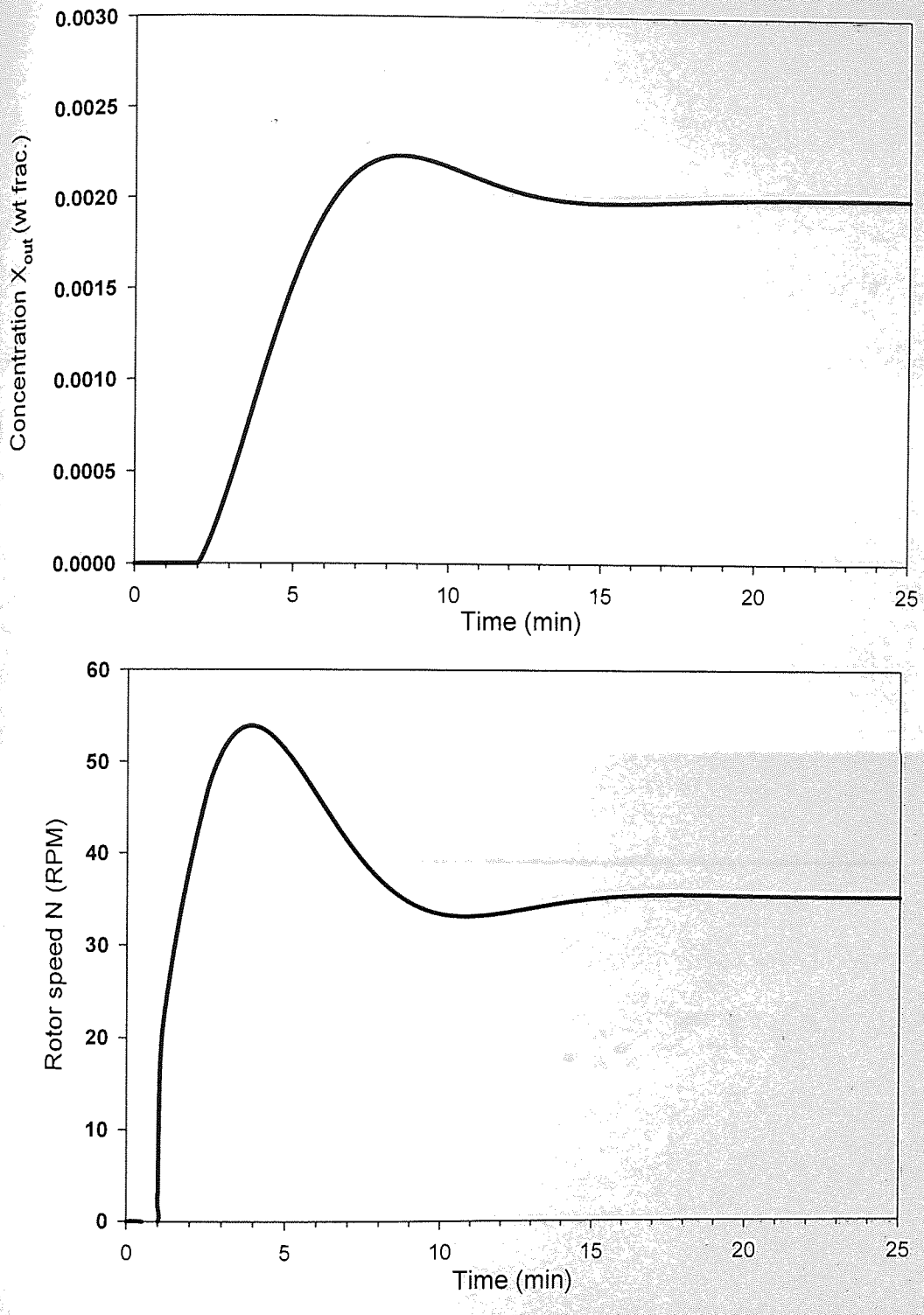

Figure (6.11) IMC single loop response for a step change of +10% in raffinate outlet concentration $\mathbf{x_{out}}$ and the corresponding response of the manipulated variable **N.**

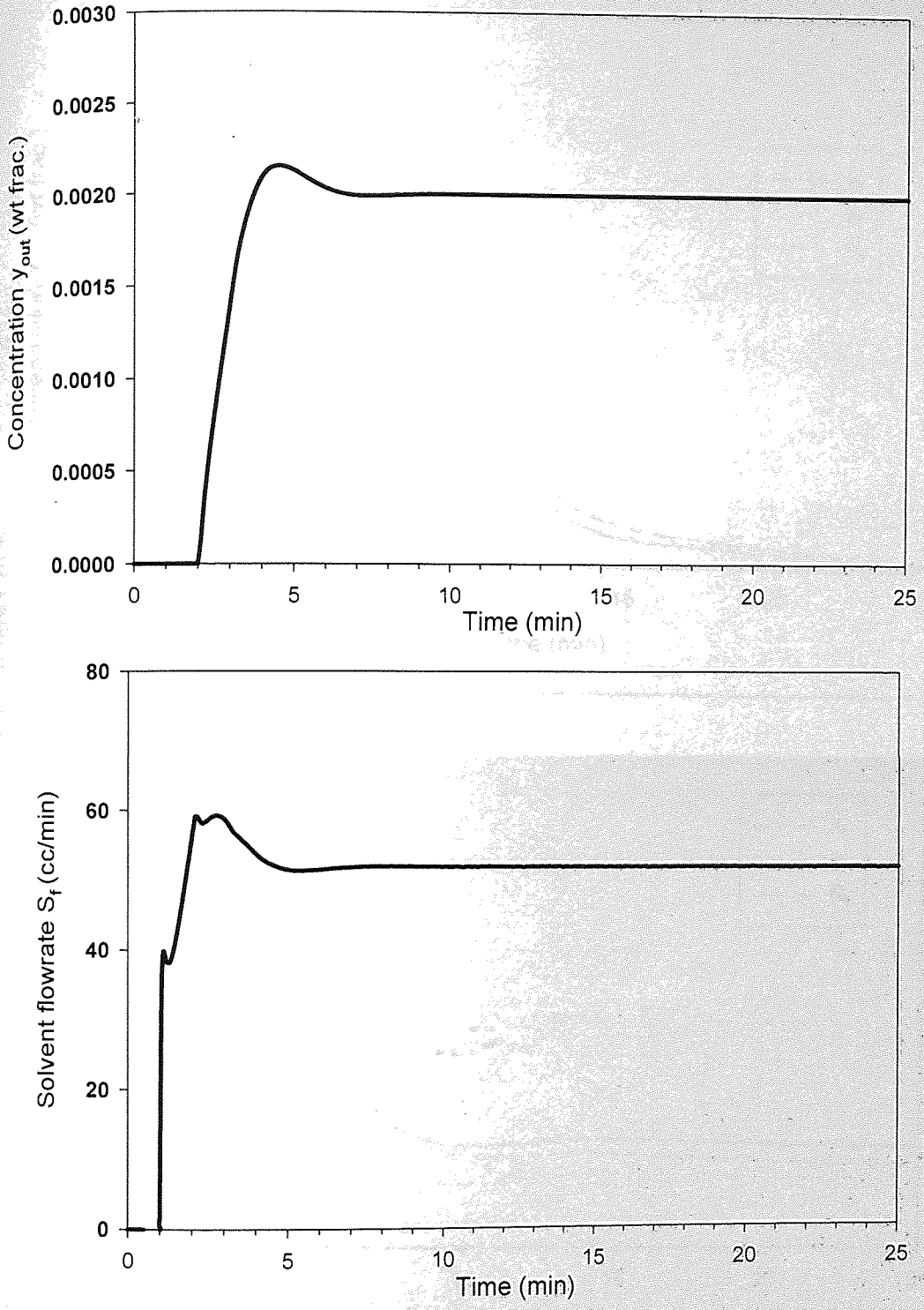

Figure (6.12) IMC single loop response for a step change of +10% in solvent outlet concentration y_{out} and the corresponding response of the manipulated variable S_f.

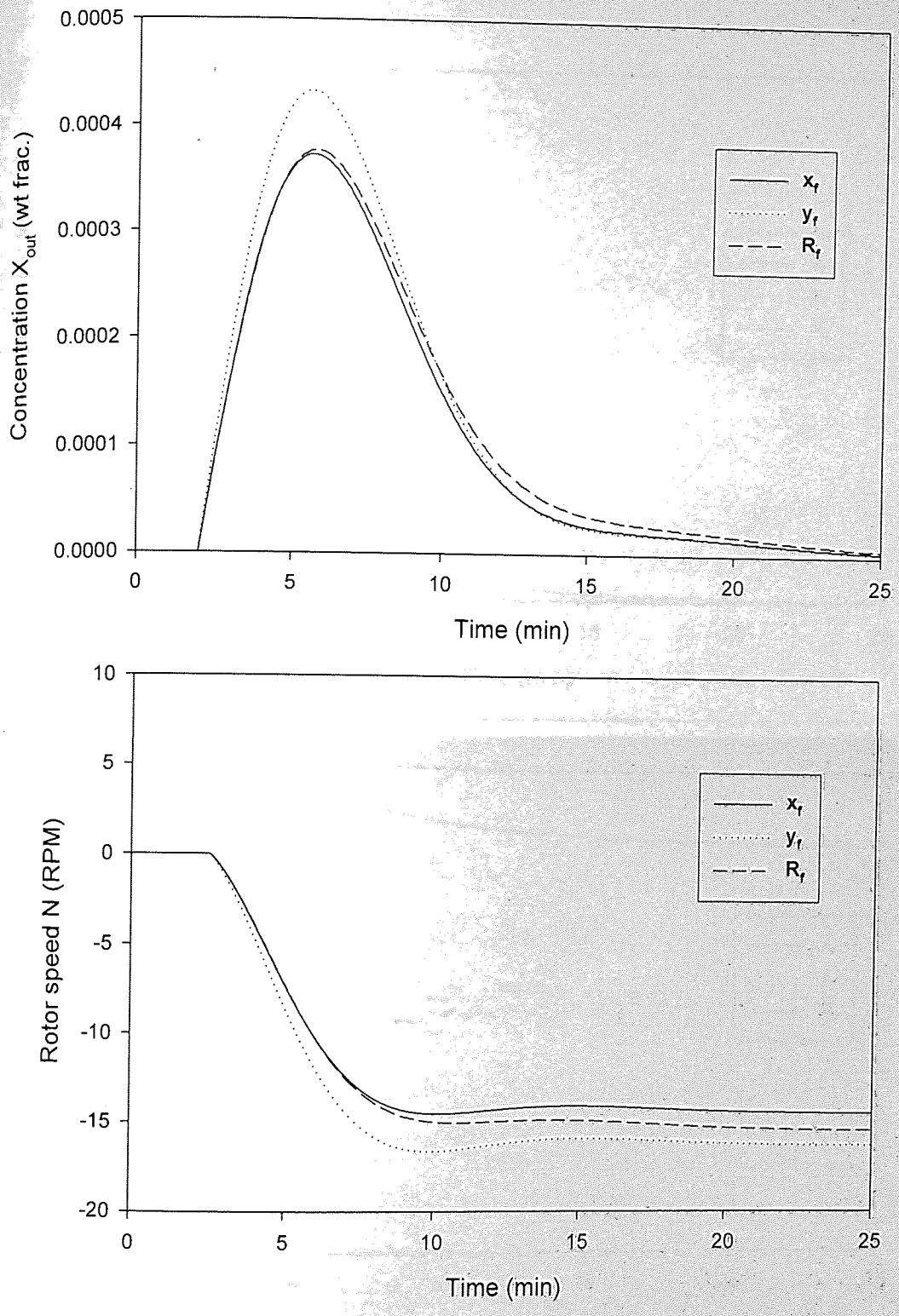

Figure (6.13) Effects of steps in loads (10% in x_f, 0 to 0.002 wt frac. in y_f and 10% in R_f) on the outlet raffinate concentration x_{out} for the N-x_{out} closed loop using IMC scheme.

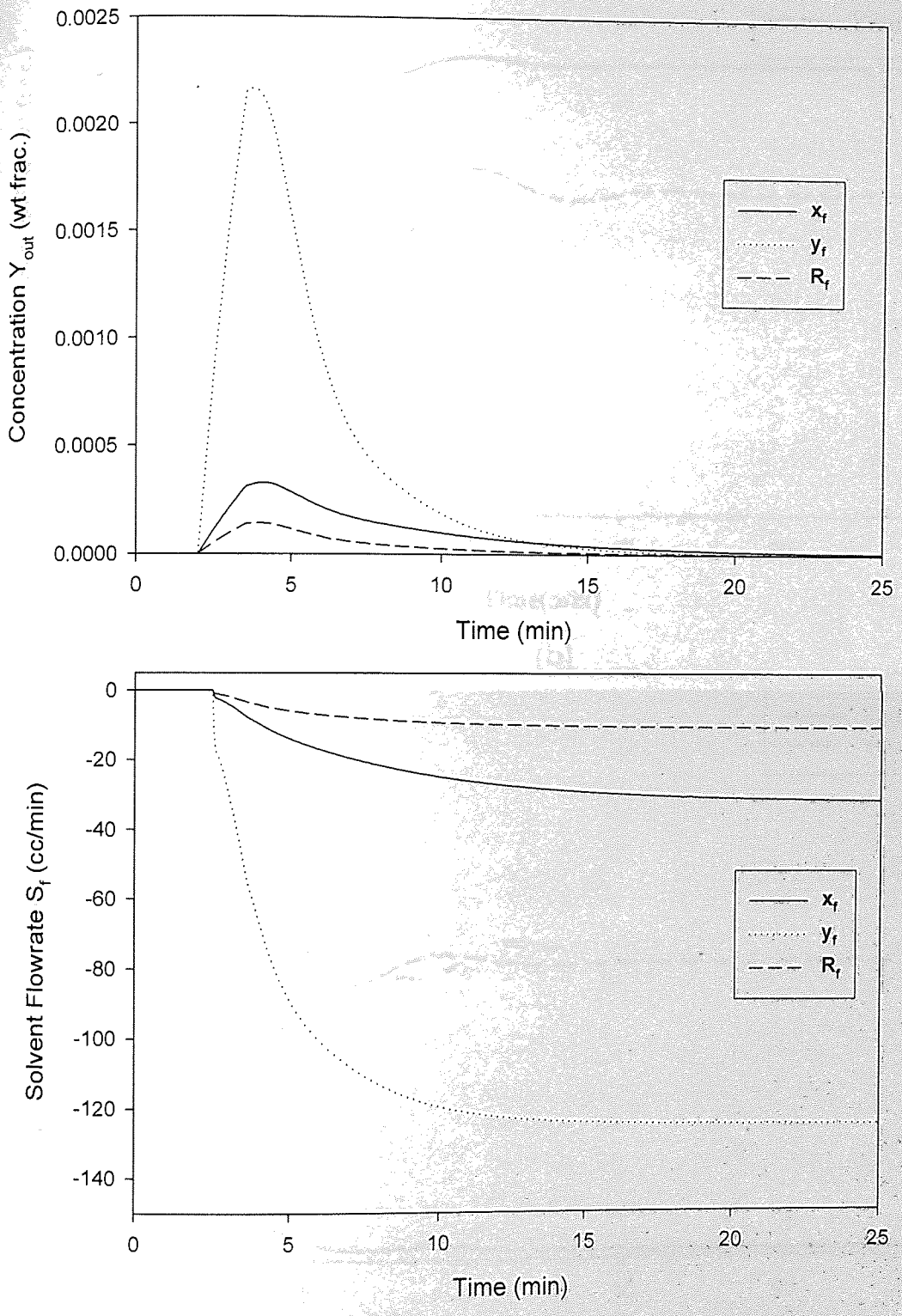

Figure (6.14) Effects of steps in loads (10% in x_f, 0 to 0.002 wt frac. in y_f and 10% in R_f) on the outlet extract concentration y_{out} for the S_f-y_{out} closed loop using IMC scheme.

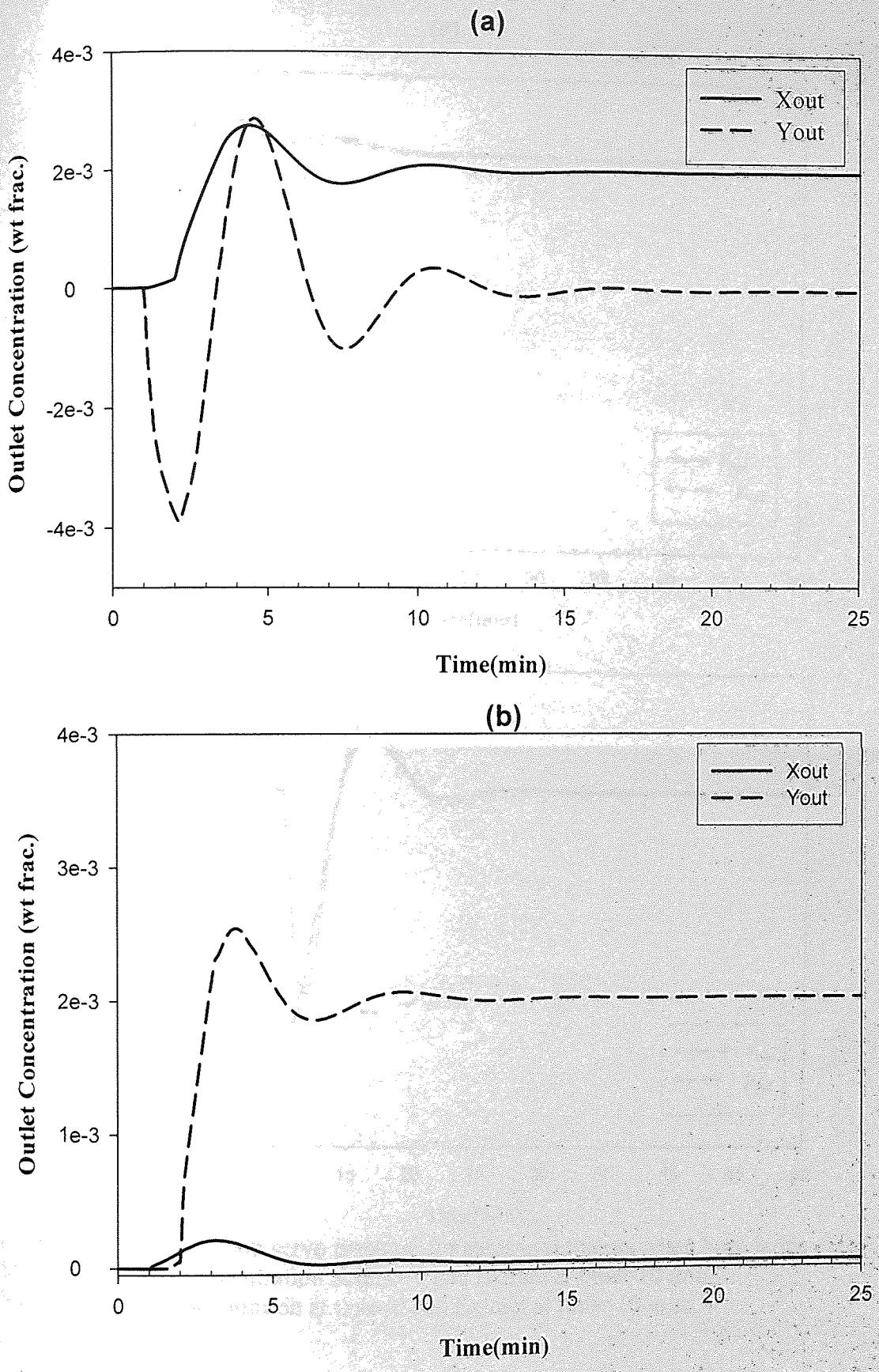

Figure(6.15) IMC close loop servo response for both loops closed

(a) Step in Raffinate concentration x_{out}.

(b) Step in Extract concentration y_{out}.

(a)

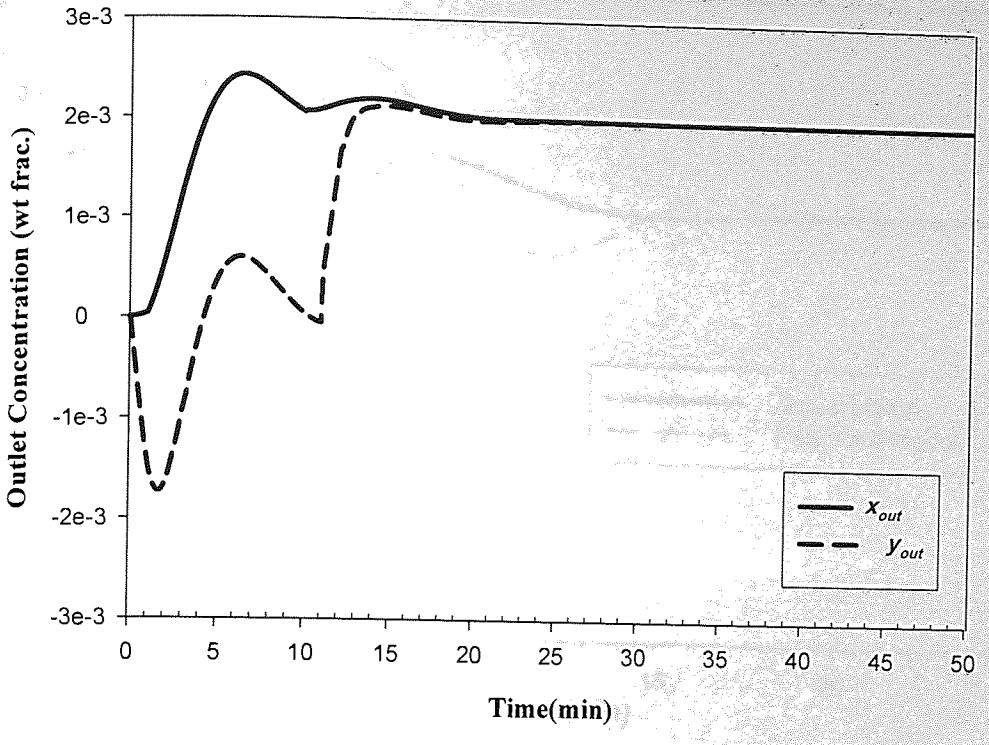

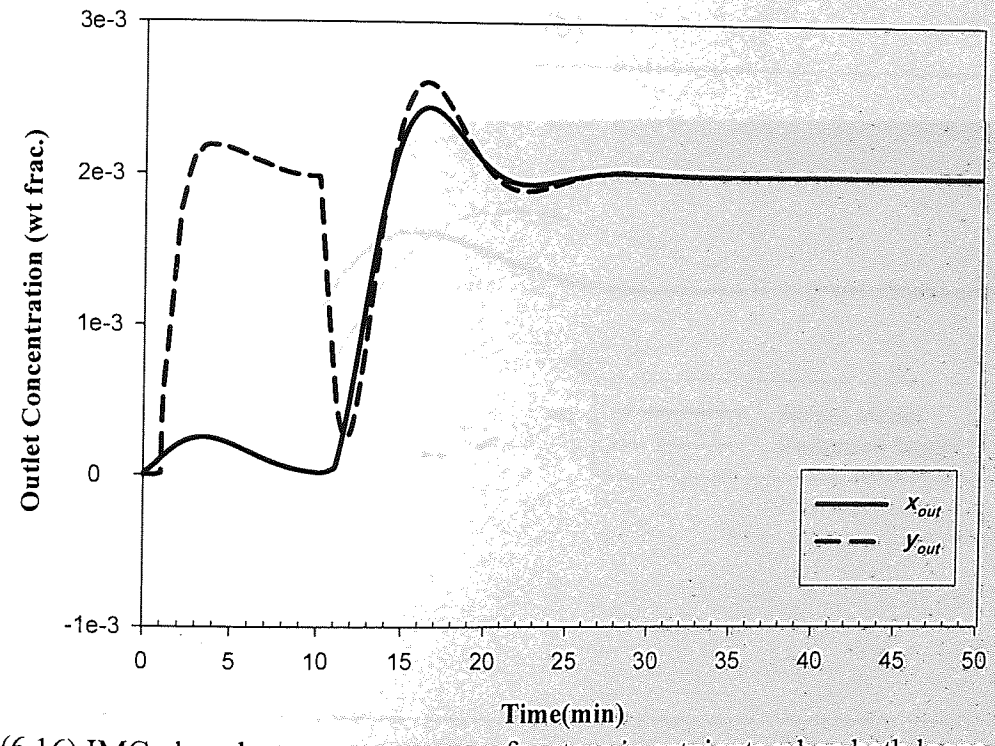

igure(6.16) IMC close loop servo response for steps in setpionts when both loops close
ı) Step in Raffinate concentration at time=0 and Extract at time=10 min.
ı) Step in Extract concentration at time=0 and Extract at time=10 min.

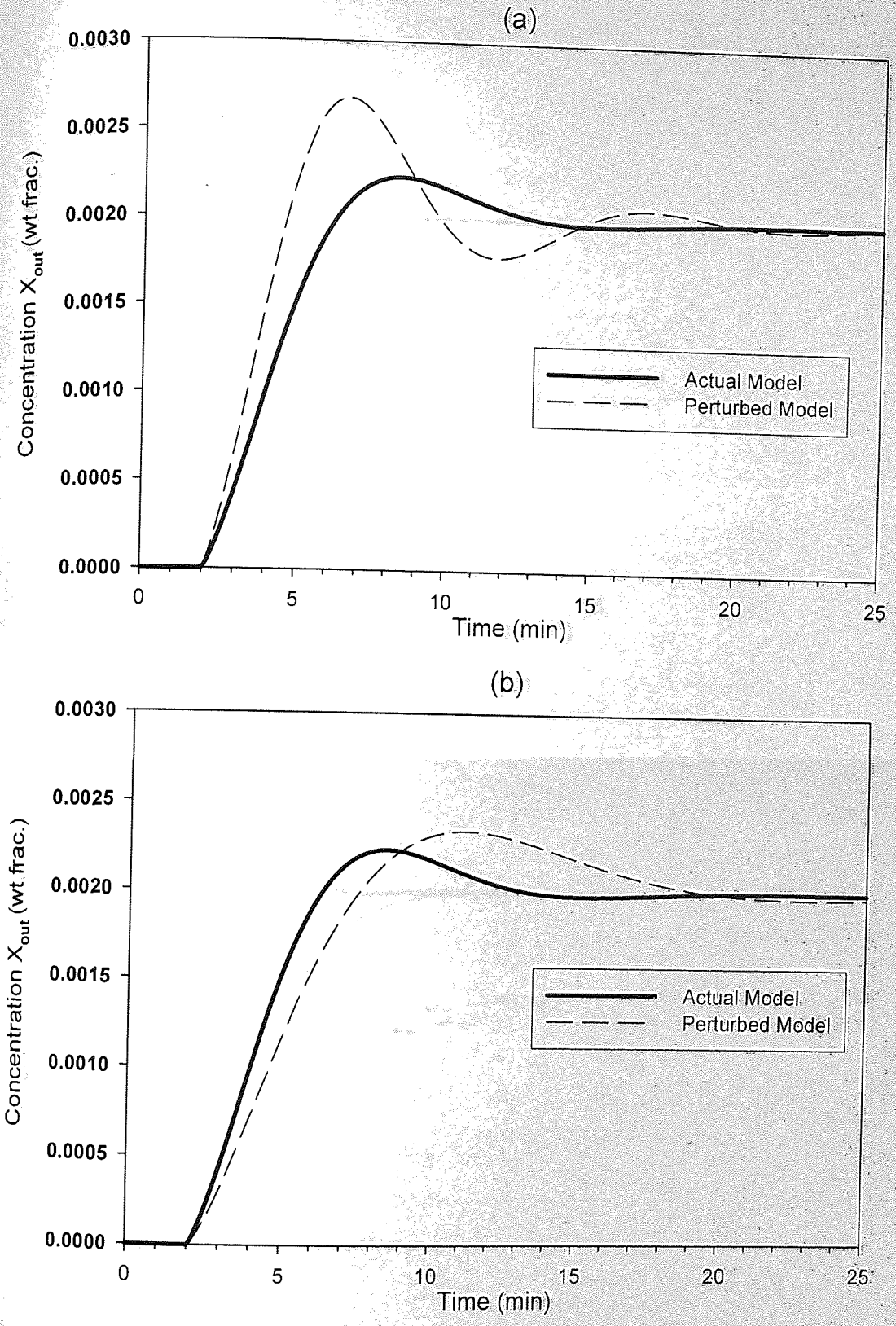

Figure (6.17) The ***N-x_{out}*** single loop servo response in raffinate outlet concentration x_{out} by 10% , with:

(a) process gain mismatch of 50%.

(b) process response time mismatch of 50%.

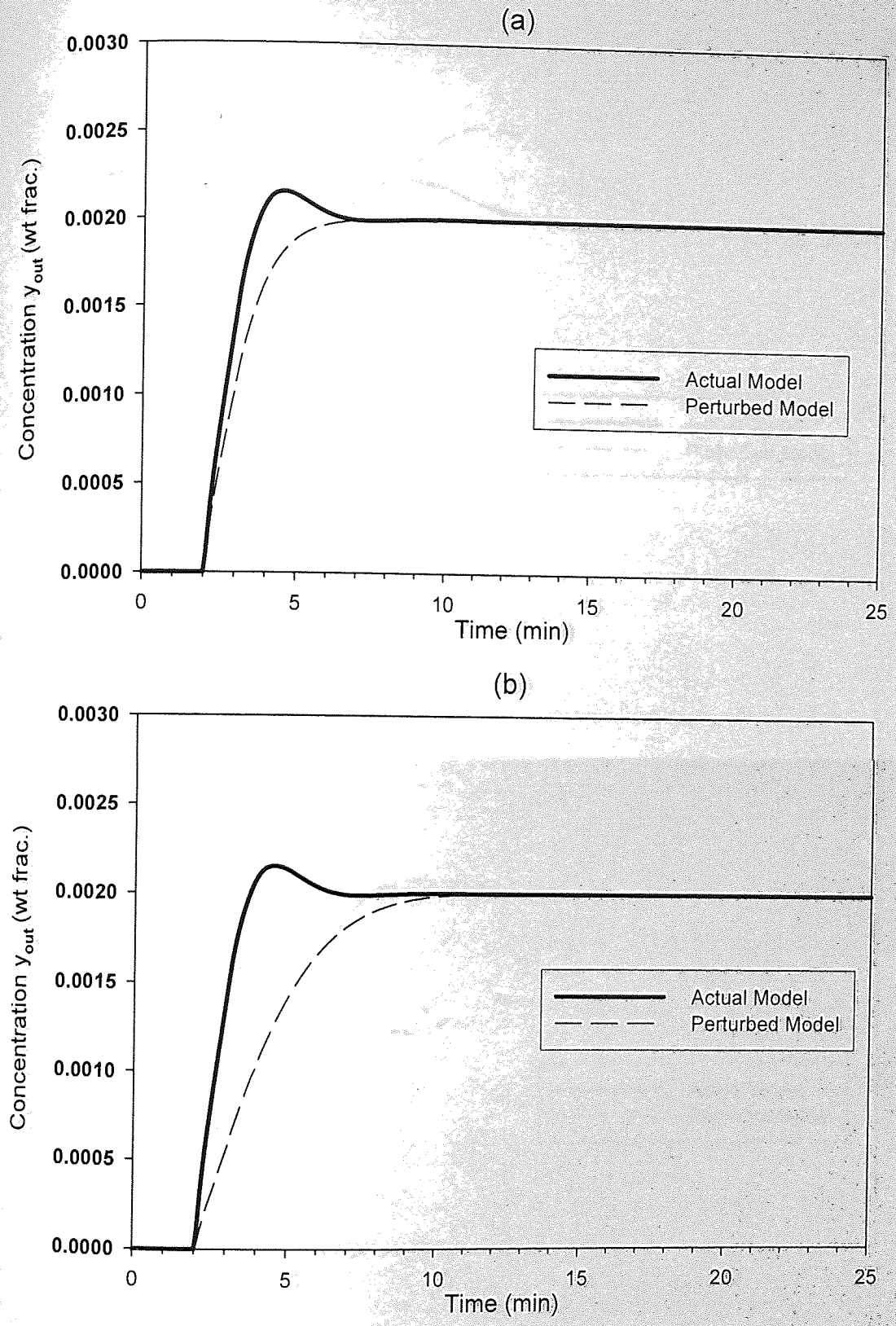

Figure (6.18) The ***S-y$_{out}$*** single loop servo response in extract outlet concentration y_{out} by 10% , with:

(a) process gain mismatch of 50%.

(b) process response time mismatch of 50%.

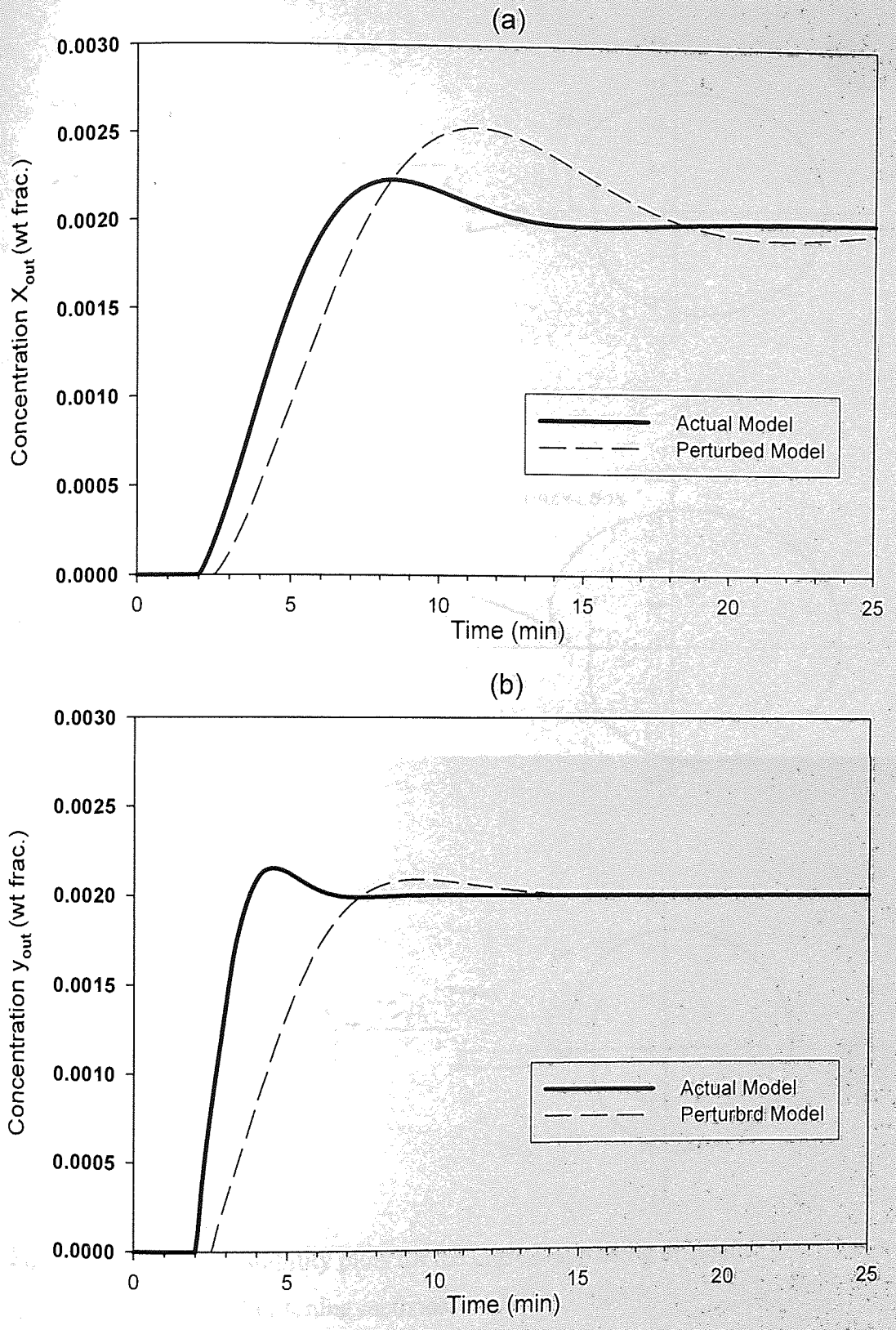

Figure (6.19) The multi-loop servo response for 10% steps in the outlet concentrations $x_{out}$and y_{out} for a 50% process gain mismatch.

(a) N-x_{out} loop response.

(b) S-y_{out} loop response.

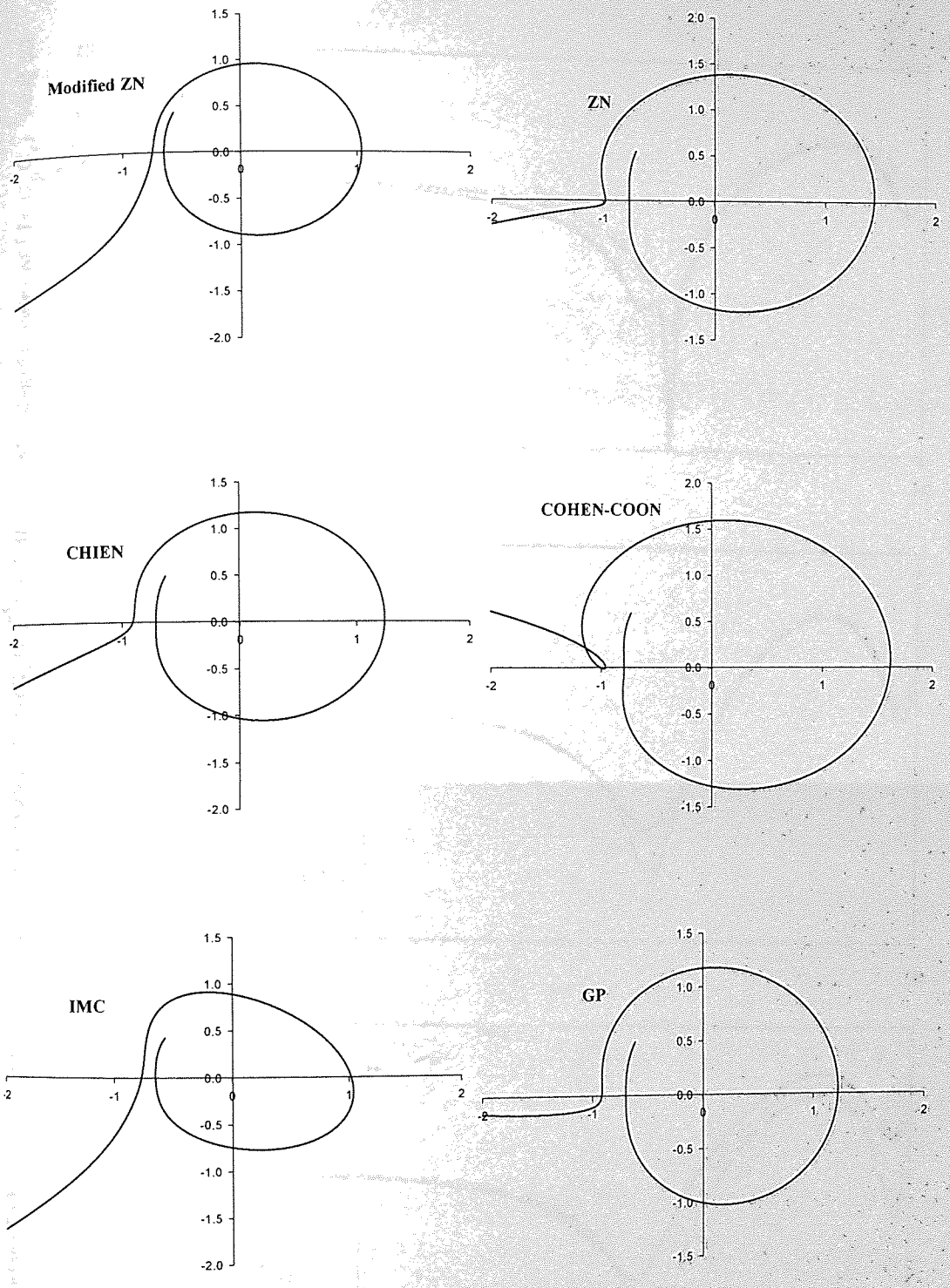

Figure(6.20) Nyquist stability plots for the closed loop using different controller tuning methods.

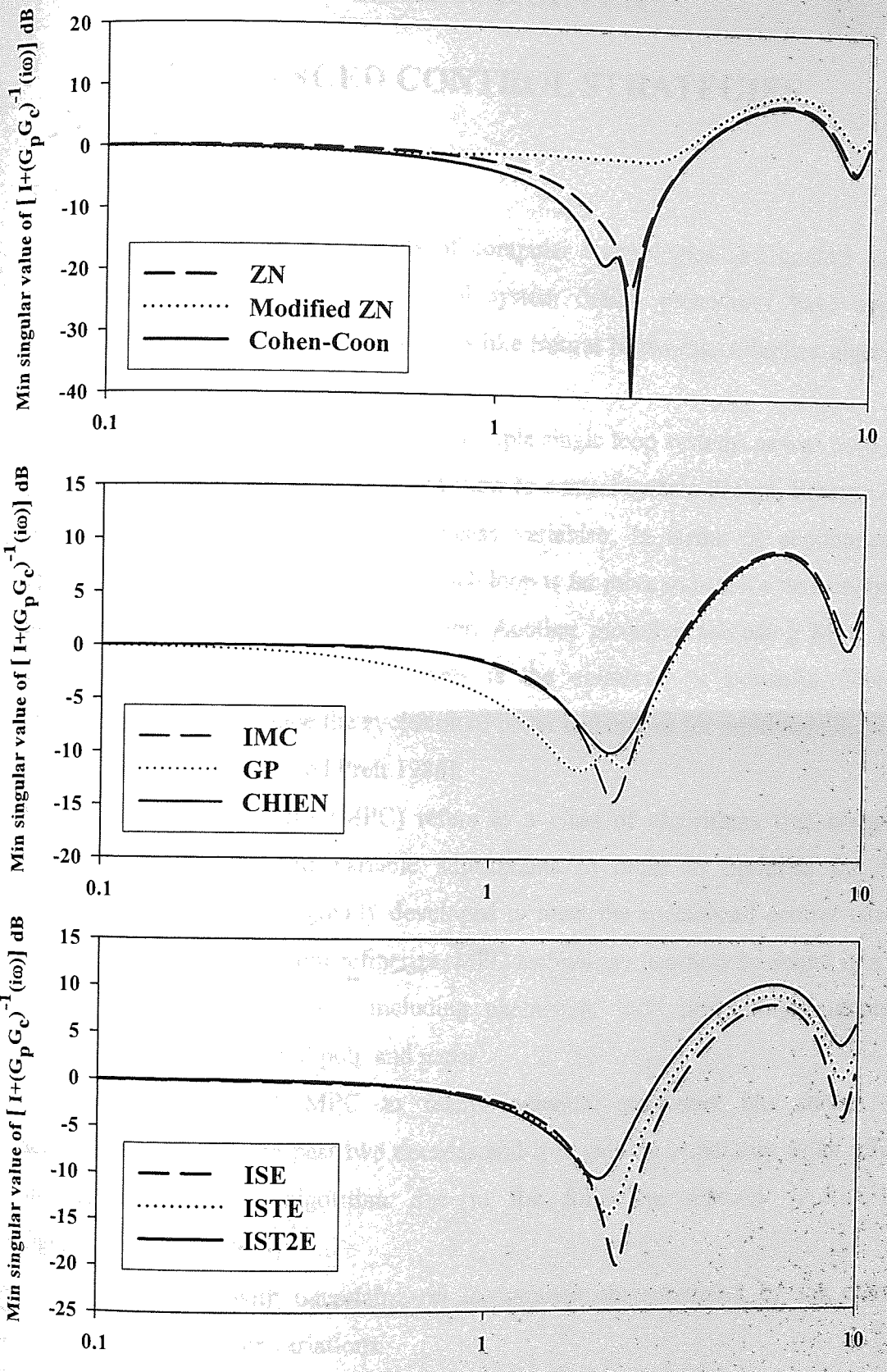

Figure(6-21) Doyle-Stein robustness criterion for the different controllers settings.

CHAPTER SEVEN

ADVANCED CONTROL STRATEGIES

7.1 Introduction:

Motivated by the advancements of computer technologies and control analysis techniques, more sophisticated control system design procedures have appeared during the past two decades. Techniques like Neural Networks, Adaptive algorithms, Model predictive are a few examples.

Treating the multivariable system as a multiple single loop systems as was done in the previous chapter, resulted in a limited view to control system design, because of the probable interactions among the process variables. In terms of economics, the operation of a separate controller for each loop is far more expensive than controlling the whole process using one controller. Another incentive for using MPC in the control of complicated MIMO plants is the existence of powerful, low cost microprocessors that made the evolution of better techniques for multivariable process control a reality [Garcia and Prett 1986].

Model Predictive Control (MPC) refers to a class of algorithms that compute a sequence of manipulated variable adjustments in order to optimise the future behaviour of a plant. Originally developed to meet the specialized control needs of power plants and petroleum refineries, MPC technology can now be found in a wide variety of application areas including chemicals, food processing, automotive, aerospace, metallurgy, and pulp and paper.

The application of MPC to many industrial processes has shown great accomplishments in the past two decades and it is gaining popularity as an efficient and reliable control algorithm due to the following features [Arkun, 1994; Ogunnaike et. al., 1994]:

- Deals with uncertainty in the process characteristics by the effect of parameter variations.
- Handles uncertainty in the environment from external disturbances.
- Manages the nonlinearities of the process introduced by multiple operating regimes.

- Can be used for situations of changing control objectives.
- Used for the characterization of a performance index amenable to controller design.
- Handles processes with time delays, inverse response and other difficult process dynamics encountered by most industrial processes.
- Manages situation where there is interaction between variables involved in the control strategy.
- Eliminates problems of stability created by constraints. These constraints restrict the use of the tuning guidelines for the unconstrained case, [Zafiriou, 1990].

Due to these merits offered by the use of the MPC, and the real need of adopting an efficient control algorithm for the liquid-liquid extraction process which suffers from all the potential problems mentioned above, a dedicated study of the MPC design was conducted using the reduced order identified models. The functions sought in the design and implementation of the MPC algorithm can be summarized as follows [Arkun, 1994]:

- drive the CV's to their steady-state optimal values (dynamic output optimization)
- drive the MV's to their steady-state optimal values using remaining degrees of freedom (dynamic input optimization).
- prevent excessive movement of MV's and exhibit smooth behaviour of actuators.
- eliminate as far as possible any loop interaction present in the process and stabilise the effect of any specific excitation on other variables.
- prevent violation of input constraints imposed by practical considerations and at the same time achieve the desired control objective.

Process knowledge is captured in the form of model suitable for on line control computations. For the MPC, four types of models can be used namely; *Impulse response models, Step response models, Auto regressive, Integrated Moving average,* and *finally State space models.*

7.2 Synthesis of Model Predictive Controller

Model Predictive Control (MPC) is a technique in which a process model is used to forecast future process behaviour, and the sequence of future control inputs is computed as the solution to an open-loop optimization problem. The first element of the optimal input sequence is used as the process input. The remaining elements of the input sequence are discarded and the optimization is repeated at each sampling time. Feedback from measurements is considered by correcting the model prediction based on the error between the measurement and prediction. Many methods are available for this correction. Several recent reviews (Morari and Lee, 1999, Qin and Badgwell, 1997) summarize the theoretical formulations and industrial implementations of MPC.

The MPC predicts controller moves from the forecast future process behaviour by solving an optimisation problem to minimize set-point error. The major components of the MPC are shown in Figure(7.1).

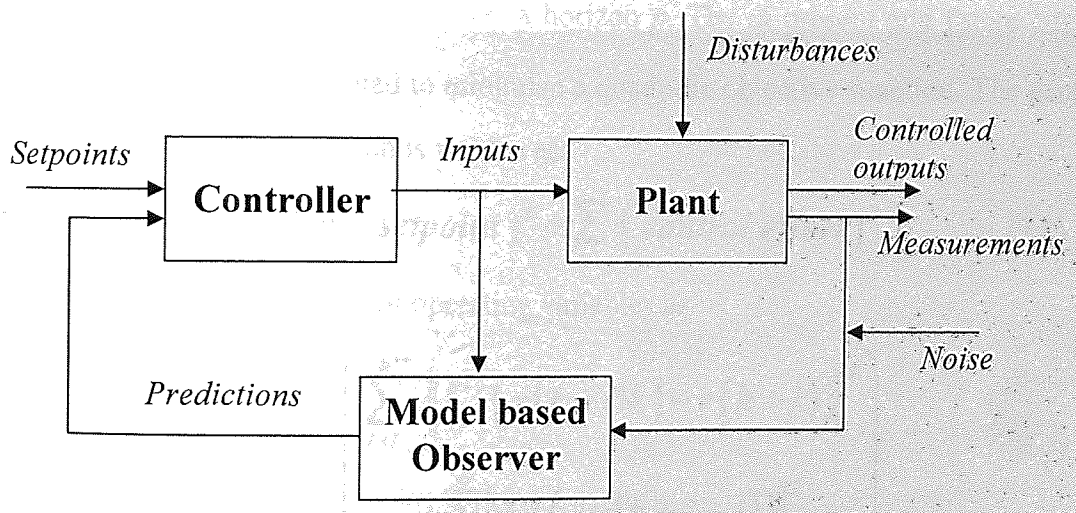

Figure(7.1) The main components of the MPC loop.

We can derive the MPC control law by referring to the following figure(7.2).

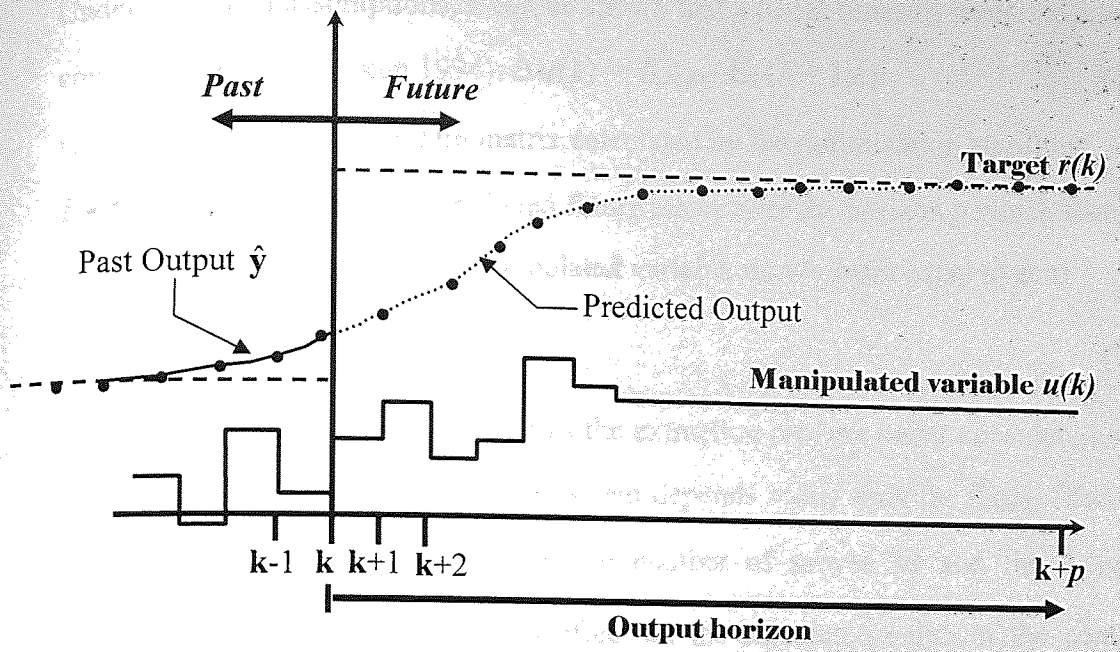

Figure(7.2) The optimization control law for MPC.

For any assumed set of present and future control moves $\Delta u(k), \Delta u(k+1), \ldots, \Delta u(k+m-1)$ the future behaviour of the process outputs $y(k+1|k), y(k+2|k), \ldots, y(k+p|k)$ can be predicted over a horizon p. The m present and future control moves $(m \leq p)$ are computed to minimize a quadratic objective function. The general form of the objective function is written as:

$$\text{Min}\left[\sum[\,\textit{prediction} - \textit{setpoint}\,]^2 + \sum[\,\textit{control effort}\,]^2\right] \qquad (7.1)$$

It can be expressed in terms of operating variables as :

$$\min_{\Delta u(k)\ldots\Delta u(k+m-1)} \left(\sum_{l=1}^{p} \left\| \Gamma_l^y \left(y(k+l|k) - r(k+l) \right) \right\|^2 + \sum_{l=1}^{m} \left\| \Gamma_l^u \left(\Delta u(k+l-1) \right) \right\|^2 \right) \qquad (7.2)$$

The Γ_l^y and Γ_l^u refer to the weighting matrices to penalize particular components of y or u at certain future time intervals. $r(k+l)$ is the (possibly time-varying) vector of future reference values (set points). Though m control moves are calculated, only the first one $(\Delta u(k))$ is implemented. At the next sampling interval, new values of the measured outputs are obtained, the control horizon is shifted forward by one step, and the same computations are repeated. This control law is referred to as "moving horizon" or "receding horizon".

Under the stated assumptions, it can be shown that a linear time-invariant feedback control law results (Arkun 1994): $\Delta u(k) = K_{MPC}\, E_P(k+1|k)$ (7.3)

where K_{MPC} is controller gain matrix calculated by the optimization algorithm, and $E_P(k+1|k)$ is the vector of predicted future errors over the horizon p which would result if all present and future manipulated variable moves were equal to zero

$$\Delta u(k) = \Delta u(k+1) = \ldots = 0 \qquad (7.4)$$

For open-loop stable plants such as the extraction process under consideration, the closed-loop nominal stability of the system depends solely only on K_{MPC}. The MPC parameters namely; the horizon p, the number of moves m and the weighting matrices Γ_l^y and Γ_l^u have direct effect on the calculated value of the controller gain. No precise conditions on these parameters exist which guarantee closed-loop stability. In general, decreasing m relative to p makes the control action less aggressive and tends to stabilize a system. For $p = 1$, nominal stability of the closed-loop system is guaranteed for any finite m, and time-invariant input and output weights. More commonly, Γ_l^u is used as a tuning parameter. Increasing Γ_l^u always has the effect of making the control action less aggressive [Morari and Ricker 1998].

To test the robustness of the control design, i.e., its sensitivity to modelling errors, model mismatches in process gains and process time constants are introduced into the models and the controllers behaviour are studied. 50% model mismatch in model parameters was chosen for the robustness study. The time response of both the perturbed and the original models and then compared, and a conclusion can then be drawn about the reliability and sensitivity of the model to modelling errors.

The practical control objective involves constraints criteria in addition to satisfying some performance criteria. These constraints are functions of variables to be kept within bounds due to physical, operational or safety limitations. They can be divided into two categories [Garcia and Prett 1986].

- Hard constraint: no dynamic violations of the bounds are allowed at any time.
- Soft constraints: violations of bounds can be allowed for satisfying criteria.

For this reason the study of any control system must involve such limitations. One of the basic features of the MPC algorithm is that it is capable of handling such

limitations in input and output variables effectively. This means that it is capable of restricting the actuators moves to be within two bounds and it also can assure that the outputs are not to exceed certain quality limits. The MPC is tested for operation under constraints in the input and output variables, and compared with that of unconstraint conditions.

7.3 Results and Discussions

The MPC system design approach was used with the identified reduced order extractor model. The closed loop was simulated to account for all input/output variables (MIMO) including loads of the system. The simulation was done using MATLAB MPC toolbox. The details of the program is given in Appendix(G). The MPC simulation and control algorithm is shown the flowchart of Figure(7.3).

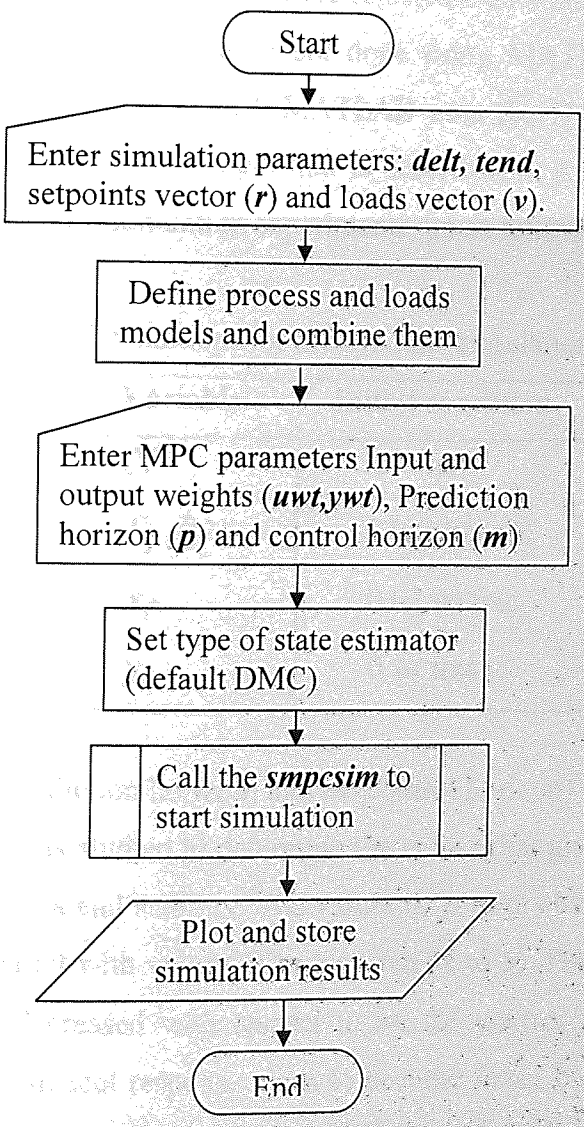

Figure(7.3) The MPC simulation algorithm.

The program variables used in the chart are described below:

delt: the sampling period for the system.

tend: the desired duration of the simulation (min).

r: the setpoint matrix consisting of 1 row and 2 columns.

v: the loads matrix consisting of 1 row and 3 columns.

uwt: matrix of weights that will be applied to the changes in the manipulated variables.

ywt: matrix of weights that will be applied to the setpoint tracking errors.

p: number of sampling periods in the prediction horizon.

m: the input horizon (number of moves) as in DMC.

The 2×2 system was simulated for 25min, with a 0.5 min sampling period. The prediction horizon and control horizon were selected after some preliminary testing as explained next. All simulation runs were done using MATLAB model predictive control toolbox version 6 release 12. MATLAB uses the Dynamic Matrix Control (DMC) form. The details of this algorithm is described in Appendix(B). The initial conditions of the dynamic simulation experiments are as follows:

Table(7.1) Initial conditions for the dynamic simulation experiments.

Variable	Initial condition
N	400 rpm
S_f, R_f	250 cm^3/min
x_f	0.02 wt frac
y_f	0 wt frac

The effect of ***p*** (prediction horizon) and ***m*** (control horizon) on the performance of the MPC algorithm was studied to determine the values that give the best response in terms of control criteria and stability. The values of ***p*** were changed within the range (5 to 15) and compared with values of ***m*** between (2 to 5). From figure(7.4) we can notice that as ***p*** is decreased with respect to ***m***, the control action becomes more aggressive and the transient response tends to become faster but closer to instability. Another (often more effective) way is to use blocking for the control horizon. In the case of blocking, each element of the vector ***m*** indicates the number of steps over

which $\Delta \mathbf{u} = \mathbf{0}$ during the optimization. For example, $\boldsymbol{m}$ = [2 3] defines 2 blocks of control moves, the first block : $\Delta \mathbf{u(k+1)} = \mathbf{0}$ and the second block: $\Delta \mathbf{u(k+3)} = \Delta \mathbf{u(k+4)} = \mathbf{0}$. This is interpreted as $\mathbf{u(k+1)} = \mathbf{u(k)}$ and $\mathbf{u(k+4)} = \mathbf{u(k+3)} = \mathbf{u(k+2)}$. After some trials, the choice of $\boldsymbol{m}$ as a raw vector with three blocks $\boldsymbol{m}$=[2 3 5] gave good performance and a more stable response for both variables. A value of $\boldsymbol{p}$=15 and $\boldsymbol{m}$=[2 3 5] were chosen and fixed for the subsequent experiments.

Next the effect of varying the input weight factor on the controller response was investigated. This was done by a trial and error procedure to select the best value that gives good performance and robustness. The MPC simulation was performed using different input weight factors (Γ_l^u). The range [0.001–0.01] was investigated. The responses for such range are shown in Figure(7.5) for both output variables x_{out} and y_{out}. As the input factor decreases the control becomes more aggressive and response gets faster and less robust, a value less than the range tested will give an unstable response. The value 0.005 for both loops (i.e. Γ^u =[0.005 0.005]) was found to give good performance characteristics, so it was selected for the rest of the experiments.

The output weight factor (Γ_l^y) was left equal to the default value of unity (i.e. Γ^y =[1 1]). This is to give an equal emphasis to both concentration outputs because of the identical importance of their control.

After detecting best simulation parameters, the MPC system was tested for both *servo* (setpoint change) and *regulatory* (load change) performance to investigate its reliability as a MIMO control scheme.

The *servo* response characteristics were tested first. Figure(7.6) gives the MPC response to a +10% step in raffinate outlet concentration x_{out} with corresponding manipulated variables moves. The system approaches steady state smoothly without overshoot and the other controlled variable (y_{out}) didn't undergo any significant change during the simulation. This indicates that the MPC was capable of handling the setpoint change efficiently, and isolated the other loop from any interaction. Also it is noticed that the manipulated variables moves were not aggressive and there values were stabilised during the first five minutes of the simulation time. This shows that the MPC handled the excitation without turbulent manipulated variable moves.

Similar response characteristics were observed in the solvent outlet concentration y_{out}. This is shown in Figure(7.7). As expected, the MPC proved to be capable of

stabilising the response smoothly within a short time, with least manipulated variable moves and isolated any loop interaction.

The *regulatory* response characteristics of the control system was tested for the three loads namely; feed concentration (x_f), solvent concentration (y_f) and feed flowrate (R_f). Figures (7.8-7.10) show these responses respectively. In general, it can be noticed that the load variables have greater effect on actuating solvent flow rate compared to the rotor speed manipulated variables. This can be attributed to the results of the input magnitudes test conducted in the previous chapter, where it was found that the solvent flowrate has the highest row sum value of the $G^{-1}G_d$ matrix, which means it has higher power for rejecting disturbance than the rotor speed. The greatest move span in the solvent flowrate is that due to the solvent concentration load (0 to -130). This is compared to (0 to 32) for the feed concentration and (0 to -10) for the feed flowrate. This gives an indication of the high mass transfer effect associated with variations in the solvent concentration which needs more effort for the actuator to be stabilized. This result agrees with previous disturbance rejection tests in the controllability analysis.

The three load responses have approximately similar trends. The responses start with a sudden change in both outlet variables x_{out} and y_{out}, then after approximately 2 min the system transient starts to settle back to the same steady state final value. The response settling times for the three loads are 4, 6, and 5 min respectively. This means that the system comes to rest after the excitations in a fairly short time, preventing any further disturbance to propagate through the system. We can conclude that the MPC was able to reject the disturbances efficiently and within reasonable time. Also it is clear that the y_f is the most difficult load to reject. This agrees with the controllability analysis results presented in chapter 6.

The effect of model mismatch was studied by testing the dynamics of the system for variations in the operational parameters namely process gain, time constants and time delay. A +50% mismatch in each of these parameters was introduced and the system response for set point disturbances was studied. This was done for the case of 10% step change in raffinate outlet concentration as well as 10% set point change in solvent outlet concentration as shown in Figures (7.11). A -50% mismatch test was performed and the corresponding system responses for the two controlled variables are shown in Figures (7.12).

The transient deviations from the actual model were insignificant comparable to the severe mismatch of +50% and -50% in the operational parameters. This indicates that the behaviour of the MPC controller is robust even under large modelling deviations.

Next the problem of control under constrained input variables was investigated. The control action can also be computed subject to hard constraints on the manipulated variables and the outputs. MPC can handle two types of constraints namely,

Manipulated variable constraints:

$$umin\ (l) \leq u(k+l) \leq umax\ (l)$$

Output variable constraints:

$$ymin\ (l) \leq y(k+l \mid k) \leq ymax\ (l)$$

where ***umin(l), umax(l), ymin(l),*** and ***ymax(l)*** are minimum and maximum bounds of the ***l*** th input and output variable constraints.

For this case the system response to a series of setpoint changes was compared for the two cases of constrained and unconstrained manipulated variables. The operation of the MPC algorithm was performed under practical imposed limitations on the actuating variables. Usually these types of constraints hinder the controller from driving the process to the desired output or at least make the control task hard to be accomplished within the specified performance criteria.

The following input variables moves constraints were considered for both deviations in the rotor speed $\hat{RPM}$ and the solvent feed flowrate $\hat{S}_f$ (expresses as perturbation variables) as:

$$-40 \leq \hat{RPM} \leq 40$$
$$-60 \leq \hat{S}_f \leq 60 \qquad (7.5)$$

The limits were chosen to be in size that reflects the effects of constraints under the setpoint step change of 0.002 in the output variables. This was done by setting the input limitation vector ***ulim***=[*-40 -60 40 60 1 100*]. The first four numbers in the ***ulim*** vector are the constraints bound, and the last two numbers specify the limits on the rate of change of the manipulated variables. A value of 1 is selected to the rotor speed and a value of 100 for the solvent flowrate. This reduces the rate of change of the rotor speed to prevent fast actuation. The simulation code is written in the MATLAB code and given in Appendix(G). The effects of loop interactions have no

appreciable effect on the overall dynamics of the system and are handled efficiently by the MPC controller.

Figure(7.13) shows the comparison for the two cases of unconstrained and constrained simulation of the MPC controlled process.

We comprehend that for the case of input constrained control, the MPC was able to drive the system dynamics to the desired values effectively without violating the limitations assigned for the manipulated variables. Of course there were some differences between the transients of the two cases in terms of set point tracking time and damping of response, but in terms of control criteria, the constrained case was acceptable with slower response than the unconstrained one especially for the raffinate case. This proves the ability of the MPC to control the extraction process effectively when limitations are imposed on the input variables movements.

For practical considerations, sometimes it is necessary to impose some limitations on the quality of the output. This may be due to economical and safety considerations or to limitations on solvent recovery schemes that restricts the recovery of solvents between certain limits. This case was considered by subjecting the control system to a series of step changes for the two cases of constrained and unconstrained controlled variables. Figure(7.14a) shows the controlled and manipulated variables MPC profiles including an upper bound constraint on the raffinate concentration x_{out}. The deviation in output raffinate concentration was limited to 0.0021 (i.e. $\hat{x}_{out} < 0.0021$) by setting the value of ***ylim*** vector in the simulation program to: ***ylim***=[*-inf -inf 0.0021 inf*] where ***inf*** denotes no bound (infinity). The MPC algorithm forced the process to produce a raffinate not exceeding this limit throughout the simulation time.

Figure(7.14b) shows the effect of imposing a lower bound constraint on the extract concentration y_{out} on the controlled and manipulated variables profiles. The deviation in output extract concentration was limited to -0.0021 (i.e. $\hat{y}_{out} > -0.0021$) by setting the value of ***ylim*** vector in the simulation program to: ***ylim***=[*-inf -0.0021 inf inf*]. Although the extract concentration hasn't high overshoot as the case of the raffinate one, The MPC algorithm will always guarantee that the its profile will never exceed this lower bond throughout the simulation time.

Figure(7.15) shows the effect of output variables constraints of both the extract concentration y_{out} and the raffinate concentration x_{out} on the controlled and

manipulated variables profiles. The constraints were written as $\hat{x}_{out} < 0.0021$ and $\hat{y}_{out} > -0.0021$. The ***ylim*** vector includes both bounds and is written as: ***ylim=[-inf -0.0021 0.0021 inf]***. The MPC was successful again in bounding the process response between the two limits imposed by the concentration constraints. In this case it is noticed that the output profiles were very tight and especially the extract profile which settles within 2 min and has a rise time of 1 min. This fast response is due to the fast actuation of the corresponding manipulated variables.

From the manipulated variables response figures, it can be noticed that the solvent feed flowrate undergoes fast changes at the start of each step change. It is worth mentioning that it is undesirable in practice to perform vigorous corrective actions due to consequences resulting from fast mechanical actuation such as the rapid wear-out of the valves and performance degradation of motors, that's why it is always preferred to build an unconstrained control system unless it is unavoidable. Nonetheless, these tests provide a clear picture on the capability of the MPC algorithm to handle output constraints safely and efficiently. This ability of handling input-output process variables limitations is one of the unique features associated with Model based predictive control schemes.

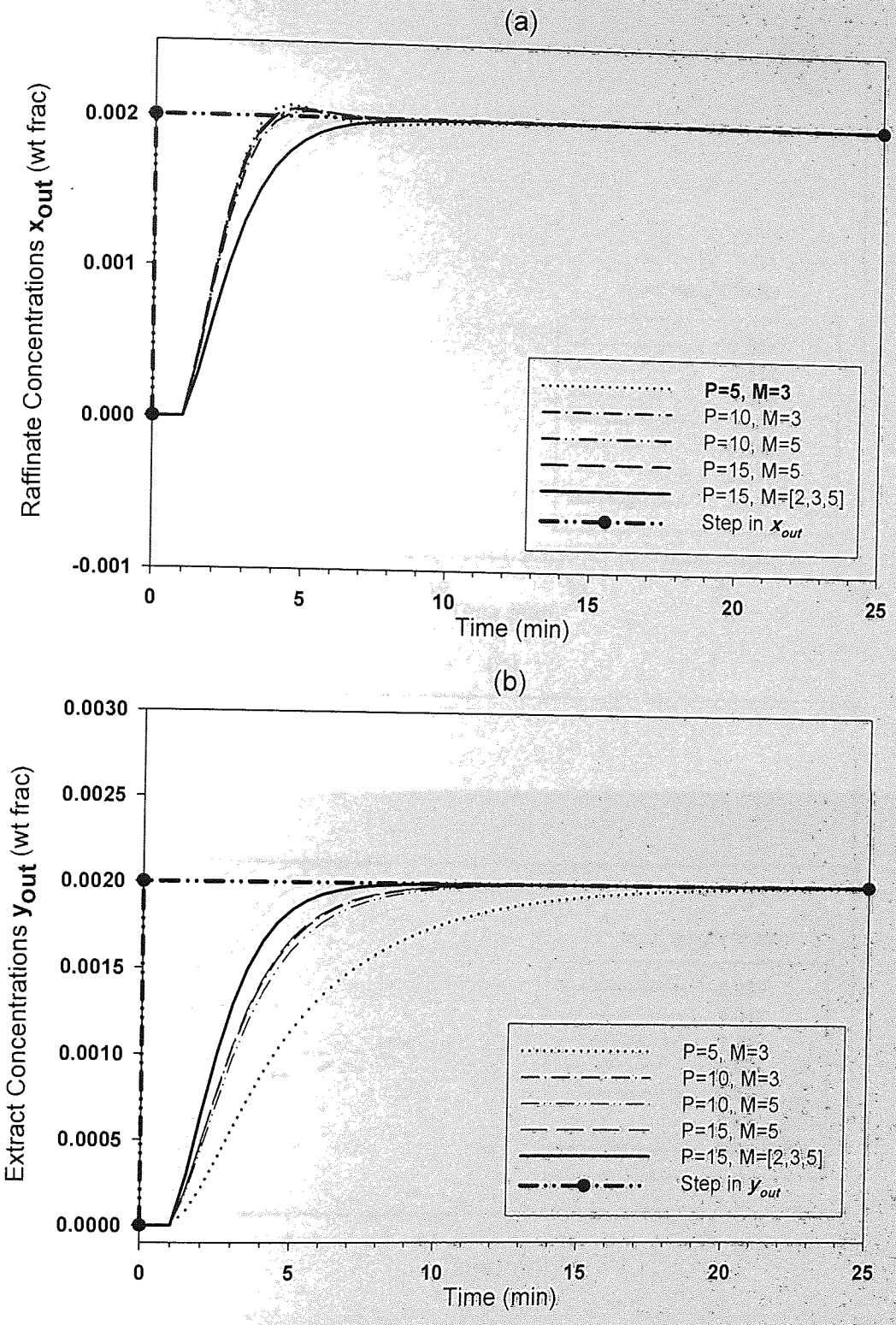

Figure (7.4) Effect of values of Prediction horizon (P) and Control horizon (M) on the response of the MPC controller response for a 10% step change in both Raffinate and Extract concentrations x_{out} and y_{out} :
(a) Raffinate concentration x_{out}.
(b) Extract concentration y_{out} .

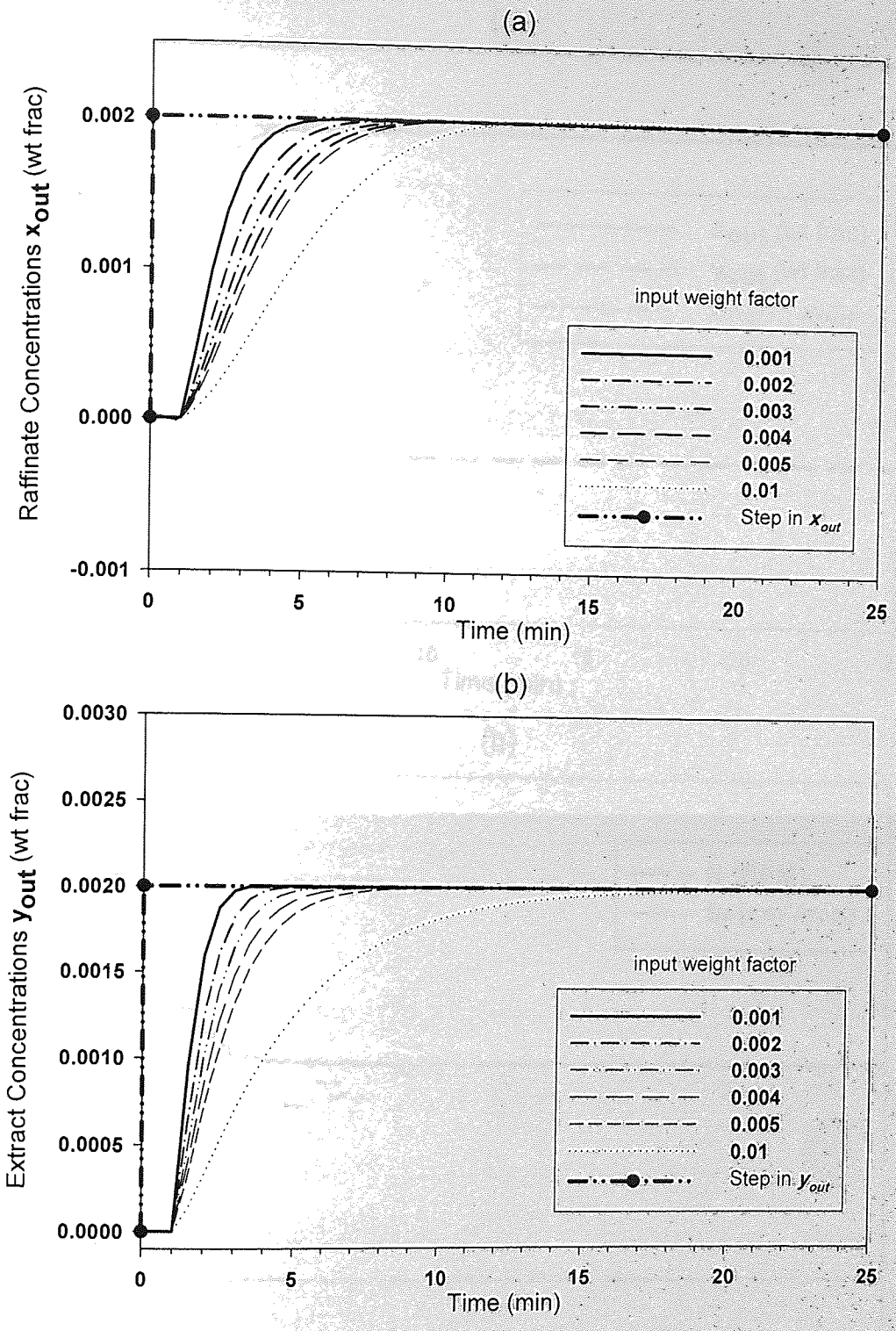

Figure (7.5) Effect of input weight factors on the response of the MPC controller, 10% step change in both Raffinate and Extract concentrations x_{out} and y_{out} :
(a) Raffinate concentration x_{out}.
(b) Extract concentration y_{out} .

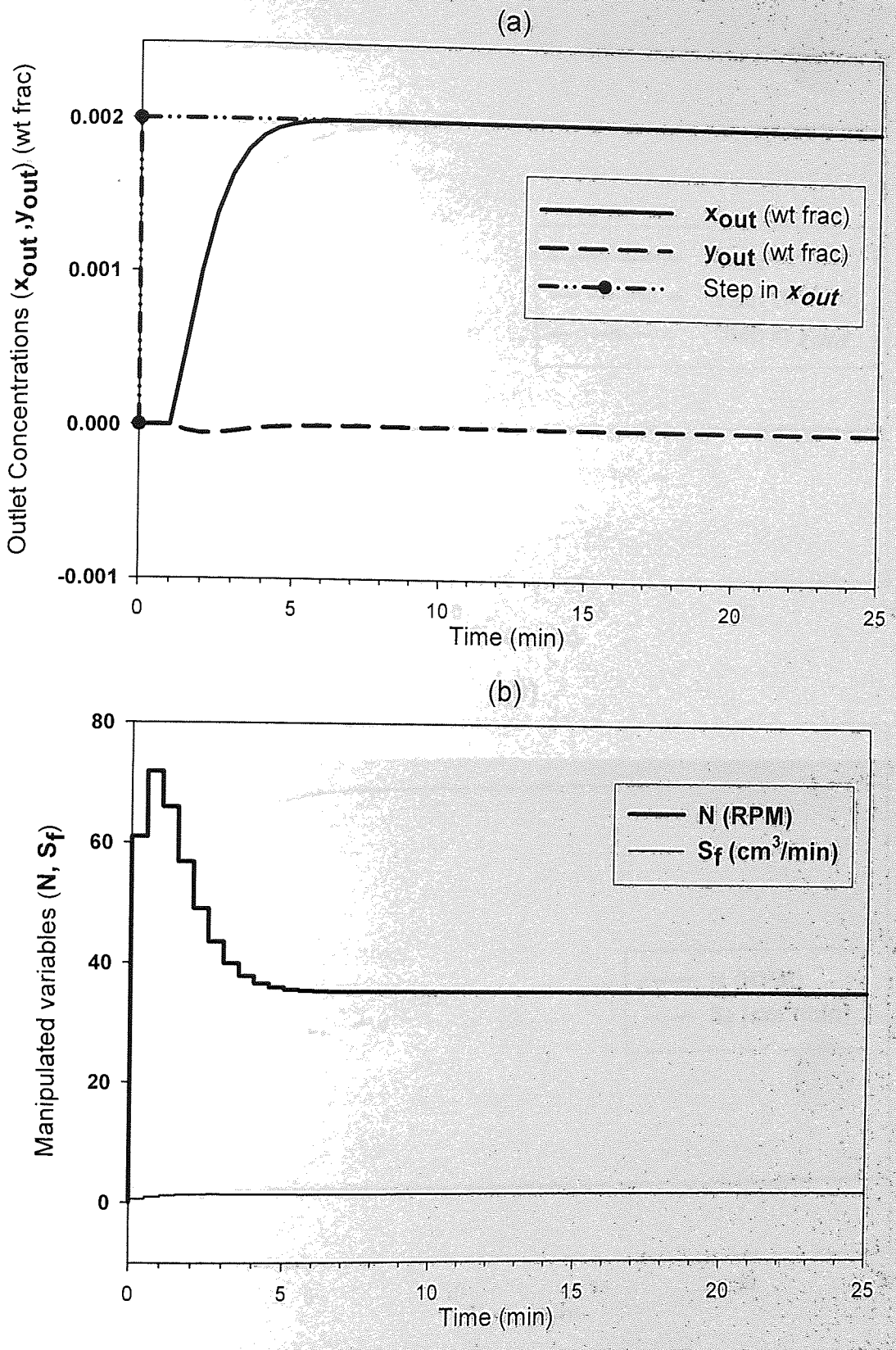

Figure (7.6) MPC Response for a 10% step in the raffinate outlet concentration x_{out} (wt frac.):
(a) Controlled variables (x_{out} ,y_{out}).
(b) Manipulated variables (N, S_f).

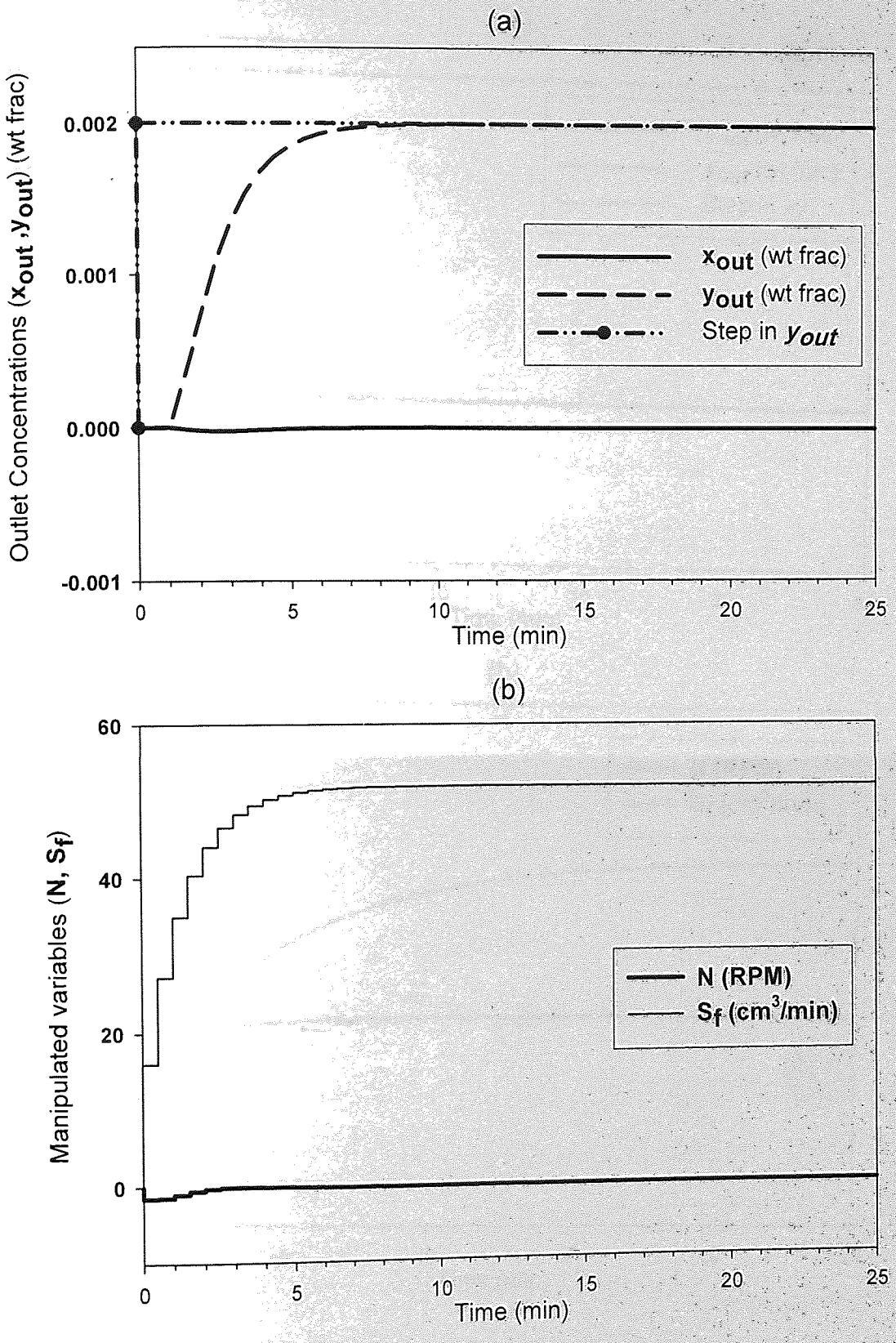

Figure (7.7) MPC Response for a 10% step in the solvent outlet concentration y_{out} (wt frac.):
(a) Controlled variables (x_{out} ,y_{out}).
(b) Manipulated variables (N, S_f).

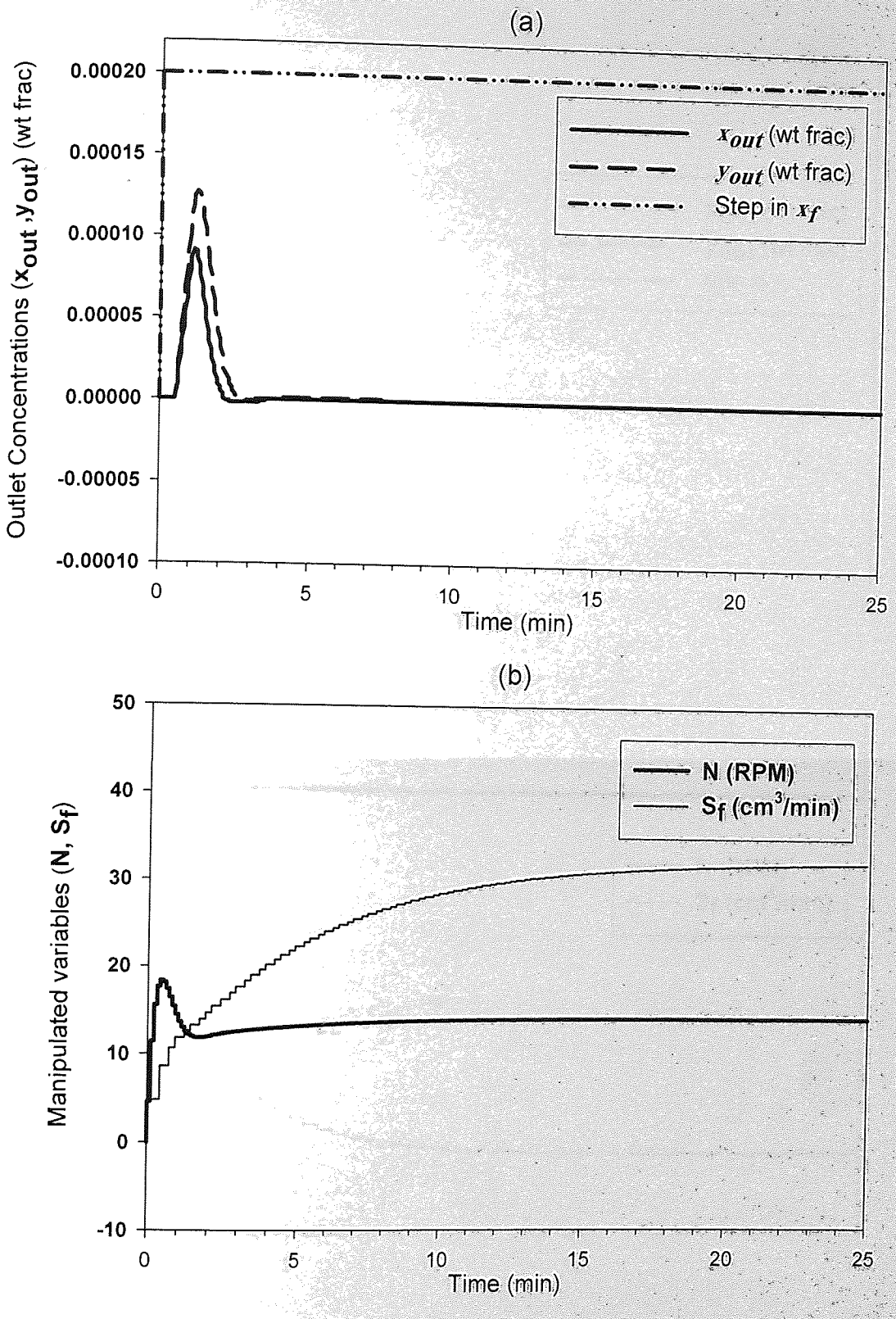

Figure (7.8) MPC Response for a 10% step in the Feed concentration x_f (wt frac):
(a) Controlled variables (x_{out}, y_{out}).
(b) Manipulated variables (N, S_f).

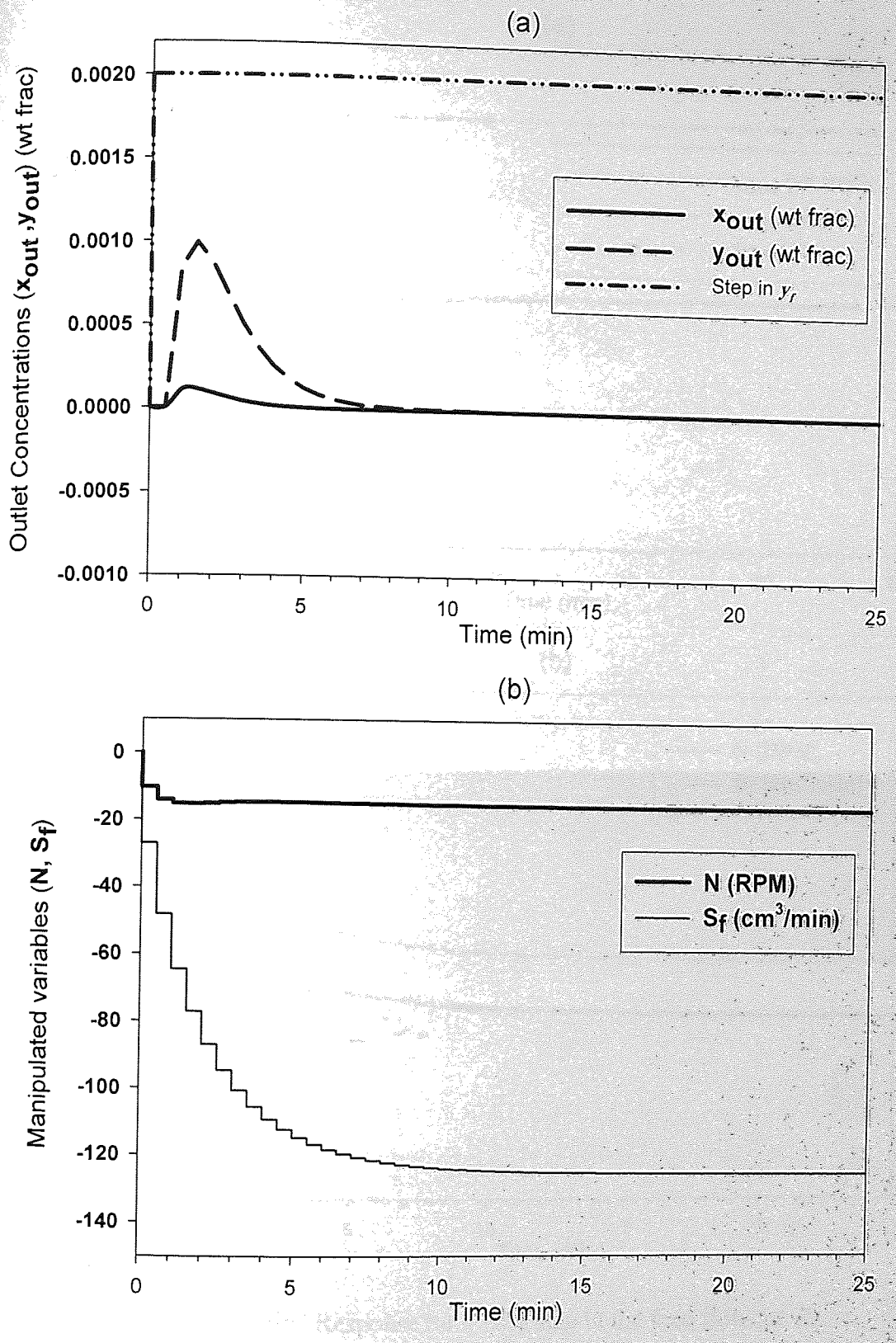

Figure (7.9) MPC Response for a 0 to 0.002 step in the Solvent concentration y_f (wt frac.):
(a) Controlled variables (x_{out} ,y_{out}).
(b) Manipulated variables (N, S_f).

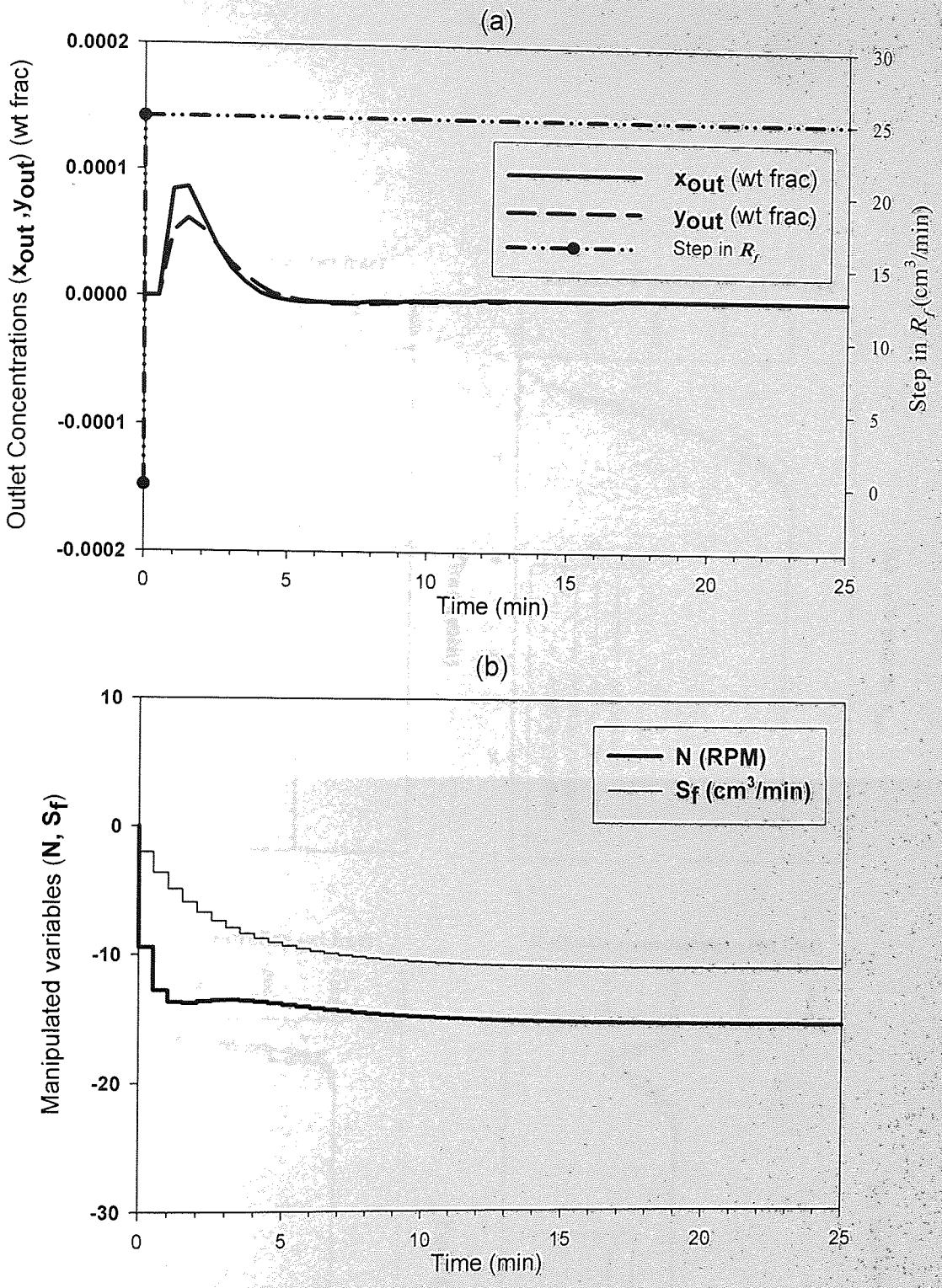

Figure (7.10) MPC Response for a 10% step in the feed flowrate R_f (cm^3/min):
(a) Controlled variables (x_{out} ,y_{out}).
(b) Manipulated variables (N, S_f).

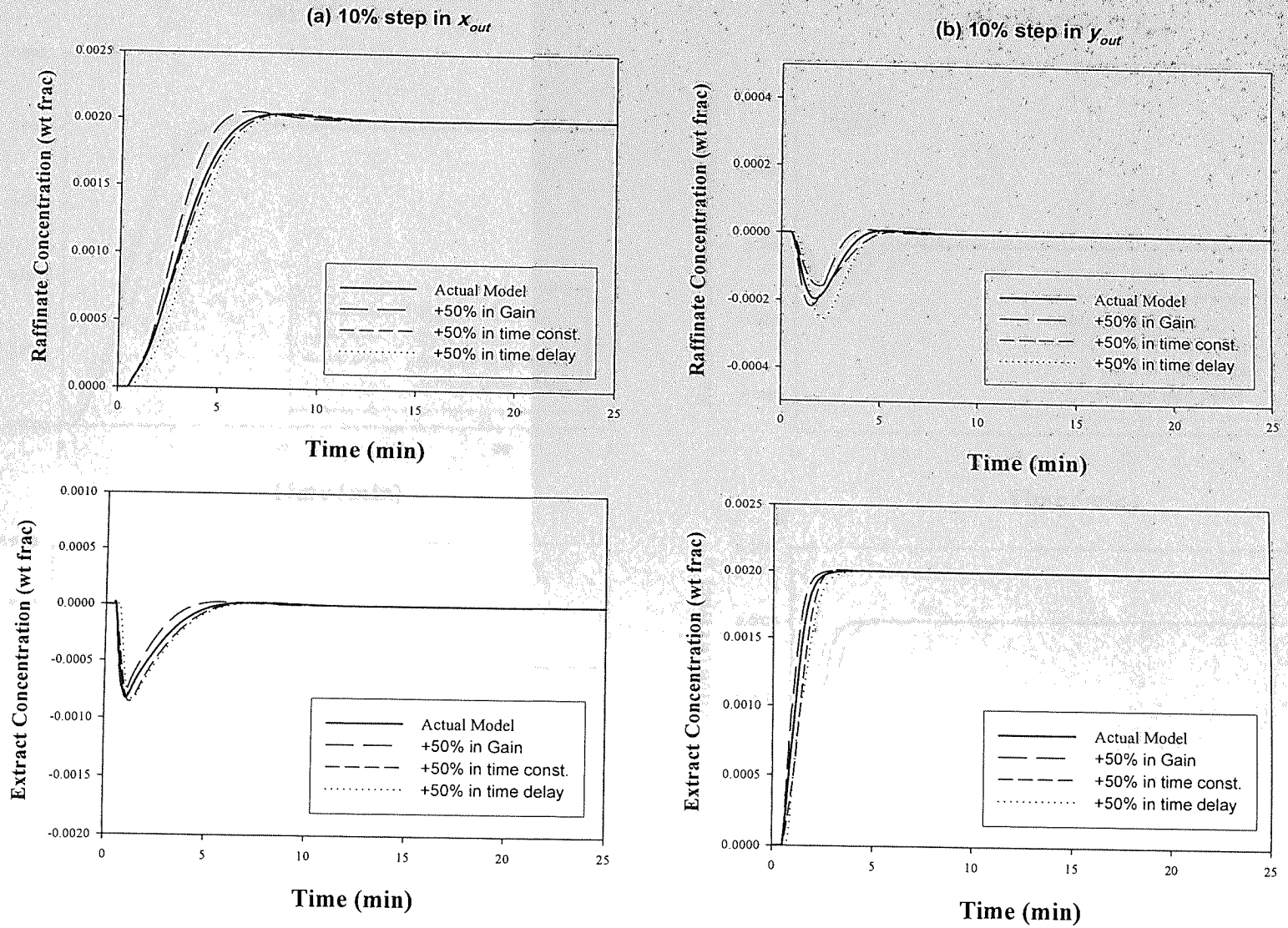

Figure (7.11) Modelling mismatch of +50% in (Gain, Time constant and Time delay) for the MPC controller:
(a) 10% step change in Raffinate x_{out} .
(b) 10% step change in Extract y_{out}.

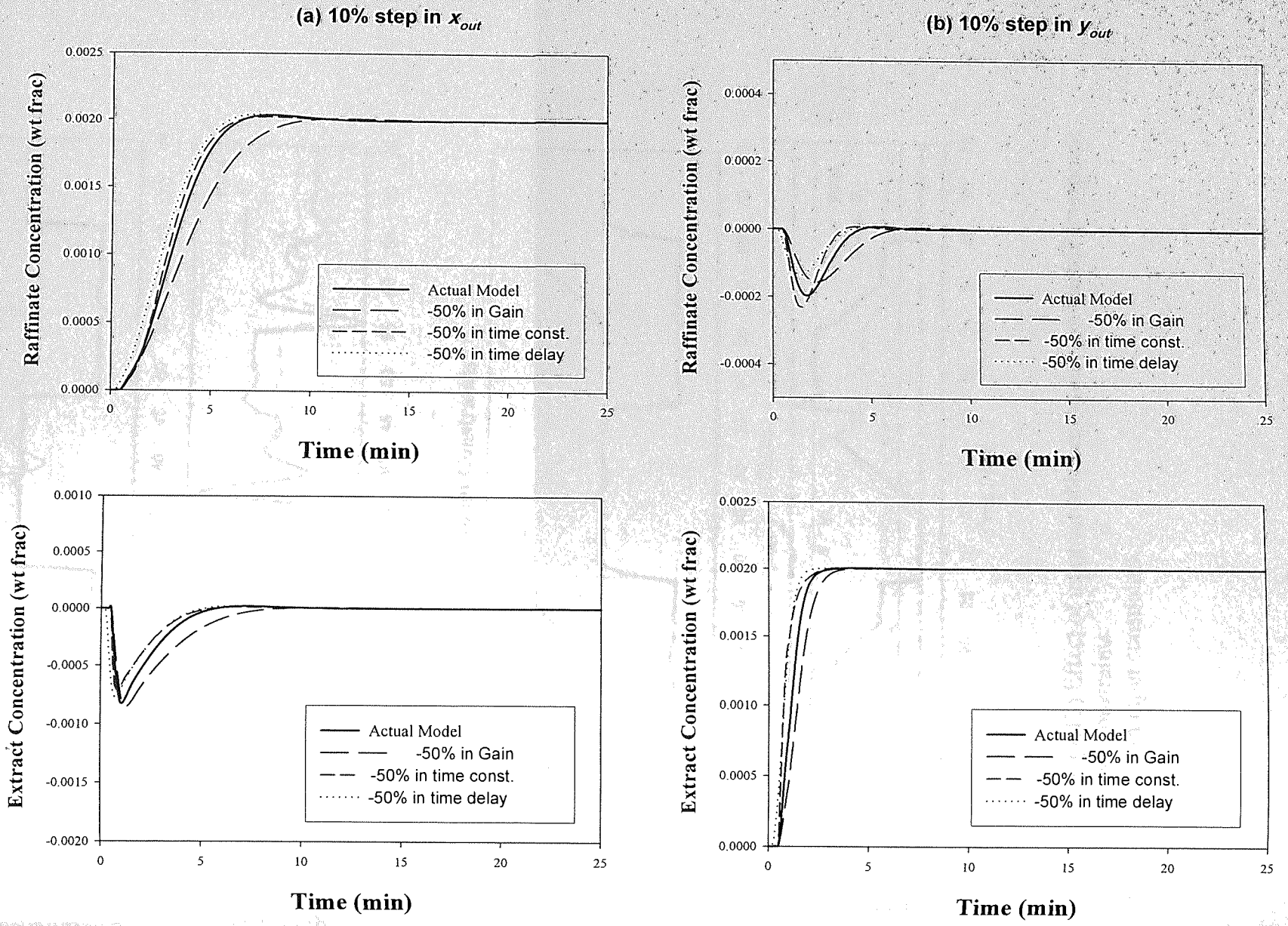

Figure (7.12) Modelling mismatch of -50% in (Gain, Time constant and Time delay) for the MPC controller:
(a) 10% step change in Raffinate x_{out}.
(b) 10% step change in Extract y_{out}.

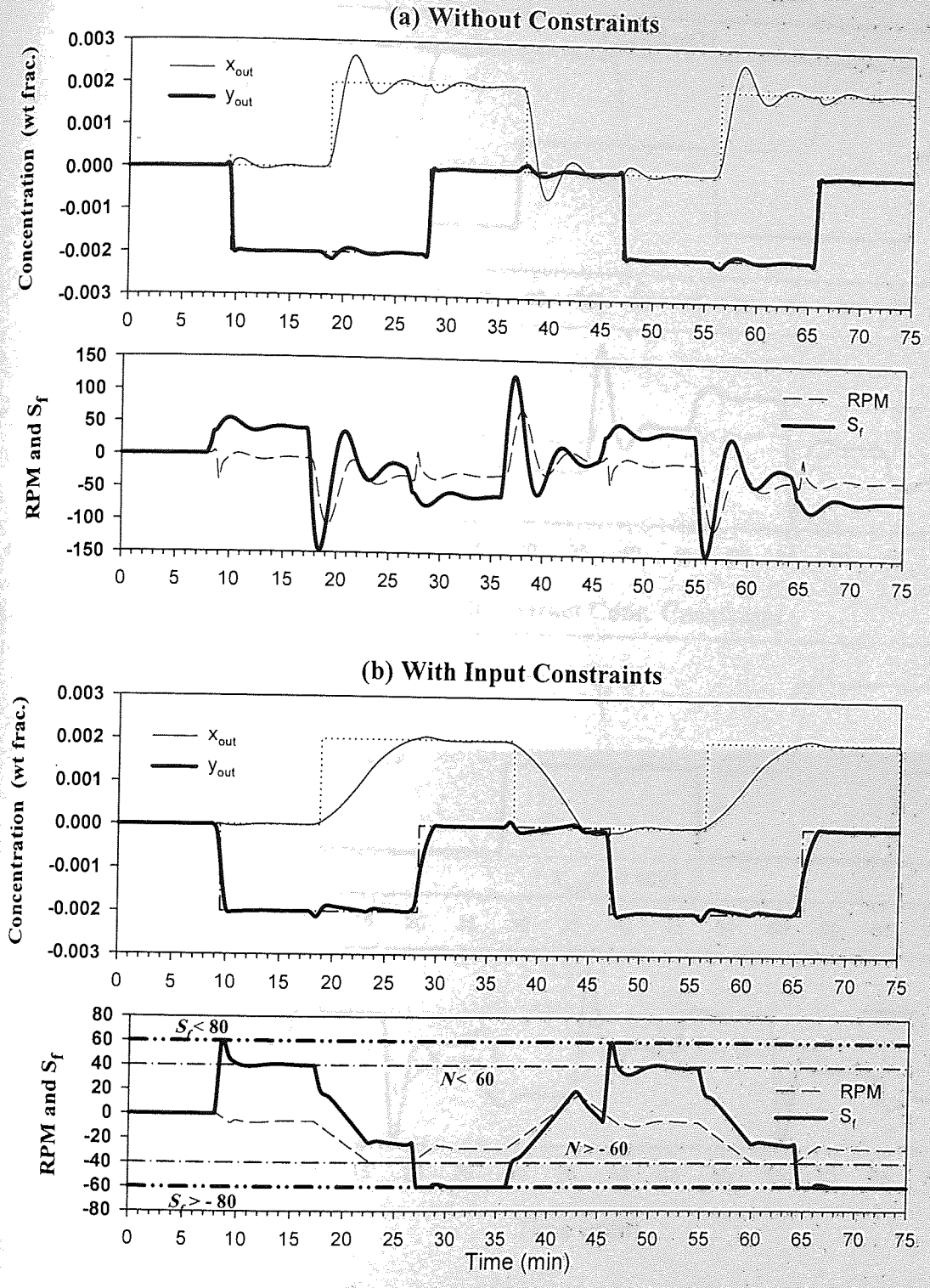

Figure (7.13) Effect of input variables constraints on the MPC response
(a) No constraints.
(b) With input constraints.

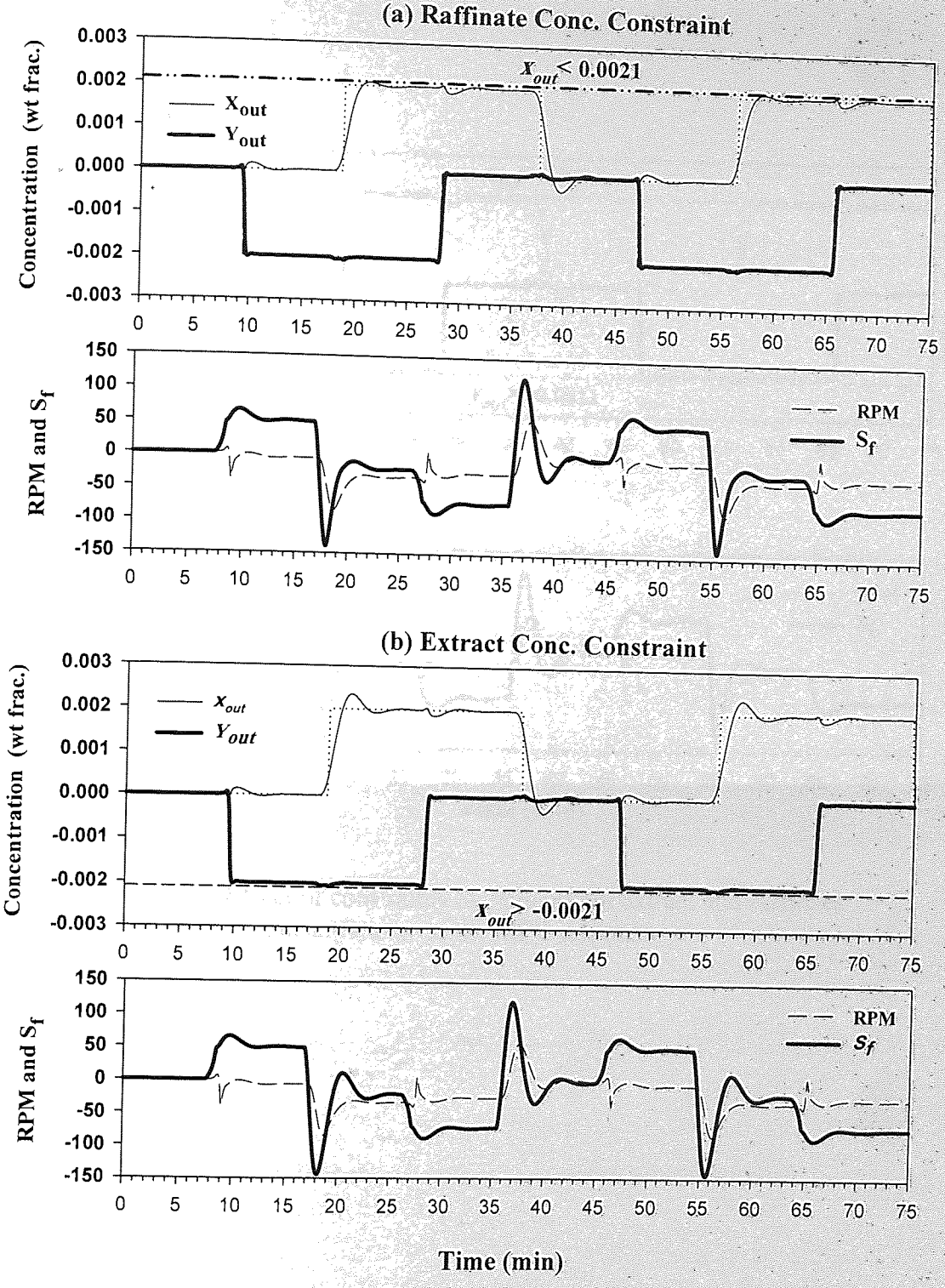

Figure (7.14) Effect of output constraints on the performance of the MPC algorithm.

(a) Raffinate concentration constraints.

(b) Extract concentration constraints.

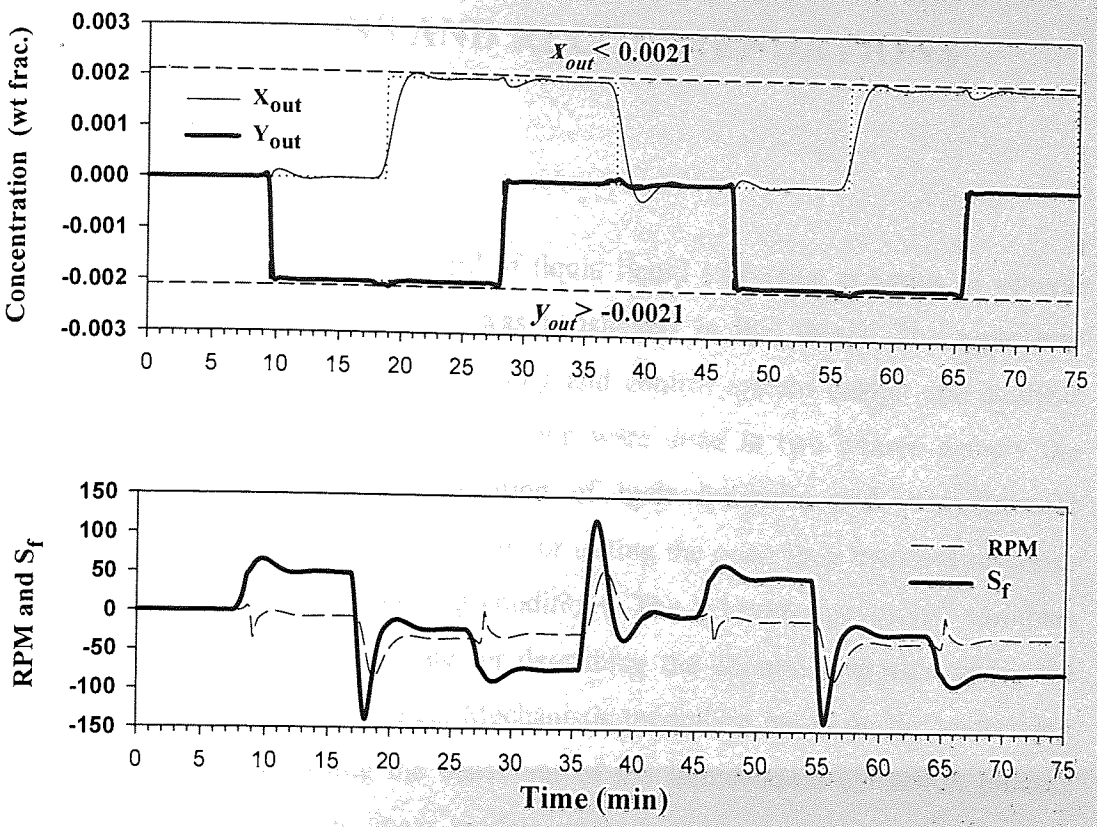

Figure (7.15) Effect of constraints on both output extract and raffinate concentrations on the MPC response.

CHAPTER EIGHT
CONCLUSIONS AND RECOMMENDATIONS

8.1 CONCLUSIONS

The problem of dynamics and control of liquid-liquid extraction columns in general and the Scheibel column in particular was considered in this thesis. The topic was investigated using an experimental, modelling and control system design and analysis approach. The experiments on Scheibel column were done in two phases namely the steady state experiments for the evaluation of hydrodynamics and mass transfer characteristics, and the dynamic experiments for testing the open loop transient response of the column under different operating conditions. The selected operational variables cover conditions which are appropriate for describing the column operation under the solute concentration range investigated. Mechanistic modelling based on the underlying physics and chemistry governing the behaviour of the liquid-liquid extraction process was performed. Reduced order linear models were then generated from the rigorous mechanistic model using system identification techniques. These simplified models were then used for designing and analysing a control system. The control study conducted in this research was preceded by a controllability analysis, to understand the ability of the process to achieve and maintain specific control objectives which is a prime goal for a reliable control system design. Different control algorithms were considered including conventional control algorithms, model based control strategies and Model Predictive Control algorithm. The closed loop testing results using different control algorithms were compared in terms of efficiency, stability and robustness.

The study was conducted and the results obtained were presented and discussed in the previous chapters. The following conclusions can be drawn from the different phases of the work; experimental data measurements, modelling, simulation, system identification and control system design and analysis:

- The preliminary experimental investigations were necessary for establishing a thorough understanding of the intrinsic of the column dynamics and explore the effects of the operating parameters on the behaviour of the column. The study explored the hydrodynamic and flooding characteristics of the column. Based on these findings the operational ranges for the deferent operating conditions was determined. The other phase of this part was concerned with the gathering of experimental data needed for correlating the column parameters and physical properties. This study had clearly shed light on the fact that these parameters are dependent on column and experimental setup.

- The steady state sampling technique used for continuous and dispersed phases was adequate, provided that the sample size is small enough and withdrawn carefully so not to contaminate it with the other phase. This technique cannot be applied for an online measurement due to limitations in time and cost of analysis. Therefore, the column open loop solute concentration profiles were detected using on-line refractometry with reasonable accuracy. The effect of measurement noise in the concentration profiles was within the tolerable limits.

- Modelling the extraction operation is a challenging goal. This is due to the complex nature of this process. The strategy adopted here is to use a mixing stage back-flow stagewise model. This rigorous model proved to be adequate for describing the hydrodynamics and mass transfer of the column. The mixing stages at the entrances of the contactor approximate the damping and delaying action of the phase separation volumes (single phase) located between the interfaces and the contactor ends (ends effects).

- The rigorous model developed accounts for the changes in the holdup as well as mass transfer non-idealities and backmixing with respect to rotor speed and phase flow ratio. The holdup correlation shows the high dependency on rotor speed and gives a reasonable method for describing the transients of holdup within the range of the selected operational variables. Under non-flooding operating conditions,

the holdup coefficient was found to be a direct function of operational parameters. It increases with the increase of rotor speed and phase flow ratio due to the droplets size reduction and the increase of dispersed phase flow rate relative to the continuous phase.

- To account for the limitation in the assumption of oscillatory drop behaviour with no mass transfer in the settling zones, the mass transfer non-idealities were described through the inclusion of mass transfer coefficient weight factor. This factor was back-calculated by minimizing the sum of the squared difference between experimental and calculated concentration profiles. It was later assumed that the mass transfer weight factor could be considered uniform throughout the column without degrading model prediction accuracy. The use of mass transfer weight factor gave good correction to the mass transfer non-idealities. The comparison of experimental step testing profiles with the model predicted ones indicate the good resemblance of the model to the actual process. The small discrepancy noticed in some of the cases might be due to the experimental shortcomings in the control of interface level and the existence of unmeasured noise in feed flowrates. The calculated values of this factor indicate that for low and moderate operating conditions there is low mass transfer contribution in the calming zones. This effect becomes significant under high conditions of operating conditions. Under these conditions the assumption of no mass transfer in the calming zones becomes unrealistic and the mass transfer weight factor corrects for this assumption.

- Axial diffusion effects were incorporated in the rigorous model through the use of backmixing coefficients. The values of these coefficients were calculated using optimization techniques to fit the experimental profiles to the model predicted values. The results showed that the values of the dispersed phase backmixing coefficient were very small and were, therefore, assumed to be negligible for the purpose of the study. On the other hand the continuous phase backmixing coefficient was of a significant value and was also correlated as a function of rotor

speed and flow phase ratio. This correlation was later incorporated into the rigorous model for proper simulation of the column operation.

From the observed behaviour of the column data, we can conclude that backmixing effect is substantial for the high range of operating conditions. The large packing height has great effect in preventing the dispersed phase backmixing and minimize the continuous phase backmixing by its baffling action to the rotational flow patterns. The packing role reduces as the operating conditions are increased.

- The rigorous dynamic model representing the behaviour of the liquid-liquid contactor was very complex to be adapted for developing different control algorithms. Therefore, system identification technique using the multivariable asymptotic method of identification was employed to represent the dynamic behaviour of the extractor with more simplified models. The derived input-output reduced order models were simple to implement and more relevant for control system design. The validation of these simple models confirmed the quality of the identification through their capability to describe dynamic data. Therefore, the development of conventional and unconventional control schemes based on these models can be practiced with confidence. However, the obtained linear models were examined in terms of sensitivity of controllers to model parameters perturbations due to variations in operating conditions.

- The controllability analysis investigated the properties and expected behaviour of the plant under closed loop conditions. This is very important for better understanding of the process control system to be built and implemented. In this study the analysis revealed that the model is functional controllable and stable for the whole range of bandwidth of operation. Furthermore it showed that the system is open loop stable and that further closed loop analysis would be fruitful. It also indicated that the extraction process is less sensitive to input signals where proper scaling for such signals is deemed necessary by the careful selection of transmitter gains. Although analysis of the condition number of the transfer function matrix

for a wide range of process operation frequency range indicated that the process is well conditioned at low frequencies close to steady state, however, special precautions should be taken when controlling the process at high frequencies. On the other hand, the disturbances were well aligned with the direction of the plant inputs implying that disturbance rejection is easily attained by carefully manipulating inputs. The analysis of inputs magnitude needed to reject process disturbances concluded that among the three disturbances encountered for the process the *feed concentration* and *solvent concentration* were more difficult to reject than *feed flowrate*, and that the *solvent concentration* was the most difficult disturbance to reject by the input. These parameters warrant more careful consideration for control system design.

- The control configuration synthesis tools applied for the extraction process under investigation suggested that the loops interaction for the low spectrum of frequencies was minimum and that it was possible to decompose the multivariable system into two almost independent control loops namely; (*rotor speed-raffinate concentration*) and (*solvent feed flowrate-extract concentration*) loops. On the other hand, at regions of high frequency, the pairings become less dependent on the choice of input-output variables, and elimination of interaction that develop at such conditions is recommended. It is worthwhile mentioning that the extraction contactors are usually operated close to these high frequency regions in order to achieve the most efficient operation near flooding conditions. Therefore, the need for more advanced control system must be stressed.

- Adopting conventional SISO control loop strategies for the control system design of each loop revealed that the closed loop response is sluggish and oscillatory but with stable behaviour. Some of the controllers gave inadequate behaviour in terms of stability and speed of response. Combining the loops in a multi-SISO configuration revealed that controlling the column with such schemes is slower, more oscillatory and subject to interaction among individual loops. Robustness tests showed that uncertainty in model parameters due to operating conditions

variations has a noticeable effect on the system behaviour and this in turn hinders the use of such control strategies for handling safe and efficient operation of the extraction columns.

- The MIMO implementation of the control system design was achieved by considering an MPC strategy. The servo and regulatory responses of the contactor indicate non-oscillatory, stable and fast control loops. The MPC algorithm was more efficient in handling loop interactions, time delays, and variables constraints. In addition, the MPC was less sensitive to modelling mismatch encountered in the model parameters compared to the case where conventional control schemes were used. The conclusion was to recommend the use of the MPC algorithm for the multivariable control of the extraction column.

8.2 RECOMMENDATIONS FOR FUTURE WORK

The research results attained in this work evoke some suggestions for future work in the field of modelling, dynamics and control of liquid-liquid contactors.

- The experimental investigation carried out in this work for the contactor under study, covered the most practical operating conditions. Nevertheless, other factors must be investigated to complete the understanding of the column behaviour. The study can be extended to include mass transfer direction, other types of chemical systems, online dispersed phase holdup measurements using conductivity, photographic or ultrasonic measurement techniques, online concentration measurements for both phases, and online drop size distribution throughout the column.

- Although this work has been applied for Type I Scheibel column, which is the original configuration of this contactor, the same research methodology should be applied to the other two improved types (Type II, and Type III). The effect of

column geometry refinements on the overall dynamic and control behaviour of the contactor can be investigated.

- The extraction process is performed under isothermal conditions, however, under special applications, chemical reactions may accompany the extraction process. Heat effects become profound that cannot be ignored in the process dynamics. More investigations should be devoted for modelling, simulation and control system design for such applications.

- The reduced order model was identified based on the simulations of the rigorous model for practical operating conditions and as such, they are limited to the conditions they were derived from. System identification should be used with other set of operating conditions in order to explore the performance of the various control algorithms under such conditions. The uncertainty in the identified model parameters and its effect on control system design were considered in this work through the robustness study. To overcome the sensitivity of the control system design to model uncertainty, on-line identification methodology can be adopted, which could be employed as part of an adaptive control scheme.

- Other advanced control algorithms such as Neural Networks, Fuzzy logic and Nonlinear Model Predictive Control algorithms should be tested for the extraction process and compared with the MPC algorithm used in this work. This will give a clearer picture on the relative efficiency of these algorithms and their practical implementation for controlling the extraction process.

- It is recommended that the proposed model predictive control system design in this work be implemented in real time applications.

LIST OF REFERENCES

1. Al-Aswad K. K. M., Mumford C. J. and Jeffreys G. V., "**The Application of Drop Size Distribution and Discrete Drop Mass Transfer Models to Assess the Performance of a Rotating Disc Contactor**", *AIChE J* Vol.31(9), p.1488 (1985).

2. Al-Faize, M. M., Jeffreys, G. V., Mumford, C. J. and Oloidi, J. O., "**Mass Transfer characteristics of Single and Pairs of Large Oscillating Drops**", Vol.103, p.369 (1987).

3. Al-Khani, A., Le Lann, M.V., Najim, K. and Casamatta, G., "**Model Reference Adaptive Control System of Liquid-Liquid Extraction Column**", *ISEC 86,* pp.I-151 to I-160, (1986).

4. Allen, P., Kropholler, H. W., and Spikins, D. J.,"**Use of a Ferranti Argus computer for control of a liquid extraction process",** *Chemical Engr.*, London, No.201, p.CE182 (1966).

5. Aly, G. and Ottertun, H., "**Dynamic behaviour of Mixer-Settlers Part III. Testing mathematical models using flow rates as input signals** ", *J. Appl. Chem. Biotechnol.* Vol.23, p.643 (1973).

6. Andersen, H. W., Rasmussen, K. H. and Jørgensen, S. B., "**Advances in Process Identification",** Proceedings of the Fourth International Conference on Chemical Process Control , *CPC IV, CACHE*, Padre Island, Texas, p.237-269, (1991).

7. Anderson, W. J. and Pratt H. R. C. ,"**Wake shedding and circulatory flow in bubble and droplet-type contactors**" *Chem. Eng. Sci.* Vol.33, p.995 (1978).

8. Arkun,Y., "**Model Predictive Control : A Tutorial**", *National AIChE meeting,* Atlanta, (1994).

9. Astorm, K. J., Panagopoulos, M. H. and Hagglund, T., "**Design of PI Controllers based on Non-Convex Optimization**", *Automatica*, Vol.34, No.5, pp.585–601,(1998).

10. Baird, L., and Hanson, C., *Handbook of Solvent Extraction,* Wily-Interscience (1983).

11. Bauermann, H. D. and Blass, E. ,"**Modelling of pulsed sieve tray columns** " *Germ. Chem. Eng.* 1, 99(1978).

12. Beetner, G. A. , Frey, A. L. , and Bautista, R. G., "**Analysis of Two-Phase Countercurrent Fluid Flow in a Multis Tage Mixer-Settler Extractor**", *Transact. Soc. Mining Eng. AIME* ,Vol.254, p.349 (1973).

13. Bibaud, R. E., and Treybal, R.E., "Axial mixing and extraction in mechanically agitated liquid extraction tower", *AIChE J.*, Vol.12, pp.472-477, (1966).

14. Biery, J. C., , "**The Transient Startup Behavior of a Liquid-Liquid Extraction Pulse Column**", Ph.D. dissertation, *Iowa State Univ.* (1961).

15. Bobrow, S. , Ponton, J. W. , and Johnson, A. I. ,"**Application of a Modular Computer Simulation System to the Control of a Reactor Train**" *A. I. Can. J. Chem. Eng.* Vol.49, p.391(1971).

16. Bonnet, J. C. and Jeffreys, G. V., "**Hydrodynamics and mass transfer characteristics of a Scheibel extractor. Part I: Drop size distribution, holdup, and flooding** ", *AIChE J.,* Vol.31, No.5, p.788 (1985).

17. Bonnet, J. C., M. Sc. Thesis, "**Hydrodynamics and Mass Transfer in Scheibel Extractor**", Aston University, Birmingham, UK (1982).

18. Bristol, E. H., "**On a new measure of interactions for multivariable process control**", *IEEE Trans. Automat. Control.* AC-11, pp.133-134 (1966).

19. Burns, D. D., and Smith, C. R. , "**Singular Value Analysis: A Geometrical Structure for Multivariable Processes**", *AIChE Winter Meet.* (1982).

20. Burkhart, L.E., "**Hydrometallurgical Process Fundamentals: Composition Control of Extractors**", *NATO Conf. series VI: Material Science*, pp.515-528,(1984).

21. Burns, P. E., and Hanson, C. , "**Transient Response of a Multistage Mixer_Settler**", *Brit. Chem. Eng.,* 12, No.1, pp75 (1964).

22. Burton, W. R. and Mills, A. L., "**Computer calculation of flowsheets for reprocessing nuclear fuels**", *Nuclear Engr.,* Vol.8, p.248, (1962).

23. Cadman, T. W. and Hsu, C. K., "**Dynamics and control of multi-stage liquid extraction**" *Transac. Inst. Chem. Eng.* ,Vol.48, p.432 (1973).

24. Champagne, F., "**Transient Solution to The Equations Describing a Differential Counter-current Extraction Process** ", M.S. Thesis, *Univ. of Washington* (1962).

25. Chartres, R. H. and Korchinsky W. J., "**Modelling of liquid-liquid extraction columns: predicting the influence of drop size distribution**", *Transactions of the Institution of Chemical Engineers,* Vol.53, no.4, Oct. 1975, pp.247-54. UK.

26. Chiang, C. L. and S.Y. MAK, "**Hydrodynamics in York-Scheibel Columns**", *Chem. Eng. Comm.*, Vol.88, pp.11-22, (1990).

27. Chien, K. L., Hrones J. A. and Reswick J. B., "**On the Automatic Control of Generalized Passive Systems.**" *Trans. ASME,* Vol.74, pp.175-185, (1952).

28. Chiu, L. L., "**Dynamic Response of a Liquid-Liquid Extraction Column to Step Change in Feed Composition** ", M. Eng. Thesis, *Univ. of Florida* (1963).

29. Clarke, D.W. C. Mohtadi and P.S. Tuffs "**Generalized Predictive Control: I. The Basic Algorithm**" Automatica, 23(2), 137 (1987).

30. Clements, W. C., "**Pulse Testing for Dynamic Analysis. Part 1: An Investigation of Computational Methods and Difficulties in Pulse testing. Part 2: Application of Pulse Testing to flow and Extraction Dynamics** ",Ph.D. dissertation, *Vanderbilt Univ.* (1963).

31. Cohen, G. H. and Coon, G. A., "**Theoretical Consideration of Retarded Control**", *Trans. ASME*, Vol.75, p.827, (1953).

32. Critchfield, C. E. M. ,"**Safety in Solvent Extraction Plants-Europe**" *J. Am. Oil Chem. Soc.*, Vol.53,p.295 (1976).

33. Cutler, C., Morshedi, A. Haydel, J. ,"**An industrial perspective on advanced control**", *AIChE Annual Meeting*, Washington, D.C. (1983).

34. Cutler, C. R. and Ramaker, B. L., "**Dynamic Matrix Control – A Computer Control Algorithm**", *Proc. ACC*, San Francisco, Paper WP5-B (1980).

35. Demarthe, J. M., "**Liquid-liquid extraction. Transient region studies. Effect of hydrodynamics on the operation of the equipment**", *CEA Report* A-R-4350 (1973).

36. Dillido, B. A. and Walsh T. J., "**Computer Simulation of Pulsed Columns**", *Ind. Eng. Chem.* 53,801 (1961).

37. Donald E. S., "**Error Analysis**", Lock Haven University, Lock Haven, PA, 17745 (1996), (http://www.lhup.edu/~dsimanek/errors.htm).

38. Doninger, J. E., "**The Dynamic Behaviour of a Packed Liquid Extraction Column**", Ph.D. dissertation. *Northwestern Univ.*, Evanston, Illinois (1965).

39. Doyle J. and Stein G., "**Multivariable Feedback Design: Concepts for a Classical/Modern Synthesis**", *IEEE Trans. Autom. Control*, AC-26, 1,Feb.(1981).

40. Drown, D. C. and Thomson, W. J., "**Fluid Mechanic Considerations in Liquid-Liquid Settlers**", *Ind. Eng. Chem. Process. Des. Devel.* Vol.12, p.197(1977).

41. Elkins, L. O. "**Steady State and Dynamic Analyses of Continuous Counter-current Liquid-Liquid Extraction Columns**"., Ph.D. dissertation, *Vanderdilt Univ.*, (1966),

42. El-Rifai, M. A., "**Composition Dynamics in Multi-Mixer-Settler Extractive Reaction Batteries**", *Chem. Eng. Sci.* Vol.30, p.79(1975).

43. Erskine W., PhD. Thesis, "**Predictive Control of an Extraction Column**", *Iowa State Univ.*, Ames, Iowa, (1968).

44. Evans, D. R., Ph. D. Thesis, "**Dynamic Testing in the Control of Pulse Column**", *Iowa State Univ.*, Ames, Iowa, (1965).

45. Flett, D.S., Cutting, G.W. , and Carey, P., "**Computer Control of Solvent Extraction Processes: Development of an Equilibrium Mathematical Model**", paper presented at *IMPC 10th Congress*, p.1147 (1973).

46. Foster, H. R., Jr, "**Transient Solution to The Equations Describing a Stagewise Counter-current Extraction Process**", M.Sc. Thesis, *Univ. of Washington* (1964).

47. Franklin, G. F., Powell, J. D. and Baeini, A. E., "**Feedback Control of Dynamic Systems**", Addison-Wesley Reading, MA (1986).

48. Franks, R. G. E. , ***Mathematical Modelling in Chemical Engineering***, Wiley, NY, (1966).

49. Freudenberg, J.S. and Looze, D.P.,"**Right half plane poles and zeros and design tradeoffs in feedback systems**", IEEE Transactions on Automatic Control AC-30(6), pp.555-565, (1985).

50. Garcia, C. E. and Prett, D. M., "**Advances in industrial Model-Predictive Control**", Chemical Process Control – *CPCIII, CACHE Elsevier*,(1986).

51. Garcia, C.E. and Morari, M., "**Internal Model Control–1. A Unified Review and Some New Results**", *Ind. Eng. Chem. Process Des. Dev.*, Vol.21(2), pp.308-323 (1982) .

52. Garner, F. H. and Tayeban, M.,"**The Importance of the Wake in Mass Transfer from both Continuous and Dispersed Phase Systems**", *Anales de Fisicay Quimica*, Vol.56b, pp.479-490 (1960).

53. Gaudernack, B. and Michelsen, O. B., "**Control of a solvent extraction process for rare earth separation by means of a computer-based, on-stream XRF analytical system",** Proceedings of the International Solvent Extraction Conference (ISEC 79), Toronto , Special Vol.21, *Canadian Institute of Mining and Metallurgy*, Montereal, p.754 (1979).

54. Gerardo, M., Cole, J. D., Naugle, N. W., Preisig, H. A. and Holland, C. D., "**A New criterion for the Pairing of Control and Manipulated Variables**", *AIChE Jornal*, Vol.32, No.9, pp.1439-1449, (1986).

55. Gilbert, J. C., and Lemarechal, C., "**Some Numerical Experiments with Variable-Storage Quasi-Newton Algorithms**", *Math. Prog.* Vol.45, pp.407-435, (1989).

56. Gorez, R, "**A survey of PID Auto-Tuning Methods**". *Journal A*, Soft Vision, Belgium, Vol.38 (1), pp.3-10, (1997).

57. Gray, R. I. and Prados, J. W., "**The dynamics of a packed gas absorber by frequency response analysis",** *AIChE Journal*, Vol.9,p.211 (1963).

58. Gray, R. I., Ph.D. thesis, "**The Dynamics of a Packed Gas Absorber by Frequency Response Analysis**", University of Tennesee, Knoxville, Tenn., (1961).

59. Grosdidier, P., B. Froisy and M. Hammann, "**The IDCOM-M Controller**" in Proc. IFAC Workshop on Model-Based Process Control, T.J. McAvoy, Y. Arkun and E. Zafiriou (eds.), pp.31-36, Pergamon Press, Oxford (1988).

60. Grunberg L., and Nissan, A. H., "**Mixture Law for Viscosity**", *Nature* 164, pp.799-800 (1949).

61. Hackl, A., Solar, W. and Ziebland, G. , "**Recommended Systems for Liquid Extraction Studies**", T. Misek, *Ed. Europ. Fed. Chem. Eng. Prague* (1978).

62. Hale, J. C., D. Sc. Thesis,"**Frequency-Domain Response of Pulsed Column Extractors**", *Univ. of Virginia*, Charlottesville, Va.,(1966).

63. Halligan, J. E. and Smutz, M., "**Prediction of the approach to steady state of a mixer-settler extractor",** *Sep. Science*, Vol.1, p.173, (1966).

64. Hang, C. C., and Sin, K. K. , "**On-line Auto-tuning of PID Controllers Based on the Cross-Correlation Technique**", *Report CI-91-4, National University of Singapore*, Dept. of Electrical Engineering (1991).

65. Hanson, C. and Sharif, M., "**Hydrodynamic Studies on Two Multistage Mixer-Settlers**", *Can. J. Chem. Eng.*, Vol.43, p.132 (1970).

66. Hays, J. R., Clements, W. C., and Harris, T. R., "**The frequency domain evaluation of mathematical models for dynamic systems",** *AIChE J*, 13, 374 (1967).

67. Heyberger A., Kratky, M. and Prochazka, J., "**Parameter Evaluation of Extractor With Backmixing**", *Chem. Eng. Sci.* Vol.38, No.8, pp.1303-1307, (1983).

68. Ho, W. K., Hang, C. C., and Cao, L. S., "**Tuning of PID Controllers Based on Gain and Phase Margin Specifications**", *Automatica*, Vol.31, No.3, pp.497-502 (1995).

69. Hoclet, O. , Chazal, G. and Rouyer, H., "**Hybrid simulation of the dynamics of a battery of mixer-settlers",** *CEA Conference*, p.1579 (1970).

70. Holt, B.R. and Morari, M., "**Design of Resilient Processing Plants, VI: The effect of Right-Half-Plant Zeros on Dynamic Resilience**", *Chem. Eng. Sci.*, Vol.27, pp.59-74, (1985).

71. Honekamp, J. R. and Burkhart, L. E., "**Role of the Packing in a Scheibel Extractor**", *I.&E.C. Proc. Des. and Dev.*, Vol.1, No.3, p.176 (1962).

72. Hovd, M and Skogestad, S., "**Controllability Analysis for Unstable Processes**" *Proc IFAC Workshop on Interactions Between Process Design and Control*, London Great Britain (1992).

73. Hsu, C. K., *Trans. Instn. Chem. Engrs.*,"**Transfer Functions of Multistage Separation Processes**", Vol.49, p.T209 (1971).

74. Huang, C. J., M. Sc. Thesis, "**Rate of Approach to Steady-State in Continuous Liquid-Liquid Extraction**", Univ. of Toronto, Toronto (1956).

75. Isdale, J. D., MacGillivary, J. C. and Cartwright, G., "**Prediction of Viscosity of Organic Liquid Mixtures by a Group Contribution Method**", *Natl. Eng. Lab. Report*, East Kilbride, Glasgow, Scotland (1985).

76. Jarvis, R. C. F., M. Eng. Thesis, *McMaster Univ.*, Hamilton, Ontario, (1971).

77. Jaswon, M. A. and Smith, W., **Counter-current transfer processes in the non-steady state",** *Proc. Royal Soc.* (London),A225, p.226 (1954).

78. Justice, R. G. and Schnelle, K. B. , Jr., "Frequency response to single phase longitudinal dispersion two phase extraction in packed beds using pulse testing methods", Paper 46B presented at the *AIChE Meeting*, Philadelphia, December, (1965)

79. Justice, R. G., Ph.D. Thesis, "**Frequency Response of Single Longitudinal Dispersion and Two-Phase Extraction in Packed Beds Using Pulse Testing Methods**", , *Vanderbilt Univ.*, Nashville, Tennessee (1964).

80. Kikiudai, T., Michel, P. , Rouyer, H. and G. Chazal," **Analogue simulation of mixer-settlers. Response of a 30% tributyl phosphate uranium extraction section to a limited concentration of acid and uranium**", paper presented at *CEA Conference*, p.1129 (1967).

81. Kramers H., and Alberda, G., "**Physical Factors in Chemical Reaction Engineering**", *Chem. Eng. Sci.*, Vol.2, p.173 (1953).

82. Lapidus, L. and Amundson, N. R., "**Stagewise Absorption and Extraction Equipments**" *Ind. Eng. Chem.*,Vol.42,p.1071 (1950).

83. Lavergne, E. A. L., Ph.D. Thesis ,"**Transient Behaviour of a Packed Liquid-Liquid Extraction Tower**", *Univ. of Toronto* (1956).

84. Le Lann, M. V., Najim, K. and Casamatta, G., "**Generalized Predictive Control of a Pulsed Liquid-Liquid Extraction Column**", *Chem. Eng. Commun.* Vol. 48, pp 237-253 (1986).

85. Libhaber, M., Blumberg, P., and Kehat, E., "**Dynamic Simulation of the Main Extraction Batteries of the Phosphoric Acid Process**", *I&E.C. Process. Des. Devel.* 13,39 (1974).

86. Ljung, L., "**Asymptotic Variance Expressions for Identified Black Box Transfer Function Models**", *IEEE Trans. On Auto. Cont.*, AC-30, pp.834-844, (1985).

87. Ljung, L., "**System Identification: Theory for the User**", Prentice-Hall, Englewood Cliffs, NJ, (1987).

88. Ljung L., Glad T.,"**Modeling of Dynamic Systems**", Prentice Hall Professional, (1994).

89. Lung Chien, I., "**IMC-PID Controller Design-An Extension**"., *Proceedings, IFAC Symposium;* Adaptive Control of Chemical Processes Conference, Copenhagen, Denmark, (1988).

90. Marshall, W. R. Jr. and Pigford. R. L., ***The Application of Differential Equations to Chemical Engineering Problems***, Univ. of Delaware (1947).

91. McDonald, C.R. and Wilkinson, W.L. , "**Automatic control of a multiple-mixer solvent extraction column**", *Proceedings of the International Solvent Extraction Conference (ISEC 77)*, Toronto Special Vol.21 (1977).

92. McSwain, C. V. and Durben, L. D., "**Backflow-cell model for continuous two-phase nonlinear mass-transfer operations including nonlinear axial holdup and mixing effects**", *Sep. Science*, Vol.1, p.677 (1966).

93. Mehra, R.K. and Rouhani, R., "**Theoretical Considerations on Model Algorithmic Control for Non-minimum Phase Systems**", *Proc. ACC*, Paper TA8-B, (1980).

94. Mills, A.L. , Oliphant, A.J. , and Paskinsor, M., "**Optimization and control of solvent extraction processes**", *Atom* , p.237 (1967).

95. Mills, A.L. and Bell, P.C., "**Automatic control and response characteristics of small scale solvent extraction equipment**", *Proceedings of the International Solvent Extraction Conference (ISEC 71)*, The Hague (1971).

96. Morari M., "**Internal Model Control–Theory and Applications**", *Proc. of PRP Automation 5, 5th International IFAC/IMEKO Conference on Instrumentation and Automation in the Paper, Rubber, Plastics and Polymerization Industries*. Antwerp, Belgium, 1-18 (1983).

97. Morari, M. and Lee, J. H., "**Model Predictive Control: Past, Present and Future**". *Comput. Chem. Eng.*, Vol.23, pp.667-682, (1999).

98. Morari, M. and Zafiriou, E., "***Robust Process Control***", Prentice-Hall, New-Jersey, USA, (1989).

99. Morari, M. and Ricker, N. L., "**Model Predictive Control Toolbox for use with MATLAB**", User Guide, *The MathWorks, Inc.*, (1998).

100. Morari, M. and Zafiriou, E., "**Design of Resilient Processing Plants. New Characterization of The Effect of RHP-Zeros**," *Chem. Eng. Sci.*, Vol.42, 10, pp.2425-2428 (1987).

101. Nabeshima, M. , Kitahara M., Tanaka C. and Shuto M. ,"**Dynamic simulation code "DYNAC" for the PURX extraction cycle coposed of pulse columns**", *I. Chem. E. Symposium Series,* No.103, pp.307-321 (1987).

102. Najim, K., M.V. Le Lann and G. Casamata, "**Learning Control of a Pulsed Liquid-Liquid Extraction Column**", *Chem. Eng. Sci.*, Vol.42, pp.1619-1628 (1987).

103. Najim, K. and Le Lann, M. V., "**Control of a Pulsed Liquid-Liquid Extraction Column Based on a Multilevel System of Automata**", *Chem. Eng. Comm.*, Vol.70, pp.107-126, (1988).

104. Niedrlinski, A., "A, **Heuristic Approach to the Design of Linear Multivariable interacting Control Systems**", *Automatica*, Vol.7, (1971).

105. Ochsenfeld W., H-J. Bleyl, D. Ertel, F. Heil, and G. Petrich, "**Studies on fast reactor fuel reprocessing in Karlsruhe**", *Proceedings of the Fast Reactor Fuel Reprocessing Symposium*, Dounreay,pp.77-91, May (1977).

106. Ogata, K., "***Modern Control Engineering***", 2nd edn. Prentice-Hall, Englewood Cliffs, NJ. (1990).

107. Ogunnaike, B.A. and Ray W. H. , ***Process Dynamics, Modeling, and Control***, Oxford university press, (1994).

108. Oloidi J.O., Jeffreys G.V., and Mumford C.J., "**Mass Transfer Characteristics of a Pilot Scale Sieve Plate Extraction Column (SPC)**", *I. CHEM. E. SYMPOSIUM SERIES*, NO. 103, p.117 (1987).

109. Pang, K. H. and Johnson A. I.,"**A minimum time operation policy for a liquid-liquid extraction column**", *Can. J. Chem. Eng.*, Vol.49, p.529, (1971)

110. Perez de Ortiz E. S. ,"**Maragoni Phenomena, Science and practice of liquid-liquid extraction**", *Oxford engineering science series* 27, Vol.1, pp.157-209 (1992).

111. Petzold L. R., "***A Description of DASSL: A Differential/Algebraic System Solver***", SAND82-8637, (September 1982).

112. Pollock G. C. and Johnson, A. I. , ***Ion Exchange and Solvent extraction***, chap.2, Vol.6, Marcel Dekker, New York (1974).

113. Pollock G. C. and Johnson, A. I., "**The Dynamics of Extraction Processes. Part III: The Determination of Steady State and Transient Concentration Profiles**", *Can. J. Chem. Eng.*, 48, 64 (1970).

114. Pollock, G. C. and Johnson, A. I., "**The Dynamics of Extraction Processes. Part I: Introduction and Critical Review of Previous Work**", *Can. J. Chem. Eng.* Vol.47, p.565(1969).

115. Pollock, G. C., M.Eng. Thesis, "**Simulation of a Mixer-Settler Liquid Extraction Column** " *McMaster Univ.*, Hamilton Ontario,(1965).

116. Pratt, H. R. C. and Stevens, G. W., "**Science and Practice of Liquid-Liquid Extraction**", Vol.1, p417, *Clearendon Press*, (1992).

117. Prett, D. M. Gillette, R. D., "**Optimization and constrained multivariable control of a catalytic cracking unit**", *Proceedings of the Joint Automatic Control Conference*. (1980).

118. Prett, D. M. Gillette, R. D.,"**Fundamental Process Control**", Butterworth, Stoneham (1988).

119. Qin, S. J. and Badgwell, T. A.,"**An Overview of Industrial Model Predictive Control Technology**", in Jerey C. Kantor, Carlos E. Garcia, and Brice Carnahan, editors, Fifth International Conference on Chemical Process Control, *AIChE Symposium Series 316*, 93, pp.232-256. (1997).

120. Rawlings, J. B.; Meadows, E. S. and Muske, K. R., "**Nonlinear Model Predictive Control: A Tutorial and Survey**", *ADCHEM'94 Proc.*, Kyoto, Japan, pp.203-214 (1994).

121. Ribeiro, L. M., Regueiras, P. F. R., Guimaraes, M. M. L. and Cruz-Pinto, J. J. C., "**Efficient Algorithms for the Dynamic Simulation of Agitated Liquid-Liquid Contactors**", *Advances in Engineering Software*, Vol.31, pp.985-990, (2000).

122. Richalet, J.A., A. Rault, J.D. Testud and J. Papon, "**Model Predictive Heuristic Control: Applications to Industrial Processes**" Automatica, 14, pp.413-428 (1978).

123. Ricker, N.L. "**Use of Quadratic Programming for Constrained Internal Model Control**" Ind. Eng. Chem. Proc. Des. Dev., 24, 925-936 (1985).

124. Rivera, D. E., Morari, M. and Skogestad, S., "**Internal mode control. 4. PID controller design**", *I.&E.C. Chem. Process Des. Dev.*, Vol.25:1, pp.252-265 (1986).

125. Rose, P. M., and Kintner, R. C., "**Mass Transfer from Large Oscillating Drops**", *AIChE J.*, Vol.12, pp.530-534 (1966).

126. Rosenbrock, H. H., "**The Future of Control**", *Automatica*, Vol.13, pp.389-392 (1977).

127. Rosenbrock, H. H., "***State space and Multivariable Theory***", Nelson London (1970).

128. Rouyer, H. and Kikindai, T., "**Mechanism of the transition regime in mixer-settlers. Extraction of uranium",** *Comptes Rend. Acad. Sci. Ser. C.*, 270, p.271 (1970).

129. Rouyer, H. and Demarthe, J. M.,"**Computer calculation in design and development of liquid-liquid extraction processes",** *Bull. Inform. Sci. Techn. Comm. Energ. Atomique* ,134, pp.49-56, (1973).

130. Rouyer, H., "**Use of analog and hybrid computers for determination of transitory regimes in mixer-settlers",** *Comptes Rend. Acad. Sci. Ser. C.*, 270, p.580 (1970).

131. Scali, C., Semino, D. & Morari, M., "**Comparison of internal model control and linear quadratic optimal control for SISO systems**", *I.&E. C.* Research Vol.31:8:pp.1920-1927 (1992).

132. Scheibel, E. G.,"**Fractional liquid extraction I.",** *Chem. Eng. Progr.*, Vol.44,p.681 (1948).

133. Scheibel, E. G., "**Scheibel Columns**" in ***Handbook of Solvent Extraction***, Wily-Interscience, p.419 (1983).

134. Seber, G. A. F. and Wild, C. J., ***Nonlinear regression***, Wiley (1989).

135. Seborg, D. E., Edgar T. F. and Mellichamp, D. A., "**Process Dynamics and Control**", Wiley, New York (1989).

136. Seibert, A. F. and Fair, J. R. , "**Hydrodynamics and Mass Transfer in Spray and Packed Liquid-Liquid Extraction Columns**", *In. Eng. Chem. Res.*, Vol.27, pp.470-481 (1988).

137. Sereno, A. M. and Anderson, T.F. ,"**Dynamic Simulation of Liquid-Liquid Operations Using Simplified Non-Linear Model**", *Comput. Chem. Engng.*, Vol.11, No.2, pp.177-185, (1987).

138. Setpoint, Inc. SMC-Idcom: "**A State-of-the-Art Multivariable Predictive Controller**". Product literature from Setpoint, Inc. (1993).

139. Skogestad, S. and Morari, M., "**Implications of Large RGA Elements on Control Performance**", *I.&E.C. Res.*,Vol.26, pp.2323-2230, (1987).

140. Skogestad, S., Morari, M.and Doyle, J. C., "**Robust Control of Ill-Conditioned Plants: High Purity Distillation**", *IEEE Trans. Autom. Control*, Vol.33,12, pp.1092-1105, (1988).

141. Sleicher, C. A. , "**Fluid Dynamics**",Industrial and Engineering Chemistry, 8th Annual Review, *Chemical Engineering Reviews*, Vol.52, p.347, (1960).

142. Souhrada, F., Landau J. and Prochazka J.,"**Dynamic Simulation of a Stagewise Mass Transfer Process with Back-Mixing**", *Can J. Chem. Eng.*, 48, 322 (1970).

143. Sovova, H. and Havlicek, A., "**Transient Behaviour of Holdup in a Reciprocating Plate Extraction Column**", *Chemical Engineering Science*, Vol.41, No.10, pp.2579-2583, (1986).

144. Staffin, H. K., "**Transient Characteristics of Continuous Extraction with Agitation**", Ph.D. Thesis, *Polytech. Inst. Of Brooklyn*, Brooklyn, NY (1959).

145. Steiner, L., Horvath, M. and Hartland, S., "**Prediction of Drop Diameter, Hold-Up and Backmixing Coefficients in Liquid-Liquid Spray Columns**" *Can. J. Chem. Eng,* Vol.56, no.1, pp.9-18, (1978).

146. Swati M., "**Modeling of liquid-liquid extraction column: A Review**", Reviews in Chemical Engineering, Vol.16(3), 199, (2000).

147. Takamatsu, E. N., ***Memoirs of the Faculty of Engineering***, Kyoto Univ., Kyoto, Japan, Vol.25, Part 2, p. 233, April (1963).

148. Tsouris C., Kirou, V.I., and Tavlarides, L. L.,"**Drop Size Distribution and Holdup Profiles in a Multistage Extraction Column**", *AIChE Journal*, Vol.40, No.3, pp.407-418, (1994).

149. Tsouris, C. and Tavlarides, L. L., "**Control of dispersed phase volume fraction in multistage extraction column contactor**", *Chem. Eng. Sci.*, Vol.46, p.2857 (1991).

150. Van Velsen D., Cardozo, R. L. and Langenkamp, H. , "**Liquid Viscosity and Chemical Constitution of Organic Compounds: A new correlation and a compilation of literature data**", *Euratom 4735e, Joint Nuclear Research Centre*, Ispra Establishment, Italy (1972).

151. Vembe, P.E., "**Instrumentation and control of the solvent extraction section in the Falconbridge Matte Leach Process",** Proceedings of the International Solvent Extraction Conference (ISEC 77), Toronto, Special Vol. 21 *Canadian Institute of Mining and Metallurgy*, Monterial, 1079, p.761. (1977).

152. Wahlberg, B., "**Model Reduction of High-Order Estimated Models, the Asymptotic ML Approach**", *International Journal of Cont*, Vol.49(1), pp.169-192., (1989).

153. Wang, P. S. M. , Ingham, J., and Hanson, C.,"**Further studies on the performance of a Graesser raining bucket liquid/liquid contactor",** *Transact. Inst. Chem. Eng.* Vol.55, p.196 (1977).

154. Watjen, J. W., and Hubbard, R. M.,"**The Dynamic Behaviour of a Pulsed Plate Extraction Column**", *AlChE Journal*, Vol.9, p.614 (1963).

155. Weast R. C., Astle, M. J. and William, H. B. , ***Handbook of Chemistry and Physics***, 73rd ed., CRC Press Inc., Boca Raton, FL (1993).

156. Weinstein, O., Semiat, R., Lewin, D. R., "**Modeling, simulation and control of liquid-liquid extraction columns**", Chemical Engineering Science, Vol.53(2), 325-339, (1998).

157. Whitman, W. G.,"**The Film Theory of Absorption**", *Chem. And Met. Eng.* Vol.29, pp.147-151 (1923).

158. Wichterlova, J. and Rod, V., "**Dynamic Behaviour of the Mixer-Settler Cascade. Extractive Separation of the Rare Earths**", *Chemical Engineering Science*, Vol.54 , pp.4041-4051 (1999).

159. Wolff, E. A., "**Studies on Control of Integrated Plants**", Ph.D. Thesis, University of Trondheim, The Norwegian Institute of Technology, (1994).

160. Yaw, C. L., Miller, J. W., Schorr, G. R. and Patel, P. M., "**Correlation Constants for Chemical Compounds**", *Chem. Eng.* Vol.83(25), pp.153-161 (1979).

161. Yoswathana, N., Casamatta G. and Najim K.," **Adaptive control of a liquid-liquid extractor**", *IFAC Adaptive Control of Chemical Processes*, pp.53-59 (1985).

162. Young, H. D., "***Statistical Treatment of Experimental Data***". McGraw-Hill, (1962).

163. Yu, C. and Luyben, W., "**Design of Multi-loop SISO Controllers in Multivariable Processes**", *Ind. Eng. Chem. Process Des.*, Vol.25, No. 2, pp.498-503, (1986).

164. Zafiriou, E. , "**Robust Model Predictive Control of Processes with Hard Constraints**", *Comput. and Chem. Eng.*, 14, 359-371 (1990) .

165. Zhu, Y. C. and Ge, X. H., "**Tai Ji ID Automatic Closed Loop Identification Package for Model Based Process Control**", *Journal A.* , Vol.38(3), pp.42-45, (1987).

166. Zhu, Y.C., "**Multivariable Process Identification for MPC: the Asymptotic Method and its Applications**", *J. Proc. Cont.* Vol.8, No.2, pp. 101-115, (1998).

167. Zhu, Y.C. and Backx, T.,"**Identification of Multivariable Industrial Processes; for Simulation, Diagnosis and Control**", Springer-Verlag, London (1993).

168. Zhuang M. and Atherton D. P., "**Automatic tuning of optimum PID controllers**" *IEE Proc. Control theory Appl.*, Vol. 140, No. 3, pp. 216-224, (1993).

169. Ziegler, J. G., and Nichols, N. B. ," **Optimum settings for automatic controllers**". *Trans. of the ASME*, Vol.64, pp.759-768, (1942).

170. Ziegler, J. G. and Nichols, N.B. , 1943,"**Process Lags in Automatic Control Circuits**", *Trans. of the ASME*, Vol.65, pp.433-444, (1943).

171. Zimmermann, A., Gourdon, C., Joulia,., X., Gorak, A., and Casamatta, G. , **"Simulation of a Multi-Component Extraction Process by a Non-Equilibrium Stage Model Incorporating a Drop Population Model"**, *European Symposium on Computer Aided Process Engineering-1*, pp.S403-S410, (1990).

APPENDIX (A)
EXPERIMENTAL SETUP AND MEASUREMENTS

A.1 THEORY OF CRITICAL ANGLE REFRACTOMETRS:

The most widely used refractometers depend on the so called "critical angle phenomenon". A prism having a refractive index η_p greater than that of the liquid η is used . As shown in Figure(A.1), when light passes through the interface between the liquid and the prism at an incidence angle i_c along the direction of maximum refraction it forms a sharp dividing line (critical boundary) between a light and a dark region inside the prism. The ray labelled (3) in Figure (A.1). The angle of refraction r_c is called "critical angle of reflection". A ray travelling in the reverse direction of the arrow in Figure(A.1) and striking point O at an angle slightly greater than r_c would not pass into the liquid, but would be totally reflected as though the interface were a mirror.

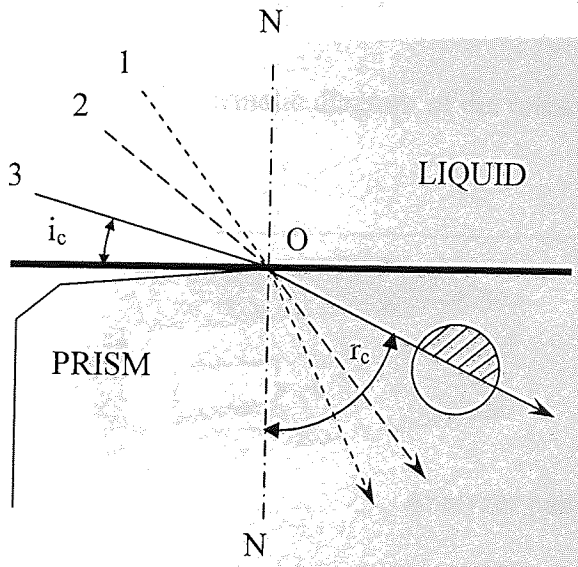

Figure (A.1) The principle of critical angle refractometer.

The refractometer determines the refractive index η at the critical angle. It is defined as:

$$\eta = \eta_p \frac{\sin r_c}{\sin i_c} \qquad \text{(A.1)}$$

In the online refractometer this is done real-time, and measurements of η is done with time and recorded on a recorder or sent to a storage media like a PC backing store.

Figure (A.2) shows a cross sectional schematic diagram of the refractometer measuring cell, which is installed on the outlet raffinate stream and connected to a PC for continuous logging of refractive index with respect to time.

Figure (A.3) shows the Anacon Process Refractometer Model 47 and the measuring cell used in the experimental study of the Scheibel extractor.

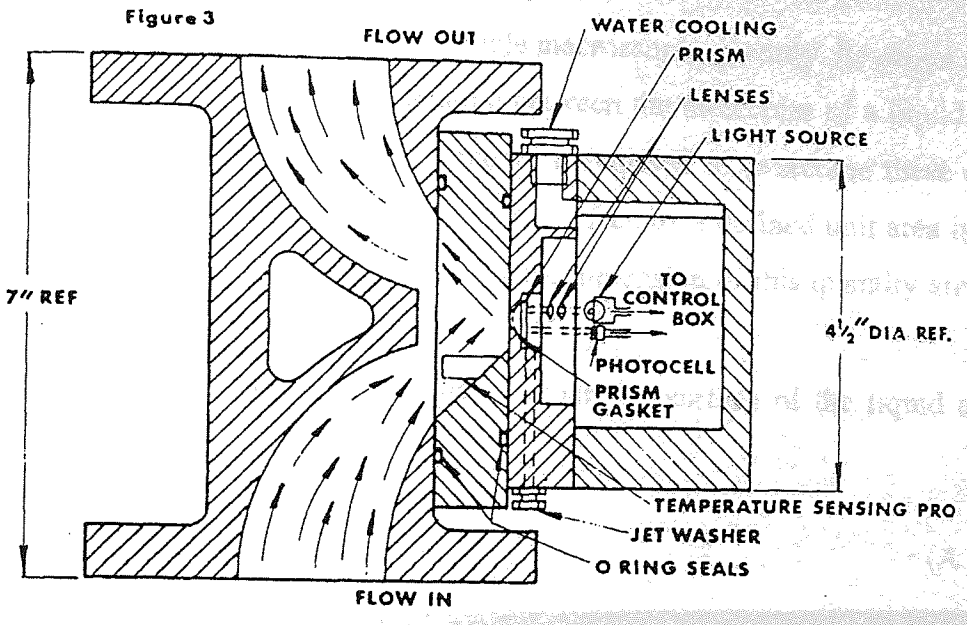

Figure (A.2) cross sectional schematic diagram of the refractometer measuring cell.

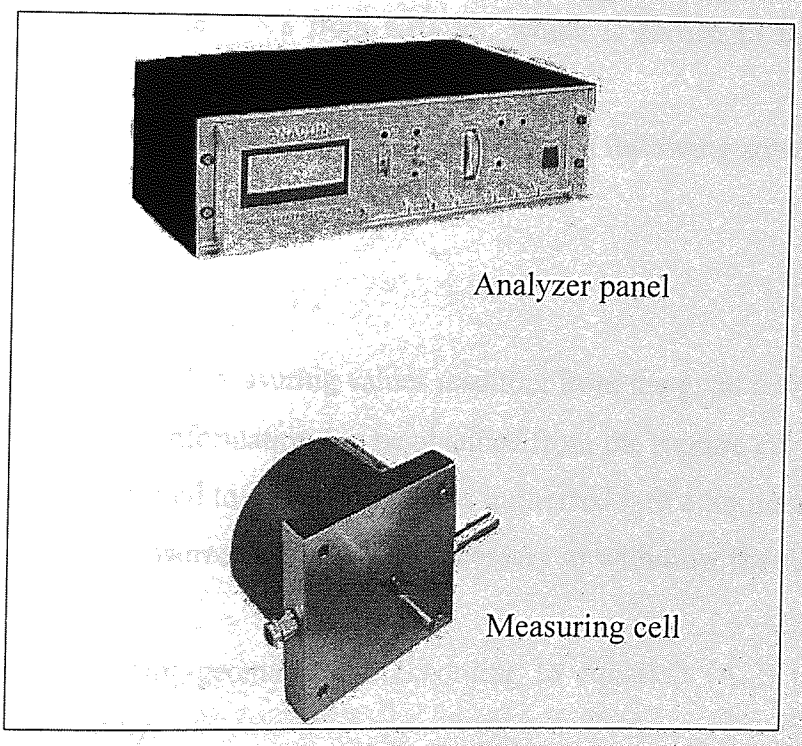

Figure (A.3) The Anacon process refractometer model 47.

A.2 SURFACE TENSION:

In the general language of today surface tension (at the phase border liquid/gas) and interfacial tension (at the phase-border liquid/liquid) are distinguished. Since surface tension is only a special case of interface tension the latter term will be used for both phenomena in the following description.

Interface tension is a physically measurable macroscopic quantity. Its origin lies in the intermolecular attraction forces operating between the molecules of a liquid. In order to increase the surface of the liquid, energy is required to overcome these attraction forces. The work required for increasing the surface by a defined unit area is referred to as specific surface work. The value and the dimension of this quantity are equal to the surface tension, σ.

It is defined by the force K by means of which the surface of the liquid acts on a straight edge line of the length l.

$$\sigma = \frac{K}{l} \qquad \text{(A.2)}$$

The interface tension is expressed in mN/m.

A.2.1 Measuring The Interfacial Tension by the Ring Method:

The Interfacial Tensiometer K8 from KRUSS, which is shown in figure (A.4) has been used for the experimental measurement.

The ring method still enjoys general popularity. It offers following advantages:

- No influence on the wetting angle
- Simple handling
- Short measuring time
- High resolution of measuring values resulting from the great contact-length
- Supplementary information can be obtained from the rupture curve

A platinum ring connected to a balance beam is immersed into a liquid and afterwards slowly withdrawn. Measured is the force K necessary to withdraw the ring against the interface tension.

With respect to the ring-geometry and according to equation (A.2) the interfacial tension is expressed by:

$$\sigma = \frac{K}{4\pi r} \qquad \text{(A.3)}$$

The radius r corresponds to the average value of outer and inner ring-diameter. The factor 2 of the denominator of equation (A.3) takes into account that the force affects both, the inner and the outer side of the ring.

In order to obtain absolute values, the result of the measured interface tension has to be multiplied by a correction factor F. This factor takes into consideration the ring dimensions and the volume of the liquid elevated above the level of the liquid surface due to the ring-geometry.

$$\sigma = \frac{K}{4\pi r} F \qquad \text{(A.4)}$$

A.2.2 Preparation of the measurement

Pt-Ir-ring has to be handled with extreme care because only an undamaged ring, ensure incontestable measuring values. To prevent damage, the ring must fall from the wooden sleeve on a soft base. For cleaning they are washed in pure Acetone or distilled water and then glowed in a Bunsen flame until they reach dark-red colour (white heat is to be avoided, otherwise the welds might get loose).

After locking the torsion balance with screw pin of the ring or plate is inserted into the ring guidance of the balance. Whenever ring is changed the balance must be locked in order to protect the sensitive system. The surface plane of the ring has to be completely flat. This can be checked by turning the ring around its axle and looking at the same time at the ring surface plane from a vertical point of view. The ring is not supposed to be out of true.

After that the sample-vessel is cleaned by means of Chromo-Sulphuric acid, boiled for a considerable time in distilled water and briefly flamed prior to use with a Bunsen burner. The measuring vessel consists of refractory glass: after being washed it may also be glowed lightly with the Bunsen burner. Our practical experience has shown that a thorough cleaning of the glass vessels with Acetone and consecutive drying is sufficient.

The liquid to be analysed is poured into the cooled glass jar and then placed on the measuring table respectively the thermostat vessel. Between the latter and the table a minimal distance of 1.5-2cm should be ensured. If this is not the case the required

distance has to be adjusted by means of the micrometer screw. When working with the flat table it is important to take care that the distance from the ring to the vessel walls is equal on all sides.

Prior to each measurement the circuit division has to be set to 0 by means of screw. The illumination can be switched on with switch. After releasing the arrest screw the light pointer should settle on the middle line of the dark screen. If this is not the case the zero position has to reset by turning the zero adjustment-screw, to be found at the backside of the head part. In this state the balance will swing freely around its zero-position. The instrument is now ready for measurement.

A.2.3 Calibration

The interfacial tensiometer is calibrated in this work with double distilled water (interface tension at 20°C = 72.6 mN/m).

If another value should be obtained in the course of time, in particular when using a new ring, it is best to operate with a correction factor. If the value obtained for water at 20°C is not 72.6 mN/m but 73.0 mN/m, the correction factor will be equal to the quotient of the theoretical and indicated value: $\frac{72.6}{73.0} = 0.994$.

A.2.4 Interface tension between two liquids

When measuring the interface tension between two liquids which are not miscible with each other, (e.g. Oil and water) and when the measurement is to be performed by drawing up the ring, it is first immersed into the specific lighter phase and the balance system is adjusted to 0. Afterwards a new sample vessel is filled up to the middle with the heavier phase; the ring is cleaned and then immersed into the heavier phase. The lighter phase is pipetted above carefully. Measurement is performed analogue to (A.2.2).

When measuring the interface tension between two liquids the phenomenon of over-elongation should be particularly utilized to detect the end point, since after breaking through from one liquid into the other the ring is wetted with the second liquid and thus rendered useless in this form for repeating the measurement. In this case the instrument has to be emptied, the ring and sample vessel have to be cleaned before the measurement can be repeated.

For several systems (e.g. water/chloroform) it is necessary to measure the interface tension by pushing the ring through the upper into the lower phase. In this case the security-screw against overturning has to be removed. The turning of screw has to be performed in clockwise-direction.

The interface tension values thus measured show accuracy of 0.05 mN/m corresponding to DIN 53914 and to ASTM D 971-50.

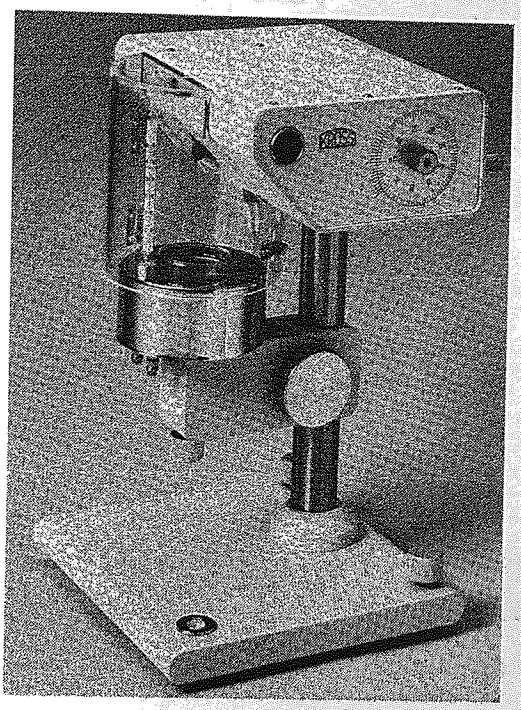

Figure (A.4) Interfacial Tensiometer K8 from KRUSS.

A.3 DATA ACQUISITION AND LOGGING BOARD

A.3.1 Overview:

The DT2811 is a half-size, low-cost analogue and digital I/O board designed for use with the IBM PC and compatible microcomputer systems. The DT2811 features three subsystems, each of which performs a distinct function: analogue to digital conversion (A/D); digital to analogue conversion (D/A); and digital I/O. The DT2811 is typically used for industrial process control and laboratory research in low noise environments. The board can be plugged into any one of the fully bussed ISA expansion slots in the IBM PC or compatible computer back plane. Table (A.1)

highlights the main features of the DT2811.

TABLE (A.1) MAIN FEATURES OF DT2811

Model	***A/D***				***D/A***	
	Range	Resolution	Gain	Max Throughput	Range	Resolution
DT2811-PGL	0-5V ±5V ±2.5V	12 bit	1 10 100 500	20 kHz 2.5 kHz	0-5 V ± 5 V ± 2.5V	12 bit

A.3.2 A/D Conversion Subsystem:

The main component of the A/D subsystem is a monolithic analogue to digital converter, which acquires analogue voltage inputs from the outside world through sensors such as thermocouples and pressure transducers, and converts them into 12-bit digital codes. In this work it has been used to accept analogue signals produced by the online refractometer. The board then transmits this code to the host computer which processes it according to the software preloaded in the computer's memory and commands issued to the processor by the operator during the execution of the program. The A/D subsystem is equipped with a gain circuit, which permits software programmable amplification of the input signal.

The A/D subsystem provides 16 single-ended or 8 differential input channels for A/D conversions. It can be configured for uni-polar or bipolar input ranges of 0 to +5V, ±5V, and ±2.5V. The DT2811 provides 12-bit resolution of the input voltage. The output code is straight binary for uni-polar inputs and offset binary for bipolar inputs.

The DT2811 can operate in single or continuous conversion modes. In the single conversion mode, the DT2811 performs conversion on a selected channel and stops at the completion of the conversion.

Another channel (or the same channel) must be selected for the next conversion operation. In the continuous conversion mode, repetitive hardware triggered

conversions can be performed on a selected channel. The conversions come to a halt when the trigger is disabled.

A/D conversion operations can be monitored either by polled I/O or by interrupts. In the polled I/O mode, the program polls the A/D Control/Status Register repeatedly for an indication of the completion of the ongoing A/D conversion. In the interrupt mode, the board automatically generates an interrupt to the host processor at the completion of an A/D conversion.

The throughput of the A/D subsystem depends on a variety of factors, such as the triggering method and the gain applied to the input signal. In the polled I/O mode, a maximum throughput of 20 kHz (20K conversions per second) can be achieved with repetitive hardware triggers applied to a single channel.

A.4 EXPERIMENTAL APPARATUS:

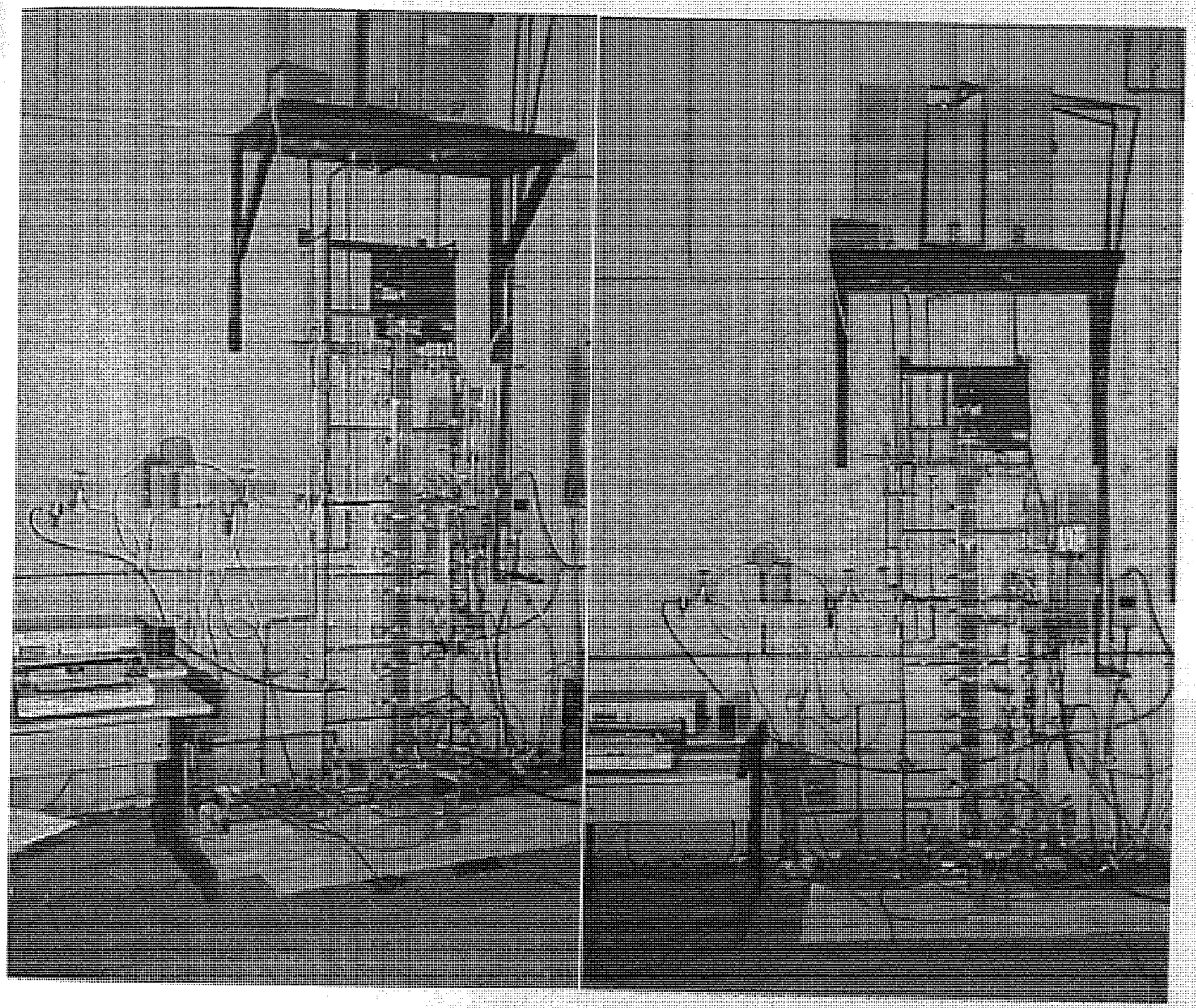

Figure (A.5) Different views of the Scheibel extraction column with instrumentations.

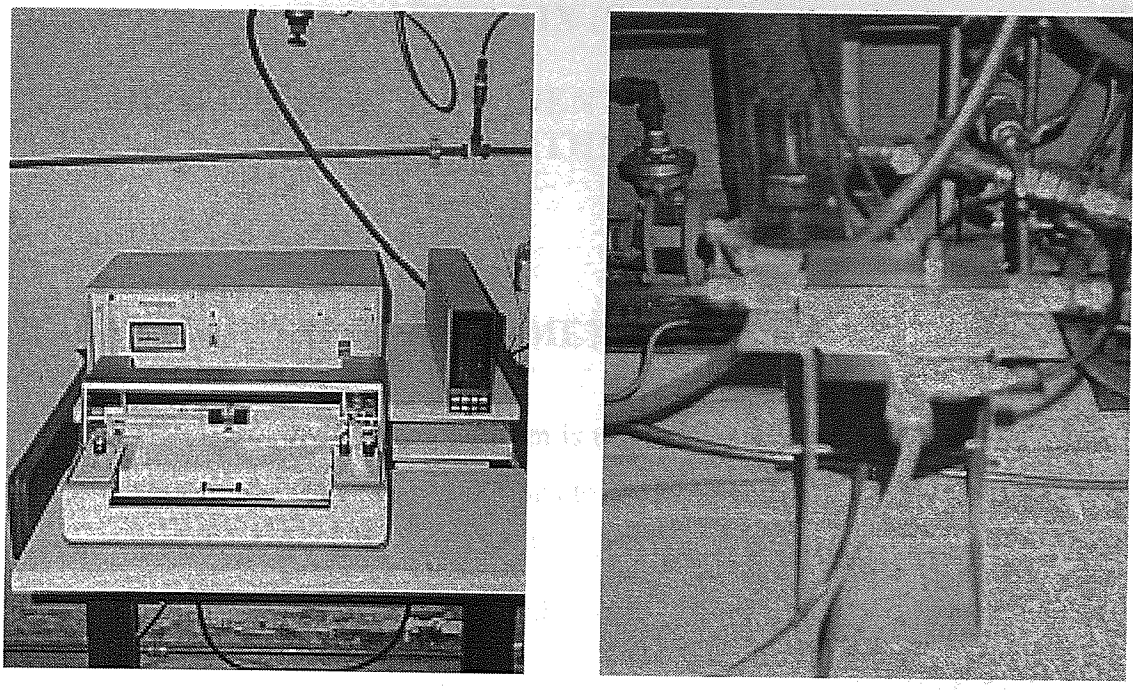

Figure (A.6) ANACON online refractometer with its measurement cell.

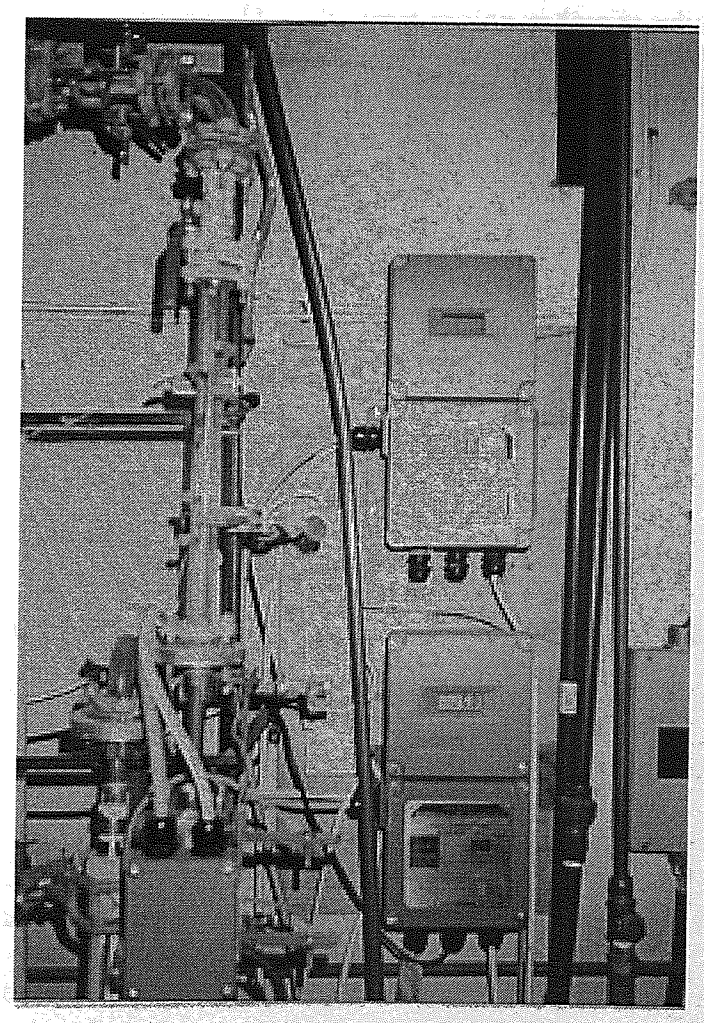

Figure (A.7) Online digital flowmeters.

APPENDIX (B)

OPTIMIZATION, SYSTEM IDENTIFICATION AND DMC ALGORITHMS

B.1 LEVENBERG-MARQUARDT METHOD (LM)

The *Levenberg-Marquardt (LM)* algorithm is used to solve nonlinear least squares problems. It is very useful for finding solutions to complex fitting problems. It can be thought of as a trust-region modification of the Gauss-Newton algorithm. Levenberg-Marquardt steps $\boldsymbol{a}_k$ are obtained by solving sub-problems of the form :

$$min\left(\tfrac{1}{2}\left\|\boldsymbol{f}'(\boldsymbol{x}_k)\boldsymbol{a}_k+\boldsymbol{f}(\boldsymbol{x}_k)\right\|_2^2 : \left\|\boldsymbol{D}_k\boldsymbol{a}\right\|_2 \le \Delta_k\right) \qquad \text{(B.1)}$$

for some $\Delta_k > 0$ and scaling matrix $\boldsymbol{D}_k$. The trust-region radius is adjusted between iterations according to the agreement between predicted and actual reduction in the objective function. For a step to be accepted, the ratio:

$$\rho_k = \frac{\boldsymbol{r}(\boldsymbol{x}_k)-\boldsymbol{r}(\boldsymbol{x}_k+\boldsymbol{s}_k)}{\boldsymbol{r}(\boldsymbol{x}_k)-\tfrac{1}{2}\left\|\boldsymbol{f}'(\boldsymbol{x}_k)\boldsymbol{a}_k+\boldsymbol{f}(\boldsymbol{x}_k)\right\|_2^2} \qquad \text{(B.2)}$$

must exceed a small positive number. (typically 0.0001). If this test is failed, the trust region is decreased and the step is recalculated. When the ratio is close to one, the trust region for the next iteration is expanded.

Levenberg-Marquardt codes usually determine the step by noting that the solution of (B.2) also satisfies the equation

$$\left(\boldsymbol{f}'(\boldsymbol{x}_k)^T\boldsymbol{f}'(\boldsymbol{x}_k)+\lambda_k\boldsymbol{D}_k^T\boldsymbol{D}_k\right)\boldsymbol{a}_k = -\boldsymbol{f}'(\boldsymbol{x}_k)^T\boldsymbol{f}(\boldsymbol{x}_k) \qquad \text{(B.3)}$$

for some $\lambda_k \ge 0$. The Lagrange multiplier λ_k is zero if the minimum-norm Gauss-Newton step is smaller than Δ_k; otherwise λ_k is chosen so that $\left\|\boldsymbol{D}_k\boldsymbol{a}_k\right\|_2 = \Delta_k$.

Equations (B.3) are simply the normal equations for the least squares problem

$$min\left\{\left\|\begin{bmatrix} f'(x_k) \\ \lambda_k^{1/2} D_k \end{bmatrix} a + \begin{bmatrix} f(x_k) \\ 0 \end{bmatrix}\right\|_2^2 : a \in \Re^n\right\} \qquad \text{(B.4)}$$

Efficient factorization of the coefficient matrix in (B.4) can be performed by a combination of Householder and Givens transformations.

For further details regarding the application of this method, refer to Seber *et al.* (1989).

In this work, the statistical analysis software STATGRAF was used for implementing the LM method for the nonlinear optimization problem of fitting the mass transfer weight factors to the experimental profiles.

B.2 QUASI-NEWTON METHODS (QN)

Quasi-Newton (QN) or *variable metric* methods attempt to generate an estimate of the inverse of the Hessian matrix. This is then used to determine the next iteration point. It can be used when the Hessian matrix is difficult or time-consuming to evaluate. Instead of obtaining an estimate of the Hessian matrix at a single point, these methods gradually build up an approximate Hessian matrix by using gradient information from some or all of the previous iterates x_k visited by the algorithm. Given the current iterate x_k, and the approximate Hessian matrix B_k at x_k, the linear system $B_k d_k = -\nabla f(x_k)$ is solved to generate a direction d_k. The next iterate is then found by performing a line search along d_k To obtain the new approximate Hessian matrix B_{k+1} from the previous approximation B_k we use the fundamental theorem of integral calculus. If we define

$$s_k = x_{k+1} - x_k, \qquad y_k = \nabla f(x_{k+1}) - \nabla f(x_k) \qquad \text{(B.5)}$$

then this theorem implies that

$$\left\{\int_0^1 \nabla^2 f(x_k + ts_k)dt\right\} s_k = y_k \tag{B.6}$$

The matrix in braces can be interpreted as the average of the Hessian matrix on the line segment $[x_k, x_k + s_k]$. This result states that when this matrix is multiplied by the vector s_k, the resulting vector is y_k.

In view of these observations, we can make B_{k+1} mimic the behavior of $\nabla^2 f$ by enforcing the *quasi-Newton condition* $B_{k+1}s_k = y_k$

This condition can be satisfied by making a simple low-rank update to B_k. The most commonly used family of updates is the Broyden class of rank-two updates, which have the form

$$B_{k+1} = B_k - \frac{B_k s_k (B_k s_k)^T}{s_k^T B_k s_k} + \frac{y_k y_k^T}{y_k^T s_k} + \phi_k \left[s_k^T B_k s_k\right] \upsilon_k \upsilon_k^T \tag{B.7}$$

where $\phi_k \in [0,1]$ and

$$\upsilon_k = \left[\frac{y_k}{y_k^T s_k} - \frac{B_k s_k}{s_k^T B_k s_k}\right] \tag{B.8}$$

The choice $\phi_k = 0$ gives the Broyden-Fletcher-Goldfarb-Shanno (BFGS) update, which practical experience, and some theoretical analysis, has shown to be the method of choice in most circumstances. The Davidon-Fletcher-Powell update, which was proposed earlier, is obtained by setting $\phi_k = 1$. These two update formulae are known universally by their initials BFGS and DFP, respectively.

Updates in the Broyden class remain positive definite as long as $y_k^T s_k > 0$. Although the previous condition holds automatically if f is strictly convex, it can be enforced for all functions by requiring that α_k satisfy the curvature condition. Some codes avoid enforcing the curvature condition by skipping the update if $y_k^T s_k \leq 0$.

Many optimisation codes implement this method. These codes differ in the choice of update (usually BFGS), line-search procedure, and the way in which $\boldsymbol{B}_k$ is stored and updated. We can update $\boldsymbol{B}_k$ by either updating the Cholesky decomposition of $\boldsymbol{B}_k$ or by updating the inverse of $\boldsymbol{B}_k$. In either case, the cost of updating the search direction by solving the system $\boldsymbol{B}_k \boldsymbol{d}_k = -\nabla f(\boldsymbol{x}_k)$.

is on the order of $\boldsymbol{n}^2$ operations. Updating the Cholesky factorization is widely regarded as more reliable, while updating the inverse of $\boldsymbol{B}_k$ is less complicated. Indeed, if we define $\boldsymbol{H}_k = \boldsymbol{B}_k^{-1}$.

then a BFGS update of $\boldsymbol{B}_k$ is equivalent to the following update of $\boldsymbol{H}_k$:

$$\boldsymbol{H}_{k+1} = \left(\boldsymbol{I} - \frac{\boldsymbol{s}_k \boldsymbol{y}_k^T}{\boldsymbol{y}_k^T \boldsymbol{s}_k} \right) \boldsymbol{H}_k \left(\boldsymbol{I} - \frac{\boldsymbol{y}_k \boldsymbol{s}_k^T}{\boldsymbol{y}_k^T \boldsymbol{s}_k} \right) + \frac{\boldsymbol{s}_k \boldsymbol{s}_k^T}{\boldsymbol{y}_k^T \boldsymbol{s}_k} \qquad \text{(B.9)}$$

When we store $\boldsymbol{H}_k$ explicitly, the direction $\boldsymbol{d}_k$ is obtained from the matrix-vector product $\boldsymbol{d}_k = -\boldsymbol{H}_k \nabla f(\boldsymbol{x}_k)$.

The availability of quasi-Newton methods renders steepest-descent methods obsolete. Both types of algorithms require only first derivatives, and both require a line search. The quasi-Newton algorithms require slightly more operations to calculate an iterate and somewhat more storage, but in almost all cases, these additional costs are outweighed by the advantage of superior convergence. For further details of this method refer to Gilbert et al. (1989).

B.3 THE ASYMPTOTIC IDENTIFICATION METHOD (ASYM)

Given a multivariable process with *m* manipulated variables (inputs) and *p* controlled variables (outputs). Denote the data sequence that is collected from an identification test as:

$$\boldsymbol{Z}^N = \{\boldsymbol{u}_1, \boldsymbol{y}_1, \boldsymbol{u}_2, \boldsymbol{y}_2, ..., \boldsymbol{u}_N, \boldsymbol{y}_N\} \qquad \text{(B.10)}$$

where $\boldsymbol{u}_t$: is a m-dimensional input vector,

y_t : is a p-dimensional output vector,

N: number of samples.

Assuming a linear discrete-time process for the generated data as:

$$y_t = G^o(z^{-1})u_t + H^o(z^{-1})e_t \qquad \text{(B.11)}$$

where z^{-1}: is unit time delay operator,

$H^o(z^{-1})$: represents the unmeasured disturbances,

e_t : is a p-dimensional noise vector.

The model to be identified has the same structure as that of equation (B.11)

The frequency response of the process is given as:

$$T^o(e^{i\omega}) : col\,[G^o(e^{i\omega}), H^o(e^{i\omega})] \qquad \text{(B.12)}$$

and that of the model as:

$$\hat{T}^n(e^{i\omega}) : col\,[\hat{G}^n(e^{i\omega}), \hat{H}^n(e^{i\omega})] \qquad \text{(B.13)}$$

where n: model polynomials degree

$col()$: column operator.

The asymptotic properties of prediction error method assume that:

$n \to \infty$ and $n^2 / N \to 0$ as $N \to 0$

and

$$\hat{T}^n(e^{i\omega}) \to T^o(e^{i\omega}) \text{ as } N \to \infty$$

The error of $\hat{T}^n(e^{i\omega})$ follows a Gaussian distribution, with covariance given as:

$$\text{cov}\left[col\left[G^o(e^{i\omega})\right]\right] \approx \frac{n}{N}(\phi_u^{-1}(\omega))^T \otimes \phi_v(\omega) \qquad \text{(B.14)}$$

where $\phi_u(\omega)$: the spectrum matrix of inputs.

$\phi_v(\omega)$: the spectrum matrix of unmeasured disturbances

$\otimes$: denotes Kronecker product

The ARX (equation error) model is estimated. This high order model is then reduced by using frequency weighted model reduction by applying the maximum likelihood principle.

The asymptotic criterion (ASYC) is used for reduced model order selection. This criterion is applied by equalizing bias error and variance error of each transfer function in the frequency range of interest. For a frequency range of $[\omega_1, \omega_2]$ the criterion is given by:

$$ASYC := \sum_{i=1}^{p}\sum_{j=1}^{m}\int_{\omega_1}^{\omega_2}\left[\left[\hat{G}_{ij}^{\,n}(\omega)-\hat{G}_{ij}(\omega)\right]^2-\frac{n}{N}\phi_{u_i}^{-1}(\omega)\phi_{v_i}(\omega)\right]d\omega \quad \text{(B.15)}$$

One of the features of the ASYM identification method is its capability of validating the model using error band matrix. The error bound matrix is defined as:

$$\left|\hat{G}_{ij}^{\,o}(\omega)-\hat{G}_{ij}^{\,n}(\omega)\right| \le 3\sqrt{\frac{n}{N}\phi_{u_i}^{-1}(\omega)\phi_{v_i}(\omega)} \quad \textbf{w.p. } 99.9\% \quad \text{(B.16)}$$

This matrix can be used for robust stability and performance analysis for the case of linear time invariant controller.

See Zhu Y. (1998) for further details.

B.4. DYNAMIC MATRIX CONTROL

Model predictive control is implemented in many forms and applied in industry under names such as (Qin and Badgwell 1997) :

- **IDCOM** : Identification and Command developed by Richalet et al. (1978).
- **DMC:** Dynamic Matrix Control, Cutler et al. (1979).
- **QDMC :** developed by García and Morshedi (1983).
- **GPC:** Generalized Predictive Control, Clarke et al. (1987).
- **IDCOM-M:** MIMO version of IDCOM developed by Setpoint, Inc. (1988).

These are only a few set of many other forms of MPC. The main ideas behind them are very similar and in its basic unconstrained form MPC is closely related to linear quadratic (LQ) optimal control. In the constrained case, however, MPC leads to an optimization problem which is solved on-line in real time at each sampling interval. MPC takes full advantage of the power available in today's control computer hardware. There are four elements shared in common by all these MPC schemes and they differ only on the way in which these elements are implemented. These elements are as follows (Ogunnaike et al. 1994):

1. Reference trajectory specification.
2. Process output prediction.
3. Control action sequence computation.
4. Error prediction update.

Dynamic Matrix Control (DMC) was pioneered in the early 1970's, by the Shell Oil company engineers and first applied it in 1973. Cutler and Ramaker, presented details of an unconstrained multivariable control algorithm which they named Dynamic Matrix Control (DMC) at the 1979 National AIChE meeting and at the 1980 Joint Automatic Control Conference. The first application of the DMC was presented by Prett and Gillette (1988). It was for an FCCU reactor/regenerator in which the algorithm was modified to handle nonlinearities and constraints.

The key features of the DMC control algorithm include:

- linear step response model for the plant.
- quadratic performance objective over a finite prediction horizon.

- future plant output behavior specified by trying to follow the setpoint as closely as possible.
- optimal inputs computed as the solution to a least-squares problem .

B.4.1 Model used in DMC

Basically there are three model forms used by the MPC schemes. These are :

1. The **finite Convolution models** which includes the impulse response model and the step response mode
2. The **discrete state-space models** also known as **ARMAX** (**A**uto**R**egressive, **M**oving **A**verage with e**X**ogenous inputs).
3. The **discrete transfer function models**

More details of these models can be found in (Prett and Gillette 1988).

The linear step response model which is a finite convolution type is utilized in the DMC. This model relates changes in a process output to a weighted sum of past input changes, referred to as input moves. Its general form is:

$$y(k)=\sum_{i=0}^{k}\beta(i)\Delta u(k-i) \tag{B.17}$$

Where:

$\beta(i)$: the process step-reponse function.

and $\Delta u(k)=u(k)-u(k-1)$.

The step response coefficients are obtained either from plant testing data or from parametric models. In this work, the later option was adopted. In MATLAB, the MPC toolbox stores the step response models in the following special format:

$$\mathbf{plant}=\begin{bmatrix} & \beta_1 & & \\ & \beta_2 & & \\ & \vdots & & \\ & \beta_n & & \\ \mathbf{nout}(1) & 0 & \cdots & 0 \\ \mathbf{nout}(2) & 0 & \cdots & 0 \\ \vdots & \vdots & \cdots & \vdots \\ \mathbf{nout}(\mathbf{n_y}) & 0 & \cdots & 0 \\ \mathbf{n_y} & 0 & \cdots & 0 \\ \mathbf{delt}2 & 0 & \cdots & 0 \end{bmatrix}_{(\mathbf{n}\cdot\mathbf{n_y}+\mathbf{n_y}+2)\times\mathbf{n_v}} \tag{B.18}$$

where: **delt2** is the sampling time and the vector **nout** indicates if a particular output is integrating or not:

nout(*i*) = 0 if output ***i*** is integrating.

nout(*i*) = 1 if output ***i*** is stable.

This format is used to represent MIMO models to be used later in MPC simulations. The ***i***th step response coefficients β_i . These coeffecents are defined as:

$$\beta_i = \begin{bmatrix} \beta_{1,1,i} & \beta_{1,2,i} & \cdots & \beta_{1,n_u,i} \\ \beta_{2,1,i} & \beta_{2,2,i} & \cdots & \beta_{2,n_u,i} \\ \vdots & \vdots & \cdots & \vdots \\ \beta_{n_y,1,i} & \beta_{n_y,2,i} & \cdots & \beta_{n_y,n_u,i} \end{bmatrix}$$

The $\beta_{k,j,i}$ is the ***i***th step response coefficient describing the effect of input ***j*** on output ***k***. The n_u and n_y are the total number of inputs and outputs repectively. This format is formulated to preserve space and simplify calculations. For further details on the use of this model format, refer to the MATLAB MPC Toolbox manual.

Let us now assume the following:

The vector of the unit step reponse function:

$$\beta = [\beta_1, \beta_2, \beta_3, \ldots, \beta_n,]^T$$

The kth time value predicted process output vector over the p-time step horizon:

$$\hat{y}_k^{\,0} = [\hat{y}_{k+1}^{\,0}, \hat{y}_{k+2}^{\,0}, \hat{y}_{k+3}^{\,0}, \ldots, \hat{y}_{k+p}^{\,0},]^T$$

The unmeasured disturbances vector on the output:

$$w_k = [w_{k+1}, w_{k+2}, w_{k+3}, \ldots, w_{k+p},]^T$$

Then the step response model can be rewritten as:

$$\Delta \mathbf{u}_k = \hat{\mathbf{y}}_k^0 + \mathbf{B}\Delta \mathbf{u}_k + \mathbf{w}_k \qquad \text{(B.19)}$$

where $\Delta \mathbf{u}_k$ is the value of $\Delta \mathbf{u}$ at ***m*** points in time beginning at time step ***k*** and defined as: $\Delta \mathbf{u}_k = [\mathbf{u}_k, \mathbf{u}_{k+1}, \mathbf{u}_{k+2}, \ldots, \mathbf{u}_{k+m-1},]^T$ and the matrix $\mathbf{B}$ is called the *"dynamic matrix"* and defined as follows:

$$\mathbf{B}=\begin{bmatrix} \beta_1 & 0 & 0 & \cdots & 0 \\ \beta_2 & \beta_1 & 0 & \cdots & 0 \\ \beta_3 & \beta_2 & \beta_1 & \cdots & 0 \\ \vdots & \vdots & \vdots & \cdots & \vdots \\ \beta_p & \beta_{p-1} & \beta_{p-2} & \cdots & \beta_{p-m+1} \end{bmatrix} \tag{B.20}$$

The columns of this matrix are the system's step-response function shifted down in order.

B.4.2 The unconstrained DMC Problem Formulation and Solution:

Starting with the step-response model equation (B.17) , the control problem becomes how to choose and implement $\Delta\mathbf{u}_k$ such that the predicted system output is caused to move and remain at the desired trajectory value y_k^* defined as:

$y_k^* = [y_{k+1}^*, y_{k+2}^*, y_{k+3}^*, \ldots, y_{k+p}^*]^T$. This means choosing $\Delta\mathbf{u}_k$ such that :

$$\mathbf{y}^*_{k+1} = \hat{\mathbf{y}}_k^0 + \mathbf{B}\Delta\mathbf{u}_k + \mathbf{w}_{k+1} \tag{B.21}$$

If we define $\mathbf{e}_{k+1} \cong \mathbf{y}^*_{k+1} - (\hat{\mathbf{y}}_k^0 + \mathbf{w}_{k+1})$ as the predicted error vector, then the control problem reduces to chooseing $\Delta\mathbf{u}_k$ to satisfy the equation :

$$\mathbf{B}\Delta\mathbf{u}_k = \mathbf{e}_{k+1} \tag{B.22}$$

This equation can be solved by finding the vector norm $\|\mathbf{e}_{k+1} - \mathbf{B}\Delta\mathbf{u}_k\|$. This is achieved by minimising some function that measures the difference between the two sides of equation B.22. For the case where the norm is the Euclidian norm, the solution is expressed as:

$$\min_{\Delta\mathbf{u}_k} (\Phi) = [\mathbf{e}_{k+1} - \mathbf{B}\Delta\mathbf{u}_k]^T [\mathbf{e}_{k+1} - \mathbf{B}\Delta\mathbf{u}_k] \tag{B.23}$$

This is the classical least squares problem which has the solution:

$$\Delta\mathbf{u}_k = \left(\mathbf{B}^T\mathbf{B}\right)^{-1}\mathbf{B}^T\mathbf{e}_{k+1} \tag{B.24}$$

In practice, a penalty against excessive control action is often incorporated in the optimization objective problem. So equation B.23 becomes:

$$\min_{\Delta u_k} (\Phi) = [e_{k+1} - B\Delta u_k]^T [e_{k+1} - B\Delta u_k] + K^2 [\Delta u_k{}^T \Delta u_k] \quad (B.25)$$

The corresponding control action equation becomes:

$$\Delta u_k = \left(B^T B + K^2 I\right)^{-1} B^T e_{k+1} \quad (B.26)$$

In order to take care of the scalling of the error vector e_{k+1} such that equally important changes in the various output variables are treated equally, a weighting matrix Γ is intorduced as a tuning parameter. Equation B.24 becomes:

$$\Delta u_k = \left(B^T \Gamma B + K^2 I\right)^{-1} B^T \Gamma e_{k+1} \quad (B.27)$$

We can conclude by stating the four MPC elements as utilized in the DMC are as follows:

1. Reference trajectory specification: A step to the desired setpoint or target value.
2. Process output prediction: Prediction is carried out using the step response model with matrix B as the main operator (equation B.22).
3. Control action sequence computation: This is done by solving equation (B.27).
4. Error prediction update: this is achieved by providing estimates for w_{k+1} (Ogunnaike et al. 1994).

B.4.3 The General Constrained DMC Problem:

In general, the DMC problem can be expressed as:

$$\min_{\Delta u_k, \ldots, \Delta u_{k+m-1}} \sum_{l=1}^{p} \varepsilon^T{}_{k+1} \Gamma \varepsilon_{k+1} + \sum_{l=1}^{m} u^T{}_{k+l-1} F u_{k+l-1} + \Delta u^T{}_{k+l-1} R \Delta u_{k+l-1} \quad (B.28)$$

where the elements the weighting matrices of Γ, F and R as well as the prediction horizon p and control moves m are the tuning parameters. ε_{k+1} is the residual error vector defined as:

$$\varepsilon_{k+1} = e_{k+1} - B\Delta u_k . \quad (B.29)$$

For the case where constrains are involved, then the problem becomes a quadratic programming (QP) problem (Garcia and Prett 1986). In this case, equation B.28 is augumented with the constraint equations. The solution to this kind of problems can be put as following:

$$\min_{\mathbf{v}} \Phi(\mathbf{v}) = \frac{1}{2}\mathbf{v}^T\mathbf{Q}\mathbf{v} + \mathbf{q}^T\mathbf{v} \qquad \text{(B.30)}$$

subject to $\Lambda^T\mathbf{v} \geq \eta$

where $\mathbf{v}$ is the collective vector of all control moves an is defined as: $\mathbf{v} = \left[\mathbf{u}_k, \mathbf{u}_{k+1}, \ldots, \mathbf{u}_{k+m-1}\right]^T$.

The parameters of equation B.30 are $\mathbf{Q}$ and Λ are related to the tuning parameters of equation B.28 subject to some hard constraints.The vectors $\mathbf{v}$ and η are linear functions of the tuning parameters as well as being functions of the output prediction vector ,$\hat{\mathbf{y}}$ and the past inputs $\mathbf{u}(k-1), \mathbf{u}(k-2), \cdots, \mathbf{u}(k-n)$. Many solutions algorithms are available for this QP problem (Ricker 1985).

APPENDIX (C)
MODEL SIMULATION PROGRAM

C.1 USER INTERFACE:

This is a Graphical User Interface (GUI) used to execute the simulation program. It is written using Visual Basic for Application under MS Excel. The flow diagram in Figure (C.1) shows the main steps of execution for the interface. All input is done through textboxes and for step changes the user has the option of either entering the new value directly in the text-box or to use the positive or negative 10% step buttons. The execution of the user interface is transparent to the user i.e. the details of the simulator are hidden to the user, and there is no way of user intervention for program execution. This prevents any unintentional effect on the core simulator or its components.

C.2 MODEL SIMULATION PROGRAM

The main Scheibel extractor simulation program is written using FORTRAN POWER STATION development language that uses both FORTRAN 77 and FORTRAN 90 instruction sets.

As shown in Figure (C.2) the main program starts by retrieving start-up and step data from the data file created by the user interface program. It then sets the values for the mass transfer weight factors and backmixing coefficients data for each stage. The time is initialised to zero, time increment to 1 min and final simulation time to 25 min.

At the beginning of simulation the routine **INIT** is called to initialise the flowrates, holdup and concentration profiles and to evaluate integration vector **Y** and derivative vector **dY.** The flowchart for **INIT** is shown in Figure (C.3).

The flow then is returned to the main program where the **DASSL** integrator parameters are set. Then the integrator is called for the current time value T to integrate the model equations until T+dT. The **DASSL** integrator is explained in section C.3. At the current time interval [T,T+dT] **DASSL** calls the model equations routine **RES** shown in Figure (C.4).

The routine **RES** starts by updating holdup and concentration profiles then it calculates flowrate profiles by calling the routine **FLOW**. Then the derivative (**DELTA**) of the upper mixing stage concentration differential equation is calculated. Then a loop is started to calculate the vector for stages 2 to N. Then the lower mixing stage derivative is calculated. The mass transfer rate is calculated by routine **RATE** that calls the routine **MASS** to calculate the mass transfer coefficient at each stage.

The program flow returns back to the main program. After the integrator finds the solution at T+dT , the program stores flowrates, holdup and concentration transient profiles at time at this time step in the output data file. The time is advanced by dT and the integration process is repeated until time reached Tfinal. At this point the simulation reaches steady state. Final simulation Time Tfinal is changed and the process of integration is repeated for the new period [T,Tfinal]. At the end of disturbances the flow of execution goes to the subroutine **PLOT** where the profiles are plot in a separate window.

The data for all transient profiles are stored in a unified array called RESULTS. It contains vectors for time, the two phases concentrations at each stage, flow rates, and holdups. These data are first scaled to fit within the graphics window allocated for plotting, then the built-in graphical routines provided in Fortran Power station are used to plot the profiles for the whole range of simulation.

C.3 DASSL (DAE) INTEGRATOR

The integration of the DAEs is done the DASSL integrator which uses backward differentiation formulae (BDF) to approximate the derivatives y'. This converts the differential equations to a system of nonlinear algebraic equations, which are then solved at each time-step by Newton's method.

A detailed description of the method of solution employed in DASSL and a description of its method of employed are given in Appendix (D).

From the experimental findings obtained, it was realized that a simulation time of 25 min was enough to describe the whole spectrum of transient response of the column, so the integration time was set to be 25 min with an interval of 1 min.

The accuracy of integration was set by selecting both, the absolute and the relative integration tolerance variables equal to 1e-6. The calculation of the Jacobian matrix needed by the Newton algorithm was done eternally by the program.

For the dynamic step testing simulation runs, DASSL was called for the interval [0,25] min to calculate the column steady state profile then the variable step change was introduced and the integrator was used for another interval using the previously calculated steady state profile as initial values for the integrated variables. The same was done for the next step disturbances.

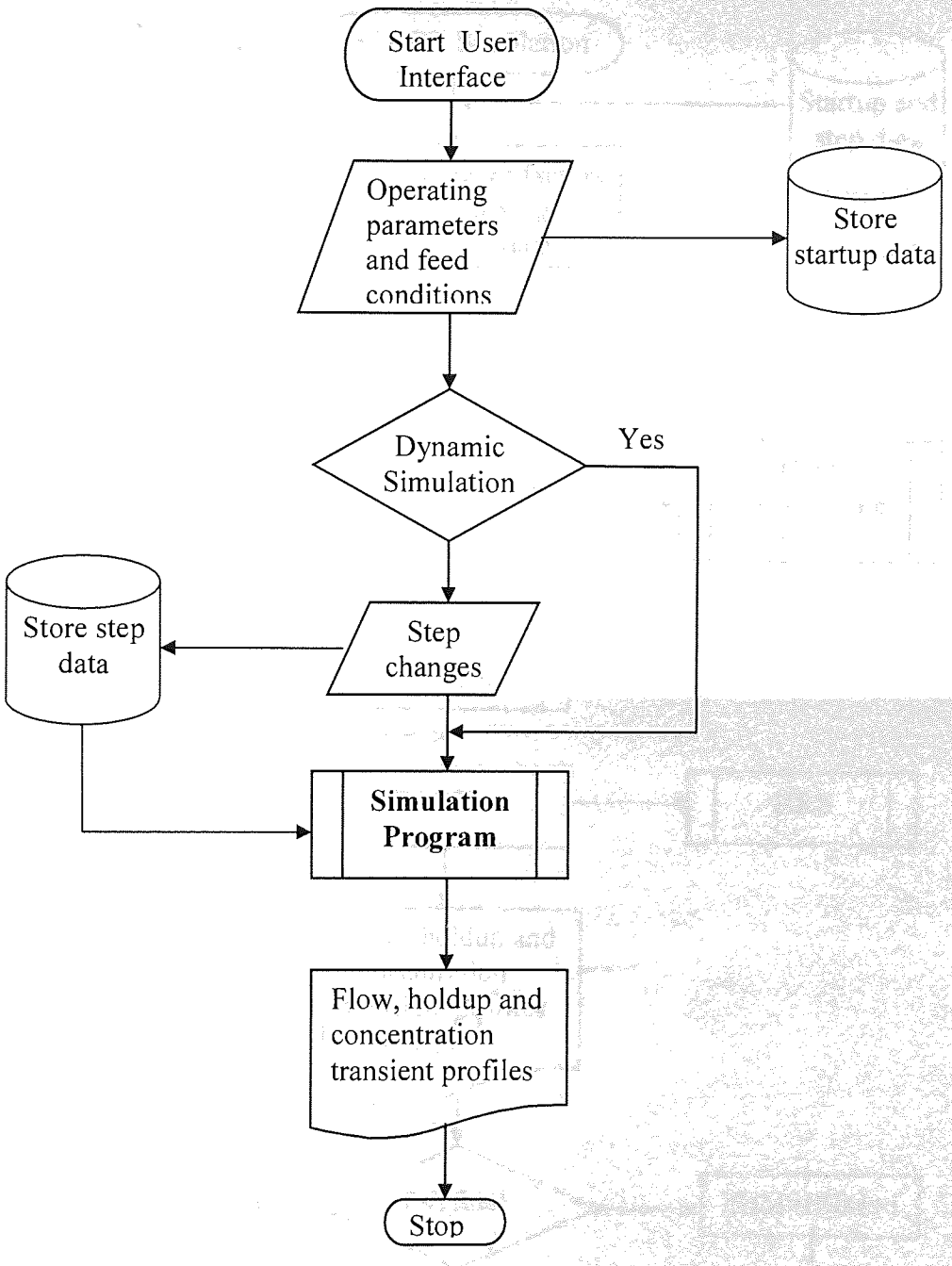

Figure (C.1) Flowchart of the simulation program user interface.

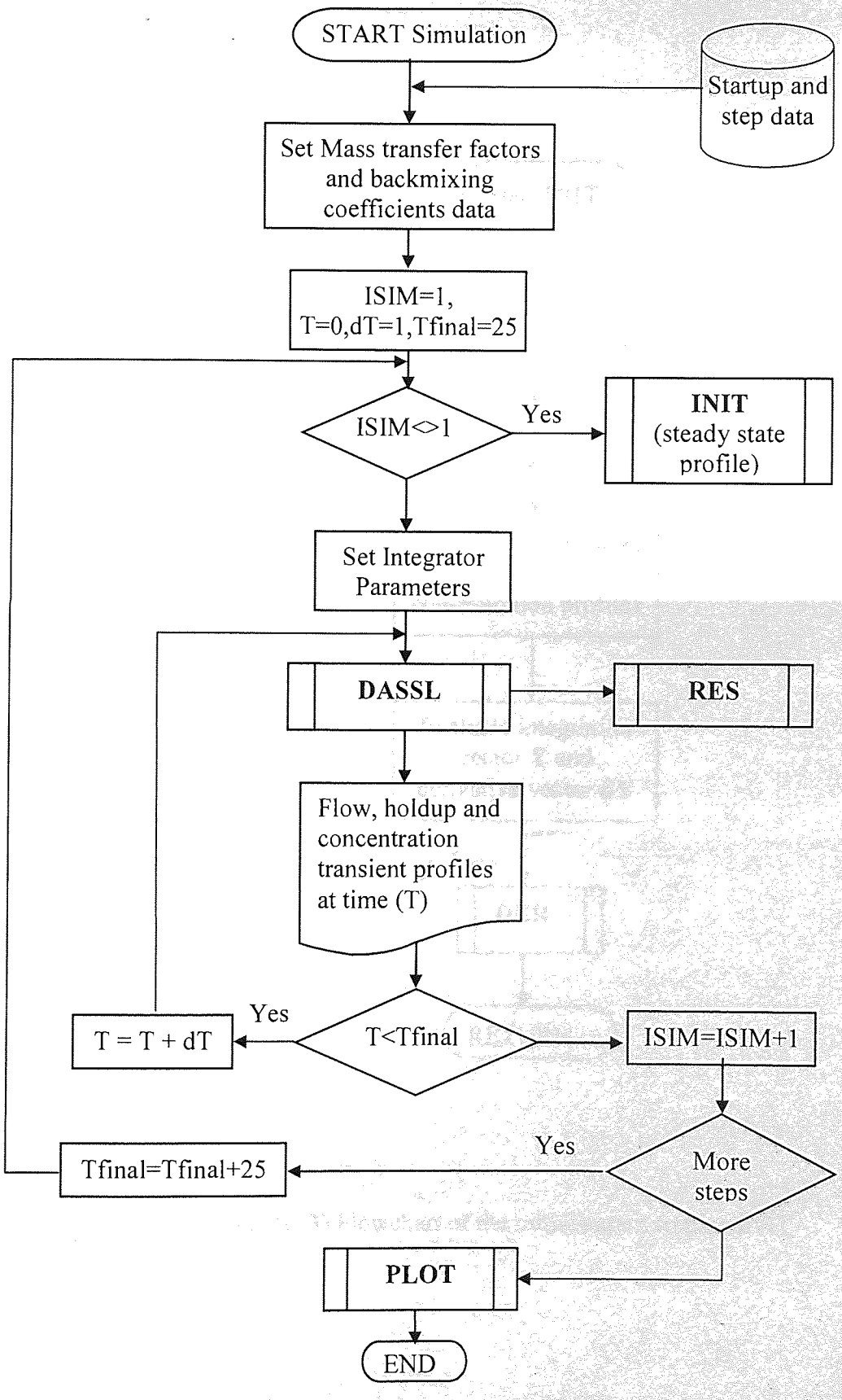

Figure(C.2) Flowchart for the MAIN model simulation program.

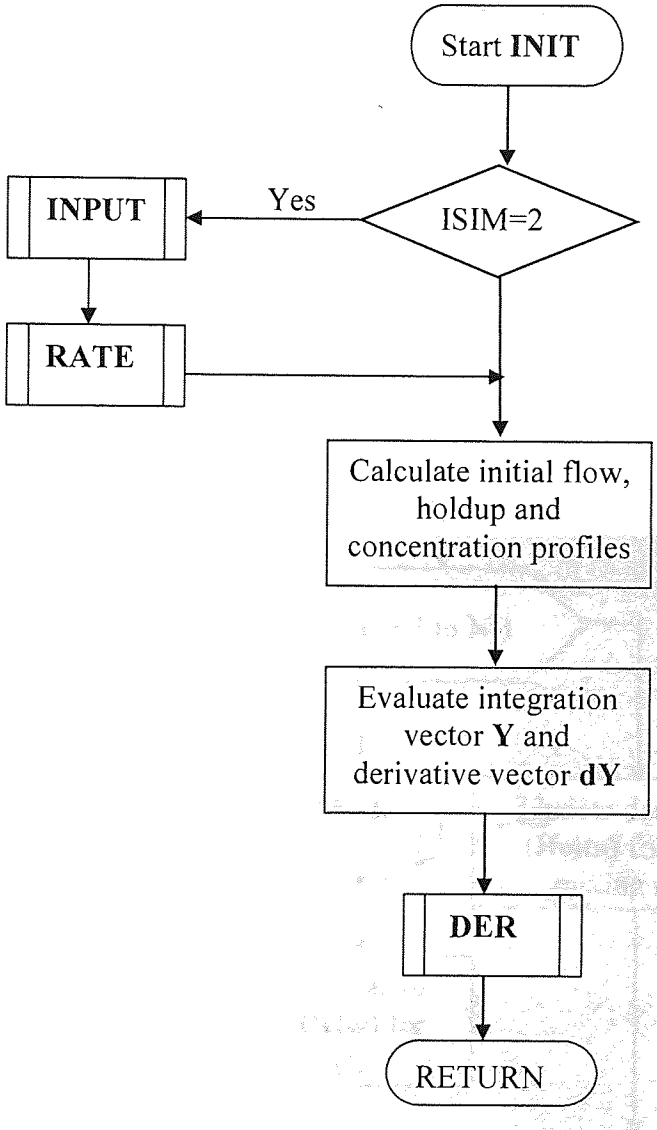

Figure (C.3) Flowchart of the initialisation routine INIT.

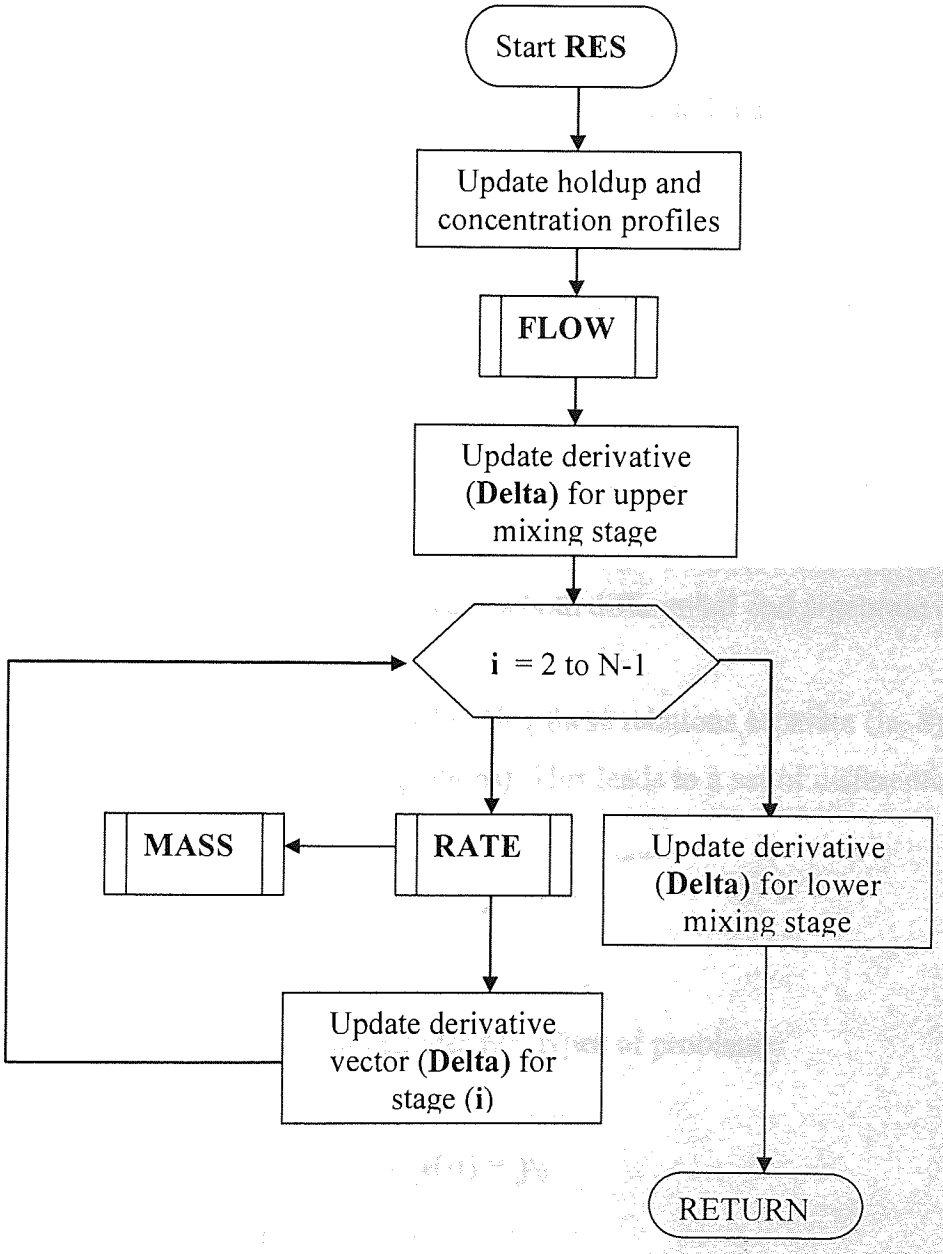

Figure (C.4) Flowchart of the model equations routine RES.

APPENDEX(D)

SOLVING DIFFERENTIAL-ALGEBRAIC EQUATIONS (DAEs)

D.1. INTRODUCTION:

A system of Ordinary Differential Equations (ODEs) is defined:

$$y' \ (= dy/dt) \ = f(y, t), \ y(0) \ = y0$$

In chemical engineering, it is frequently required to deal with problems that involve one or more of the following type of equations:

- conservation laws (mass and energy balance),
- constitutive equations (equations of state, pressure drops, heat transfer...),
- design constraints (desired operations...).

The combination of these equations involves both differential and algebraic equations to be solved simultaneously.

Solution of these equations is done by keeping these relations separate (ie. Sparating the differential from the algebraic equations). This leads to a set of differential and algebraic equations (DAEs):

$$F(y, y', t) \ = \ 0 \ \text{ with } y(0) = y_0$$

This is a Fully Implicit form that includes two types of problems:

- Linear Implicit DAEs:

  $$Ay' \ + f(y,t) \ = \ 0 \ \text{ with } y(0) = y_0$$

- Semi-implicit DAEs:

  $$x' \ = f(x, z, t)$$
  $$g(x, z, t) \ = \ 0$$

where:

x - differential variables

z - algebraic variables, $\mathbf{y}^T = [\mathbf{x}^T \ \mathbf{z}^T]$

For consistency, we consider the semi-explicit form only.

To solve DAEs, extensions of ODE solvers are implemented using two approaches:

1. Nested Approach:
   - *given* x_n, *solve* $g(x_n, z_n) = 0 \Rightarrow z_n\ (x_n)$ *using ODE method,*
   - *evolve* $x_{n+1} = F(x_n, z_n(x_n), t_n)$

   This is the most common approach, it requires $z = z(x)$ (implicit function)

   It is required if only an explicit method is available (e.g., explicit Euler or Runge-Kutta) and can be expensive due to inner iterations.
2. Simultaneous Approach:

   Solve $x' = f(x, z, t)$, $g(x, z, t)=0$ *simultaneously using an implicit solver to evolve both* x *and* z *in time.*

   It requires an implicit solver. The integration is much more efficient, and provides for more flexible problem specification.

The way this is done is as follows:

Consider a Backward Difference Formula (BDF) solver. For a semi-explicit system, we can write:

$$x_{n+1} = h\beta_{-1} f(x_{n+1}, z_{n+1}, t_n) + \sum_{j=0,k} a_j\, x_{n-j}$$

$$g(x_{n+1}, z_{n+1}, t_{n+1}) = 0$$

and we can solve this system for x_{n+1}, z_{n+1} using Newton's method. At iteration l:

$$\begin{bmatrix} 1 - h\beta_{-1}\dfrac{\partial f}{\partial x} & -h\beta_{-1}\dfrac{\partial f}{\partial z} \\ \dfrac{\partial g}{\partial x} & \dfrac{\partial g}{\partial z} \end{bmatrix} \begin{bmatrix} \Delta x_{n+1} \\ \Delta z_{n+1} \end{bmatrix} = - \begin{bmatrix} x^l_{n+1} - \sum_{j=0}^{k} x_{n-j}\alpha_j - h\beta_{-1} f(x^l_{n+1}, z^l_{n+1}, t_{n+1}) \\ g(x^l_{n+1}, z^l_{n+1}, t_{n+1}) \end{bmatrix}$$

and note that the Jacobian matrix is nonsingular at $h = 0$ as long as $\dfrac{\partial g}{\partial z}$ is nonsingular

(a necessary condition for the implicit function $z(x)$)

Thus if $\dfrac{\partial g}{\partial z}$ is nonsingular, both the nested and simultaneous approaches should work.

D.2. DESCRIPTION OF DASSL DAE SOLVER :

DASSL (Differential Algebraic System Solver) is designed for the numerical solution of implicit systems of differential/algebraic equations written in the form

$$F(t, y, y') = 0,$$

where F, y, and y' are vectors, and initial values for y and y' are given. Systems of differential/algebraic equations (DAE) arise in several diverse applications in the physical world. Problems of this type occur frequently in the numerical method of lines treatment of partial differential equations, in the simulation of electronic circuits, where they are sometimes called semistate equations, and in the dynamic analysis of mechanical and industrial systems. These problems can all be solved using DASSL. It uses double-precision variables to increase the degree of accuracy. The derivatives y' are approximated by backward differentiation formulae (BDF), and the resulting nonlinear system at each time-step is solved by Newton's method.

DASSL, normally chooses its own integration step based on the tolerances that you provide, the integration time interval, and the magnitude of the state derivatives, but it also gives a chance to set the initial and maximum integration step sizes; this is useful in dealing with stiff or difficult problems but, as usual, caution is required. DASSL also chooses its own integration order, which goes up as the problem becomes easier to solve, but it allows setting the upper limit on this number; again, caution is required.

A consistent set of derivatives can also be computed by DASSL when the integration is about to begin, an internal restart takes place (change in the nature of some model equations, like the change that occurs in going from a system whose volume is constant to one whose volume is not), or a discrete controller action at the start of a new sampling period. The user is given the opportunity to say when to compute the consistent set.

D.3. DESCRIPTION OF THE CALLING SEQUENCE FOR THE PACKAGE DASSL:

The general syntax for the DASSL subroutine is as follows:

```
CALL DDASSL(res, neq, t, y, yprime, tout, info, rtol,
            atol, idid, rwork, lrw, iwork, liw, rpar,
            ipar, jac)
```

DDASSL is the double precision implementation of DASSL. The following is a description of each parameter used in the calling statement:

RES subroutine (external)

This subroutine is used to describe to DASSL what the system of differential/algebraic equations is. The subroutine RES has the following form:

```
subroutine res(t, y, yprime, delta, ires, rpar, ipar)
```

Within this RES subroutine are several parameters:

t (input) : The independent variable.

y (input) : The dependent variable.

yprime (input) : The first derivative of the dependent variable.

delta (output) : This array must be defined as the residual of the differential algebraic system. That is, if equation system is of the form : $F(t, y, y')=0$, then delta(*) would essentially be the left-hand side of the above.

ires (output) : This is a flag to signal to the DASSL routine. You probably shouldn't change this unless the RES routine gets an illegal input. In this case, set ires to -1. In all other cases, ires should be 0.

rpar(*)(input) : This is an array of double precision extra parameters that your problem might have above and beyond y, y', and t. DASSL doesn't change this array. The user can dimension it freely.

ipar(*) (input) : This is the integer analogy to rpar.

neq (input) : This is the number of equations you have in your differential/algebraic system.

The rest of DASSL calling parameters are descriped bellow:

t (input/output) : Set this array to the initial value of the solution vector.

y(*)(input/output) : Set this to the initial point of the integration.

yprime(*)(input/output) Set this array to the initial values of the first derivative of the

solution vector.

tout (input) : This is the point at which the solution is desired. The DASSL routine will not step past this point.

info(*)(input) : This array is used by DASSL to enable the user to provide more information about the problem to be solved. This should be dimensioned to 15. The elements have the following control over the code:

info(1) : Set this to 0 for the first call of the program.

info(2) : If the user wants both the absolute and relative error tolerances to be scalars, then set info(2) = 0. If both vectors, then set info(2) = 1.

info(3) : To integrate step-by-step from t to tout, set info(3) = 1. To only get the solution vector at time tout, then set info(3) = 0.

info(4) : To handle solutions at a great many specific values ***tout*** efficiently, this code may integrate past tout and interpolate to obtain the result at ***tout***. Sometimes it is not possible to integrate beyond some point ***tstop*** because the equation changes there or it is not defined past ***tstop***. If the integration can be carried out without any restrictions on the independent variable t, then set info(4) = 0. Otherwise, set info(4) = 1 and define the time tstop by setting rwork(1) = tstop.

info(5) : If it is required that DASSL evaluate a Jacobian matrix using finite differences, set info(5) = 0. Otherwise, set info(5) = 1 and define a subroutine jac for evaluating the matrix of partial derivatives.

info(6) : If it is required to solve the problem using a full (dense) matrix (and not a special banded structure), then set info(6) = 0 (this is the case for our system solution). Otherwise, read the documentation for DASSL.

info(7) : A maximum stepsize can be set so that the code will avoid passing over very large regions. If the code is to decide on its own maximum stepsize then set info(7) = 0. Otherwise, set info(7) = 1 and define the maximum stepsize h_{max} by setting rwork(2) = h_{max}.

info(8) : Differential/algebraic systems may occasionally suffer from severe scaling difficulties on the first step. If the user know a great deal about the scaling of your problem, he can help to alleviate this problem by specifying an initial stepsize h_0. If the code is to define its own initial stepsize then set info(8) = 0. Otherwise, set info(8) = 1 and define

h_0 by setting rwork(3) = h_0.

info(9) : This item enables controlling the maximum order of the BDF scheme used. If it is set info(9) = 0 this tells DASSL to use the fifth-order BDF.

info(10) : If the solutions to the system of equations will always be nonnegative, it may help to set this parameter. However, it is probably best to try the code without using this option first, and only to use this option if that doesn't work very well. If it is set to 0 then the code will solve the problem without invoking any special nonnegativity constraints. Otherwise, set info(10) = 1.

info(11) : If the initial values of y, y', and t are consistent (i.e., $F(t, y, y') = 0$), then set info(11) = 0. If not, set info(11) = 1 and set yprime(*) as an initial approximation of y.

info(12) - info(15) : Not used, but info(*) must be dimensioned to 15 anyway.

rtol and atol (input) : These are the relative and absolute error tolerances for the problem, respectively. These can be either scalars or arrays (see also the information under info(2)). They control, of course, the local error and not the global error.

rwork(*) (workspace) : This workspace array has the dimension ***lrw***. It probably shouldn't be changed unless one of the info flags that asks to change an ***rwork*** component is set.

lrw (input) : Unless the case of using a banded Jacobian (info(6) = 1), it should be set to $lrw = 40 + 9neq + neq^2$

iwork(*) (workspace) : This workspace array has the dimension ***liw***.

liw (input) : This is the dimension of the iwork array. Set it to $liw = 20 + neq$

rpar(*) and ipar(*) (input, optional) : These arrays are used for communication between the main program and the RES subroutine. These arrays are used for extra parameters in the differential/algebraic system and dimension freely.

JAC (external) : An analytical Jacobian matrix subroutine must be provided whenever possible in the problem. If it is not possible (such as in our case), set

info(5)=0 and treat JAC as a dummy parameter. Otherwise, provide a routine of the form : ***subroutine JAC(t, y, yprime, pd, cj, rpar, ipar)***

to define the matrix of partial derivatives in ***pd***. The components of this subroutine are as follows:

t, y(*), yprime(*) (input) : These are the independent variable, dependent variable, and first derivative respectively. The subroutine JAC shouldn't change these values, just use them to calculate the Jacobian matrix.

pd(*,*)(output) : This is the partial derivative array. It should be dimensioned as pd(neq,neq). In the JAC subroutine pd should be set as:

$$pd(i,j) = \frac{df_i}{dy_j} + c_j \frac{df_i}{dy_j'}$$

The only exception to this is if the banded Jacobian option is used.

cj (input) : This is a scalar that shouldn't be changed. Just use it as indicated above in pd.

rpar(*) and ipar(*)(input) : These are the real and integer parameter arrays that are used for communication between the code and the JAC subroutine.

APPENDIX (E)
IDENTIFIED MODELS

The extraction process was modeled using the Tai Ji identification package. The result of identification is given in three forms which all represent the same open loop transfer function of the process under consideration. The continuous Laplace domain linear model was given in chapter(5). The other two equivalent forms are described below.

E.1 Discrete Transfer Function

In dealing with sampled data systems, the model should be given in a way relevant to the discrete nature of the process. The Discrete transfer function has the general form, $Y(z)=G(z)u(z)$. It related the z-transform of the output variables to that of the input variables. The extractor model will be given as:

$$\begin{pmatrix} x_{out} \\ y_{out} \end{pmatrix} = \begin{pmatrix} \frac{-7.396\times10^{-6}z - 6.36\times10^{-6}}{z^2 - 0.7394z} & \frac{-2.259\times10^{-6}z^{-1}}{z - 0.7189} & \frac{0.1539z^{-4}}{z - 0.7394} & \frac{0.05771z + 0.04663}{z^2 - 0.6528z} & \frac{6.731\times10^{-6}z + 5.278\times10^{-6}}{z^2 - 0.6147z} \\ \frac{5.508\times10^{-5}z^2 - 3.982\times10^{-5}z - 1.817\times10^{-6}}{z^3 - 0.7789z^2 + 0.001475z} & \frac{-3.07\times10^{-5}z^{-1}}{z - 0.2036} & \frac{0.08541z + 0.07275}{z^2 - 0.7254z} & \frac{0.508z + 0.1373}{z^2 - 0.073z} & \frac{1.861\times10^{-6}z^{-1}}{z - 0.7371} \end{pmatrix} \begin{pmatrix} N \\ S_f \\ x_f \\ y_f \\ R_f \end{pmatrix}$$

E.2 Discrete State Space Model

The general form of the discrete state space model is as follows:

$$x_{k+1} = Ax_k + Bu_k$$
$$y_{k+1} = Cx_k + Du_k$$

Matrices A ,B ,C and D for the extraction column are as follows:

$$A=\begin{pmatrix}
-0.30193 & 0 & 0 & 0 & 0 & 0 & 0 & 0 & 0 & 0 & 0 \\
0 & -6.519 & -1.5814 & 0 & 0 & 0 & 0 & 0 & 0 & 0 & 0 \\
0 & 1 & 0 & 0 & 0 & 0 & 0 & 0 & 0 & 0 & 0 \\
0 & 0 & 0 & -0.33009 & 0 & 0 & 0 & 0 & 0 & 0 & 0 \\
0 & 0 & 0 & 0 & -1.5917 & 0 & 0 & 0 & 0 & 0 & 0 \\
0 & 0 & 0 & 0 & 0 & -0.30195 & 0 & 0 & 0 & 0 & 0 \\
0 & 0 & 0 & 0 & 0 & 0 & -0.32102 & 0 & 0 & 0 & 0 \\
0 & 0 & 0 & 0 & 0 & 0 & 0 & -0.42646 & 0 & 0 & 0 \\
0 & 0 & 0 & 0 & 0 & 0 & 0 & 0 & -2.6173 & 0 & 0 \\
0 & 0 & 0 & 0 & 0 & 0 & 0 & 0 & 0 & -0.48657 & 0 \\
0 & 0 & 0 & 0 & 0 & 0 & 0 & 0 & 0 & 0 & -0.30507
\end{pmatrix}$$

$$B=\begin{pmatrix}
0.003906 & 0 & 0 & 0 & 0 \\
0.015625 & 0 & 0 & 0 & 0 \\
0 & 0 & 0 & 0 & 0 \\
0 & 0.001953 & 0 & 0 & 0 \\
0 & 0.007813 & 0 & 0 & 0 \\
0 & 0 & 0.5 & 0 & 0 \\
0 & 0 & 0.5 & 0 & 0 \\
0 & 0 & 0 & 0.5 & 0 \\
0 & 0 & 0 & 1 & 0 \\
0 & 0 & 0 & 0 & 0.003906 \\
0 & 0 & 0 & 0 & 0.001953
\end{pmatrix}$$

$$C=\begin{pmatrix}
-0.0040798 & 0 & 0 & -0.0013581 & 0 & 0.35671 & 0 & 0.25633 & 0 & 0.00327 & 0 \\
0 & 0.022445 & 0.005249 & 0 & -0.0078536 & 0 & 0.36981 & 0 & 1.8219 & 0 & 0.0011054
\end{pmatrix}$$

$$D=\begin{pmatrix}
0 & 0 & 0 & 0 & 0 \\
0 & 0 & 0 & 0 & 0
\end{pmatrix}$$

APPENDIX (F)

PID Controller Tuning Algorithms

F.1 PID Controller Algorithm

Conventional controllers are PID controllers, and depending on the manufacturer, one of the following three PID algorithms are used:

The ideal algorithm:
$$CO = K_C\left(E + \frac{1}{\tau_I}\int_0^t E.dt + \tau_D\frac{dE}{dt}\right) \quad \text{(F.1)}$$

The independent gain algorithm:
$$CO = K_{CP}.E + K_{CI}\int_0^t E.dt + K_{CD}\frac{dE}{dt} \quad \text{(F.2)}$$

The interacting algorithm:
$$CO = K_C\left(E + \frac{1}{\tau_I}\int_0^t E.dt\right)\left(1 + \tau_D\frac{dE}{dt}\right) \quad \text{(F.3)}$$

where :

CO = Controller Output,
K_{CP} = Proportional Constant,
K_{CI} = Integral Constant,
K_{CD} = Differential Constant,
K_C = Controller Gain,
τ_I = Reset Time,
τ_D = Rate Time,
and the error is defined as:
E = (Process Variable – Set Point)

The ideal algorithm is the most widely used one, and it is adopted in this study. The primary benefit from the integral term is the reduction of steady state error while the differential term helps improve the responsiveness and stability. Also notice that, the proportional term always produces the same output with the same given error, while the integral term always accumulates and the differential term produces an output only when there is a change.

The use of PID controller needs the evaluation of its terms namely K_C , τ_I, τ_D. The procedure for this is called controller tuning. The following is a brief description of the tuning methods used in this study.

F.1.2 Ziegler Nichols Methods :

These methods are based on empirical observations of PID tuning strtigies.They obtaining a closed-loop response of ¼ decay ratio (ζ=0.2) and 50% overshoot for a setpoint change. The method is either performed in an open-loop or in a closed-loop manner.

F.1.2.1 ZN Open Loop Reaction Rate Tuning Method

It was originally proposed in 1942 by John G. Ziegler and Nathaniel B. Nichols, and remains popular today because of its simplicity and its applicability to any process governed by a model. In order to begin tuning with this methodology, the process must be at steady-state condition. With the controller in manual (operator overwrites the PID controller output), the controller output is changed by a small amount and the process is monitored. From the process reaction curve, the following measurements are made:

$$K = \text{Effective process gain} = \frac{\text{ultimate value of output}}{\text{magnitude of the step change}} \qquad \text{(F.4)}$$

$$\tau = \text{Effective time constant} = \frac{\text{ultimate value of output}}{\text{slope of tangent at inflexion point}} \qquad \text{(F.5)}$$

θ = Effective time delay.

Then the PID constants are calculated as shown in Table F.1.

F.1.2.2 ZN Closed Loop Tuning Method

This version of the ZN method is based on the determination of response stability margins. Its is some times called the ultimate sensitivity method. In this methodology, the controller is placed into automatic with low gain, no integral or derivative term. Thereafter the gain is increased gradually, making small changes in the set point, until oscillations start. Then the gain is adjusted to make the oscillations continue with constant amplitude. The gain (Ultimate Gain, K_u) and Period (Ultimate Period, P_u) are noted. The K_u and P_u are properties of the system in which the oscillations continue with constant amplitude. Then the PID constants are calculated using Table F.1. Some of the disadvantages of the ZN methods are

- The closed loop system obtained is too oscillatory for ζ=0.2.
- It gives too large overshoot.

- Sensitive to process variations.
- Can only be used on a restricted class of processes.

F.1.3 Cohen-Coon Method (CC)

Based on the concept of achieving a quarter decay ratio, Cohen and Coon (1953), developed their rules by modifying the classical ZN settings. This method has the same limitations of the ZN method ;

- These rules are applicable for the limited range of $0.1 < \theta/\tau < 1.0$.
- Resolution, measurement errors decrease stability margins.
- ¼ decay ratio not conservative standard (too oscillatory).
- Interactions are ignored (decreased stability limits).
- The presence of time delay gives inaccurate results.

Table F.1 gives the values of CC rules.

F.1.4 Modified Z-N settings for PID control

Astrom and Hagglund (1998) modified the conventional ZN method by interpreting the Ziegler-Nichols frequency domain method as finding controller parameters so that the critical point, defined as the point where the Nyquist curve intersects the negative real axis, is moved to the point of -(0.6 + *j*0.28).
The modified Ziegler-Nichols method (MZN) is described briefly as follows. Given a point *A* on the Nyquist curve of the process $g(s)$:

$$A = g(i\omega) = r_a e^{i(-\pi+\varphi_a)} \tag{F.6}$$

find a controller $k(s)$ to compensate for $g(s)$ such that this point is moved to:

$$B = g(i\omega)k(i\omega) = r_b e^{i(-\pi+\varphi_b)} \tag{F.7}$$

The solution to these two equations is:

$$K_c = \frac{r_b \cos(\varphi_b - \varphi_a)}{r_a}$$

$$\omega\tau_D - \frac{1}{\omega\tau_i} = \tan(\varphi_b - \varphi_a) \tag{F.8}$$

Note that the controller gain K_c is uniquely given , but τ_i and τ_D are not. An additional condition must thus be introduced to determine these two latter parameters uniquely. A common method is to specify a relation between τ_i and τ_D as $\tau_D = \alpha\tau_i$ where α is recommended to be equal to 0.25. Another method (Zhuang and Atherton 1993) which can generally yield better performance is to specify α as given below by:

$$\alpha = \frac{0.413}{3.302\kappa + 1} \qquad \text{(F.9)}$$

where κ is the process-normalized gain defined as: $\kappa = \left| \frac{g(0)}{g(i\omega_c)} \right|$

It is important for one to know where to move the critical point for best performance of this method with the help of some knowledge of the process.

Table (F.1) direct PID controller tuning rules.

Tuning Method	K_C	τ_I	τ_D
ZN (*Reaction Curve*)	$\frac{1.2}{K}\left(\frac{\tau}{\theta}\right)$	2.0θ	0.5θ
ZN (*Closed loop*)	$0.6K_u$	$P_u/2$	$P_u/8$
Cohen-Coon	$\frac{1}{K}\left(\frac{4\tau}{3\theta}+\frac{1}{4}\right)$	$\frac{\theta\left[32+6(\theta/\tau)\right]}{13+8(\theta/\tau)}$	$\theta\left(\frac{4}{11+2(\theta/\tau)}\right)$
Modified ZN	$K_c = \frac{r_b\cos(\varphi_b-\varphi_a)}{r_a}$	$\frac{\tan(\varphi_b-\varphi_a)+\sqrt{\tan^2(\varphi_b-\varphi_a)+4\alpha}}{2\omega\alpha}$	$\alpha\tau_i$

F.1.5 Gain and Phase Margin Assignment

Gain and phase margin are important measures of system robustness. They are related to damping of the system and can therefore serve as performance measure.

Ogata (1990) and Franklin et al (1986) have designed controllers based on gain margin and phase margin criteria. Their calculation procedure was a graphical trial and error using bode plots.

Ho et al. (1995) have introduced some approximations in the previous calculations so that more straight-foreword calculations can be performed.

For a process and controller transfer functions : $G_p(s)$ and $G_c(s)$ the specified gain and phase margins A_m and ϕ_m are defined as:

$$A_m = \frac{1}{\left|G_c(i\omega_p)G_p(i\omega_p)\right|} \tag{F.10}$$

$$\phi_m = arg\left[G_c(i\omega_g)G_p(i\omega_g)\right] + \pi \tag{F.11}$$

where ω_p is the phase crossover frequency and ω_g is the gain crossover frequency.

The above equations can be solved for a given second order process with dead time(K, τ, τ', θ) and specifications (A_m and ϕ_m) to calculate controller parameters (K_c, τ_I, τ_D) and crossover frequencies (ω_g, ω_p) with some approximation to yield :

$$K_c = \frac{\omega_p \tau}{A_m K} \tag{F.12}$$

$$\tau_I = \left(2\omega_p - \frac{4\omega_p^2\theta}{\pi} + \frac{1}{\tau}\right)^{-1} \tag{F.13}$$

$$\tau_D = \tau'$$

where ω_p is given by: $\dfrac{A_m\phi_m + \frac{1}{2}\pi A_m(A_m - 1)}{(A_m^2 - 1)\theta}$

F.1.6 Chien, Hrones, and Reswick (CHR) method

This method was based on the dynamic behaviour of a multi-capacity passive system compared to that of a single-capacity system of appropriate time constant with a finite time delay. The authors; Chien, Hrones, and Reswick (1952) indicated that the later system reproduced the dynamic behaviour of the multi-capacity system and they characterised this system by a single parameter they called "*the lag-delay ratio*

$r = \tau / \theta$". An analogue computer was used to fit the data. For a PID controller, two sets of controller tuning parameters where calculated, one based on the quickest response without overshoot and the second based on the quickest response with 20% overshoot. The tuning rules for these two cases are shown in table(F.4) for both cases of *servo* and *regulatory* control.

Table(F.2) PID controller parameters for the CHR tuning method.

PID Controller tuning parameters	Fastest response with 0% overshoot		Fastest response with 20% overshoot	
	Set point	Load	Set point	Load
K_c	$0.6\frac{r}{K}$	$0.95\frac{r}{K}$	$0.95\frac{r}{K}$	$1.2\frac{r}{K}$
τ_I	$1.667\theta K$	$2.5\frac{\theta K}{r}$	$1.429\theta K$	$1.667\frac{\theta K}{r}$
τ_D	$0.3\frac{\theta r}{K}$	$0.4\frac{\theta r}{K}$	$0.45\frac{\theta r}{K}$	$0.5\frac{\theta r}{K}$

F.1.7 Optimum Tuning Methods

In order to tune a PID controller, the criteria that "the constants are defined at their best". This is accomplished by defining a cost function, mainly derived on how the controller reacts to a given disturbance. Given that we want to optimise the controller so that the process variable stays around the set point as a "time integral" performance criteria can be used. The tuning process usually involves minimizing a function of $\varepsilon(t) = y_{set} - y$. This method depends on the form of integral function used. In general the optimisation cost function is written as:

$$J_n(\theta) = \int_0^\infty t^n e(\theta, t)^2 .dt \qquad \text{(F.14)}$$

Table F.3 gives some of these methods with the corresponding value of constant n in the objective function.

Table F.3 optimum tuning methods

Method	(n) in Equ.(F.4)
ISE: Integral of error squared	0
ITSE: Integral of time multiplied by error squared	1
ISTSE : Integral of time squared multiplied by error squared	2

F.2 Model Based Control:

In the following section the general model based control tuning methods will be discussed, in these methods, the structure of the model of the process is explicitly involved in the controller design in contrast to the previous methods where the model is not part of the design procedure. Two design methods will be considered, the direct synthesis and the Internal Model Control.

F.2.1 Direct Synthesis (Minimal Prototype Design):

The most straightforward design approach of all is to directly solve for the controller given a desired closed-loop transfer function (Ljung and Glad 1994). A typical block diagram for a feedback control system is depicted in Figure (F.1).

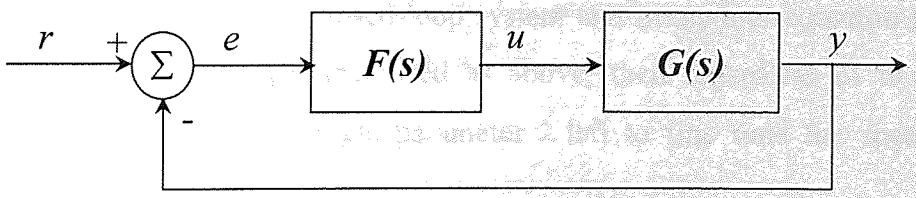

Figure (F.1) Block diagram of linear feedback control system

Based on the block diagram we get

$$G_c(s) = \frac{Y(s)}{R(s)} = \frac{G(s)F(s)}{1+G(s)F(s)} \qquad \text{(F.15)}$$

Then solving for $F(s)$ yields :

$$F(s) = \frac{1}{G(s)} \frac{Y(s)/R(s)}{1-Y(s)/R(s)} \qquad \text{(F.16)}$$

From this it can be observed that if perfect control (infinite gain) is desired, i.e. $Y(s)/R(s) = 1$ it would require $F=\infty$. A common choice of $Y(s)/R(s)$ is:

$$\frac{Y(s)}{R(s)} = H(s) = \frac{1}{\lambda s + 1} \qquad \text{(F.17)}$$

which gives a step response exponentially approaching the set-point. The tuning then consists of selecting an appropriate value of λ. This can be done via trial and error (some rules of thumb can usually be given) or by computer simulation tests on the model before implementing on the real process.

For the case where a dead-time is available in the process model, then the desired closed loop system must involve a dead-time as:

$$\frac{Y(s)}{R(s)} = \frac{e^{-\theta s}}{\lambda s + 1} \qquad \text{(F.18)}$$

However, for a PID controller where a pure derivative action is present, it is impossible to physically realize this controller in practice or it may not be in the PID form and too complicated. This problem can be resolved by using a second order desired closed-loop system. For example

$$\frac{Y(s)}{R(s)} = \frac{1}{(\lambda s + 1)^2} \qquad \text{(F.19)}$$

It can be seen that once a model for the process has been found, all that needs to be done is to decide on a desired closed-loop system and insert into equation (F.15). If the desired closed-loop is parameterised as above, then regardless of the process model order, there is only a single parameter λ left to fine tune the speed of the system.

One drawback of the direct synthesis approach, is that the response may be unnecessarily slow for input disturbances, due to that the controller cancels the plant. The cancellation causes another, more important problem, though. Some processes cannot or should not be inverted. An example of the first category is processes with time delay, where inversion corresponds to predicting the input ahead of time. Example of processes that should not be inverted are ones with a zero in the right-half plane, since this would correspond to introducing an unstable pole in the controller. Even though it would be cancelled in the closed-loop transfer function it leads to an internally unstable process, i.e. infinite control signals would be required.

There is, however, a solution to this problem, and it is to not invert that part of the dynamics. One way to do that is to factorise the plant as $G(s) = G^{+}(s)\, G^{-}(s)$ where $G_{+}(s)$ contains all the non-invertible dynamics (and has $G^{+}(0) = 1$). Then $G^{+}(s)$ is retained in the desired closed-loop system, i.e.

$$\frac{Y(s)}{R(s)} = G^{+}(s)\, H(s) \qquad \text{(F.20)}$$

where $H(s)$ is the desired closed loop system. After insertion into (F.15) results in the controller

$$F(s) = \frac{1}{G(s)} \frac{G^{+}(s)\, H(s)}{1 - G^{+}(s)\, H(s)} = \frac{1}{G^{-}(s)} \frac{H(s)}{1 - G^{+}(s)\, H(s)} \qquad \text{(F.21)}$$

F.2.2 Internal Model Control (IMC):

The direct synthesis approach suffers from the following limitations:

- The resulting controller may be physically realizable.
- If there are RHP zeros in the process, the resulting controller will be unstable.
- Unmeasured disturbances and modeling errors are not considered.

The IMC approach was first developed by Garcia and Morari (1982), in order to overcome the previously mentioned difficulties. This method is more robust and it gives the control engineer a different perspective on the control design problem. IMC is based on the block diagram shown in Figure F.2 (everything within dashed lines belongs to the controller):

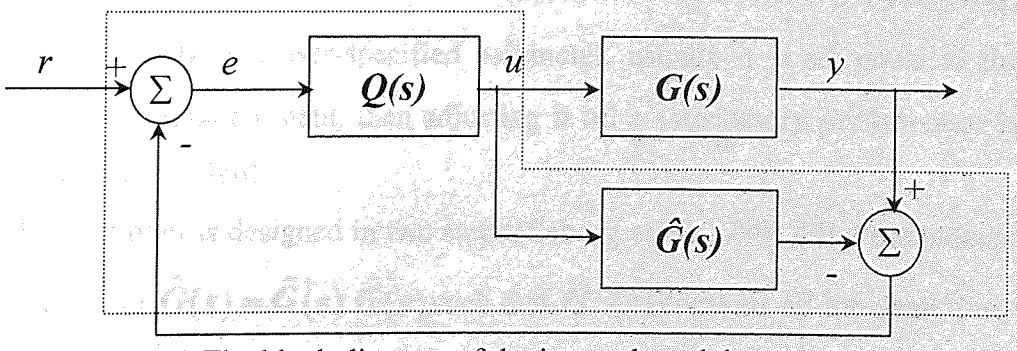

Figure F.2 The block diagram of the internal model control.

The $G(s)$ represents the true process and $\hat{G}(s)$ represents the plant model. The term (internal model) comes from the fact that the controller contains a model of the plant $\hat{G}(s)$. The controller design is then to choose the transfer function $Q(s)$.

Using block diagram algebra on Figure F.2 we can put:

$$U(s)=\frac{Q(s)}{1-Q(s)\hat{G}(s)}\big(R(s)-Y(s)\big) \tag{F.22}$$

Hence, if this is compared with $U(s)$ from Figure F.1 which is expressed as: $U(s)=F(s)\big(R(s)-Y(s)\big)$, it follows that the IMC obviously corresponds to:

$$F(s)=\frac{Q(s)}{1-Q(s)\hat{G}(s)} \tag{F.23}$$

From this argument it is clear that any conventional controller can be reformulated to IMC and vice versa.

For a perfect model (i.e. $\hat{G}(s)=G(s)$) and no disturbances, the signal in the feedback path is zero. Hence the closed-loop system is simply found as:

$$Y(s)=G(s)Q(s)R(s) \tag{F.24}$$

If we use $H(s)=G(s)Q(s)$ then it follows that $Q(s)$ should be selected as:

$$Q(s)=\frac{1}{\hat{G}(s)}H(s) \tag{F.25}$$

Where the filter has a transfer function of the form:

$$H(s)=\frac{1}{\left(\tau_f s+1\right)^n} \tag{F.26}$$

For most chemical processes, it is found that a first order filter i.e, n=1 is satisfactory. Filter time constant, τ_f, is a user-specified parameter, usually it is set equal to the open-loop dominant time constant, then adjusting it till a satisfactory performance is obtained (Rivera *et al.* 1986).

The IMC controller is designed in two steps (Seborg et al. 1989). First the process model is factored as $\hat{G}(s)=\hat{G}^{+}(s)\,\hat{G}^{-}(s)$ such that $\hat{G}^{+}(s)$ contains all the dead times and right half plane zeros; consequently $\hat{G}^{-}(s)$ is stable. Then the IMC controller is defined as:

$$Q(s) = \frac{1}{\hat{G}(s)} H(s) \qquad \text{(F.27)}$$

The relationship between the feedback controller Figure F.2 and IMC controller Figure F.1 is:

$$F(s) = \frac{Q(s)}{1 - Q(s)G(s)} \qquad \text{(F.28)}$$

PID controller settings for some process models are reported by Lung Chien. (1988), Table F.4 lists the PID controller design parameters for the control loops under consideration.

Table (F.4) IMC-PID tuning rules (Lung Chien, 1988)

Parameter	**1st order model with delay**	**2nd order model with delay**
K_C	$\frac{1}{k}\frac{\tau + 0.5\theta}{\tau_f + 0.5\theta}$	$\frac{1}{k}\frac{\tau_1 + \tau_2}{\tau_f + \theta}$
τ_I	$\tau + 0.5\theta$	$\tau_1 + \tau_2$
τ_D	$\frac{\tau\theta}{2\tau + \theta}$	$\frac{\tau_1\tau_2}{\tau_1 + \tau_2}$

SIMULINK closed loop control system simulation diagrams

The previously mentioned controller tuning algorithms, were simulated using the SIMULINK block diagram simulation program running under MATLAB package. The single and multi-loop diagrams for both conventional PID and IMC controllers are shown in the figures (F3-F6) shown below.

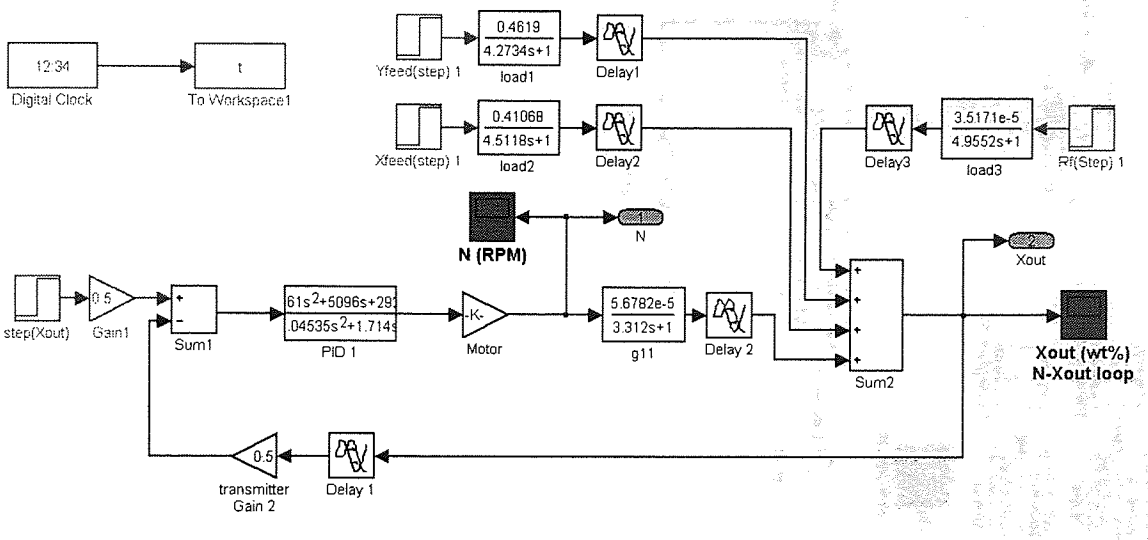

Figure(F.3) IMC SIMULINK single loop simulation flow diagram.

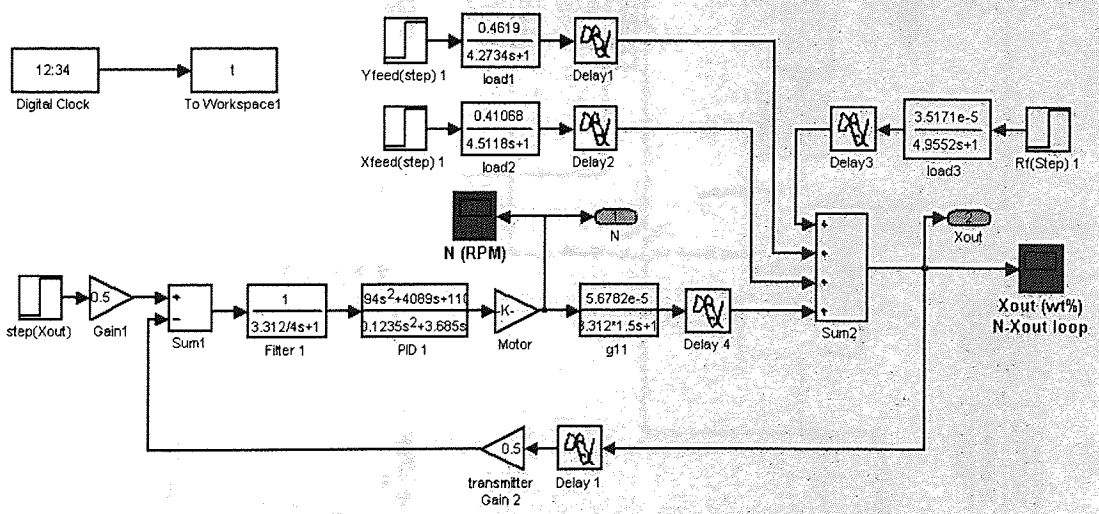

Figure(F.4) IMC SIMULINK single loop simulation flow diagram.

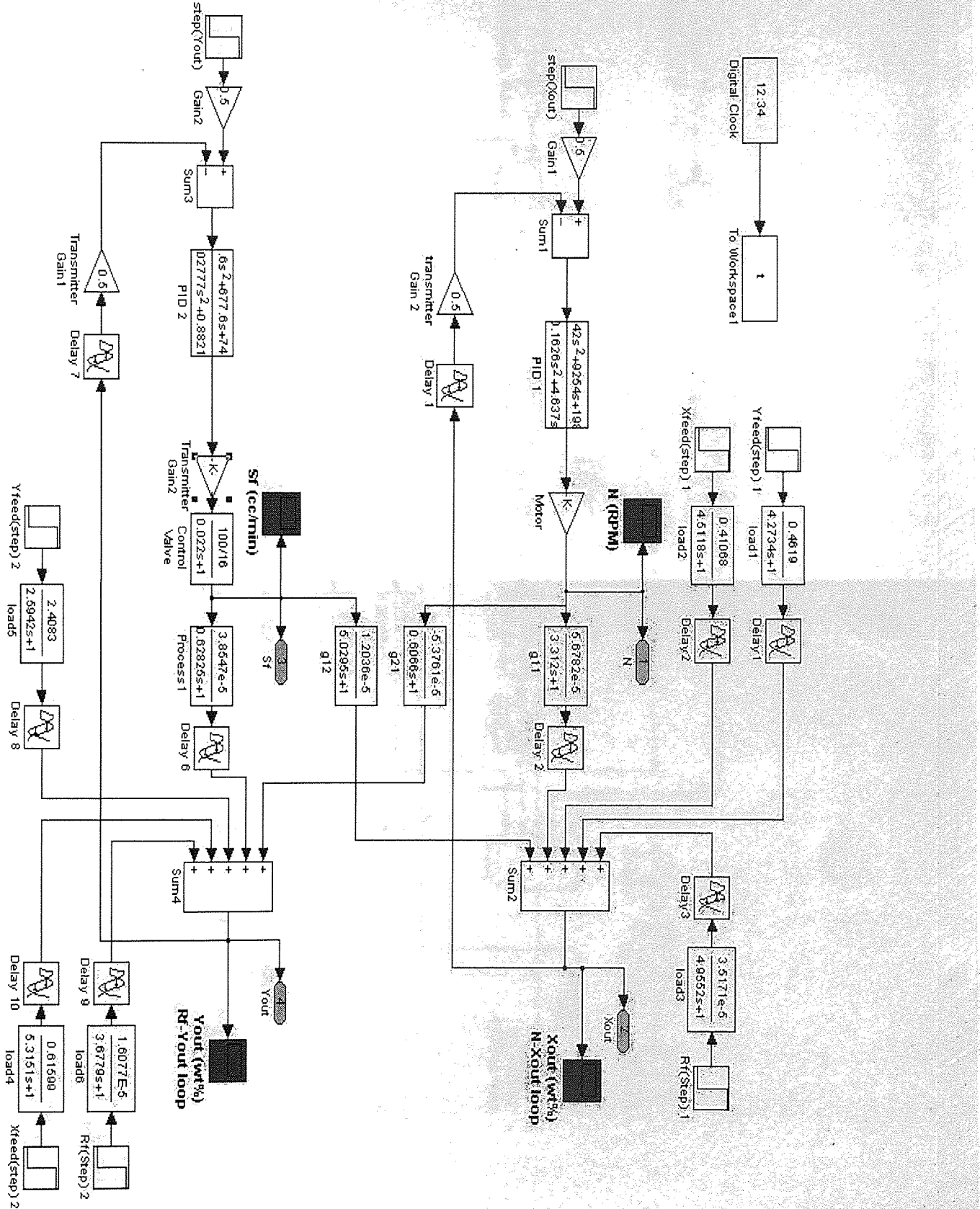

Figure(F.5) SIMULINK Multi-loop simulation flow diagram of the extraction process using conventional PID controllers.

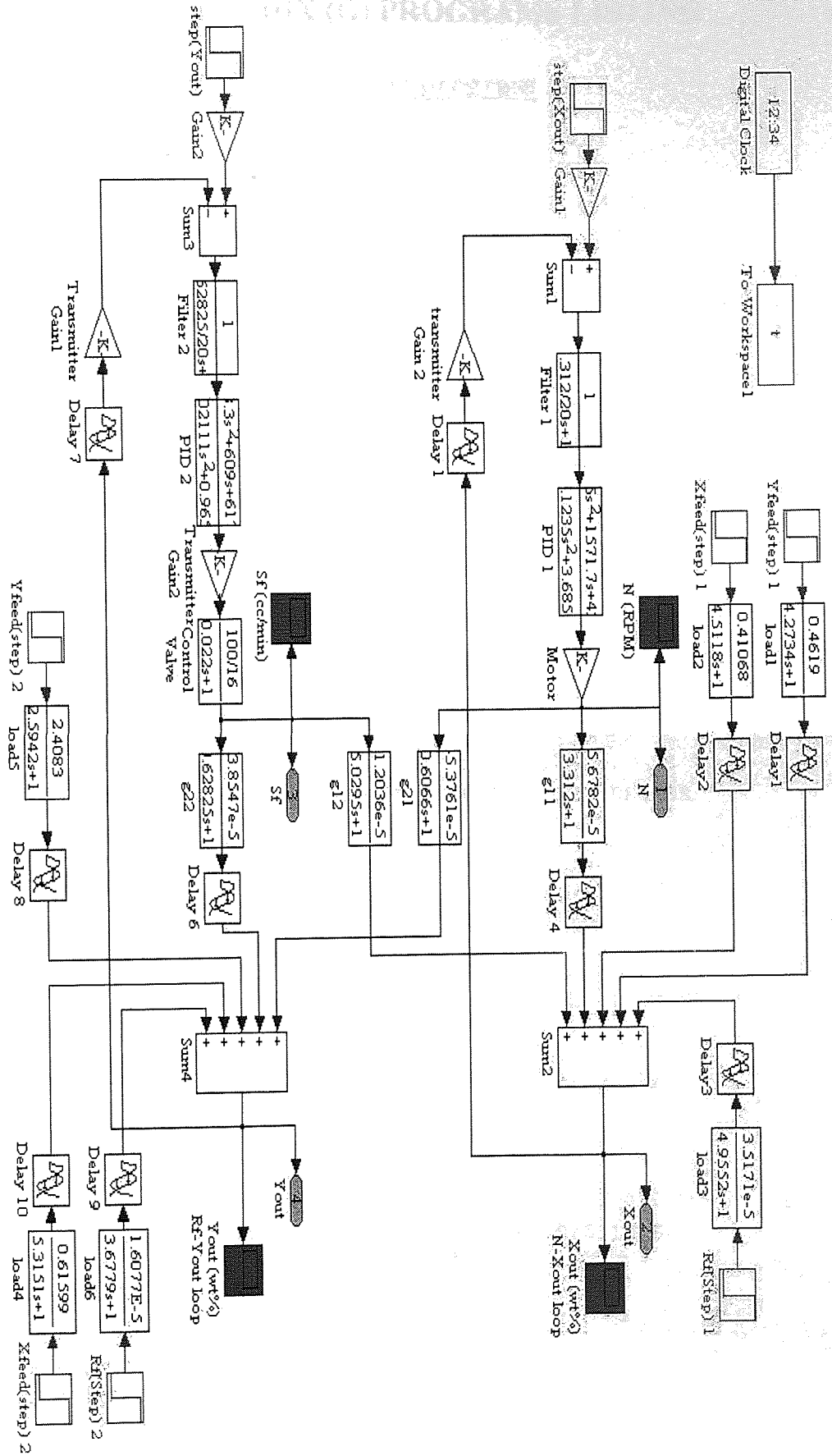

Figure(F.6) SIMULINK Multi-loop simulation flow diagram of the extraction process using IMC controller.

APPENDIX (G) PROGRAMS LISTING

G.1 Nyquis Stability Criterion test program

```
      USE MSIMSL
      REAL KP(4,4),KC(4)
      DIMENSION RESET(4),DERACT(4),TAU(4,4,4),D(4,4)
      COMPLEX GM(4,4),B(4,4),Q(4,4),YID(4,4),C(4,4)
      COMPLEX DET,WFUNC
C PROCESS TRANSFER FUNCTION DATA :
      DATA KP(1,1),KP(1,2),KP(2,1),KP(2,2)/-5.4782e-5,-0.8036e-5,
     &                                      8.2015e-4,-3.047 e-3/
      DATA
      TAU(1,1,1),TAU(1,1,2),TAU(1,2,1),TAU(1,2,2)/0.,0.,0.252,0.0/
      DATA TAU(2,1,1),TAU(2,1,2),TAU(2,2,1),TAU(2,2,2)
     &                                      /3.112, 5.0295,
     &                                       6.2667,0.62825/
      DATA D(1,1),D(1,2),D(2,1),D(2,2)/0.5,1.,
     &                                 0.5,1./
C CONTROLLER TRANSFER FUNCTION DATA:
C     DATA KC(1),KC(2)/2148.,1082./
C     DATA RESET(1),RESET(2)/3.77,1.027/
C     DATA DERACT(1),DERACT(2)/0.3304,0.2465/

      DO 1 I=1,2
      DO 1 J=1,2
      TAU(3,I,J)=0.0
      TAU(4,I,J)=0.0
   1  CONTINUE
C SET INITIAL FREQUENCY AND NUMBER OF POINTS PER DECADE
      W=0.001
      DW=(10.)**(1./1000.)
      N=2
      OPEN(1,FILE='D:\NYQ.DAT',STATUS='UNKNOWN')
C MAIN LOOP FOR EACH FREQUENCY
      WRITE(6,10)
      WRITE(1,10)
  10  FORMAT(' FREQ    REAL    IMAG    DB      DEG')
 100  CALL PROCESS(GM,W,N,KP,TAU,D)
      CALL CONTROL(B,W,N,KC,RESET,DERACT)
      CALL MCRCR (N, N, GM, N, N, N, B,N, N, N, Q, N)
      CALL IDENTITY(YID,N)
      CALL MATADD(YID,Q,C,N)
      DET=C(1,1)*C(2,2)-C(1,2)*C(2,1)
      DB=20.*ALOG10(CABS(DET))
      WFUNC=DET-1.
      DEG=ATAN(AIMAG(WFUNC)/REAL(WFUNC))*180.0/3.1416
      IF(REAL(WFUNC).LT.0.0)DEG=DEG-180.
      WRITE(6,2)W,WFUNC,DB,DEG
      WRITE(1,2)W,WFUNC,DB,DEG
   2  FORMAT(1X,5F15.5)
      W=W*DW
C STOP IF FREQUENCY IS GREATER THAN 10
      IF(W.LT.10.0)GO TO 100
      CLOSE(1)
      STOP
      END
      SUBROUTINE CONTROL(B,W,N,KC,RESET,DERACT)
      DIMENSION KC(4),RESET(4),DERACT(4)
```

```
      COMPLEX B(4,4),ZINT,ZL
      REAL KC
      ZINT(X)=CMPLX(0.,W*X)
      ZL(X)=CMPLX(1.,X*W)
      DO 10 I=1,N
        DO 10 J=1,N
        B(I,J)=CMPLX(0.,0.)
        IF(I.EQ.J) THEN
        B(I,J)=CMPLX(KC(I),0.)*ZL(RESET(I))/ZINT(RESET(I))*
     &     ZL(DERACT(I))/ZL(0.05*DERACT(I))
        ENDIF
  10  CONTINUE
      RETURN
      END
      SUBROUTINE PROCESS(GM,W,N,KP,TAU,D)
      DIMENSION KP(4,4),TAU(4,4,4),D(4,4)
      COMPLEX GM(4,4),ZL,ZD
      REAL KP
      ZL(X)=CMPLX(1.,X*W)
      ZD(X)=CMPLX(COS(W*X),-SIN(W*X))
      DO 10 I=1,N
      DO 10 J=1,N
10    GM(I,J)=KP(I,J)*ZD(D(I,J))*ZL(TAU(1,I,J))/ZL(TAU(2,I,J))
     + /ZL(TAU(3,I,J))/ZL(TAU(4,I,J))
      RETURN
      END
c-----------------------------------------------------------------------
c     Matrix Addition: C  =  A  +  B
      SUBROUTINE MATADD(A,B,C,N)
      COMPLEX A(4,4),B(4,4),C(4,4)
      DO 10 I=1,N
      DO 10 J=1,N
   10 C(I,J)=A(I,J)+B(I,J)
      RETURN
      END
c     Form the Identity Matrix  I
      SUBROUTINE IDENTITY(B,N)
      COMPLEX B(4,4)
      DO 20 I=1,N
      DO 10 J=1,N
      B(I,J)=CMPLX(0.0,0.0)
      IF(I.EQ.J) B(I,J)=CMPLX(1.,0.0)
      10 CONTINUE
      20 CONTINUE
      RETURN
      END
```

G.2 Doyle-Stien Robustness test program

```
      USE MSIMSL
      REAL KP(4,4),KC(4)
      DIMENSION RESET(4),DERACT(4),TAU(4,4,4),D(4,4),
     &          WK(4),WKEIG(12),SVAL(4)
      COMPLEX GM(4,4),B(4,4),Q(4,4),QIN(4,4),YID(4,4)
      COMPLEX A(4,4),ASTAR(4,4),H(4,4),CEIGEN(4),WA(24),VECT(4,4)

C PROCESS TRANSFER FUNCTION DATA :
```

```
      DATA KP(1,1),KP(1,2),KP(2,1),KP(2,2)/-5.4782e-5,-0.8036e-5,
     &                                      8.2015e-4,-3.047e-3/
      DATA
      TAU(1,1,1),TAU(1,1,2),TAU(1,2,1),TAU(1,2,2)/0.,0.,0.252,0.0/
      DATA TAU(2,1,1),TAU(2,1,2),TAU(2,2,1),TAU(2,2,2)
     &                                      /3.112, 5.0295,
     &                                       6.2667,0.62825/
      DATA D(1,1),D(1,2),D(2,1),D(2,2)/0.5,1.,
     &                                 0.5,1./
C CONTROLLER TRANSFER FUNCTION DATA:
C     DATA KC(1),KC(2)/2148.,1082./
C     DATA RESET(1),RESET(2)/3.77,1.027/
C     DATA DERACT(1),DERACT(2)/0.3304,0.2465/

      OPEN(9,FILE='D:\NYQ-ROBUST\ROB.DAT',STATUS='UNKNOWN')
      DO 1 I=1,2
      DO 1 J=1,2
      TAU(3,I,J)=0.0
      TAU(4,I,J)=0.0
    1 CONTINUE

C SET INITIAL FREQUENCY AND NUMBER OF POINTS PER DECADE
      W=0.1
      DW=(10.)**(1./200.)
      N=2
      WRITE(6,10)
      WRITE(9,10)
   10 FORMAT(' FREQUENCY    SINGULAR VALUES')
      IA=4
      M=N
C MAIN LOOP FOR EACH FREQUENCY
  100 CALL PROCESS(GM,W,N,KP,TAU,D)
      CALL CONTROL(B,W,N,KC,RESET,DERACT)
      CALL MCRCR (N, N, GM, IA, M, M, B,IA, N, N, Q, IA)

      CALL IDENT(QIN,N)
      CALL LINCG (N, Q, IA, QIN, IA)

      CALL IDENT(YID,N)
      CALL MADD(YID,QIN,A,N)

      CALL CONJT(A,ASTAR,N)
      CALL MCRCR (N, N, ASTAR, IA, N, N, A,IA, N, N, H, IA)
      CALL EVLCG (N, H, IA, CEIGEN)

      DO 6 I=1,N
    6 SVAL(I)=SQRT(REAL(CEIGEN(I)))
      WRITE(6,7) W,(20.*ALOG10(SVAL(I)),I=1,N)
      WRITE(9,7) W,(20.*ALOG10(SVAL(I)),I=1,N)
    7 FORMAT(1X,4F15.5)
      W=W*DW
C STOP IF FREQUENCY IS GREATER THAN 10
      IF(W.LT.10.)GO TO 100
      CLOSE(9)
      STOP
      END
      SUBROUTINE CONTROL(B,W,N,KC,RESET,DERACT)
      DIMENSION KC(4),RESET(4),DERACT(4)
      COMPLEX B(4,4),ZINT,ZL
      REAL KC
      ZINT(X)=CMPLX(0.,W*X)
```

```
      ZL(X)=CMPLX(1.,X*W)
      DO 10 I=1,N
        DO 10 J=1,N
        B(I,J)=CMPLX(0.,0.)
        IF(I.EQ.J) THEN
        B(I,J)=CMPLX(KC(I),0.)*ZL(RESET(I))/ZINT(RESET(I))*
     &          ZL(DERACT(I))/ZL(0.05*DERACT(I))
        ENDIF
  10  CONTINUE
      RETURN
      END
      SUBROUTINE PROCESS(GM,W,N,KP,TAU,D)
      DIMENSION KP(4,4),TAU(4,4,4),D(4,4)
      COMPLEX GM(4,4),ZL,ZD
      REAL KP
      ZL(X)=CMPLX(1.,X*W)
      ZD(X)=CMPLX(COS(W*X),-SIN(W*X))
      DO 10 I=1,N
      DO 10 J=1,N
10    GM(I,J)=KP(I,J)*ZD(D(I,J))*ZL(TAU(1,I,J))/ZL(TAU(2,I,J))
     + /ZL(TAU(3,I,J))/ZL(TAU(4,I,J))
      RETURN
      END
c-----------------------------------------------------------------------
c     Matrix Addition
      SUBROUTINE MADD(A,B,C,N)
      COMPLEX A(4,4),B(4,4),C(4,4)
      DO 10 I=1,N
      DO 10 J=1,N
   10 C(I,J)=A(I,J)+B(I,J)
      RETURN
      END
c     Form the Identity Matrix
      SUBROUTINE IDENT(B,N)
      COMPLEX B(4,4)
      DO 20 I=1,N
      DO 10 J=1,N
      B(I,J)=CMPLX(0.0,0.0)
      IF(I.EQ.J) B(I,J)=CMPLX(1.,0.0)
      10 CONTINUE
      20 CONTINUE
      RETURN
      END
c      Form Conjugate Transpose
      SUBROUTINE CONJT(A,B,N)
      COMPLEX A(4,4),B(4,4)
      DO 10 I=1,N
      DO 10 J=1,N
      B(I,J)=A(J,I)
      Z=AIMAG(B(I,J))
  10  B(I,J)=CMPLX(REAL(B(I,J)),-Z)
      RETURN
      END
```

G.3 Plant & Disturbance condition number program (MATLAB m-file)

```
w=logspace(-2,0,100);
s=i*w;
```

```
g11 = tf([-5.4782e-5],[3.312 1]);
g21 = tf([3.5071E-004 8.2015E-005],[1 6.519 1.5814]);
g12= tf([-0.8036E-005],[5.0295  1]);
g22 = tf([-3.047e-5],[0.62825 1]);

d11 = tf([0.5907],[3.312 1]);
d12 = tf([0.3005 ],[2.3449 1]);
d13 = tf([3.117e-5],[2.0552 1]);
d21 = tf([0.57599],[3.015  1]);
d22 = tf([0.69612],[0.38208 1]);
d23 = tf([0.7077e-5],[3.2779 1]);

Gp=[freqresp(g11,s) freqresp(g12,s);freqresp(g21,s) freqresp(g22,s)]
Gd=[freqresp(d11,s) freqresp(d12,s) freqresp(d13,s);freqresp(d21,s)
freqresp(d22,s) freqresp(d23,s)]
G=[g11 g12;g21 g22]
for i=1:100
nor(i)=norm(inv(Gp(:,:,i))*Gd(:,3,i),inf)
Condit(i)=Cond((Gp(:,:,i)))
DistCond1(i)=(norm(inv(Gp(:,:,i))*Gd(:,1,i),2)/norm(Gd(:,1,i),2))*norm
(Gp(:,:,i))
DistCond2(i)=(norm(inv(Gp(:,:,i))*Gd(:,2,i),2)/norm(Gd(:,2,i),2))*norm
(Gp(:,:,i))
DistCond3(i)=(norm(inv(Gp(:,:,i))*Gd(:,3,i),2)/norm(Gd(:,3,i),2))*norm
(Gp(:,:,i))

all = [w', Condit', DistCond1', DistCond2' ,DistCond3', nor']';
fid = fopen('d:\mine\Final\id\Analysis.txt','w');
fprintf(fid,'    w      Condition     DistCond1     DistCond2
DistCond3    Norm\n')
fprintf(fid,'%10.5f %12.8f %12.8f %12.8f %12.8f %12.8f\n',all);
fclose(fid);

semilogx(w,Condit,w,DistCond1,w,DistCond2,w,DistCond3)
semilogx(w,nor)
end;
```

G.4 Loops Interaction Analysis program (MATLAB m-file)

```
g11=-5.4782e-5; g12=-0.8036E-005;   g21=8.2015E-005; g22=-3.047e-5;
L=1/(1-(g12*g21/(g11*g22)));
w=logspace(-3,1,100);
s=i*w;
p11 = -5.4782e-5./(3.112*s+1);
p21 = (3.5071E-004*s+8.2015E-005)./(s.^2+6.519*s+ 1.5814);
p12= -0.8036E-005./(5.0295*s+ 1);
p22 = -3.047e-5./(0.62825*s+1);
L12=-p12.*p21./(p11.*p22-p12.*p21);
RGA=[L L-1; L-1 L];
lam12=sign(real(L12)).*abs(L12);
lam11=1-lam12;
for i=1:length(p11)
detG(i)=rank([p11(i) p12(i);p21(i) p22(i)])
end
semilogx(w,lam11,'-k',w,lam12,':k')
xlabel('Frequency rad/min')
ylabel('lam,1-lam')
text(0.1,17.5,'lam')
text(0.1,-14,'1-lam')
G=[p11 p12;p21 p22]
```

```
GG=[g11 g12;g21 g22];
all = [w', lam11', lam12']'
fid = fopen('d:\RGA.txt','w');
fprintf(fid,'    w      lamda1    lamda2\n')
fprintf(fid,'%10.5f %12.8f %12.8f \n',all);
fclose(fid);
[U S V]=svd(G);
Niederlinski=(det(GG)./(g12*g21));
H=[0 g12/g11; g21/g22 0];
Eigen=eig(H);
```

G.5 MATLAB m-file for the MPC control of the extraction system

```
clear
delt =0.05;          %sampling period.
ny = 2;              % no of output variables.
tend=25;             % time period for simulation.

% Set up the model and calculate its step response.
g11 = poly2tfd(-5.4782e-5, [3.112  1],0,0.5);
g21 = poly2tfd([3.5071e-4 8.2015e-5],[1.582 6.5191 1],0,0.5);
g12 = poly2tfd(-0.8036e-5, [5.0295  1],0,1);
g22 = poly2tfd(-3.047e-5, [0.6281 1],0,1);

% Defines the effect of u inputs
umod = tfd2mod(delt,ny,g11,g21,g12,g22);

g13 = poly2tfd(0.5907,    [3.312 1],0,4);
g23 = poly2tfd(0.576,     [3.015 1],0,0.5);
g14 = poly2tfd(0.3005,    [2.3449 1],0,0.5);
g24 = poly2tfd(0.6961,    [0.3821 1],0,0.5);
g15 = poly2tfd(3.117e-5, [2.0552 1],0,0.5);
g25 = poly2tfd(0.7077e-5,[3.2779 1],0,1.0);
% Defines the effect of d input
dmod = tfd2mod(delt,ny,g13,g23,g14,g24,g15,g25);
% Combines the two models.
pmod = addmd(umod,dmod);
% assume perfect modeling
imod = pmod;
% default (unity) weights on both outputs.
ywt = [ ];
% weights on both inputs
uwt = [0.001  0.005];
P =50;                    % prediction horizon
M=[2 3 4];                % control horizon
% Calculate the unconstrained controller gain.
Ks = smpccon(imod,ywt,uwt,M,P);
r = [0.00 0.002];         % setpoints for the two outputs.
% Simulate the response of the closed loop system with inputs.
[y,u] = smpcsim(pmod,imod,Ks,tend,r);
t=0:delt:tend;
nt=length(t);
ulim = [ ];               % default (no) constraints on u variables.
Kest = [ ];               % default (DMC) state estimator.
z = [0 0];                % default (zero) measurement noise.
v = [0.00 0.00 0];        % step in measured disturbance.
[y,u] = smpcsim(pmod,imod,Ks,tend,r,ulim,Kest,z,v);
% Save and plot results results.
subplot(2,1,1)
plot(t,y(:,1),t,y(:,2));
title('Control variables');
```

```
ylabel('Concentration wt frac.');
h = legend('Xout','Yout',1);
subplot(2,1,2)
stairs(t,u);
text(100,100,'Manipulated variables');
xlabel('Time (min)');
ylabel('RPM and Sf');
h = legend('RPM','Sf',1);
n=length(t);
yyy=[t' u y]
fid=fopen('d:\MPC\MPC_XY.dat','w+');
fprintf(fid,' Time        RPM          Sf        Xout        Yout\n') ;
for j=1:n
    fprintf(fid,'%5.1f  %f %f %f %f\n',yyy(j,:));
   end
```

G.6 MATLAB m-file for the MPC control of the extraction system with input constraints:

```
clear
delt=0.05;          %sampling period.
ny=2;               % no of output variables.
tfinal=100;         % Final simulation time.
tend=75;            % End of simulation time.

% Set up the model and calculate its step response.
g11 = poly2tfd(-5.4782e-5, [3.112  1],0,0.5);
g21 = poly2tfd([3.5071e-4 8.2015e-5],[1.582 6.5191 1],0,0.5);
g12 = poly2tfd(-0.8036e-5, [5.0295  1],0,1);
g22 = poly2tfd(-3.047e-5, [0.6281 1],0,1);
model=tfd2step(tfinal,delt,ny,g11,g21,g12,g22);
plant=model;        % No plant/model mismatch

P=23;               % Prediction horizon.
M=10 ;              % Number of moves (input horizon).
% Input and output weights.
ywt=[10 5];  uwt=[0.0005 0.0005];

% Simulate the closed-loop response for a pulse train of steps in
% the setpoints with input constraints
[rr,tt] = gensig('square',tend/2,tend,delt);    % generate a train of
square pulses signal.
for i=1:(tend/delt)
r1(i,1)=rr(i)*(0.002) ;
r1(i,2)=rr(i)*(-0.002);
end;
o1=tend/delt-7*(tend/delt)/8;
o2=tend/delt-(tend/delt)/8+1;
r(1:o2,1)=r1(1:o2,1);
r(1:o2,2)=r1(o1:(tend/delt),2);
r(o2+1:tend/delt,1)=0.002;
r(o2+1:tend/delt,2)=0.00;

% define input and output constraints.
ulim=[-40 -60 40 60 1 100];
ylim=[];
% Simulate the closed loop with input constraints.
[y,u]=cmpc(plant,model,ywt,uwt,M,P,tend,r,ulim,ylim);
```

```
% Save and plot results results.
plotall(y,u,delt)
subplot(2,1,1)
plot(tt,y(:,1),tt,y(:,2),tt,r(:,1),tt,r(:,2));
title('Control variables');
ylabel('Concentration wt frac');
h = legend('Xout','Yout',1);
subplot(2,1,2)
stairs(tt,u);
text(100,100,'Manipulated variables');
xlabel('Time (min)');
ylabel('RPM and Sf');
h = legend('RPM','Sf',1);
yyy=[tt r u y]
fid=fopen('d:\mine\Final\MPC\MPC_Constraint.dat','w+');
fprintf(fid,' Time     r1        r2     RPM          Sf        Xout
Yout\n') ;
fprintf(fid,'%5.1f  %f %f %f %f %f %f\n',yyy');
fclose(fid);
```

G.7 Dynamic Simulation of the Solvent Extraction Column (FORTRAN version)

```
      USE MSFLIB
      IMPLICIT REAL*8 (A-H,O-Z)
      EXTERNAL RES
      REAL*8 NN,KO ,P(5)
      COMMON /PAR/IODIR,HX(20),HY(20),XC(20),YC(20),R(20),S(20),E(20),A
     +,B,KO(20)
      COMMON /C/NN,A1,A2,A3,A4,A5,DENA,DENW,DENT
      COMMON /CON/NEQ,XF(20),YF(20),RF,SF,V,AREA,VS
      COMMON /DATA1/ XE(20),YE(20)
      COMMON /DES/N
      COMMON /RESULT/ results(1500,14),TSTOP,ITER
      CHARACTER*80 TEXT , NAMEI*50, IODIR*80
C     WORKING DATA PATH
      IODIR="D:\MINE\extraction\winsim\"
      ISIM=1
      LIO=LEN_TRIM(IODIR)
      NAMEI=IODIR(:LIO) // 'PARAM.TXT'
      OPEN(9,FILE=NAMEI,STATUS='OLD')

C     NO OF COLUMN STAGES
      N=9
      N=N+2
      ITER=0

  11  DO WHILE (.NOT. EOF(9))
      READ(9,111)TEXT
      READ(9,*)A,B,FRAC
      READ(9,111)TEXT
C
C     INPUT FEED CONDITIONS :
C     -----------------
C
C     BACKMIXING COEFFICIENTS
C     FLOW RATE UNIT  (L/HR)
C     CONC. UNIT      (MASS FRAC.)
C     ROTOR SPEED     (RPM)
C
      READ(9,*)YF(1),YF(2),SF
      READ(9,111)TEXT
      READ(9,*)XF(1),XF(2),RF
      READ(9,111)TEXT
      READ(9,*)NN
      READ(9,111)TEXT
      DO 10 I=1,N
       XE(I)=XF(2)
       YE(I)=YF(2)
 10   CONTINUE
      FRAC1=FRAC
      FRAC2=FRAC
      FRAC3=FRAC
 111  FORMAT(A)
      P(1)=FRAC1
      P(2)=FRAC2
      P(3)=FRAC3
      P(4)=A
      P(5)=B
      CALL OBJECT (ISIM,P)
```

```
      ISIM=ISIM+1
      END DO
C-----------------------------------------------------------------------
      CLOSE(9)
      CLOSE(11)
      OPEN (UNIT = 10, FILE = 'USER', IOFOCUS = .TRUE.)
      CALL Plot
      PAUSE
      END

      SUBROUTINE OBJECT(ISIM,P)
      USE MSFLIB
      IMPLICIT REAL*8 (A-H,O-Z)
      EXTERNAL RES,PRINTOUT
      PARAMETER (IS=100,LRW=10000,LIW=500)
      REAL*8 Y(IS),YP(IS),RWORK(LRW),P(5),TIME(200)
      DIMENSION  INFO(15), IWORK(LIW)
      REAL*8 NN,KO
      COMMON /OPT/FRAC1,FRAC2,FRAC3
      COMMON /CON/NEQ,XF(20),YF(20),RF,SF,V,AREA,VS
      COMMON /PAR/IODIR,HX(20),HY(20),XC(20),YC(20),R(20),S(20),E(20),A
     +,B,KO(20)
      COMMON /C/NN,A1,A2,A3,A4,A5,DENA,DENW,DENT
      COMMON /CAL/NCALLS
      COMMON /DES/N
      COMMON /RESULT/ results(1500,14),TSTOP,ITER
      CHARACTER*80 IODIR
      DATA TOUT,DTOUT,TPRINT/1.0,1.0,1.0/
      INTEGER(4)  OLDTC
      SF=SF*(1500./60.)
      RF=RF*(1500./60.)
      NN=NN/60.0

   60 FRAC1=P(1)
      FRAC2=P(2)
      FRAC3=P(3)
      A=P(4)
      B=P(5)
      MEQUIL=1
      NC=3
      MODEL=2
      IOUT=6
      LIO=LEN_TRIM(IODIR)
      IF (ISIM.EQ.1) THEN
      CALL INIT(ISIM,Y,YP,N)
      OPEN (8,FILE=IODIR(:LIO)//'OUTPUT',STATUS='UNKNOWN')
      OPEN (11,FILE=IODIR(:LIO)//'TXY.TXT',STATUS='UNKNOWN')
      ELSE
      OPEN (8,FILE=IODIR(:LIO)//'OUTPUT',ACCESS='APPEND',STATUS='OLD')
      OPEN (11,FILE=IODIR(:LIO)//'TXY.TXT',ACCESS='APPEND',STATUS='OLD')
      ENDIF

      NERR = 0
      ITOL = 1
      ATOL=1.0E-6
      RTOL=1.0E-6
      NEQ = 2*N
      NOUT = 25
      TSTOP=NOUT
      RWORK(1)=TSTOP
      DO 115 I = 1,15
```

```
 115  INFO(I) = 0
      INFO (11)=1
      INFO (8 )=1
      INFO (4 )=1
      TO=1.0E-6
      RWORK(3)=TO
      IF (ISIM.EQ.1)T =0.0D0
      KK=1
      CALL FLOW(N,Y,YP)
C      CALL PRINTOUT(T,N)
C     ITER=ITER+1
      TFLAG=TPRINT
      XO=1.0
      XFIN=NOUT

      IF (ISIM.GT.1)GO TO 45
 1    CALL DDASSL(RES,NEQ,T,Y,YP,TOUT,INFO,RTOL,ATOL,IDID,
     &            RWORK,LRW,IWORK,LIW,RPAR,IPAR,JAC)
      HU = RWORK(7)
      NQU = IWORK(8)
      IF (TOUT.GE.TFLAG) THEN
      TIME(KK)=TFLAG
      ITER=ITER+1
      CALL PRINTOUT(T,N)
      TFLAG=TFLAG+TPRINT
      KK=KK+1
      ENDIF
      IF (IDID .LT. 0) GO TO 175
      TOUT = TOUT + DTOUT
      IF (TOUT.LE.TSTOP) GOTO 1
 175  CONTINUE
      IF (IDID .LT. 0) THEN
      PRINT*,' UBNORMAL TERMINATION IDID = ',IDID
      ENDIF
      GO TO 999
C-----------------------------------------------------------------------
C     DISTURBANCE
C-----------------------------------------------------------------------
   45 XO=XFIN+1
      XFIN=ISIM*25
      INFO(11)=1
      NOUT=XFIN
      TSTOP=NOUT
      RWORK(1)=TSTOP
      TFLAG=XO
      GOTO 1
C-----------------------------------------------------------------------
  999 IF(ISIM.EQ.1) CALL STORE(N,Y,YP)
      NST = IWORK(11)
      NFE = IWORK(12)
      NJE = IWORK(13)
      ERO=  IWORK(14)
        OLDTC = SETTEXTCOLORRGB(#00FFFFFF)
      WRITE (6,180) NST,NFE,NJE,ERO
  180 FORMAT(//1X,32H FINAL STATISTICS FOR THIS RUN../
     1  1X,18H NUMBER OF STEPS =,I5/
     2  1X,18H NUMBER OF F-S   =,I5/
     4  1X,18H NUMBER OF J-S   =,I5/
     5  1X,16H ERROR OVERRUN =,E10.2)
       CLOSE (8)
       CLOSE (11)
```

```
      RETURN
      END

      SUBROUTINE INIT (ISIM,Y,YP,N)
      IMPLICIT DOUBLE PRECISION(A-H,O-Z)
      COMMON /OPT/FRAC1,FRAC2,FRAC3
      COMMON /CON/NEQ,XF(20),YF(20),RF,SF,V,AREA,VS
      COMMON /PAR/IODIR,HX(20),HY(20),XC(20),YC(20),R(20),S(20),E(20),A
     +            ,B,KO(20)
      COMMON /C/NN,A1,A2,A3,A4,A5,DENA,DENW,DENT
      COMMON /DATA1/ XE(20),YE(20)
      COMMON /CAL/NCALLS
      COMMON /RESULT/ results(1500,14),TSTOP,ITER

      CHARACTER*80  IODIR
      DIMENSION  Y(1),YP(1) ,X0(20),Y0(20)
      REAL*8 NN,KO,KX,M

      XF(3)=   1-XF(2)-XF(1)
      YF(3)=   1-YF(2)-YF(1)
C
C  STEADY STATE DISPERSED PHASE FRACTIONAL HOLDUP CORRELATION
C -------------------------------------------------------------
C
C    E = A1+A2*(N)^A3+A4*(N*S/R)^A5
C
      A1=0.0549565
      A2=1E-8
      A3=8.10603
      A4=0.00007412
      A5=2.71254

      IF (ISIM.EQ.2) THEN
      CALL INPUT(N,Y,YP)
      CALL  RATE(1,Y(1),Y(N+1),KX,M,XS)
      RETURN
      ENDIF
 111  FORMAT(A)
      DO 10 I=1,N
      S(I)=(SF*(1-YF(2)))/(1-YE(I))
      R(I)=(RF*(1-XF(2)))/(1-XE(I))
      E(I)= A1+A2*(NN)**A3+A4*(NN*(S(I)/R(I)))**A5
      X0(I)=XE(I)
      Y0(I)=YE(I)
  10  CONTINUE
  11  FORMAT(4(3X,F15.5))
C
      Y(1)=X0(1)
      Y(1+N)=Y0(1)
      DO 2 I=2,N-1
      I1=I
      I2=I+N
      Y(I1) =X0(I)
      Y(I2) =Y0(I)
   2  CONTINUE
      Y(N)=X0(N)
      Y(2*N)=Y0(N)
      CALL DER(N,Y,YP)
      RETURN
      END
      SUBROUTINE RATE(II,XX,YY,KX,M,XS)
```

```
      IMPLICIT REAL*8 (A-H,O-Z)
      COMMON /OPT/FRAC1,FRAC2,FRAC3
      COMMON /CON/NEQ,XF(20),YF(20),RF,SF,V,AREA,VS
      COMMON /PAR/IODIR,HX(20),HY(20),XC(20),YC(20),R(20),S(20),E(20),A
     +,B,KO(20)
      COMMON /C/NN,A1,A2,A3,A4,A5,DENA,DENW,DENT
      REAL*8 M,NN,KX,KO
      CHARACTER*80 IODIR
      XO=XX
      YO=YY
      NC=3
      J=2
C-----------------------------------------------------------------------
-
C       CALCULATION OF MASS TRANSFER COEFF. KX
C-----------------------------------------------------------------------
-
      M=0.868582+0.086806*XX**(-0.483142)
      XS=YO/M
      XX=XO
      YY=YO
      CALL MASS(II,M,V,XX,YY,KX)
      KO(II)=KX
      RETURN
      END
      SUBROUTINE RES(T,Y,YP,DELTA,IRES,RPAR,IPAR)
      IMPLICIT DOUBLE PRECISION(A-H,O-Z)
      COMMON /CON/NEQ,XF(20),YF(20),RF,SF,V,AREA,VS
      COMMON /PAR/IODIR,HX(20),HY(20),XC(20),YC(20),R(20),S(20),E(20),A
     +,B,KO(20)
      COMMON /CAL/NCALLS
      COMMON /DES/N
      COMMON /RESULT/ results(1500,14),TSTOP,ITER
      COMMON /C/NN,A1,A2,A3,A4,A5,DENA,DENW,DENT
      COMMON /CONST/R1F1,R1F2,R1F3,S1F1,S1F2,S1F3,
     &      RIF(5,20),SIF(5,20),
     &      RNF1,RNF2,RNF3,SNF1,SNF2,SNF3
      DIMENSION Y(1),YP(1),DELTA(1)
      REAL*8 NN,M,KX,KO
      CHARACTER*80 IODIR

      DO 2 I=1,N
      I1=I
      I2=I+N
      XC(I)=Y(I1)
      YC(I)=Y(I2)
      HX(I)=V*(1-E(I))
      HY(I)=V*E(I)
    2 CONTINUE
      CALL FLOW(N,Y,YP)
C
C                          *** STAGE 1 ***
C
      I1=1
      I2=N+1
      QQ1= (R(2)*XC(2)-R(1)*XC(1))/HX(1)
      DELTA(I1)=YP(I1)-QQ1
      QQ2=0
      DELTA(I2)=YP(I2)-QQ2

C
```

```
C                          *** STAGE 2 ***
C
      I1=2
      I2=N+2
      CALL  RATE(2,XC(2),YC(2),KX,M,XS)
      QX=KX*(XC(2)-XS)
      QQ1= ((1+A)*(R(3)*XC(3)-R(2)*XC(2))-QX)/HX(2)
      DELTA(I1)=YP(I1)-QQ1
      QQ2=(B*YC(3)*S(3)-(1+B)*YC(2)*S(2)+SF*YF(2)+QX)/HY(2)
      DELTA(I2)=YP(I2)-QQ2

C
C                          *** STAGE I ***
C
      DO 1 I=3,N-2
      I1=I
      I2=I+N
      CALL  RATE(I,XC(I),YC(I),KX,M,XS)
      QX=KX*(XC(I)-XS)


      QQ1=(1+A)*R(I+1)*XC(I+1)-(1+2*A)*R(I)*XC(I)+A*XC(I-1)*R(I-1)-QX
      QQ1=QQ1/HX(I)
      DELTA(I1)=YP(I1)-QQ1
      QQ2=B*YC(I+1)*S(I+1)-(1+2*B)*YC(I)*S(I)+(1+B)*YC(I-1)*S(I-1)+QX
      QQ2=QQ2/HY(I)
      DELTA(I2)=YP(I2)-QQ2
    1 CONTINUE
C
C                          *** STAGE N-1 ***
C
      I1=N-1
      I2=N+(N-1)
      CALL  RATE(N-1,XC(N-1),YC(N-1),KX,M,XS)
      QX=KX*(XC(N-1)-XS)

      QQ1=(XF(2)*RF+A*XC(N-2)*R(N-2)-(1+A)*XC(N-1)*R(N-1)-QX)/HX(N-1)
      DELTA(I1) =YP(I1)- QQ1
      QQ2=((1+B)*(S(N-2)*YC(N-2)-S(N-1)*YC(N-1))+QX)/HY(N-1)
      DELTA(I2)=YP(I2)-  QQ2
C
C                          *** STAGE N ***
C
      I1=N
      I2=2*N

      QQ1=0
      DELTA(I1) =YP(I1)- QQ1
      QQ2=(S(N-1)*YC(N-1)-S(N)*YC(N))/HY(N)
      DELTA(I2)=YP(I2)-  QQ2
      RETURN
      END

      SUBROUTINE DER(N,Y,YP)
      IMPLICIT DOUBLE PRECISION(A-H,O-Z)
      COMMON /CON/NEQ,XF(20),YF(20),RF,SF,V,AREA,VS
      COMMON /PAR/IODIR,HX(20),HY(20),XC(20),YC(20),R(20),S(20),E(20),A
     +,B,KO(20)
      COMMON /RESULT/ results(1500,14),TSTOP,ITER
      DIMENSION Y(1),YP(1)
      REAL*8 KO,M,KX
```

```
      CHARACTER*80  IODIR

      DO 2 I=1,N
      I1=I
      I2=I+N
      XC(I)=Y(I1)
      YC(I)=Y(I2)
    2 CONTINUE
C
C                          *** STAGE 1 ***
C
      YP(1)=0
      YP(N+1)=0

C
C                          *** STAGE 2 ***
C
      I1=2
      I2=N+2
      CALL  RATE(1,XC(2),YC(2),KX,M,XS)
      QX=KX*(XC(2)-XS)
      YP(I1)=((1+A)*(R(3)*XC(3)-R(2)*XC(2))-QX)/(V*(1-E(2)))
      YP(I2)=(B*YC(3)*S(3)-(1+B)*YC(2)*S(2)+SF*YF(2)+QX)/(V*(E(2)))
C
C                          *** STAGE I ***
C
      DO 1 I=3,N-2
      I1=I
      I2=I+N
      CALL  RATE(I,XC(I),YC(I),KX,M,XS)
      QX=KX*(XC(I)-XS)

      QQ1=(1+A)*R(I+1)*XC(I+1)-(1+2*A)*R(I)*XC(I)+A*XC(I-1)*R(I-1)-QX
      YP(I1)=QQ1/(V*(1-E(I)))

      QQ2=B*YC(I+1)*S(I+1)-(1+2*B)*YC(I)*S(I)+(1+B)*YC(I-1)*S(I-1)+QX
      YP(I2)=QQ2/(V*(E(I)))
    1 CONTINUE
C
C                          *** STAGE N-1 ***
C
      I1=N-1
      I2=2*N-1
      CALL  RATE(N-1,XC(N-1),YC(N-1),KX,M,XS)
      QX=KX*(XC(N-1)-XS)
      YP(I1)=(XF(2)*RF+A*XC(N-2)*R(N-2)-(1+A)*XC(N-1)*R(N-1)-QX)
     &/(V*(1-E(N-1)))
      YP(I2)=((1+B)*(S(N-2)*YC(N-2)-S(N)*YC(N-1))+QX)/(V*(E(N-1)))
C
C                          *** STAGE N ***
C

      YP(N)=0
      YP(2*N)=0
   54 CONTINUE
      RETURN
      END

      SUBROUTINE MASS (II,M,V,XX,YY,K)
      IMPLICIT REAL*8 (A-H,O-Z)
      REAL*8 M,NN,NE,KC,KD,K,KO
```

```
      COMMON /DES/N
      COMMON /RESULT/ results(1500,14),TSTOP,ITER
      COMMON /OPT/FRAC1,FRAC2,FRAC3
      COMMON /C/NN,A1,A2,A3,A4,A5,DENA,DENW,DENT
      COMMON
/PAR/IODIR,HX(20),HY(20),XC(20),YC(20),R(20),S(20),E(20),A
     +,B,KO(20)
      CHARACTER*80  IODIR

C-----------------------------------------------------------------------
C
C  PHYSICAL PROPERTIES UNITS TO BE USED :
C  -------------------------------------
C
C     DENSITY              [=]  GM/CM^3
C     VISCOSITY            [=]  P = GM / CM S
C     DIFFUSIVITY          [=]  CM^2/S
C     SURFACE TENSION      [=]  DYN/CM =  GM/S^2
C     DROP DIAMETER        [=]  CM
C     VELOCITY             [=]  CM/S
C
C     MASS TRANSF. COEFF.  [=]  CM/S
C
C-----------------------------------------------------------------------
C
C  SYSTEM : WATER - ACETONE - TOLUENE
C
      DENW= 0.99777
      DENA= 0.79200
      DENT= 0.86600
      VISA= 0.32
      VIST= 0.55
      DIFC=1.82630E-5
      DIFD=2.21084E-5

      DENC=XX*DENA+(1-XX)*DENW
      DEND=YY*DENA+(1-YY)*DENT
      GAT=-0.772
      VISC=1.E-2*(0.99694+2.611*XX-1.2307*XX**2    )
      VISD=1.E-2*(EXP( (YY*(DLOG(VISA))) + ((1-YY)*(DLOG(VIST)))
     &  +((1-YY)*YY*GAT) )  )
      XS=XX+YY
      SURF=33.479243-95.050177*XS+275.917068*XS**2.0

      DR=2.2
      HM=2.5.0
      HS=12.0
      AREA=3.14569*(8/2)**2.0
      V=HM*AREA
      VM=V
      VS=HS*AREA
C ... SAUTER MEAN DROP DIAMETER (CM)
      WE=(DR**3 * (NN)**2 * DENC)/(SURF)
      D32=DR*(1.763+16.117*E(II))*WE**(-0.907)

C ... ROTOR TIP SPEED VELOCITY     (CM/S) .

      V0=3.14153*DR*NN
      V0=V0/2
      REDROP=(DEND*D32*V0)/VISD
```

```
C ... MASS TRANSFER COEFFECIENT  (CM/S)
      F1=0.2
      F2=3.6131
      F3=-2.2565
      F4=0.2798
      F5=0.5526
      F6=-0.2582
      F7=0.2775
      REC=(DENC*D32*V0)/VISC
      SC=VISC/(DENC*DIFC)
      NE=2
      W=( (SURF*(D32**0.225/1.242)/(D32/2)**3)*((NE*(NE+1)*(NE-1)*
     &  (NE+2))/((NE+1)*DEND+NE*DENC) ))**0.5
      KD=0.45*(W*DIFD)**0.5
      KC=(50.0+0.0085*REC*SC**0.7)*(DIFC/D32)
      K=1.0/( 1.0/KC + 1/(M*KD) )

C ... INTERFACIAL AREA     (1/CM)

      AI=(6*E(II)*VM)/D32

C ... OVERALL MASS TRANSFER COEFF. K=KO*A*V*FRAC

      FRAC(II)=F1+F2*(NN)**F3+F4*(S(II)/R(II))**F5+
     &F6*(NN*(S(II)/R(II)))**F7
      Aim=AI
      AIs=(6*e*VS)/D32
      AK1=60*K*AIm
      AK2=60*K*AIs*FRAC(II)
      K=AK1+AK2
      RETURN
      END
      SUBROUTINE STORE(N,Y,YP)
        IMPLICIT REAL*8 (A-H,O-Z)
      COMMON /PAR/IODIR,HX(20),HY(20),XC(20),YC(20),R(20),S(20),E(20),A
     + ,B,KO(20)
      REAL*8 Y(1),YP(1),KO
      CHARACTER*80 IODIR
      LIO=LEN_TRIM(IODIR)
      OPEN(10,FILE=IODIR(:LIO)//'STEADY.DAT',STATUS='UNKNOWN')
      DO 1 I=1,N
      WRITE (10,20)E(I),Y(I),Y(I+N),R(I),S(I)
    1 CONTINUE
      WRITE(10,'(A)') '  '
      DO 2 I=1,N
      WRITE (10,20)YP(I),YP(I+N)
    2 CONTINUE
   20 FORMAT(5(1X,F15.7))
   30 FORMAT(5X,I2,6X,F12.5,4X,F12.5)
      CLOSE(10)
      RETURN
      END
C-----------------------------------------------------------------------
      SUBROUTINE INPUT (N,Y,YP)
        IMPLICIT REAL*8 (A-H,O-Z)
      COMMON /PAR/IODIR,HX(20),HY(20),XC(20),YC(20),R(20),S(20),E(20),A
     +,B,KO(20)
      REAL*8 Y(1),YP(1),KO
      CHARACTER*1 BLANK
      CHARACTER*80 IODIR
```

```
      LIO=LEN_TRIM(IODIR)
      OPEN(10,FILE=IODIR(:LIO)//'STEADY.DAT',STATUS='UNKNOWN')
      DO 1 I=1,N
      READ (10,20)E(I),Y(I),Y(I+N),R(I),S(I)
   1  CONTINUE
      READ(10,'(A)')BLANK
      DO 2 I=1,N
      READ (10,20)YP(I),YP(I+N)
   2  CONTINUE
   20 FORMAT(5(1X,F15.7))
      CLOSE(20)
      RETURN
      END
C-----------------------------------------------------------------------
      SUBROUTINE FLOW (N,Y,YP)
      IMPLICIT REAL*8 (A-H,O-Z)
      COMMON PAR/IODIR,HX(20),HY(20),XC(20),YC(20),R(20),S(20),E(20),A
     +,B,KO(20)
      COMMON /RESULT/ results(1500,14),TSTOP,ITER
      COMMON /CON/NEQ,XF(20),YF(20),RF,SF,V,AREA,VS
      COMMON /C/NN,A1,A2,A3,A4,A5,DENA,DENW,DENT
      REAL*8 Y(1),YP(1),KO,NN
      CHARACTER*80 IODIR
      B=0.0
      A=-2.859-2.463*(NN)**(-0.8)+0.156*(SF/RF)**2+
     &4.031*(NN*(SF/RF))**(-0.1);
      DO 1 I=1,N
        I1=I
        I2=I+N
        XC(I)=Y(I1)
        YC(I)=Y(I2)

        E(I)= A1 + A2*NN**A3 + A4*(NN*(SF/RF))**A5
        HX(I)=V*(1-E(I))
        HY(I)=V*E(I)
 1    CONTINUE
      S(1)=(HY(1)*YP(1)+SF*(1-YF(2))+B*S(2)*(1-YC(2)))/
     +     ((1+B)*(1-YC(1)))
      DO 2 I=2,N-1
      S(I)=(HY(I)*YP(I+N)+(1+B)*S(I-1)*(1-YC(I-1))+
     +     B*S(I+1)*(1-YC(I+1)))/((1+2*B)*(1-YC(I)))
   2  CONTINUE
      S(N)=(HY(N)*YP(2*N)+(1+B)*S(N-1)*(1-YC(N-1)))/
     +     ((1+B)*(1-YC(N)))

      R(N)=(HX(N)*YP(N)+RF*(1-XF(2))+A*R(N-1)*(1-XC(N-1)))/
     +     ((1+A)*(1-XC(N)))
        DO 22 I=N-1,2,-1
      R(I)=(HX(I)*YP(I)+(1+A)*R(I+1)*(1-XC(I+1))+
     +     A*R(I-1)*(1-XC(I-1)))/((1+2*A)*(1-XC(I)))
  22  CONTINUE

      R(1)=(HX(1)*YP(1)+(1+A)*R(2)*(1-XC(2)))/((1+A)*(1-XC(1)))
      RETURN
      END
C-----------------------------------------------------------------------
      SUBROUTINE PRINTOUT(T,N)
      USE MSFLIB
      IMPLICIT REAL*8 (A-H,O-Z)
      COMMON
/PAR/IODIR,HX(20),HY(20),XC(20),YC(20),R(20),S(20),E(20),A
```

```
     +,B,KO(20)
      COMMON /CON/NEQ,XF(20),YF(20),RF,SF,V,AREA,VS
      COMMON /RESULT/ results(1500,14),TSTOP,ITER
      REAL*8 KO
      CHARACTER IODIR*80,C*1
      TYPE (windowconfig) wc
      LOGICAL status /.FALSE./
c  Set the x & y pixels to 800X600 and font size to 8x12
      wc.numxpixels = 800
      wc.numypixels = 600
      wc.numtextcols = -1
      wc.numtextrows = -1
      wc.numcolors = -1
      wc.title= "CALCULATED COLUMN PROFILES"C
      wc.fontsize = #0008000C
      if (.NOT.status) status = SETWINDOWCONFIG(wc)

      IF(T.EQ.0) WRITE(8,11)
      C=','
      WRITE(8,112)T,C,XF(2),C, YC(1),C ,YC(N),C ,XC(1),C ,XC(N),
     1               C, S(1), C , S(N),C, R(1), C, R(N),
     2               C, HY(1),C , HY(N),C, HX(1),C,HX(N)
      write(11,113)T,XC(1),YC(N)
      RESULTS(ITER,1)=T
      RESULTS(ITER,2)=YC(1)  ;      RESULTS(ITER,3)=YC(N)
      RESULTS(ITER,4)=XC(1)  ;      RESULTS(ITER,5)=XC(N)
      RESULTS(ITER,6)=S(1)   ;      RESULTS(ITER,7)=S(N)
      RESULTS(ITER,8)=R(1)   ;      RESULTS(ITER,9)=R(N)
      RESULTS(ITER,10)=HY(1) ;      RESULTS(ITER,11)=HY(N)
      RESULTS(ITER,12)=HX(1) ;      RESULTS(ITER,13)=HX(N)
 11   FORMAT('TIME ,',6X,6Hyf(2),,
     1       7X,6H Y(1),,7X,7H Y(N) ,,7X,6H X(1),,4X,10H    X(N) ,,
     2       4X,6H S(0),,7X,7H S(N) ,,7X,6H R(1),,4X,10H    R(N) ,,
     3       4X,7H Hy(1),,7X,8H Hy(N) ,,7X,7H Hx(1),,4X,7H Hx(N)   )
 112  FORMAT(F7.3,A,F10.6,2X,A,2X ,12(F10.6,2X,A ) )
 113  FORMAT(F7.3,2x,F10.6,2X ,F10.6 )
 888  RETURN
      END
C-------------------------------------------------------------------
-
      SUBROUTINE Plot
      USE MSFLIB
      IMPLICIT REAL*8 (A-H,O-Z)
      COMMON /RESULT/ results(1500,14),TSTOP,ITER
      COMMON /XY/XMIN,XMAX,YMIN,YMAX
      REAL XARR(1500),YARR(1500,15),XMIN,XMAX,YMIN,YMAX,MX,MY
      INTEGER(2) LOCX,LOCY ,X0,Y0,DX,DY
      INTEGER(2) fontnum, numfonts
      character(8) AXMIN,AXMAX,AYMIN,AYMAX ,AMX,AMY
      TYPE  (xycoord)  xy
      TYPE (windowconfig) wc
      LOGICAL status /.FALSE./
      wc.numxpixels = 800
      wc.numypixels = 600
      wc.numtextcols = -1
      wc.numtextrows = -1
      wc.numcolors = -1
      wc.title= "TRANSIENT CONCENTRATION PROFILES"
      wc.fontsize = #0008000C
      if (.NOT.status) status = SETWINDOWCONFIG(wc)
      NPTS=TSTOP
```

```
      PRINT*,NPTS
      do  12 I=1,NPTS
      XARR(i)=RESULTS(I,1)
      DO 1 J=3,4
      YARR(I,J)=RESULTS(I,J)
1     CONTINUE
       PRINT*,XARR(I),YARR(I,3),YARR(I,4)
12    CONTINUE
      X0=150        ; DX=500
      Y0=100        ; DY=400
      CALL SCAL(NPTS,3,4,XARR,YARR,X0,Y0,DX,DY)
      DUMMY = FOCUSQQ (10)
         OLDTC = SETCOLOR(15)
         dummy = RECTANGLE($GBORDER,X0-1,Y0-1,X0+DX+1,Y0+DY+1 )
         OLDTC = SETCOLOR(17)
         dummy = RECTANGLE($GFILLINTERIOR,X0,Y0,X0+DX,Y0+DY )
         OLDTC = SETCOLOR(15)
         dummy=RECTANGLE($GBORDER,X0+DX-170,Y0+DY-110,X0+DX-20,Y0+DY-20)
         OLDTC = SETCOLOR(11)
         locx  =  XARR(1)
         locy  =  YARR(1,3)
         CALL MOVETO( locx, locy, xy  )
      DO I=2,NPTS
         locx  =  XARR(I)
         locy  =  YARR(I,3)
         dummy = LINETO( locx, locy  )
      END DO

      OLDTC = SETCOLOR(10)
         locx  =  XARR(1)
         locy  =  YARR(1,4)
         CALL MOVETO( locx, locy, xy  )
      DO I=2,NPTS
         locx  =  XARR(I)
         locy  =  YARR(I,4)
         dummy = LINETO( locx, locy  )
      END DO
      MX=XMIN+(XMAX-XMIN)/2
      MY=YMIN+(YMAX-YMIN)/2
      CALL CONV(XMIN,XMAX,YMIN,YMAX,MX,MY,AXMIN,AXMAX,
     +    AYMIN,AYMAX,AMX,AMY)
      numfonts = INITIALIZEFONTS ( )
      fontnum = SETFONT ('t''Arial''h18w10e')
      OLDTC = SETCOLOR(15)
      CALL SETGTEXTROTATION(0)
      CALL moveto(X0-100,Y0+DY-10,xy)
      CALL OUTGTEXT(AYMIN)
      CALL moveto(X0-100,Y0+(DY/2)-10,xy)
      CALL OUTGTEXT(AMY)
      CALL moveto(X0-100,Y0,xy)
      CALL OUTGTEXT(AYMAX)
      CALL moveto(X0-20,Y0+DY+20,xy)
      CALL OUTGTEXT(AXMIN)
      CALL moveto(X0+(DX/2)-20,Y0+DY+20,xy)
      CALL OUTGTEXT(AMX)
      CALL moveto(X0+DX-40,Y0+DY+20,xy)
      CALL OUTGTEXT(AXMAX)
      K=10
      I1=DX/K
      I2=DY/K
      do i=1,K
```

```
      CALL moveto(X0+I1*i,Y0+DY,xy)
      dummy = LINETO( X0+I1*i,Y0+DY-10  )
      CALL moveto(X0,Y0+I2*i,xy)
      dummy = LINETO(X0+10,Y0+I2*i  )
      end do
      fontnum = SETFONT ('t''Arial''h18w10i')
      CALL moveto(X0-130,Y0+(DY/2)+60,xy)
      CALL SETGTEXTROTATION(900)
      CALL OUTGTEXT('Concentration (wt%)')
      call moveto(X0+(DX/2)-30,Y0+DY+50,xy)
      CALL SETGTEXTROTATION(0)
      CALL OUTGTEXT('Time (min)')
      OLDTC = SETCOLOR(11)
      call moveto(X0+DX-150,Y0+350,xy)
      CALL OUTGTEXT('EXTRACT')
      OLDTC = SETCOLOR(10)
      call moveto(X0+DX-150,Y0+300,xy)
      CALL OUTGTEXT('RAFFINATE')
      OLDTC = SETCOLOR(15)
      fontnum = SETFONT ('t''Arial''h28w10e')
      call moveto(X0+20,Y0-60,xy)
      CALL OUTGTEXT('COLUMN OUTLETS CONCENTRATION PROFILES')
      RETURN
      END
      SUBROUTINE SCAL(NPTS,ii,jj,X,Y,X0,Y0,DX,DY)
      COMMON /XY/XMIN,XMAX,YMIN,YMAX
      REAL X(1500),Y(1500,15),XMIN,XMAX,YMIN,YMAX
      INTEGER(2) X0,Y0,DX,DY
      XMIN=X(1)
      XMAX=X(1)
      YMIN=Y(1,ii)
      YMAX=Y(1,ii)
      DO 1 I=1,NPTS
      IF (XMIN.GT.X(I) ) XMIN=X(I)
      IF (XMAX.LT.X(I) ) XMAX=X(I)
      DO 2 J=ii,jj
      IF (YMIN.GT.Y(I,J)) YMIN=Y(I,J)
      IF (YMAX.LT.Y(I,J)) YMAX=Y(I,J)
    2 CONTINUE
    1 CONTINUE
      XD=XMAX-XMIN
      YD=YMAX-YMIN
C      YMIN=YMIN-.05*YD
C      YMAX=YMAX+.05*YD
      DO 5 I=1,NPTS
      X(I)=X0+DX*(X(I)-XMIN)/(XMAX-XMIN)
      DO 21 J=ii,jj
      Y(I,J)=600-(Y0+DY*(Y(I,J)-YMIN)/(YMAX-YMIN))
   21 CONTINUE
    5 CONTINUE
  999 RETURN
      END
      SUBROUTINE CONV(XMIN,XMAX,YMIN,YMAX,MX,MY,
     +           AXMIN,AXMAX,AYMIN,AYMAX,AMX,AMY)
      character(8) AXMIN,AXMAX,AYMIN,AYMAX,AMX,AMY
      real XMIN,XMAX,YMIN,YMAX ,MX,MY
      open(7,file='test',status='unknown')
      write(7,'(f5.1,5X,f5.1,5X,f8.4,2X,f8.4,2X,f5.1,5X,f8.4)')XMIN,XM
AX
     +         ,YMIN*100     , YMAX*100 ,MX,MY*100
      close (7)
```

```
      open(7,file='test',status='UNKNOWN')
      read(7,'(6(A8,2X))') AXMIN, AXMAX , AYMIN , AYMAX ,AMX,AMY
      close (7)
      RETURN
      END
```

G.8 Solvent Extraction Column Rigorous Model (MATLAB version)

```
% Main module
% Running Stage-wise Back-mixed Extraction model
  for a ternary system (W-A-T)
clear
profile on
global A1 A2 A3 A4 A5 NN N V A B FR SF RF R S XF YF Y YP

%Setting Initial Conditions.
Init;

% Defining solver options
options = odeset('RelTol',1e-8);
% Calling Integrator
secs = cputime;
[t,x]=ode15s(@ExtModel,[0 25],Y,options);
secs = cputime - secs;
lengthx=size(x);
Y=x(lengthx(1),:)';
xAll=x; tAll=t;

% Disturbance (Select one of the five cases).
%Case 1: Solvent Concentration
         YF(1)=0.99;   YF(2)=0.01; YF(3)=0;
%Case 2: Feed Concentration
%        XF(1)=0.96;  XF(2)=0.04; XF(3)=0;
%Case 3: Rotor Speed
%        NN=450/60;
%Case 4: Solvent Flowrate
%        SF=17*(1000/60);
%Case 5: Feed Flowrate
%        RF=17*(1000/60);

% Calling Integrator again
[t,x]=ode15s(@ExtModel,[25 50],Y,options);
x(:,N)=XF(2);
x(:,N+1)=YF(2);

xAll=[xAll',x']'; tAll=[tAll',t']';

% Save results
% Vector 'Xss' returns steady-state compositions of component B at
each stage for both phases
lengthx=size(x);
Xss=x(lengthx(1),:)';

figure(1)
subplot(2,1,1); plot(tAll,xAll(:,1:11)); subplot(2,1,2);
plot(tAll,xAll(:,12:22));
figure(2)
subplot(2,1,1); plot(tAll,xAll(:,1)); subplot(2,1,2);
plot(tAll,xAll(:,22));
```

```
profile off
profile report

% Initial Conditions function
function YP=INIT
global A1 A2 A3 A4 A5 NN N V A B FR SF RF R S XF YF Y YP

% Feed variables
N=11;
NN=400/60;
YF(1)=1.0;     YF(2)=0.0;
SF=15*(1000/60);
XF(1)=0.98;  XF(2)=0.02;
RF=15*(1000/60);

%Model Parameters
F1=0.2; F2=3.6131; F3=-2.2565;  F4=0.2798;  F5=0.5526;  F6=-0.2582;
F7=0.2775;
A1=0.0549565; A2=1E-8; A3=8.10603; A4=0.00007412;  A5=2.71254; V=240;
B=0.0; A=0.0;
B=0.0;
A=-2.859-2.463*(NN)^(-0.8)+0.156*(S(I)/R(I))^2+
4.031*(NN*(S(I)/R(I)))^(-0.1);
%Initial Profiles
XF(3)=   1-XF(2)-XF(1);
YF(3)=   1-YF(2)-YF(1);

for I=1:N
      S(I)=SF;      R(I)=RF;
      E(I) = A1+A2*(NN)^A3+A4*(NN*(S(I)/R(I)))^A5;
        FR(I)=F1+F2*(NN)^F3+F4*(S(I)/R(I))^F5+F6*(NN*(S(I)/R(I)))^F7;
      X0(I)=XF(2);
      Y0(I)=YF(2);
  end
Y(1)=X0(1);     Y(1+N)=Y0(1);
for I=2:N
      I1=I;    I2=I+N;
      Y(I1) =X0(I);
      Y(I2) =Y0(I);
  end
Y(N)=X0(N);     Y(2*N)=Y0(N);

 for I=1:N
      I1=I;
      I2=I+N;
      XC(I)=Y(I1);
      YC(I)=Y(I2);
  end
% Initial derivatives
%                          *** STAGE 1 ***
YP(1)=0;     YP(N+1)=0;
%                          *** STAGE 2 ***
I1=2;
I2=N+2;
[K,M]=MTC(2,XC(2),YC(2),E(2));    KX=K; XS= YC(2)/M;   QX=KX*(XC(2)-XS);
YP(I1)=((1+A)*(R(3)*XC(3)-R(2)*XC(2))-QX)/(V*(1-E(2)));
YP(I2)=(B*YC(3)*S(3)-(1+B)*YC(2)*S(2)+SF*YF(2)+QX)/(V*(E(2)));

%                          *** STAGE I ***
for I=3:N-2
```

```
I1=I;
I2=I+N;
[K,M]=MTC(I,XC(I),YC(I),E(2)); KX=K; XS= YC(I)/M;      QX=KX*(XC(I)-XS);
YP(I1)=((1+A)*R(I+1)*XC(I+1)-(1+2*A)*R(I)*XC(I)+A*XC(I-1)*R(I-1)-
QX)/(V*(1-E(I)));
YP(I2)=(B*YC(I+1)*S(I+1)-(1+2*B)*YC(I)*S(I)+(1+B)*YC(I-1)*S(I-
1)+QX)/(V*(E(I)));
end
%                          *** STAGE N-1 ***
I1=N-1;
I2=2*N-1;
[K,M]=MTC(N-1,XC(N-1),YC(N-1),E(N-1));  KX=K; XS= YC(N-1)/M;
QX=KX*(XC(N-1)-XS);
YP(I1)=(XF(2)*RF+A*XC(N-2)*R(N-2)-(1+A)*XC(N-1)*R(N-1)-QX)/(V*(1-E(N-
1)));
YP(I2)=((1+B)*(S(N-2)*YC(N-2)-S(N)*YC(N-1))+QX)/(V*(E(N-1)));

%                          *** STAGE N ***
YP(N)=0;     YP(2*N)=0;

% Model Equations
function DELTA=ExtModel(t,x)
global A1 A2 A3 A4 A5 NN N V A B FR SF RF R S XF YF Y YP

S(1)=SF;
R(N)=RF;
%if Y(N)-XF(2)~=0   Y(N)=XF(2);   end
%if Y(N+1)-YF(2)~=0 Y(N+1)=YF(2); end

for I=1:N
E(I)= A1 + A2*NN^A3 + A4*(NN*(SF/RF))^A5;
HX(I)=V*(1-E(I));   HY(I)=V*E(I);
end
DELTA=zeros(2*N,1);
% Composition of A in the Continuous phase for all stages
XC=x(1:N)';
% Composition of A in the Dispersed phase for all stages
YC=x(N+1:2*N)';
XC(N)=XF(2);
YC(1)=YF(2);

%                      Algebraic Equations

R(N)=RF;
R(N-1)=(HX(N-1)*DELTA(N-1)+RF*(1-XF(2))+A*R(N-2)*(1-XC(N-
2)))/((1+A)*(1-XC(N-1)));
for I=N-2:-1:3
R(I)=(HX(I)*DELTA(I)+(1+A)*R(I+1)*(1-XC(I+1))+ A*R(I-1)*(1-XC(I-
1)))/((1+2*A)*(1-XC(I)));
end
R(2)=(HX(2)*DELTA(2)+(1+A)*R(3)*(1-XC(3)))/((1+A)*(1-XC(2)));
R(1)=(HX(1)*DELTA(1)+R(2)*(1-XC(2)))/(1-XC(1));

S(1)=SF;
S(2)=(HY(2)*DELTA(2+N)+SF*(1-YF(2))+B*S(3)*(1-YC(3)))/((1+B)*(1-
YC(2)));
for I=3:N-2
S(I)=(HY(I)*DELTA(I+N)+(1+B)*S(I-1)*(1-YC(I-1))+B*S(I+1)*(1-
YC(I+1)))/((1+2*B)*(1-YC(I)));
end
S(N-1)=(HY(N-1)*DELTA(N+N-1)+S(N)*(1-YC(N)))/((1+B)*(1-YC(N-1)));
```

```
S(N)=(HY(N)*DELTA(N+N)+(1+B)*S(N-1)*(1-YC(N-1)))/(1-YC(N));

for ii=1:N Data (ii,1)=0; if ii==1 Data(ii,1)=t; end
    Data(ii,2)=R(ii); Data(ii,3)=S(ii); Data(ii,4)=XC(ii);
Data(ii,5)=YC(ii); Data(ii,6)=E(ii); end; Data;
%                       Differential Equations
%                          *** STAGE 1 ***
DELTA(1)=(R(2)*XC(2)-R(1)*XC(1))/HX(1);
DELTA(N+1)=0;

%                          *** STAGE 2 ***
I1=2;
I2=N+2;
[K,M]=MTC(2,XC(2),YC(2),E(2));KX=K; XS= YC(2)/M;  QX=KX*(XC(2)-XS);
DELTA(I1)=((1+A)*(R(3)*XC(3)-R(2)*XC(2))-QX)/HX(2);
DELTA(I2)=(B*YC(3)*S(3)-1+B)*YC(2)*S(2)+SF*YF(2)+QX)/HY(2);

%                          *** STAGE I ***

for I=3:N-2
  I1=I;
  I2=I+N;
  [K,M]=MTC(I,XC(I),YC(I),E(2));   KX=K;  XS= YC(I)/M;
  QX=KX*(XC(I)-XS);
  DELTA(I1)=((1+A)*R(I+1)*XC(I+1)-
        (1+2*A)*R(I)*XC(I)+A*XC(I-1)*R(I-1)-QX)/HX(I);
  DELTA(I2)=(B*YC(I+1)*S(I+1)-
        (1+2*B)*YC(I)*S(I)+(1+B)*YC(I-1)*S(I-1)+QX)/HY(I);
end

%                          *** STAGE N-1 ***

  I1=N-1;
  I2=N+(N-1);
  [K,M]=MTC(N-1,XC(N-1),YC(N-1),E(N-1)); KX=K; XS=YC(N-1)/M;
  QX=KX*(XC(N-1)-XS);
  DELTA(I1)= (XF(2)*RF+A*XC(N-2)*R(N-2)-(1+A)*XC(N-1)*R(N-1)-QX)/HX(N-
1);
  DELTA(I2)= ((1+B)*(S(N-2)*YC(N-2)-(1+B)*S(N-1)*YC(N-1))+QX)/HY(N-1);

%                          *** STAGE N ***
  DELTA(N) =0;
  DELTA(2*N)= (S(N-1)*YC(N-1)-S(N)*YC(N))/HY(N);

%Physical Properties function
function [K,M]=MTC(i,xi,yi,e)
global A1 A2 A3 A4 A5 NN N V A B FR SF RF R S XF YF Y YP
M=0.868582+0.086806*xi^(-0.483142);

DENW= 0.99777;  DENA= 0.79200; DENT= 0.86600;
VISA= 0.32;     VIST= 0.55;    DIFC=1.82630E-5;  DIFD=2.21084E-5;

DENC=xi*DENA+(1-xi)*DENW;  DEND=yi*DENA+(1-yi)*DENT;
GAT=-0.772;
VISC=0.01*(0.99694+2.611*xi-1.2307*xi^2 );
VISD=0.01*(exp( (yi*(log10(VISA))) + ((1-yi)*(log10(VIST))) +((1-
yi)*yi*GAT) )  );
XS=xi+yi;
% SURFACE TENSION (GM/S^2)
SURF=33.479243-95.050177*XS+275.917068*XS^2.0;
```

```
DR=2.2;
HM=2.5; HS=12.0;
AREA=pi*(8/2)^2;
VM=HM*AREA;
V=VM;
VS=HS*AREA;
% ... SAUTER MEAN DROP DIAMETER (CM)
WE=(DR^3 * NN^2 * DENC)/(SURF);
D32=DR*(1.763+16.117*e)*WE^(-0.907);

% ... ROTOR TIP SPEED VELOCITY     (CM/S) .

V0=3.14153*DR*NN;
V0=V0/2;
REDROP=(DEND*D32*V0)/VISD;

% ... MASS TRANSFER COEFFECIENT  (CM/S)

REC=(DENC*D32*V0)/VISC;
SC=VISC/(DENC*DIFC);
NE=2;
W=( (SURF*(D32^0.225/1.242)/(D32/2)^3)*((NE*(NE+1)*(NE-
1)*(NE+2))/((NE+1)*DEND+NE*DENC) ))^0.5;
KD=0.45*(W*DIFD)^0.5;
KC=(50.0+0.0085*REC*SC^0.7)*(DIFC/D32);
%KD=KD/7;
K=1.0/( 1.0/KC + 1.0/(M*KD) );
zz=[KC KD K];
% ... INTERFACIAL AREA     (1/CM)
AIm=(6*e*VM)/D32;
AIs=(6*e*VS)/D32;
% ... OVERALL MASS TRANSFER COEFF. K=KO*A*V*FRAC

K1=60*K*AIm;
K2=60*K*AIs*FR(i);
K=K1+K2;
```

Mathematical Modeling and Steady-State Analysis of a Scheibel Extraction Column

I. ALATIQI[1], G. ALY[2], F. MJALLI[1] and C. J. MUMFORD[3]*

[1]Department of Chemical Engineering, Kuwait University, P.O. Box 5969, Safat 13060, Kuwait
[2]Department of Chemical Engineering I, University of Lund, Box 124, S-22100 Lund, Sweden
[3]Department of Chemical Engineering and Applied Chemistry, University of Aston, Birmingham B4 7ET, United Kingdom

Aston University

Content has been removed for copyright reasons